The response of marine pelagic calcifiers to ocean alkalinity enhancement as a carbon dioxide removal technique



Sophie J. Gill

Linacre College

University of Oxford

A thesis submitted for the degree of

Doctor of Philosophy

14th January 2022

Declaration

All work presented is my own and has been conducted over the course of my time as a PhD candidate at the University of Oxford (2017-2022). Contribution by co-authors is outlined fully using the University of Oxford MPLS Division template for statement of authorship at the end of each chapter. Any information, figures and data from other publications are referenced clearly throughout the thesis.

Acknowledgements

This PhD has been a true lesson in resilience. Between failed culturing seasons in Israel, a global pandemic, and many other setbacks along the way, I can hardly believe I am writing these acknowledgements, as there were definitely times along the way I wondered if I would ever get to this point! I am beyond proud of myself for getting here and would like to thank the following people for their contribution to the success of this project.

Thank you to the Natural Environment Research Council (NERC) project NE/P019536/1 for the financial support of this PhD. Thank you to Ros, my primary supervisor, for all the engaging science over the years, but also in particular for being supportive when things were tough. I really appreciated you looking out for my wellbeing, and financially supporting a 3-month extension at the end of my PhD. Thank you also to Gideon for being my secondary supervisor; your expertise and input were always helpful. Thank you to the OceanBUG research group (past and present), in particular Joseph Snow for helping me set up so much in the lab at the start of my PhD. Thank you to Joan Zhang and Nishant Chauhan for providing feedback on a very early draft of Chapter 3. A massive thank you to Steve Wyatt in the Department of Earth Sciences, Oxford, for without fail always managing to fix things. Thank you to Isabelle Aldridge for your enthusiasm and work with the foraminifera culturing data.

A big thank you to Jonathan Erez and the team at the Department of Earth Sciences at the Hebrew University of Jerusalem, as well as at the Inter-University Institute of Marine Sciences in Eilat. In particular, thanks to Sandrine LeHouedec and David Evans, and to Adam Levi.
Thank you to Peter Ditchfield in the Department of Archaeology, Oxford, for being unendingly patient while I trialled TPC and POC measurements on your mass spectrometer. Thank you Errin Johnson in the William Dunn School of Pathology, Oxford, for always being so kind and helpful and enabling me to produce fantastic quality SEM images. Thank you to Stathys Papadimitriou at the National Oceanography Centre, Southampton, for your expertise in

measurement of Total Alkalinity on an autotitrator – I learnt so much from my visits to your lab. Thank you to Lydia Kapsenberg and James Gately for providing me with experience of science outside Oxford, and for being such fantastic collaborators. I have learnt loads from both of you.

Thank you to Office 50.15. I so appreciated always having someone to talk over the trials and tribulations of a PhD, and to have a cup of tea with. Thank you to Caroline Lister for providing me with a beautiful, peaceful place to rent during the midst of a global pandemic when I needed to finish my lab work. An incredibly heartfelt thank you goes to Ellen Cliff. I am so thankful that we started at Oxford at the same time and became such firm friends. Travelling with you to conferences was a highlight of my PhD, and one day we will travel together again, I am sure! Thank you for your true friendship, support, and fun.

Thank you to my entire family for always backing me. Thank you Mum and Dad for always believing in me and encouraging me to pursue my interests. There is no way I would have finished this PhD without your continued love and support. Thank you for letting me use your dining room as my thesis-writing room! Mum, you are an absolute trooper - your proofreading skills are unbelievably impressive, and you are officially one of the only people to ever read the entirety of my thesis. And to Ben, my fiancé, what can I say. I can't believe that I did the first two years of my PhD without you by my side! Thank you for proofreading, encouraging me, and thank you for listening to me talk about my research and showing so much interest in it. Thank you for being there for me, always. I can't wait to experience life post-thesis with you.

Abstract

It is apparent that in order to reach international climate goals, it will not be sufficient to simply reduce greenhouse gas emissions. There must also be a degree of removal of legacy emissions from our atmosphere to remain within 1.5-2 ^{o}C of warming relative to pre-industrial values. Several carbon removal schemes have been proposed which use the ocean as the site of removal, termed marine Carbon Dioxide Removal (mCDR). Meta-analysis of mCDR literature conducted as part of this thesis has revealed that there are six key "elimination" criteria that must be satisfied in order for any mCDR scheme to be viable. There are three main "elimination" criteria which are currently lacking from peer-reviewed mCDR publications: (i) completion of field trials, pilot studies and demonstration projects, (ii) assessment of governance/finance/social aspects of mCDR, and (iii) accurate quantification of CO_2 drawdown/CDR potential. The mCDR scheme of Ocean Alkalinity Enhancement (OAE), which involves raising surface ocean Total Alkalinity (TA) to shift the carbonate buffer system such that it absorbs more atmospheric CO_2, has great potential as an mCDR technique due to its co-benefits and relative advancement compared to other mCDR methods.

However, the growth and calcification response of major pelagic calcifiers to OAE (the coccolithophores and the foraminifera) are as yet unquantified. This thesis has constrained these responses for two key "endmember" species of coccolithophore (*E. huxleyi* and *C. braarudii*) and five key species of planktonic foraminifera (*G. ruber*, *G. siphonifera*, *G. bulloides*, *G. sacculifer* and *O. universa*) using *in-vitro* experiments. Growth and calcification response to OAE has been found to be species- and taxa-specific, similar to responses to ocean acidification studies. There is evidence that *G. siphonifera*, *G. ruber* and *O. universa* may have an optimum reproductive success at TA ~ 3000 µmol kg^{-1}, but calcification responses of planktonic foraminifera in enhanced TA did not change, although these were subject to high variability. *E. huxleyi* did not change its calcification per cell under simulated air-equilibrated OAE (CO_2-replete conditions), whereas *C. braarudii* decreased its calcification per cell. In simulated non-equilibrated OAE (CO_2-limited conditions), *E. huxleyi* increased its calcification per cell. Even if therefore the risk of calcification per cell increasing for major calcifiers is minimal, thereby providing no re-release of CO_2 to the atmosphere through a calcification feedback, the growth of *E. huxleyi* was fertilised by increased availability of HCO_3^- during both air-equilibrated and non-equilibrated OAE scenarios. Therefore, larger populations of this major bloom-forming coccolithophore could contribute to an overall increased amount of calcification and re-release of atmospheric CO_2. The lack of fertilisation of *C. braarudii* by increased supply of HCO_3^- reveals a fundamental difference between the

“opportunistic” carbon acquisition of *E. huxleyi* and the “static” carbon acquisition mechanism of *C. braarudii*. This has implications for understanding the physiology of the genii they come from, *Reticulofenestra* (*E. huxleyi*) and *Coccolithus* (*C. braarudii*). The elemental stoichiometry of *E. huxleyi* and *C. braarudii* was also constrained during experiments, and it was found that C:N of *E. huxleyi* may increase in non-equilibrated OAE scenarios. This would provide a positive feedback on carbon drawdown during OAE, and merits further investigation with the average C:N:P of pelagic organic matter during OAE.

Further work is needed with mesocosm and mesoscale field trials to constrain the overall growth, calcification, and elemental stoichiometry shifts of the pelagic ecosystem in response to OAE, in a timely manner, so that opportunities to use mCDR responsibly and equitably to reach international climate goals do not pass us by.

Table of contents

Declaration i

Acknowledgements ii

Abstract iv

List of figures x

List of tables xii

Chapter 1: Introduction……...……...1

1.1 The climate crisis and the need for Carbon Dioxide Removal…….1

1.2 Introduction to Ocean Alkalinity Enhancement as a Carbon Dioxide Removal Technique……8

1.2.1 Rationale and Principle……8

1.2.2 Extent of knowledge and potential feasibility and efficacy of techniques……..11

1.2.3 Potential scale of use……15

1.2.4 Appraisal of the potential impacts of the techniques on the marine environment (and the atmosphere where appropriate)……..16

1.2.5 Conclusions for enhancing ocean alkalinity……16

1.3 Risks and co-benefits of increased (Earth) Alkaline metal concentrations in the marine environment……...17

1.3.1 Perturbation……17

1.3.2 Current understanding……19

1.3.3 Important knowledge gaps and testable hypotheses……19

1.4 The marine biological response to Alkalinity Enhancement…….21

1.4.1 Calcification and the major calcifiers……21

1.4.2 Past work on the biological response to Alkalinity Enhancement……23

1.4.3 Analytical methods for quantifying calcification……..29

1.4.4 Biogeochemical and ecosystem impacts of Alkalinity Enhancement…….32

1.5 Thesis aims…….34

References…….35

Statements of authorship……43

Chapter 2: Meta-analysis of Ocean Carbon Dioxide Removal literature: major focus areas for research identified using elimination criteria……45

2.1 Introduction……..45

2.2 Methods……...48

2.3 Results……50

2.3.1 Broad-scale publication trends……50

2.3.2 Publication trends according to elimination criteria……...53

2.4 Discussion ……..59

2.4.1 The trajectory of OIF research can inform strategy for mCDR advancement……59

2.4.2 A rate-limiting step for advancement of mCDR: finance, governance and social aspects……..60

2.4.3 Field trials will be necessary to address elimination criteria……61

2.4.4 Supporting a strategic research agenda……61

2.5 Conclusions……62

References……63

Statement of authorship……...66

Chapter 3: The growth and calcification response of the coccolithophores *Emiliania huxleyi* and *Coccolithus braarudii* to the marine Carbon Dioxide Removal technique of Ocean Alkalinity Enhancement ……...67

3.1 Introduction……..67

3.2 Methods……...73

3.2.1 Simulation of air-equilibrated OAE……...73

3.2.2 CO_2-replete vs CO_2-limited cultures……76

3.2.3 Experimental protocol in CO_2-replete conditions……...80

3.2.4 Experimental protocol in CO_2-limited conditions……83

3.3 Results and Discussion……84

3.3.1 Growth and calcification response of coccolithophores……84

3.3.2 Implications for coccolithophore physiology……104

3.3.3 Implications for Ocean Alkalinity Enhancement……..107

3.4 Conclusions……..109

References……..109
Statement of authorship……118

Chapter 4: Changing Redfield ratio of the coccolithophores *Emiliania huxleyi* and *Coccolithus braarudii* in response to Ocean Alkalinity Enhancement: a potential positive feedback for CO_2 drawdown?…….....119
4.1 Introduction……119
4.2 Methods……121
4.2.1 Batch culturing……..121
4.2.2 C:N:P sampling and analysis……..121
4.3 Results……...126
4.4 Discussion……131
4.4.1 Biological mechanisms for shifts in elemental composition…...131
4.4.2 Implications of changing C:N:P for OAE……...133
4.5 Conclusions……..135
References……..135
Statement of authorship……139

Chapter 5: The response of planktonic foraminifera to enhanced ocean alkalinity - a conceptual study for marine Carbon Dioxide Removal……140
5.1 Introduction……140
5.2 Methods……143
5.2.1 Experimental framework……..143
5.2.2 Culturing……145
5.2.3 Handling of calcification data……..147
5.2.4 Compilation of prior data……148
5.3 Results……...151
5.3.1 Gametogenesis rate……151
5.3.2 Lifespan in culture……154
5.3.3 Calcification……157
5.4 Discussion……159
5.5 Conclusions……..161
References……..162
Statement of authorship……165

Chapter 6: Discussion and conclusions……166
6.1 Summary of research chapters……..166
6.2 Wider implications of thesis findings……169
6.3 Future work on mCDR and the response of biota……..172
6.4 Conclusions……..176
References…….....177

Appendix 1: Supplementary material for Chapter 2……180
Appendix 2: Supplementary material for Chapter 3……182
A2.1 Calculation for CO2 drawdown per unit addition of Total Alkalinity to the surface ocean……..182
A2.2 Malformation statistics……..183
Appendix 3: Supplementary material for Chapter 5……185
A3.1 Normalisation of time to gametogenesis using individual foraminifera growth rates……185
A3.2 Morphometric analyses of planktonic foraminifera……..187
A3.2.1 Methods……...187
A3.2.2 Discussion……...195
A3.3 Statistical testing of compiled literature and culture logs……196
References……..198
Appendix 4: The response of *Coccolithus braarudii* strain RCC1198 to OAE using $NaHCO_3$ under CO_2-limited conditions……199

List of figures

1.1 Projected climate scenarios……2
1.2 The geological carbon cycle and fluxes……3
1.3 Bjerrum plot……...5
1.4 Definitions of Total Alkalinity……...6
1.5 Enhancing Ocean Alkalinity……8
1.6 Effects of Enhanced Weathering……10
1.7 Changes in carbonate chemistry from Enhancing Alkalinity……...22
1.8 Dose-response curves of microalgae to elevated DIC……24
1.9 PIC:POC response of *E. huxleyi* to Total Alkalinity……..27
1.10 The "white or green ocean hypothesis"……..……..33

Box 2.1 Definitions of mCDR approaches……46

2.1 Publication times series of mCDR……...51
2.2 mCDR approach publications by year……51
2.3 Empirical, discussion and modelling publications……52
2.4 mCDR publications as a function of mCDR approach……53
2.5 Publications reporting CDR potential……..55
2.6 Counts as a function of keyword……..56
2.7 Environmental studies of mCDR……..57
2.8 mCDR governance as a function of governance level……58
2.9 Social aspects of mCDR publication……...59

3.1 Carbonate chemistry perturbation through EW/OAE……68
3.2 Equilibration tests.....75
3.3 [CO_2] in pre-inoculation culture media……75
3.4 Pre-inoculation carbonate chemistry of culture media……77
3.5 Shifts in carbonate chemistry during culturing……...78
3.6 *E. huxleyi* specific growth rate response……85
3.7 *E. huxleyi* specific growth rate – HCO_3^- fertilisation……86
3.8 *E. huxleyi* cellular calcification response……88

3.9 *E. huxleyi* cellular calcification rate response……89
3.10 *E. huxleyi* cellular calcite quota response……90
3.11 *E. huxleyi* cellular calcification rate in the CO_2-limited system……92
3.12 *E. huxleyi* cellular calcite quota in the CO_2-limited system……93
3.13 *E. huxleyi* PIC:POC in the CO_2-limited system……94
3.14 *E. huxleyi* PIC:POC in both CO_2-limited and -replete systems……95
3.15 *E. huxleyi* relative coccosphere size……96
3.16 *E. huxleyi* SEM images……97
3.17 *C. braarudii* specific growth rate response……98
3.18 *C. braarudii* cellular calcification rate response……99
3.19 *C. braarudii* cellular calcite quota response……100
3.20 *C. braarudii* PIC:POC response……102
3.21 *C. braarudii* relative coccosphere size……102
3.22 *C. braarudii* SEM images……103

4.1 POC feedback during OAE……120
4.2 Nitrate assay standard curve……123
4.3 Analytical measurement comparison: PON……123
4.4 Phosphate assay standard curve……124
4.5 Elemental ratios in *E. huxleyi* as a function of Total Alkalinity……127
4.6 Elemental ratios in *E. huxleyi* as a function of specific growth rate……128
4.7 Elemental ratios in *C. braarudii* as a function of Total Alkalinity……129
4.8 Elemental ratios in *C. braarudii* as a function of specific growth rate……130

5.1 Size-mass relationships……148
5.2 Relationship between TA and CO_3^{2-} in culturing media……150
5.3 Gametogenic success rate (Eilat, 2019)……152
5.4 Gametogenic success rate of *O. universa* (Catalina, 2014)……153
5.5 Lifespan in culture (Eilat, 2019)……154
5.6 Lifespan in culture (compiled culture log data)……156
5.7 Calcification (Eilat, 2019)……157
5.8 Calcification (compiled culture log data)……158

6.1 UVic ESCM model……175

A3.1 Normalisation of time to gametogenesis……186
A3.2a-e SEM and light microscope images of planktonic foraminifera……..188
A3.3 Foraminifera aspect ratio……194
A3.4 Foraminifera perforation……...194
A4.1 *C. braarudii* in CO_2-limited conditions – physiological response……...201
A4.2 *C. braarudii* in CO_2-limited conditions – SEM images…….202

List of tables

1.1 Table 1 from Bach et al. (2019)……18

2.1 Summary of meta-data collected…….49
2.2 mCDR elimination criteria…….54

3.1 Carbonate chemistry at cell harvest……79

5.1 Summary of carbonate chemistry in alkalinity treatments…….144
5.2 Mortality and gametogenesis rates……...147
5.3 ROUT analysis……148
5.4 Mortality and gametogenesis excluding unicellular ciliate effect……....149

A2.1 SEM images of representative liths……183
A2.2 *C. braarudii* lith statistics……..183
A2.3 *E. huxleyi* lith statistics……..184
A3.1 Proportion of individuals viewed under SEM……187
A3.2 Statistical testing of compiled culture logs…….196
A4.1 Carbonate chemistry of culture media for *C. braarudii* – CO_2-limited……..200
A4.2 C:N:P of *C. braarudii* – CO_2-limited……203

Chapter 1: Introduction

1.1 The climate crisis and the need for Carbon Dioxide Removal

The world is facing an unprecedented global challenge: tackling the climate crisis. Extreme weather events and natural disasters, such as droughts, floods, hurricanes, severe storms, heatwaves, wildfires, cold spells and landslides (UNCCS, 2019) are made more likely by the climate crisis (IPCC, 2021; IPCC, 2018: Summary for Policymakers). In 2018 alone, 315 cases of these hazards occurred, driven by the climate crisis, affecting 68.5 million people at an estimated economic cost of $131.7 billion (Fawzy et al., 2020). Climate solutions are imperative to avoid these catastrophic climate hazards to save the natural world and achieve an equitable and just society. The stabilisation of the global climate is a precondition for at least partially achieving the Sustainable Development Goals (SDGs) (Honegger et al., 2020).

It is well-established both in academia and policy that slowing global temperature increases relative to pre-industrial levels will contribute to decreasing the frequency and magnitude of the occurrence of these climate-driven hazards (IPCC, 2021; IPCC, 2018: Summary for Policymakers; GESAMP, 2019; Renforth and Henderson, 2017; National Academies of Sciences, Engineering, and Medicine, 2021). The first legally binding international climate agreement was the 2015 Paris Agreement at COP21, the aim of which was to keep global warming well below 2 °C and pursue efforts to limit it to 1.5 °C. The climate impacts at 2 °C compared to 1.5 °C are significantly more severe (IPCC, 2018: Summary for Policymakers). For example, at 1.5 °C, IPCC (2018) projections show that during summer, the Arctic Ocean will be ice-free 1 year out of every 100 years, whereas at 2 °C, the Arctic Ocean will be ice-free 1 year out of every 10 years. Coral reef habitat areas are projected to decline by 70-90% at 1.5 °C, and 99% at 2 °C (IPCC, 2018). Climate projections also show that to reach either the 1.5 °C or 2 °C targets, we will not only have to reduce our emissions but will have to remove historical CO_2 emissions from our atmosphere.

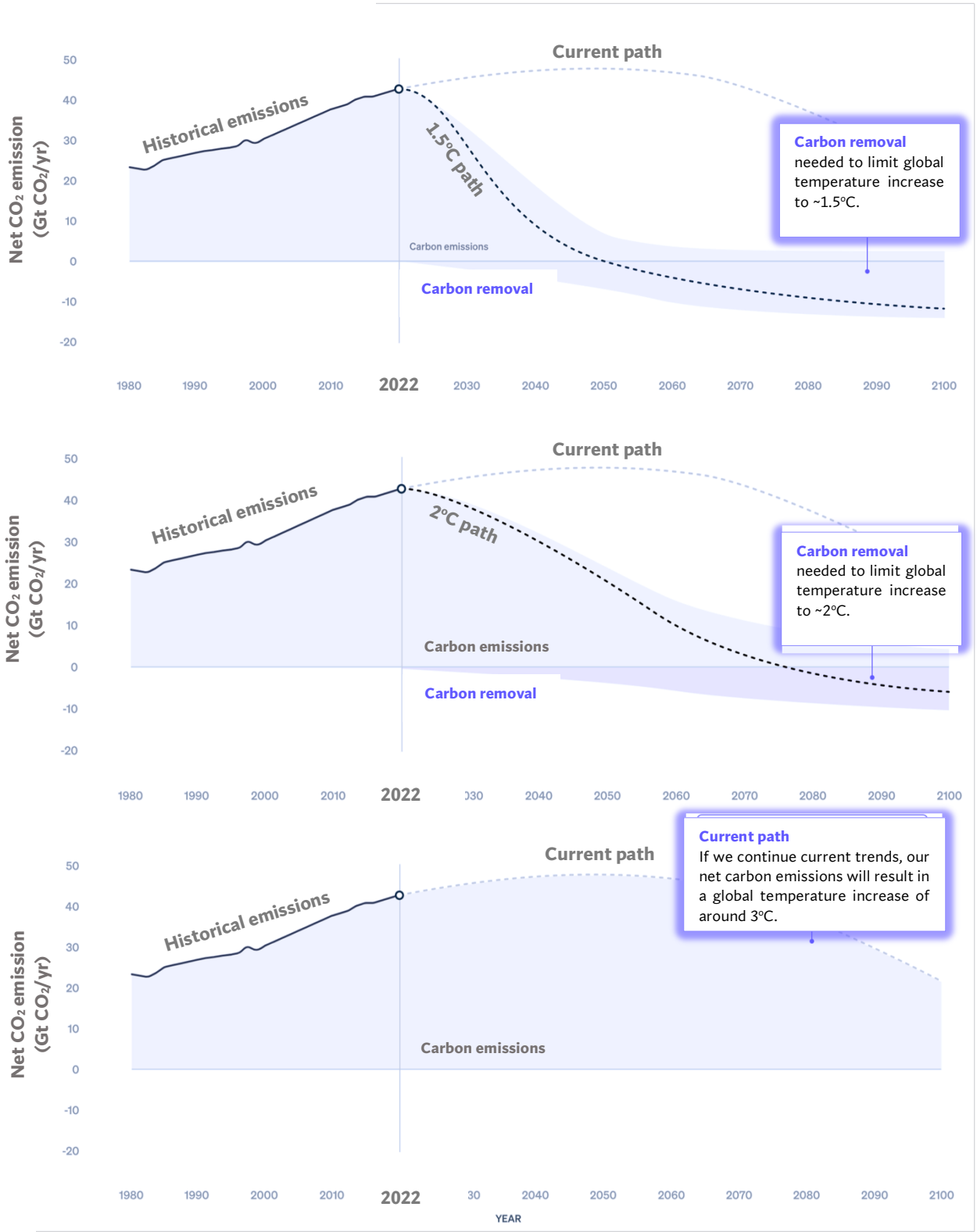

Figure 1.1: Comparison between emissions pathways for 1.5 °C, 2 °C, and 3.0 °C (or "business-as-usual") in projected climate scenarios 1980-2100. Historical emissions are projected using data from Global Carbon Project, Houghton & Nassikas (2017), and Hansis et al. (2015). "Current path" projected using SSP4-6.0 from the SSP public database (Version 2.0) and Hausfather & Peters (2020). Carbon removal pathways are projected using data from CICERO (Peters, 2018). Adapted using original figures from Stripe (2021).

For example, **Figure 1.1** (Stripe, 2021) illustrates that carbon removal is necessary to achieve climate pathways limiting global warming to 1.5 °C or 2 °C. To limit the global average temperature increase to 1.5 °C above pre-industrial levels, global emissions need to be net-zero by 2050. Fuss et al. (2014) estimated that the scenario for limiting global temperatures to between 0.9-2.3 °C above pre-industrial temperatures would require 40-220 Gt C removal from the atmosphere. Recent estimates of how much carbon dioxide removal (CDR) would be necessary to limit global warming to 1.5 °C project the use of CDR on the order of 100–1000 Gt CO_2 over the 21st century (IPCC, 2018: Summary for Policymakers).

The challenge is enormous, and there have been many different CDR schemes proposed to remove historical CO_2 emissions from our atmosphere. These range from terrestrial CDR schemes (e.g. enhanced weathering with croplands, reforestation, direct air capture) to marine CDR (mCDR) schemes, in which the ocean is the site of CO_2 removal. Due to the urgent nature of the climate crisis, there is a real need to establish a strategic research framework for mCDR (National Academies of Sciences, Engineering, and Medicine, 2021; Burns and Corbett, 2020; Lezaun, 2021; GESAMP, 2019).

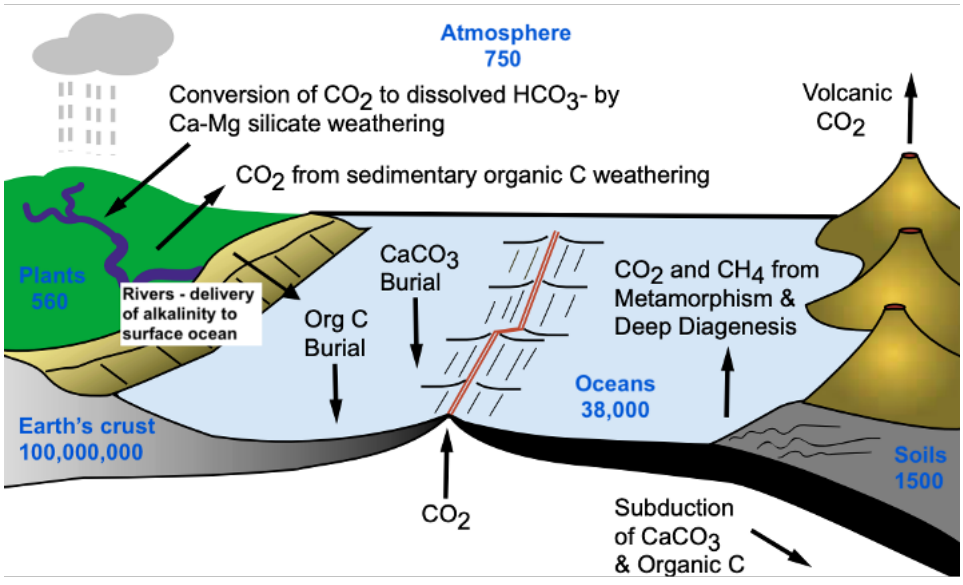

Figure 1.2: The geological carbon cycle budgets and fluxes. Carbon reservoirs shown in blue, with quantities accompanying shown in petagrams (Pg). Fluxes indicated by black arrows with accompanying labels. Diagram adapted from Berner (1999). The ocean's carbon store consists of four key reservoirs. In descending order of magnitude, these are: (1) the DIC pool (~38,000 Pg C), (2) the DOC pool (662 Pg C), (3) the POC pool (2.3 Pg C, the most dynamic C pool in the ocean with the highest turnover rate), and finally (4) the PIC pool (~0.03 Pg C) (Brewin et al., 2021).

The inspiration for many of these mCDR schemes stems from the precedent set by the role of the ocean in responding to environmental perturbations over geological timescales. The majority of carbon on Earth is stored in the lithosphere (**Figure 1.2**). The ocean stores ~50 times more carbon than the atmosphere (Berner, 1999; Renforth and Henderson, 2017), shown in **Figure 1.2**.

Raising ocean alkalinity, as a result of enhanced weathering, is one of the major long-term feedbacks on atmospheric CO_2 levels over geological timescales (Berner, 1999). In the oceans, there is an excess of conservative cations compared to conservative anions, as shown in **Figure 1.4**, where conservative means that their concentration can be assumed to be constant globally throughout the surface ocean (Zeebe and Wolf-Gladrow, 2001). This can be described chemically by the explicit conservative expression for alkalinity (Wolf-Gladrow et al., 2007), also shown in **Figure 1.4**. The sum difference between conservative cations and conservative anions is equivalent to the carbonate system components that can change their speciation in response to perturbations to ocean chemistry, i.e. the non-conservative expression for alkalinity (see **Figure 1.4**).

External perturbations of pH and alkalinity shift the carbonate system between its three major DIC components: CO_2(aq), HCO_3^-, and CO_3^{2-} (Heinze et al., 2015), related by the equilibria shown in **Equation 1.1**, where K_1 and K_2 are the first and second dissociation constants of carbonic acid. These dissociation constants are related to the concentrations of the various components of the dissolved inorganic carbonate system as follows (**Equation 1.2** and **1.3**), and dependent on temperature (T), salinity (S) and pressure (P).

$$CO_2\,(aq) + H_2O \Leftrightarrow H_2CO_3 \overset{K_1}{\Leftrightarrow} HCO_3^- + H^+ \overset{K_2}{\Leftrightarrow} CO_3^{2-} + 2H^+ \quad \textbf{(1.1)}$$

$$K_1 = \frac{[HCO_3^-][H^+]}{[CO_2]} \quad \textbf{(1.2)}$$

$$K_2 = \frac{[CO_3^{2-}][H^+]}{[HCO_3^-]} \quad \textbf{(1.3)}$$

Alkalinity can be increased by adding conservative cations to the surface ocean, for example through enhanced weathering processes on land (**Figure 1.2**). For example, the process of carbonate dissolution raises ocean alkalinity by 2 moles and ocean DIC by 1 mole per mole of carbonate dissolution (Zeebe and Wolf-Gladrow, 2001). **Equation 1.4** describes the equilibrium between calcium carbonate and its soluble constituent ions; the forward reaction denotes carbonate dissolution, and the backward reaction denotes carbonate precipitation. The solubility product (K_{sp}) of calcium carbonate is also shown.

$$CaCO_3(s) \overset{K_{sp}}{\Longleftrightarrow} Ca^{2+}(aq) + CO_3^{2-}(aq) \qquad K_{sp} = [Ca^{2+}][CO_3^{2-}] \tag{1.4}$$

Raising ocean alkalinity increases the difference between conservative cations and anions in the surface ocean, causing the carbonate buffer system to shift its speciation towards the more negatively charged end of the spectrum to make up for the extra charge imbalance; this means increased levels of HCO_3^- and CO_3^{2-}, and decreased CO_2(aq), as shown in **Figure 1.3**. Due to Henry's law, shown in **Equation 1.5**, decreased CO_2(aq) promotes dissolution of atmospheric CO_2 in the surface ocean, therefore drawing down atmospheric CO_2 (Murray, 2004). K_0 is the solubility coefficient of CO_2 in seawater.

$$CO_2(g) \overset{K_0}{\leftrightarrow} [CO_2](aq) \tag{1.5}$$

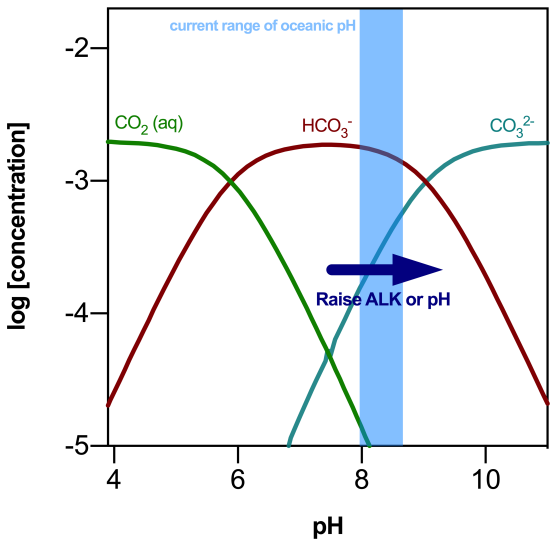

Figure 1.3: A plot showing the proportional contribution of the different inorganic carbon species to the carbonate buffer system in response to perturbations of pH and/or alkalinity, modified from Heinze et al. (2015).

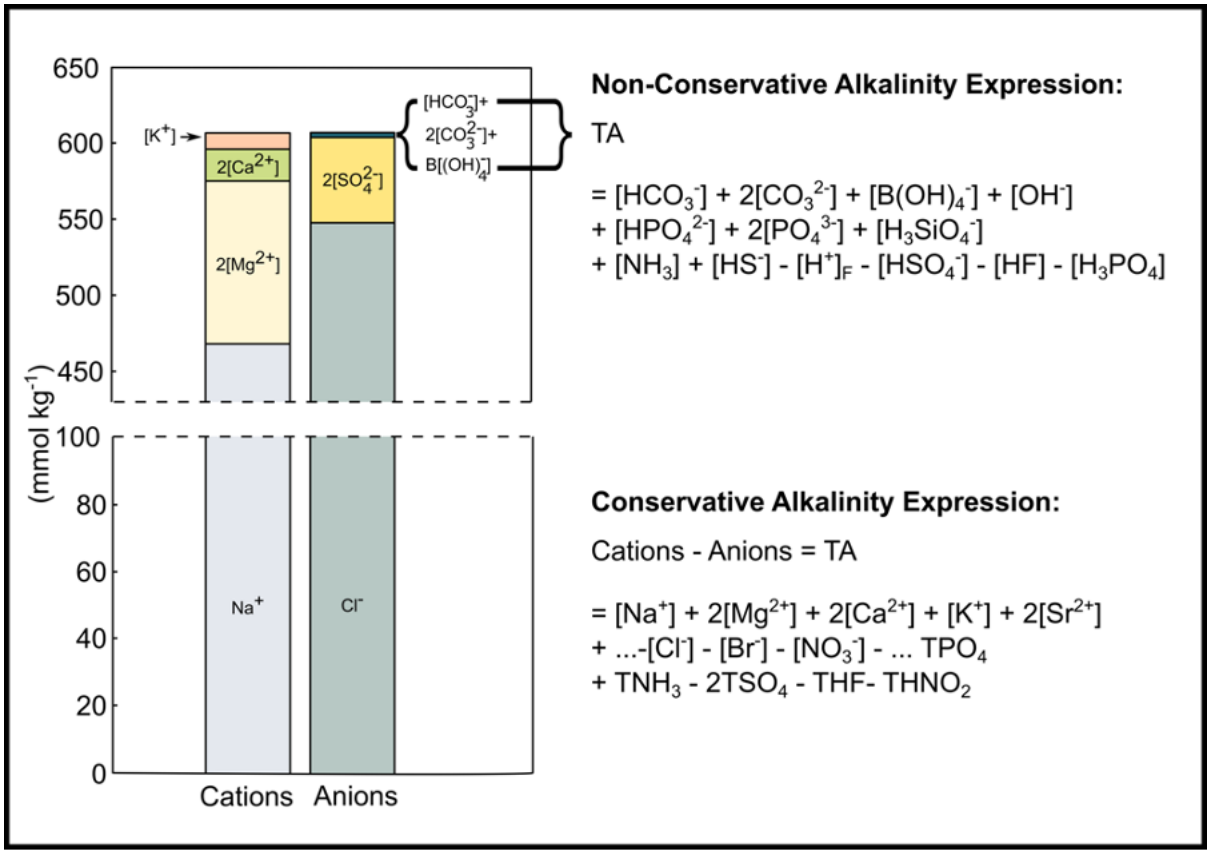

Figure 1.4: Bar chart quantifying the relationship between non-conservative and conservative definitions of alkalinity, in the context of the major ion charge balance in the modern ocean. Equations link the conservative and non-conservative definitions of alkalinity. Figure modified from Zeebe and Wolf-Gladrow (2001). Equations from Wolf-Gladrow et al. (2007).

This process of accelerated weathering in response to the warming from greater CO_2 emissions acts as a negative feedback on carbon emissions within the geological carbon cycle, and prevents "runaway" greenhouse climate effects. This is in conjunction with the longer-term process of carbonate compensation and subsequent $CaCO_3$ burial (Berner, 1999; Boudreau et al., 2018). The annual drawdown of CO_2 through natural weathering is currently ~4 Gt CO_2 per year (~1.1 Gt C per year) (Ciais et al., 2013), with annual anthropogenic CO_2 emissions dwarfing this, at ~36 billion tonnes annually (Beerling, 2019). If it is possible to accelerate or stimulate this natural weathering process to add extra alkalinity to our oceans, in theory, this could operate as an mCDR scheme. If alkalinity were to be applied uniformly to the global ocean, an increase in surface ocean alkalinity of 10% would be sufficient to adsorb 50% of fossil fuel CO_2 emissions on a 5-year timescale (Henderson et al., 2008). This idea of artificial ocean alkalinization, commonly referred to as Alkalinity Enhancement, has been

estimated to have major potential as an mCDR technique in the National Academies of Sciences, Engineering, and Medicine (2021) Research Strategy for Ocean-based Carbon Dioxide Removal and Sequestration, and could remove between 265 - 790 Gt C by 2099 (Feng et al., 2017).

Alkalinity addition would also contribute to the reversal of ocean acidification, which would have positive co-benefits for many marine organisms at risk due to rising acidity (Bach et al., 2019; Doney et al., 2009; Albright et al., 2016; Silverman et al., 2007). This is due to the fact that alkalinity enhancement raises ocean pH and $\Omega CaCO_3$ to higher values (Ilyina et al., 2013).

Addition of sufficient Ca^{2+} to fully compensate emissions of ~10 Gt C/year would require the addition of ~20 Gt Ca^{2+}/year to the surface ocean. Therefore, due to the large logistical challenges of sourcing materials containing high concentrations of conservative cations, such as mine tailings (Renforth, 2019), it is likely that alkalinity enhancement will be one of a suite of ocean-based CDR schemes used to mitigate climate change. It is also unlikely that alkalinity would be applied uniformly to the global surface ocean for this reason (Renforth and Henderson, 2017), and instead would be applied at higher concentrations in localised "hotspots" of point-source addition. 3500-4000 μmol kg^{-1} is the range of Total Alkalinity expected at point-source, and 3000 μmol kg^{-1} is the level expected once ocean circulation has evened out alkalinity addition over a larger area of the ocean, for example, an ocean basin (GESAMP, 2019; Renforth and Henderson, 2017). These values are much higher than the natural range of ocean Total Alkalinity, with an average surface value of 2300 μmol kg^{-1}, increasing to an average of 2500 μmol kg^{-1} in the deep ocean (Sarmiento and Gruber, 2006).

1.2 Introduction to Ocean Alkalinity Enhancement as a Carbon Dioxide Removal Technique

Sophie J. Gill & Rosalind E. M. Rickaby

Published as "Enhancing Ocean Alkalinity" Section 5.13, GESAMP (2019). "High level review of a wide range of proposed marine geoengineering techniques". (Boyd, P.W. and Vivian, C.M.G., eds.). (IMO/FAO/UNESCO-IOC/UNIDO/WMO/IAEA/UN/UN Environment/UNDP/ISA Joint Group of Experts on the Scientific Aspects of Marine Environmental Protection). Rep. Stud. GESAMP No. 98, 144 p.

Permission has been granted by Andrew Birchenough at the IMO for this Section 5.13 to be reproduced in this thesis. GESAMP is an advisory body consisting of specialized experts nominated by the Sponsoring Agencies (IMO, FAO, UNESCO-IOC, UNIDO, WMO, IAEA, UN, UN Environment, UNDP). Its principal task is to provide scientific advice concerning the prevention, reduction and control of the degradation of the marine environment to the Sponsoring Agencies. The report contains views expressed or endorsed by members of GESAMP who act in their individual capacities; their views may not necessarily correspond with those of the Sponsoring Agencies.

1.2.1 Rationale and principle

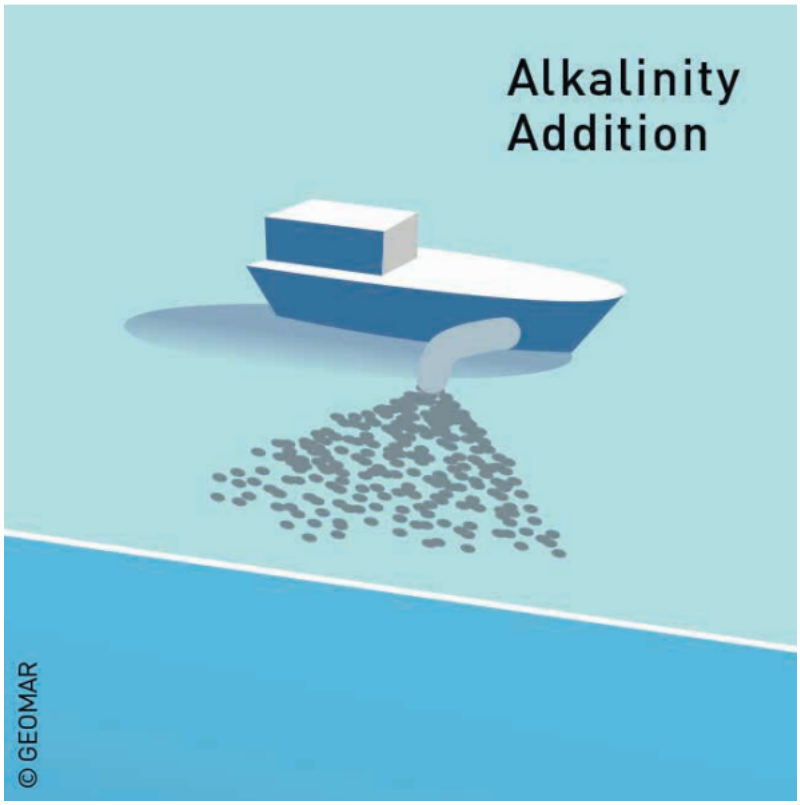

Figure 1.5: Enhancing Ocean Alkalinity.

Alkalinity is the capacity of a solution to neutralize acid. Seawater alkalinity is predominantly composed of bicarbonate (HCO_3^-), carbonate (CO_3^{2-}) and to a much smaller extent hydroxide (OH^-) anions that are charge balanced by cations other than H^+. The preceding chemical bases then constitute nearly all of seawater's alkalinity.

CO_2 dissolved in water readily forms carbonic acid, H_2CO_3, which in the case of the ocean is ≥99% dissociated and transformed to more stable forms via reactions and equilibria with the preceding seawater carbonate and hydroxide bases. It therefore follows that adding additional chemical base (alkalinity) to seawater can be useful in helping: (i) decrease surface water partial pressure of CO_2 (pCO_2) thereby increasing CO_2 uptake by the ocean, (ii) counter seawater acidity such as that generated by excess CO_2, and/or (iii) provide a vast and relatively stable storage medium for anthropogenic CO_2 in the form of mineral bicarbonate and carbonate ions (alkalinity) in seawater. Note that these 3 benefits are not independent but are interlinked and concurrent.

Enhanced ocean alkalinity also raises the carbonate saturation state of the oceans, which can help reverse the effects of ocean acidification, in particular countering its effects on calcifying organisms (e.g. corals and shellfish) that are central to marine biodiversity (e.g. (Albright et al., 2016; Marubini and Thake, 1999; Renforth and Henderson, 2017).

A source of inspiration for marine geoengineering through enhanced ocean alkalinity comes from the natural weathering process, in which globally abundant silicate (**Equation 1.6**) and carbonate minerals (**Equation 1.7**) naturally react with atmospheric CO_2 and water to consume and store excess CO_2 as stable, dissolved or solid alkaline compounds (Berner, 2004).

$$CaSiO_3 + 2CO_2 + 3H_2O\ Ca^{2+} + 2HCO_3^- + H_4SiO_4 \rightarrow 3H_2O + CO_2 + CaCO_3 + SiO_2 \quad \textbf{(1.6)}$$

$$CaCO_3 + H_2O + CO_2 \rightarrow Ca^{2+} + 2HCO_3^- \rightarrow H_2O + CO_2 + CaCO_3 \quad \textbf{(1.7)}$$

This can be compared with reactions involving synthetic bases/alkalinity e.g.:

$$Ca(OH)_2 + 2CO_2 \rightarrow Ca^{2+} + 2HCO_3^- \rightarrow H_2O + CO_2 + CaCO_3 \quad \textbf{(1.8)}$$

In each case, the first step of the reaction (first arrow) indicates dissolution and reaction with CO_2. Note that some CO_3^{2-} is also formed via equilibrium reactions. The second step of the reaction (second arrow) indicates carbonate precipitation. If, after dissolution, the aqueous constituents remain in or are delivered to the ocean, ocean C storage and alkalinity is increased. However, if carbonate precipitation occurs, CO_2 is rereleased such that approximately half the CO_2 initially consumed and stored via silicate weathering is lost (**Equation 1.6**) and all the CO_2 captured and the alkalinity generated by carbonate weathering is lost (**Equation 1.7**).

The idea of emulating the natural weathering process to drawdown atmospheric CO_2 was first proposed by Seifritz (1990), and first studied in detail by Lackner et al. (1995). They suggested that ultramafic igneous rocks could be reacted with atmospheric CO_2 to produce calcium and/or magnesium carbonates, supported by the results of preliminary experimental work. Because more than 90% of the Earth's crust is composed of alkaline minerals and mineral weathering is the primary way excess CO_2 is consumed on geologic time scales (Archer et

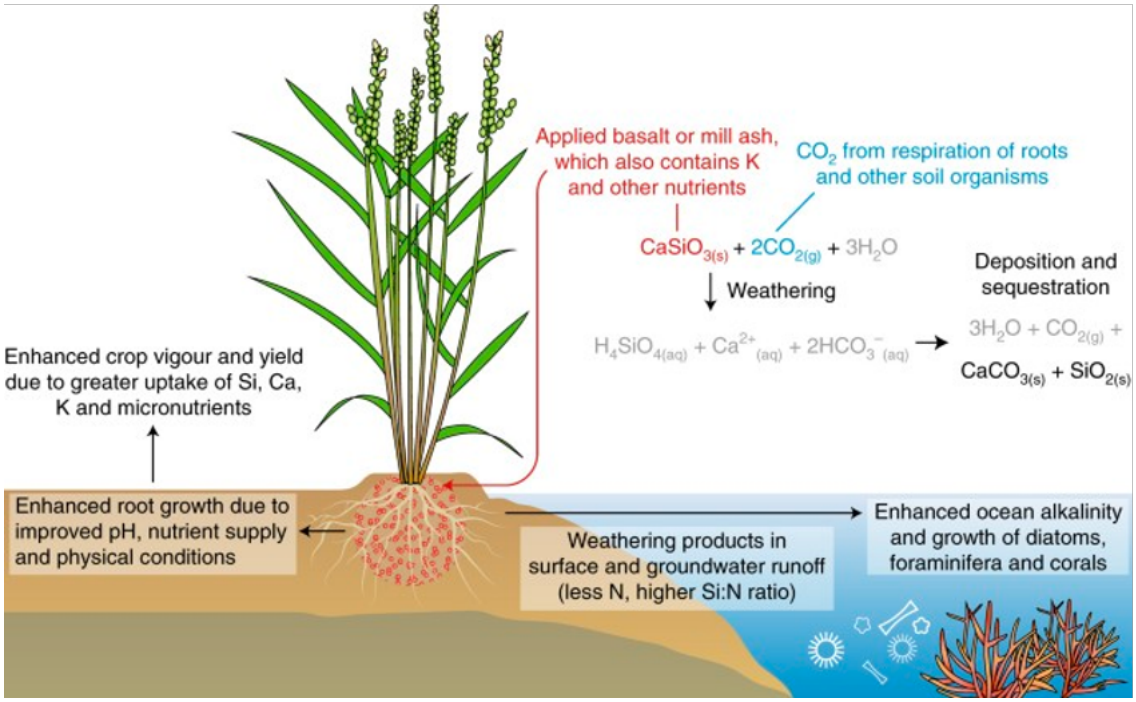

Figure 1.6: Summary of the potential effects of weathering of crushed basalt or silicate-rich wastes, such as sugarcane mill ash, applied to croplands. As silicate rocks weather, they release nutrients that can improve soil conditions and support crop production, and also generate alkaline leachate, ultimately leading to export of dissolved inorganic carbon forms to the oceans. Reprinted by permission from Nature, © 2018, D Beerling et al. (2018) 'Farming with crops and rocks to address global climate, food and soil security', Nature Plants, 4, 138-147.

al., 2009), the capacity of such processes to contribute to excess global CO_2 mitigation is thought to have no known physical limit (IPCC, 2013). Determining cost-effective and safe ways of accelerating such weathering and alkalinity generation could therefore play a major role in reducing CO_2 and ocean acidity on human time scales.

1.2.2 Extent of knowledge and potential feasibility and efficacy of techniques

Adding lime directly to the ocean

This is also known as "ocean liming" and is achieved by the calcination of limestone to produce lime (calcium oxide - CaO) or portlandite (calcium hydroxide - $Ca(OH)_2$) to bypass the slow dissolution rate of natural carbonate minerals (Henderson et al., 2008; Kheshgi, 1995; Renforth and Henderson, 2017). Lime readily dissolves in the ocean and consumes ocean and air CO_2 (see **Equation 1.8** above). The chemistry of this is well understood, but a major negative is the large energy and carbon footprint of conventional calcination. Nevertheless, alternative methods of generating hydroxide using non-fossil energy could avoid this problem (e.g. "Electrochemical enhancement…" below).

Adding carbonate minerals to the ocean

While the surface ocean is supersaturated with respect to $CaCO_3$ and therefore any added $CaCO_3$(s) will not dissolve to form alkalinity, such carbonate can dissolve in undersaturated subsurface waters (Harvey, 2008). By choosing locations where undersaturated water is present at shallow depths and where vertical advection of such water is relatively rapid (100's of years) the addition of $CaCO_3$(s) here can eventually affect surface ocean alkalinity addition and CO_2 sequestration, though on timescales likely irrelevant to mitigating more urgent excess CO_2 and surface ocean acidification problems.

Accelerated weathering of limestone (AWL)

Dissolution of carbonate minerals (e.g. $CaCO_3$(s)) can be achieved by reacting them with waste flue gas CO_2 and seawater (Caldeira and Rau, 2000; Chou et al., 2015; Langer et al., 2009; Rau, 2011; Rau and Caldeira, 1999; Rau et al., 2007). This raises seawater pCO_2 to

>0.51 kPa and lowers pH and $CaCO_3$(aq) saturation state such that when contacted with solid calcium carbonate, reaction with CO_2 spontaneously occurs (**Equation 1.7** step 1). The resulting alkalinity is discharged to the ocean. The technique does require that thousands of tonnes of seawater be used per tonne of CO_2 sequestered. The downstream use of pumped seawater that is commonly employed as cooling water in coastal power stations could be used for this. In the context of stable C storage, environmental impacts of AWL would seem favoured over direct injection of CO_2 into the ocean, though further research on environmental desirability, cost effectiveness and global capacity is needed.

Electrochemical enhancement of carbonate and silicate mineral weathering

During the course of the electrolysis of saline solutions (such as seawater) to produce hydrogen (H_2), acids that are produced in these processes can be neutralized with carbonate or silicate minerals, which leaves un-neutralized OH^- that is co-produced in electrolysis, balanced by cations such as Mg^{2+}, Ca^{2+} or Na^+. As in the case of ocean liming, these dissolved mineral hydroxides are highly reactive with CO_2 and when exposed to air remove atmospheric CO_2, forming stable, bicarbonate-rich solutions (**Equation 1.8**; (House et al., 2007; Lu et al., 2015; Rau, 2008; Rau et al., 2013). The air contacting and bicarbonate formation can occur away from the ocean or can occur after the hydroxide is added to the ocean, in the latter case increasing air → ocean CO_2 flux. In either case, the surface ocean is the recipient of the resulting (bi)carbonate alkalinity and is the medium for the ensuing carbon storage. To affect maximum CO_2-emissions negativity such systems must be powered by non-fossil electricity, yet at least some of this energy can be recovered from the H_2 produced (e.g. via the use of fuel cells). Limited experimental work has been conducted on this process. An evaluation of global capacity of such methods suggests that 100's of Gt CO_2 removal and 1000's of EJ of energy generation per year might be technically possible (Rau et al., 2018).

Brine thermal decomposition (BTD) of desalination reject brine

Desalination reject brine contains magnesium salts including magnesium chloride ($MgCl_2$), thermal decomposition of which produces magnesium oxide (MgO). MgO added to the ocean would draw down CO_2 through conversion to bicarbonate (Davies, 2018). This is similar in theory to the schemes proposed by Kheshgi (1995), essentially a variant on the ocean liming process (see above). $MgCl_2$ decomposition was shown to be achievable at temperatures <600^oC, well within the capabilities of solar energy receivers. This process has advantages over ocean liming because reject brine is potentially a logistically better raw feedstock than limestone. The total electrical requirements of the desalination plant increase by ~50% due to the dewatering of reject brine by nanofiltration, but this is offset by absorptive capacity of MgO produced through BTD.

Open ocean dissolution of olivine

Olivine or other silicate mineral particles can be added to the surface ocean (Köhler et al., 2013; Köhler et al., 2010) to affect CO_2 removal, analogous to **Equation 1.6**. However, because of very low dissolution rates per unit surface area, silicate minerals need to be ground to ≤1μm to dissolve on relevant time scales (elevated ambient ocean pH slows dissolution rates). The energy and CO_2 footprint of crushing such volumes of olivine required may be significant with additional contributions from mineral extraction and transport. For example, Hangx and Spiers (2009) estimated that a total of >60 kWh of energy would be consumed and >30 kg CO_2 emitted when finely ground olivine was used to consume 1 tonne of CO_2.

Soluble silicon (Si) derived from silicate minerals could increase diatom growth (biogeochemical models exist simulating this), and there could be additional Fe fertilization effects for silicates containing iron. (see also “Appraisal of the potential impacts…” below.) The proposed diameter of 1 μm olivine particles (1011 m^{-3}) is similar to that of the most abundant phytoplankton in the ocean, *Prochlorococcus*. Potential influences of these alien particles on food-web interactions (grazing) were not considered and are unknown. The

biochemical effects and fate of other metal impurities released from silicate minerals are also concerns and require further study.

Coastal spreading of olivine

An alternative to open ocean addition of olivine is its amendment within coastal and shelf environments where wave action and biological activity can accelerate dissolution (Montserrat et al., 2017; Schuiling and de Boer, 2011). Such methods could be incorporated into existing coastal management projects e.g. dredging operations, land reclamation, beach nourishment. Small-scale experiments have effectiveness; however, they also indicate problems such as nonstoichiometric dissolution, potential pore water saturation in the seabed, and the potential occurrence of secondary reactions which may limit the CO_2 sequestration potential.

Enhanced weathering of mine waste

Silicate and carbonate mine waste (already crushed into small particles) could be treated with microbes or spread over agricultural land to accelerate the natural weathering process, and via downstream transport ultimately add to the surface ocean (Renforth and Henderson, 2017). Use of fine particulate mine waste avoids the extra energy and cost of mineral crushing/grinding. To involve the use of the ocean, waste mineral dissolution needs to be done near the site of surface ocean addition to prevent in situ precipitation of minerals re-releasing CO_2. Mine waste is currently not well-characterised, and could contain major/trace elements, e.g. metals which would affect ocean biogeochemistry.

Amending cropland soils with crushed reactive silicates

Soil pore waters are naturally corrosive, allowing in situ acceleration of dissolution kinetics and CO_2 removal (Beerling et al., 2018; Hartmann et al., 2013; Manning, 2008; Renforth et al., 2013; Taylor et al., 2017). Products of dissolution (including increased alkalinity of rainwater) are transported to the ocean via runoff, rivers and groundwater. Slow dissolution rates at ambient temperature and pressure, combined with solubility limits of naturally occurring minerals, hamper this process. Soil pore water aqueous chemistry could enhance

precipitation of carbonate minerals, which has been widely observed in anthropogenic soils. Adding crushed reactive silicates however accelerates the natural chemical breakdown of soils which enhances CO_2 drawdown and the aqueous products are then transported to the oceans, raising alkalinity. This has the advantage that the reactions taking place can facilitate further fertilization of crops, both lowering the need for pesticides and potentially delivering better food security. Single column reactor experiments and several large-scale trials are taking place in the USA, Australia and Malaysian Borneo.

1.2.3 Potential scale of use

As explained under 'Rationale and principle', precipitation of carbonate minerals decreases the efficacy of all these techniques. Modern day surface oceans are supersaturated in calcite by ~4 times, because other ions present in seawater inhibit inorganic precipitation (Renforth and Henderson, 2017). The concentration of these ions is such that abiotic precipitation from seawater will not occur until about 20-fold saturation is achieved, meaning seawater's ability to accommodate additional carbon storage in the form of bicarbonate and carbonate alkalinity is quite significant. Nevertheless, care would be needed to stay below such limits, especially during the initial addition of alkalinity prior to subsequent ocean mixing and dilution. It is likely that the first applications of alkalinity addition would be local and coastal because this would be logistically much simpler to achieve, and because of the desire to alleviate the stress on coastal resources affected by ocean acidification e.g. shellfish/corals (Albright et al., 2016). Local addition of alkalinity could pass the inorganic precipitation threshold if addition occurs faster than the mineral dilution rate (Henderson et al., 2008), which merits further research via laboratory saturation experiments and calculations. In any case, the duration of deployment of enhanced ocean alkalinity would need to be continuous if sustained carbon dioxide removal and/or ocean acidification mitigation are required.

1.2.4 Appraisal of the potential impacts of the techniques on the marine environment (and the atmosphere where appropriate)

All of the preceding enhanced weathering and alkalinity generation schemes add divalent cations to the surface ocean (in particular Mg^{2+} and Ca^{2+}). While such ion input is part of natural mineral weathering, both the benefits and impacts of increased addition require further study. As stated above, abiotic carbonate precipitation is strongly inhibited in seawater yet biologically-mediated precipitation of $CaCO_3$ could be enhanced, possibly beyond that which can be viewed as restoration of present ocean-acidity depressed calcification. Such bio-precipitation would also release CO_2 (**Equations 1.6-8**), reducing the efficacy of the original carbon storage in dissolve alkaline form. Other ions (e.g. derived from the silicon, nickel, lead, zinc and chromium contained in carbonate and silicate minerals) introduced by these techniques could also either impede or enhance carbon fixation and other biogeochemical processes, potentially affecting marine ecosystems (Renforth and Henderson, 2017). Therefore, the marine biogeochemical and ecological response to alkalinity addition and impurities therein must be investigated before any of these approaches are implemented. This includes consideration of the ocean in the vicinity of river mouths where land-derived alkalinity would be delivered prior to dilution. In the coastal ocean, it is also possible that any change in the deposition of anthropogenic sulphate and nitrate aerosols could have significant influence on ocean alkalinity (Hunter et al., 2011).

1.2.5 Conclusions for enhancing ocean alkalinity

Insufficient research and testing has been done on these topics to allow informed decision-making on large-scale deployment. Enhancing ocean alkalinity in this way would help draw down atmospheric carbon dioxide and reverse ocean acidification. The key unknowns which require further research are:

(i) the characterisation of the minerals or other alkalinity to be used, including specific ions and materials that would accompany alkalinity addition to the ocean;

(ii) the marine biological response to these additions;

(iii) determination of the response and effects of biotic and abiotic carbonate precipitation under alkalinity addition, in particular, their impact on net C storage and lifetimes;

(iv) public acceptability;

(v) economics and cost effectiveness; and

(vi) monitoring and verification.

1.3 Risks and co-benefits of increased (Earth) Alkaline metal concentrations in the marine environment

Sophie J. Gill & Rosalind E. M. Rickaby

Published as "Risks and co-benefits of increased (Earth) Alkaline metal concentrations in the marine environment" in Bach, Lennart T., Sophie J. Gill, Rosalind E. M. Rickaby, Sarah Gore, and Phil Renforth. 'CO2 Removal With Enhanced Weathering and Ocean Alkalinity Enhancement: Potential Risks and Co-Benefits for Marine Pelagic Ecosystems'. Frontiers in Climate 1 (2019). *© 2019 Bach, Gill, Rickaby, Gore and Renforth. This is an open-access article distributed under the terms of the* ***Creative Commons Attribution License (CC BY)****. The use, distribution or reproduction in other forums is permitted, provided the original author(s) and the copyright owner(s) are credited and that the original publication in this journal is cited, in accordance with accepted academic practice. No use, distribution or reproduction is permitted which does not comply with these terms.*

1.3.1 Perturbation

It is expected that the most likely minerals to be used for EW/OAE are Ca or Mg oxides (e.g., CaO) and/or Ca or Mg silicates (e.g., Mg_2SiO_4). Ca and Mg are important ions for all organisms and in particular for calcifiers: Ca as a main ingredient and Mg as an inhibitor of precipitation which is excluded from the mineralisation space (Davis et al., 2000). Due to the high background concentrations of these alkali Earth metals in seawater, the relative change in their concentrations through addition to the surface ocean will be small (**Table 1.1**). However, it is likely that there will be considerable local perturbations through EW/OAE, and therefore Ca and Mg, at the input location for these schemes, on a regional scale. Biotic impacts through Ca or Mg may be pronounced at these perturbation hotspots before mixing through ocean currents disperses these chemicals to lower concentrations.

Component	*Residence time in the oceans[a] (years)*	*Dissolved surface ocean concentration[b] (µmol kg^{-1})*	*Natural input of dissolved element into the oceans[c] (Tmol year^{-1})*	*Source material for OAE*	*Element content in source rocks (mol kg rock^{-1})[d]*	*Amount added via OAE[e] (Tmol year^{-1})*	*N-fold the natural inputs*	*Amount added from 2020-2090 (Tmol)*	*Surface ocean concentration by 2090[f] (µmol kg^{-1})*
TA	100,000	2,000-2,500	30			250	8	17,500	25-400
Si	10,000	0-80	5-14	Dunite	6.7 ± 0.6	67	5-14	4,692	
				Carbonate	0.70	7	0.5-1.4	490	
Ca	1,000,000	8,800-11,700		Dunite	0.3 ± 0.6	3.2		225	0.3-5
				Carbonate	15	150		10,500	15-240
Mg	11,600,000	45,500-60,600	6	Dunite	10 ± 2.4	101	16	7,045	10-160
				Carbonate	0.4	4	0.7	280	0.4-6
Fe	40	Mostly <0.001		Dunite	1.4 ± 0.5	14		971	
				Carbonate	0.18	2		126	
Ni	4,000-10,000	0.002-0.012	1.5	Dunite	0.04 ± 0.01	0.4	0.3	30	
				Carbonate	0.00003	0.00003	~0.0002	0.02	

Table 1.1: Table 1 and the following figure caption are directly reproduced from Bach et al. (2019). Estimated additions of key components in an OAE scenario with 10 Gt rock year^{-1}. [a] Residence time for TA was estimated by dividing the oceanic inventory (~3 x 10^{18} mol) by riverine inputs (next column); Si from Treguer and De La Rocha (2013); Ni from Gall et al. (2013); other values from Sarmiento and Gruber (2006). [b] TA from Takahashi et al. (2014); Si from the World Ocean Atlas (https://www.nodc.noaa.gov/OC5/indprod.html); Ca and Mg from Zeebe and Wolf-Gladrow (2001) for a salinity range from 30 to 40 assuming conservative behaviour; Fe from Schlitzer et al. (2018); Ni from Gall et al. (2013). Please note that the given ranges cover most of the surface ocean but deviations can occur regionally (e.g. Fe can be considerably higher in coastal regions or when affected by dust or hydrothermal plumes). [c] TA from Amoitte Suchet et al. (2003) with only riverine alkalinity (HCO_3^-) influx considered; Si from Treguer and De La Rocha (2013); Mg from Tipper et al. (2006); Ni from Gall et al. (2013). Please note that values for Ca and Fe are not provided due to large uncertainties (Jickells et al. 2005; Fantle and Tipper, 2014). For example, inputs of DFe are hard to quantify as it is difficult to constrain solubilities of particulate Fe sources (Jickells et al., 2005; Boyd and Ellwood, 2010). [d] Please keep in mind that the element contents within source rocks for EW/OAE vary widely. Given the large globally distributed deposits of silicate and carbonate rocks, it may be possible to extract material to optimise the chemical composition or minimise the environmental impact. Such a procedure would require careful regulation and verification. [e] The assumption is that 10 Gt of rock coincide with an addition of 250 Tmol TA year^{-1}. The other elements are scaled to this mass with the molar contents per kg rock^{-1} given in the previous column. Please note that the addition of 250 Tmol TA year^{-1} for 10 Gt of rock is an (idealised) upper estimate based on the assumption that pure Mg_2SiO_4 or $Ca(OH)_2$ dissolve. In reality annual TA additions through 10 Gt rock would likely be lower because such chemical purities will not be reached. [f] Concentration increase for TA from Lenton et al. (2018) which vary regionally as indicated by the given range. The upper estimate is based on a scenario where TA was added evenly over tropical surface ocean. Please note that an even addition is probably unfeasible so that higher concentrations would very likely occur in a more realistic scenario with localised additions. Concentration increases are also provided for Ca and Mg as these should, like TA, behave conservatively.

1.3.2 Current understanding

High intracellular calcium is incompatible with life. At high intracellular concentrations, Ca^{2+} causes aggregation of proteins and nucleic acids, affects the integrity of lipid membranes, and can precipitate with cytosolic phosphate removing a major nutrient from bioavailability within the cell (Case et al., 2007). All forms of life, from their origin, need an effective system for Ca homeostasis, which keeps intracellular Ca^{2+} at concentrations low enough to prevent apatite precipitation, at levels of ~0.1 μM, and ~10,000–20,000 times lower than that in seawater (Carafoli, 1987). Although maintenance of such a large Ca^{2+} concentration gradient can be used effectively for Ca signaling as a core component of cellular regulation, it comes at a metabolic cost. Thus, any perturbation of the environmental Ca^{2+} concentration could impose an additional metabolic cost to all forms of life from bacteria to the highest eukaryotes, meaning that marine food webs could be affected by high Ca^{2+} at perturbation hotspots.

Magnesium is the second most abundant cellular cation after potassium. In comparison to Ca, high intracellular concentrations of total and free magnesium ion (Mg^{2+}) appear to be essential to regulate numerous cellular functions and enzymes, including ion channels, metabolic cycles, and signalling pathways up with intracellular concentrations ranging from 17-20 mmol kg^{-1}, just 2.5 times lower than ambient seawater (Romani, 2011). Understanding how cells regulate Mg^{2+} homeostasis remains incomplete but again must occur at some, but lesser than Ca, energetic cost to the cell (Romani, 2011).

1.3.3 Important knowledge gaps and testable hypotheses

From a biomineralization perspective, it is possible that calcification will benefit from additional Ca^{2+} in a quicklime OAE scheme (Stanley et al., 2005). The influence of Mg in an olivine scheme is more complicated. Mg is known to be a strong inhibitor of inorganic calcite precipitation through incorporation into the $CaCO_3$ lattice (Davis et al., 2000). Mg incorporation raises the dissolution rate of the advancing crystal edge, which subsequently increases the mineral solubility, resulting in corresponding reduced net calcification. Aragonite is not inhibited by Mg incorporation into the $CaCO_3$ lattice in the same way that calcite is.

Incorporation of Mg into aragonite's crystal structure has been shown experimentally to have no effect on growth rate of aragonite crystals (Berner, 1975; Gutjahr et al., 1996). Changes in the concentration of Mg in seawater relative to Ca do appear to be reflected in the plankton fossil record. Here, high Mg/Ca ratios through low absolute Ca concentrations, as in the modern ocean, promoted aragonite, and high Mg-calcite mineralizers. Conversely, low Mg-calcite mineralizers such as the coccolithophores, were more prevalent during the Mesozoic, which was characterized by oceans with low Mg/Ca and high absolute Ca^{2+} concentrations (Stanley and Hardie, 1998; Ries, 2010). Therefore, studies in palaeoceanography may be useful to elucidate future changes we could expect from EW/OAE scenarios by acting as suitable analogs.

There is also the possibility that higher Ca^{2+} and Mg^{2+} concentrations may interfere with the uptake of nutrients by phytoplankton (and/or bacteria). For example, Ca and Mg have been shown to influence Fe uptake in the freshwater cyanobacteria *Microcystis aeruginosa* (Fujii et al., 2015). It is therefore possible that Ca and Mg have similar effects on marine phytoplankton which may have implications from primary production at EW/OAE perturbation hotspots.

Given that foraminifera mineralize first by the engulfing of seawater by a membrane, the low Mg/Ca of their calcite compared to inorganic predictions suggests an active role for pumping of Mg away from the region of mineralization (Segev and Erez, 2006). Two species of benthic foraminifera incorporate more Mg into shells as Mg/Ca increases, suggestive that control on the Mg content of the mineralizing space is not strictly regulated. The greatest increase in precipitation of $CaCO_3$ was obtained at Mg/Ca of 1, and not at present-day seawater ratio (Mg/Ca = 5). Thus, it is possible that any decrease (increase) in the Mg/Ca ratio of the ocean will both increase (decrease) the degree of calcification of foraminifera, in addition to making the carbonate less (more) soluble by lowering its Mg/Ca ratio.

Pteropods are holoplanktonic gastropod molluscs which are the major producers of aragonite in the surface ocean today (Andersson et al., 2008). The response of pteropods to changing

Mg/Ca is not well-constrained due to the difficulty of keeping pteropods alive in culture (Howes et al., 2014). The origination of the pteropods and rise in prevalence during high Mg/Ca in the Cenozoic may suggest that pteropods are favored by the emerging aragonite sea conditions (Burridge et al., 2017). Accordingly, they could be influenced oppositely to coccolithophores and foraminifera by Mg/Ca alterations associated with EW/OAE.

As a first step, it will be essential to constrain the impact of elevated Ca and/or Mg on the order of magnitude predicted in **Table 1.1**. To our knowledge, no work has specifically been completed on the response of plankton other than coccolithophores or foraminifera to increased Mg, Ca or altered Mg/Ca. This work may also be important to complete for the major group of silicifiers, the diatoms, due to the competition between silicifiers and calcifiers mentioned before. If CaO were added to the ocean, thereby decreasing Mg/Ca, it is reasonable to hypothesize that coccolithophores as competitors of diatoms would be further strengthened and take a larger share of the available nutrient pool. There is huge opportunity for the utilization of palaeoceanographic studies to help with these predictions, due to the rich fossil and sediment record providing evidence of secular changes in Mg/Ca ratios over geological time showing that silicifiers have risen to open ocean dominance in high Mg/Ca oceans (Falkowski et al., 2004).

1.4 The marine biological response to Alkalinity Enhancement

1.4.1 Calcification and the major calcifiers

The vast majority of $CaCO_3$ formed in the modern ocean is by coccolithophores, foraminifera, and pteropods (Lebrato et al., 2010; Sarmiento and Gruber, 2006). Buitenhuis et al. (2019) highlight the important difference between the export of calcite to the deep ocean and the contribution to shallow pelagic calcification. There has been some debate in the literature about the relative contributions of coccolithophores, foraminifera, and pteropods to the global $CaCO_3$ budget and studies that quantify the export of calcite to the deep ocean conclude that coccolithophores and foraminifera dominate this. For example, Tyrrell and Young (2009) assert that the flux of coccoliths to the deep ocean likely contributes ~ 50% of the total vertical

$CaCO_3$ flux in open ocean waters, with foraminifera shells responsible for most of the rest. Similarly, Schiebel (2002) found that foraminiferal tests contribute between 32–80% of total calcite flux to the deep ocean. However, Buitenhuis et al. (2019) found via modelling that pteropods contribute at least 33% to the export of $CaCO_3$ at 100m and up to 89% to pelagic calcification. The contribution of pteropods (which produce aragonite shells rather than calcite shells like coccolithophores and foraminifera) is not negligible. More work will need to be completed to establish precisely the contributions of these three major plankton groups to global calcification. Still, the coccolithophores and foraminifera have been long-established as the bulk contributors to pelagic and export flux of calcite in our oceans.

As significant contributors to calcification, due to the possibility of CO_2 re-release (CO_2 leakage) that may happen as a response to Alkalinity Enhancement (either EW or OAE) (**Figure 1.7**), it will be crucial to constrain the response of these two major groups of plankton that occupy the pelagic zone.

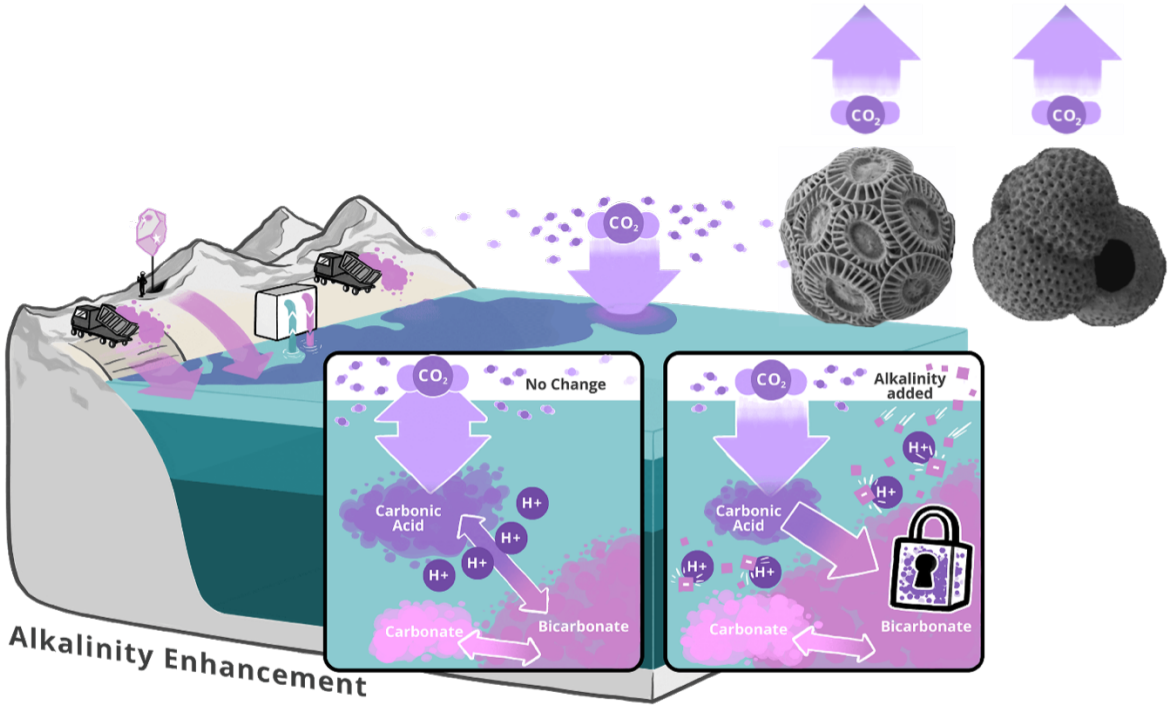

Figure 1.7: Original image from oceanCDR.net (permissions free), showing Alkalinity enhancement and the subsequent changes to carbonate chemistry. Possible feedbacks from planktonic foraminifera and coccolithophores on CO_2 re-release shown (SEM images of the coccolithophore *E. huxleyi* and the planktonic foraminifera *G. ruber* taken by S. J. Gill). Not to scale.

Coccolithophores calcify intra-cellularly by fixing inorganic carbon into calcite in the intra-cellular coccolith vesicle and subsequently secreting these onto the cell surface (De Vargas et al., 2007; Raven and Giordano, 2009; Taylor et al., 2017); this occurs at a similar or faster rate than photosynthetic carbon fixation (Anning et al., 1996). Most studies of coccolithophores focus on *Emiliania huxleyi*, as it is the model organism for coccolithophore studies (Jordan, 2009), but evidence suggests that there is a high degree of diversity in physiology among coccolithophores (Rickaby et al., 2010; Sheward et al., 2017; Anning et al., 1996).

By contrast to the coccolithophores, foraminifera calcify by employing a method of fluid-phase seawater endocytosis, where seawater is drawn directly into the cell via vacuolisation. Ions are supplied directly to the calcification site in the cell from the seawater vacuole (Bentov et al., 2009). As foraminifera calcify, they produce new calcite chambers extracellularly and add a new layer of calcite to previous chambers each time a new chamber is added (de Nooijer et al., 2009).

1.4.2 Past work on the biological response to Alkalinity Enhancement

To my knowledge, no specific studies on coccolithophore or planktonic foraminifera response to increased ocean alkalinity as a CDR technique have been published. Storage of carbon in the ocean as a CDR technique is an underrepresented area in the literature (Bellamy et al., 2012). However, studies are beginning to emerge examining the biological impacts of mCDR schemes.

It is important to note that marine biota do not physiologically respond directly to the chemical parameter of Total Alkalinity, but rather the chemical components of the carbonate system which are modified as a result of a change in Total Alkalinity. As outlined in **Section 1.1**, the parameters of the carbonate system that rise as a result of an increase of alkalinity are pH ($[H^+]$), and [DIC] (in the forms $[HCO_3^-]$ and $[CO_3^{2-}]$), and these are the variables that directly influence cell biology. $\Omega CaCO_3$ also rises during alkalinity increases, and while this does not directly influence cell biology, this parameter also affects calcifiers because it affects the

dissolution and stability of the calcite precipitated by calcifying biota. [CO_2](aq) and pCO_2 are also parameters that directly influence the cell biology of marine biota, and these fall during alkalinity enhancement before air-sea equilibration has occurred. There is also the possibility that [CO_2](aq) and pCO_2 may be constant with increasing TA in the surface ocean, if the timescale is sufficiently long enough for air-sea equilibration to occur (Bach et al., 2019).

Therefore, experimental work constraining the response of biota to alkalinity enhancement will need to link the physiological impact of each of these species of the carbonate system with the responses observed after alkalinity has been raised.

For instance, Gim et al. (2018) experimentally investigated the eco-toxicological effects, i.e. mortality rates of elevated DIC as part of an ocean alkalinity enhancement framework. They generated dose-response curves for three species of marine microalgae, none of which are calcifying: *Dunaliella salina*, *Isochrysis galbana* and *Nannochloropsis oculata*. They also investigated effects on one species of copepod, rotifer, amphipod, echinoderm, bivalve, and fish. [DIC] in their experimental conditions ranged from 3.0-190 mM, while pH ranged from 7.61-8.45. All of these species showed 100% mortality by 100mM DIC, which is ~50 times more than modern ocean concentrations of DIC.

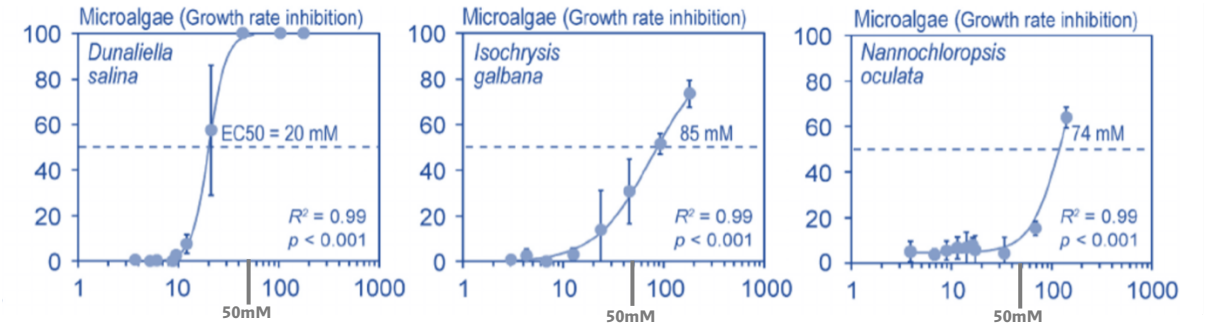

Figure 1.8: Dose-response curves for three microalgae species to elevated DIC concentrations (*x*-axis). Y-axis value is the percentage mortality rate, i.e. "eco-toxicological effects". Original figure from Gim et al. (2018).

As shown in **Figure 1.8**, growth inhibition effects on microalgae varied among species. *D. salina* was more susceptible to eco-toxicological effects from DIC than the other two species investigated, which implies taxa-specific responses to elevated DIC in microalgae. This study

claims that alkalinity enhancement must be kept to the equivalent of 11mM DIC or lower in the surface ocean to protect marine organisms. From my calculation in CO2sys[1], increasing Total Alkalinity (TA) from surface ocean reference values of ~2500 μmol kg^{-1} (Sarmiento and Gruber, 2006) to 4000 μmol kg^{-1} (a maximum expected value for alkalinity enhancement values, (Renforth and Henderson, 2017)) at present atmospheric CO_2 levels would only increase DIC concentrations to 3.3mM. Returning to **Figure 1.8**, this does not appear to have a strong eco-toxicological effect on the microalgae investigated. Therefore, this paper took DIC levels well above those that would ever be expected in a realistic alkalinity enhancement scenario, highlighting the need for realistic, application-focused work in this field.

Gore et al. (2018) have examined the response of a globally ubiquitous red calcifying macroalgae, Corallina spp. (of the family Corallinales) to an increase in TA over a 3-week laboratory experiment. They used the alkalinity anomaly technique (after Chisholm and Gattuso (1991)) to measure the calcification response of Corallina spp. in ambient seawater (TA = 2694 ± 114 μEq L^{-1}) and seawater of elevated alkalinity through added Na_2CO_3 (TA = 3454 ± 105 μEq L^{-1}). Calcification rates were ~60% higher in the elevated alkalinity treatment than ambient seawater, but primary productivity also increased markedly throughout the duration of the experiment. The study is relatively inconclusive regarding whether CO_2 consumption through increased primary productivity could outweigh CO_2 release through increased calcification, which is a crucial parameter to constrain for biological response to alkalinity enhancement.

Coral reefs are relatively well-studied for response to alkalinity addition, both in small-scale field studies (Albright et al., 2016; Silverman et al., 2007) and in laboratory experiments (Marubini and Thake, 1999). The effect seems to be positive for coral reef recovery, i.e.,

[1] Values were entered into CO2SYS v2.1 (Pierrot et al. 2006), run using the constants of Mehrbach et al. (1973) refitted by Dickson and Millero (1987).

calcification rate increases with alkalinity addition, although this is a negative feedback for CO_2 drawdown.

There have also been some studies that have examined the response of coccolithophores and foraminifera to alkalinity enhancement as a by-product of their main topic of investigation. Langer et al. (2006) measured a reduction in calcification rate of *Calcidiscus leptoporus* and *Coccolithus pelagicus* (important primary-producing coccolithophore species) during culture experiments, in response to elevated calcite saturation ($\Omega CaCO_3$ from 2 to 13, pH 7.8 to 8.7), which they postulate could be physiologically driven by lower levels of $[CO_2](aq)$.

Jonathan Erez examined benthic foraminifera response to enhanced sodium levels as a by-product of another experiment he completed (Erez, J., email correspondence, Nov 2018), where foraminifera tended to live longer in solutions with added Na i.e. raised alkalinity. Na addition in his experiments will have raised alkalinity because it is a conservative monovalent cation that appears in the explicit conservative expression for alkalinity (Wolf-Gladrow et al., 2007). The culturing completed in the seminal studies of Bijma et al., (1999), Holland et al., (2020), Russell et al., (2004), and Spero et al., (1997), suggest that pH and CO_3^{2-} are the likely physiological drivers of planktonic foraminifera geochemical ($\delta^{18}O$ and $\delta^{13}C$ of the calcite test) and calcification responses to culturing manipulations of carbonate chemistry. Many of these manipulations resulted in changes in alkalinity as an indirect consequence; although foraminiferal calcification does not appear to be impacted by elevated alkalinity, this could be due to the difficulty of assessing calcification rates (e.g., Holland et al., 2017; Allen et al., 2016).

Unfortunately, it is difficult to interpret these results directly within a realistic alkalinity enhancement framework because they may not be realistic for the ocean's chemicals during an mCDR scheme. For example, Langer et al. (2006) used hydrochloric acid and sodium hydroxide as the chemical manipulations in their experiment, which are highly unlikely to be added to the ocean for alkalinity enhancement. The Na alkalinity which Erez used in his

experiments may be more realistic; however, Ca alkalinity effects also require investigation, as outlined in **Section 1.3**, as divalent cations are a more efficient way of enhancing alkalinity and drawing down CO_2, due to double the disruption of the charge balance compared to monovalent cations.

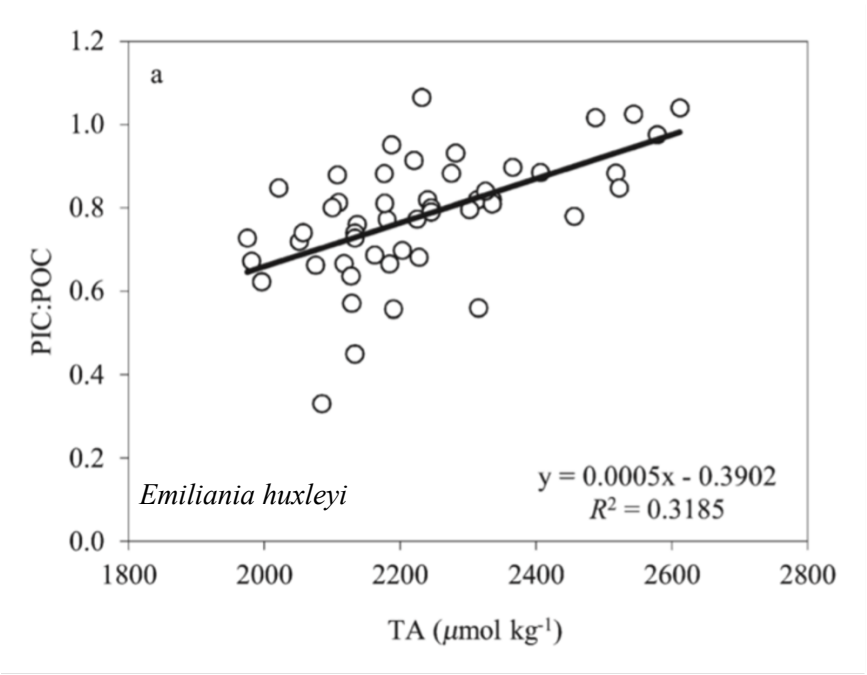

Figure 1.9: Positive relationship between PIC:POC of the coccolithophore *E. huxleyi* in culture with TA. Original figure from Findlay et al. (2011). PIC:POC is a measure of the partitioning of the DIC between the inorganic (calcification) and organic (photosynthesis) carbon fixation (Hermoso et al., 2014), and so acts as a proxy for the carbon export ratio.

There have been numerous coccolithophore and foraminifera studies focussing on ocean acidification scenarios. There seems to be a general relationship of decreased calcification and increased malformation of coccoliths with increased acidity in the species of coccolithophore including *E. huxleyi* and *Gephyrocapsa oceanica* (Beaufort et al., 2011; Riebesell et al., 2007, Riebesell et al., 2000; Zondervan et al., 2001) due to dissolution of liths driven by a decrease in $[CO_3^{2-}]$ and $\Omega CaCO_3$, and inhibition of lith formation by increasing $[H^+]$ as pH decreases (Bach et al., 2015; Cyronak et al., 2016). The same trend and drivers are recognised for the response of planktonic foraminifera to ocean acidification (Moel et al., 2009; Moy et al., 2009). Therefore, it could be suggested that there should be the opposite effect on

calcifying organisms from enhanced alkalinity, i.e. an increase in calcification because ocean alkalinisation is essentially the opposite of ocean acidification.

However, not all studies concerning the coccolithophore response to ocean acidification observe the same responses. Iglesias-Rodriguez et al. (2008) and Shi et al. (2009) both observed an increase in organic carbon production and calcification of *E. huxleyi* in response to increased pCO_2 (and decreased pH and $\Omega CaCO_3$, a measure of the thermodynamic likelihood of $CaCO_3$ dissolution, the value of which is obtained by rearranging **Equation 1.4**). This has been argued to be due to differences in the experimental design of carbonation (e.g. bubbling of CO_2 vs. addition of acid/base) (Riebesell et al., 2008), but is more likely due to strain-specific variation in observations (Ridgwell et al., 2009). Additionally, it seems likely that different species of coccolithophore respond differently to ocean acidification. For example, Langer et al. (2006) found that *C. leptoporus* exhibited optimum PIC responses to a range of pCO_2 values between 98-920 µatm, while *Coccolithus braarudii* PIC:POC was insensitive from pCO_2 149-915 µatm.

PIC:POC is a measure of the partitioning of the DIC between the inorganic (calcification) and organic (photosynthesis) carbon fixation (Hermoso et al., 2014), and so acts as a proxy for the carbon export ratio. Findlay et al. (2011) found that PIC:POC of the coccolithophore *Emiliania huxleyi* increases linearly with TA over a range of carbonate chemistries relevant to ocean acidification scenarios (see **Figure 1.9**). This was shown to be driven by linearly decreasing $[CO_2](aq)$ and more minorly by $[PO_4^{3-}]$ as a result of PRIMER multiple regression analysis. PRIMER multiple regression analysis uses the PERMANOVA+ for PRIMER software to perform multiple regression analyses. In the case of Findlay et al. (2011), this was used to assess the strength of the relationship between TA and the different components of the carbonate system, in particular PIC:POC, as well as the importance of each of the components to the relationship. However, Bach et al. (2011) ran a similar experiment to Langer et al. (2006) but found a non-linear relationship between pCO_2 and calcification rate, with a strong pH

dependence of calcification at high pCO_2, but the carbonate system parameter driving calcification responses at low pCO_2 was unclear. Therefore, it is challenging to interpret ocean acidification results for ocean alkalinity carbon storage, which could reveal a different relationship between calcification and CO_2(aq) versus HCO_3^- and CO_3^{2-}, particularly because non-air-sea-equilibrated OAE could drive [CO_2](aq) low. This variation in past results makes it difficult to accurately predict how much CO_2 may be re-released by calcification during a realistic OAE scenario. It highlights the need for culturing experiments that precisely assess the responses to OAE at relevant carbonate chemistries.

1.4.3 Analytical methods for quantifying calcification

As evidenced above, there are several ways to quantify calcification during live culturing or monitoring of biota during an experimental incubation. Calcification can either be quantified using (i) calcification rate or (ii) calcite quota. Calcification rate refers to the production rate of calcite by a given organism over a specified time period. For example, in Gore et al. (2018), the calcification of macroalgae over the course of the culturing period. Calcite quota refers to the amount of calcite per cell on each calcifying organism, and is usually reported for coccolithophore culturing studies specifically, either directly as $CaCO_3$ $cell^{-1}$ or indirectly as PIC $cell^{-1}$ (Henderiks, 2008; Hermoso et al., 2020; O'Dea et al., 2014). The term gross calcification refers only to the process of precipitation of $CaCO_3$, whereas net calcification accounts for both precipitation and dissolution of $CaCO_3$ (Bach, 2015). Net calcification and gross calcification are equivalent in conditions where $CaCO_3$ does not dissolve, i.e. where $\Omega CaCO_3 > 1$ (Morse and Arvidson, 2002).

Calcification rate can be measured using the alkalinity anomaly technique (Chisholm and Gattuso, 1991; Gore et al., 2018; Smith and Key, 1975; Gazeau et al., 2015). This method enables the quantification of calcification by measuring the Total Alkalinity of seawater samples before and after (and sometimes during the course of) an experimental incubation, and can be used for both communities (e.g. corals, as in Albright et al., (2016) where a dual tracer regression method was used to quantify alkalinity uptake by the coral reef) or organisms

(e.g. macroalgae, microalgae, etc.). Calcification is then calculated using the assumption that for every mole of $CaCO_3$ precipitated, alkalinity is lowered by 2 moles (i.e. calcification = 0.5 x ΔTA). One drawback of the alkalinity anomaly technique is that its use in culturing studies to constrain calcification rate per cell is not well-documented, although Gore et al. (2018) report accurate calcification rate data for macroalgae using this technique, and this work has also been completed successfully with calcifying cyanobacteria (Sarah Gore, personal comms, Autumn 2020) in culturing conditions according to international best practice guidelines (LaRoche et al., 2010) used for coccolithophore culturing. The assumption that calcification = 0.5 x ΔTA inherently assumes that uptake of nutrients which are conservative ions e.g. NO_3^-, PO_4^{3-}, which contribute to ΔTA by biota, negligibly affects ΔTA, and that the processes of respiration and photosynthesis do not affect ΔTA. Chisholm and Gattuso (1991) confirmed that all underlying assumptions of the alkalinity anomaly technique are correct, and no correction for nutrient changes are required in the calculation of calcification because these changes are smaller than the variation in actual calcification values. The analytical advantage of measuring calcification in this way is that alkalinity analyses are often quick and efficient using an autotitrator, and highly accurate if using Gran titration coupled with international seawater reference standards (Dickson et al., 2007). Additionally, it is possible to calculate $CaCO_3$ $cell^{-1}$ from the calcification rate per cell by dividing by the duration of the experiment, although to my knowledge no published data has used this method before.

Calcification rate of foraminifera in culture has to be measured in a unique way because foraminifera are isolated as individual specimens for culturing, and therefore alkalinity change is only negligible in the comparatively large volume of culture water for each specimen (Evans et al., 2016a). Instead of using the alkalinity anomaly technique, changes in foraminifera weight and size can be used to constrain the amount of shell mass added over the course of an experiment, and therefore the calcification rate. Foraminifera cannot be weighed at the beginning of culturing because they are suspended in the culture media. Instead, foraminifera's long-axes can be measured at the start and the end of the experiment, and then

after gametogenesis (i.e. the end of a foraminifer's life), individuals can be weighed using a micro-balance. Finally, using published mass-size relationships for a given foraminifera species, the initial weight can be back-calculated and used in conjunction with the final weight to calculate the change in shell mass over the course of the experiment, which is equivalent to the amount of calcite added per unit time, because addition of organic matter is negligible in terms of contribution to mass compared to that added by calcite. Alternatively, the total shell mass added can be used as a measure of calcification without converting to a calcification rate. These techniques are well-established (Evans et al., 2018; Kisakürek et al., 2008; Evans et al., 2016b; Lombard et al., 2009; Erez and Luz, 1983). Back-calculation of the initial weight of foraminifera relies on the accuracy of published mass-size relationships for foraminifera species (e.g. Kisakürek et al., 2011; Marshall et al., 2015; Allen et al., 2011; Hamilton et al., 2008; Lombard et al., 2010). However, this is not a source of major uncertainty because mass-size relationships are robustly tested for statistical significance and based on high sample numbers of individual foraminifera.

Coccolithophore cellular calcification can be quantified using a variety of measurements. The three most commonly used are: (i) PIC:POC analysis (e.g. Oviedo et al., 2014; Riebesell et al., 2007; Bach et al., 2015; Langer et al., 2009) (ii) Flame absorption spectroscopy to measure changes in particulate calcium (Stoll et al., 2002; Findlay et al., 2011) or (iii) SEM volume conversions, which are based on work completed using nannofossil work on coccolithophores from sediment cores (Young and Ziveri, 2000). The measurement of choice for most coccolithophore calcification studies is PIC:POC, which is carried out using acidified and non-acidified culture samples collected onto GF/F filters and subsequently analysed using a CHN analyser. The difference between the resulting measurements of TPC and POC can be used to obtain PIC values. This method has the advantage of providing a proxy for the ratio of calcification to photosynthesis (Rickaby et al., 2010; Hermoso et al., 2014) and therefore carbon export ratio, unlike other measurements of calcification. Carbon export ratio is the parameter used preferentially in modelling studies, rather than $CaCO_3$ $cell^{-1}$. PIC:POC can

also be easily compared to $CaCO_3$/cell measurements with a simple chemical conversion using the molecular masses of Ca, C, and O. There are no real analytical problems with this technique; it is routinely carried out with access to a CHN analyser. Incomplete acidification may be a foreseeable analytical problem, which would lead to overestimates of PIC values.

It is not possible to directly compare the measurement of calcification rate with the measurement of calcite/cell, or vice versa, because they provide different information about calcification (i.e. a production rate per cell vs. a cellular value). However, converting between a rate and a quota (or vice versa) would provide broadly comparable calcification data. For example, PIC $cell^{-1}$ can be easily converted to a PIC production rate or vice versa using a known growth rate, as outlined in Zondervan et al. (2002) and Aloisi (2015). If experimental methods used to obtain measurements are different, then there is a possibility of some disparity between absolute values of $CaCO_3$ $cell^{-1}$ (Ridgwell et al., 2009). Normalising to POC production (i.e. PIC:POC or $CaCO_3$:POC) produces greater agreeability between studies (Riebesell et al., 2008).

1.4.4 Biogeochemical and ecosystem impacts of Alkalinity Enhancement

There is also the possibility of more wide-ranging biogeochemical and ecosystem impacts on biota from alkalinity enhancement in the marine environment. Enhancing alkalinity raises total DIC in seawater. DIC is required for POC formation, so this process may lead to higher POC formation rates. Additional POC settling would remove higher levels of carbon from the surface ocean and reduce atmospheric CO_2 further (Henderson et al., 2008); the Redfield (C:N:P) ratio is a crucial control on this. If C:N:P is fixed, then the extent of additional POC production is likely to be small because POC production is limited by phosphate and nitrate, not by the availability of DIC (Riebesell et al., 2007). So if organisms like coccolithophores could alter their C:N:P in response to an alkalinity perturbation, this mechanism could be a potential positive feedback of enhancing ocean alkalinity to draw down atmospheric CO_2. This could be important to quantify as part of the ocean's response to any carbon dioxide removal scheme. Or indeed, if enhanced alkalinity would change ecosystem structure, and some organisms

have different Redfield ratios, then this could conceivably lead to feedbacks on CO_2 drawdown as well. There is evidence that C:N:P in marine microalgae is highly variable between species and strains (Geider and Roche, 2002), and indeed, flexible elemental stoichiometry has been observed in prokaryotes (Hillebrand et al., 2013; White et al., 2006).

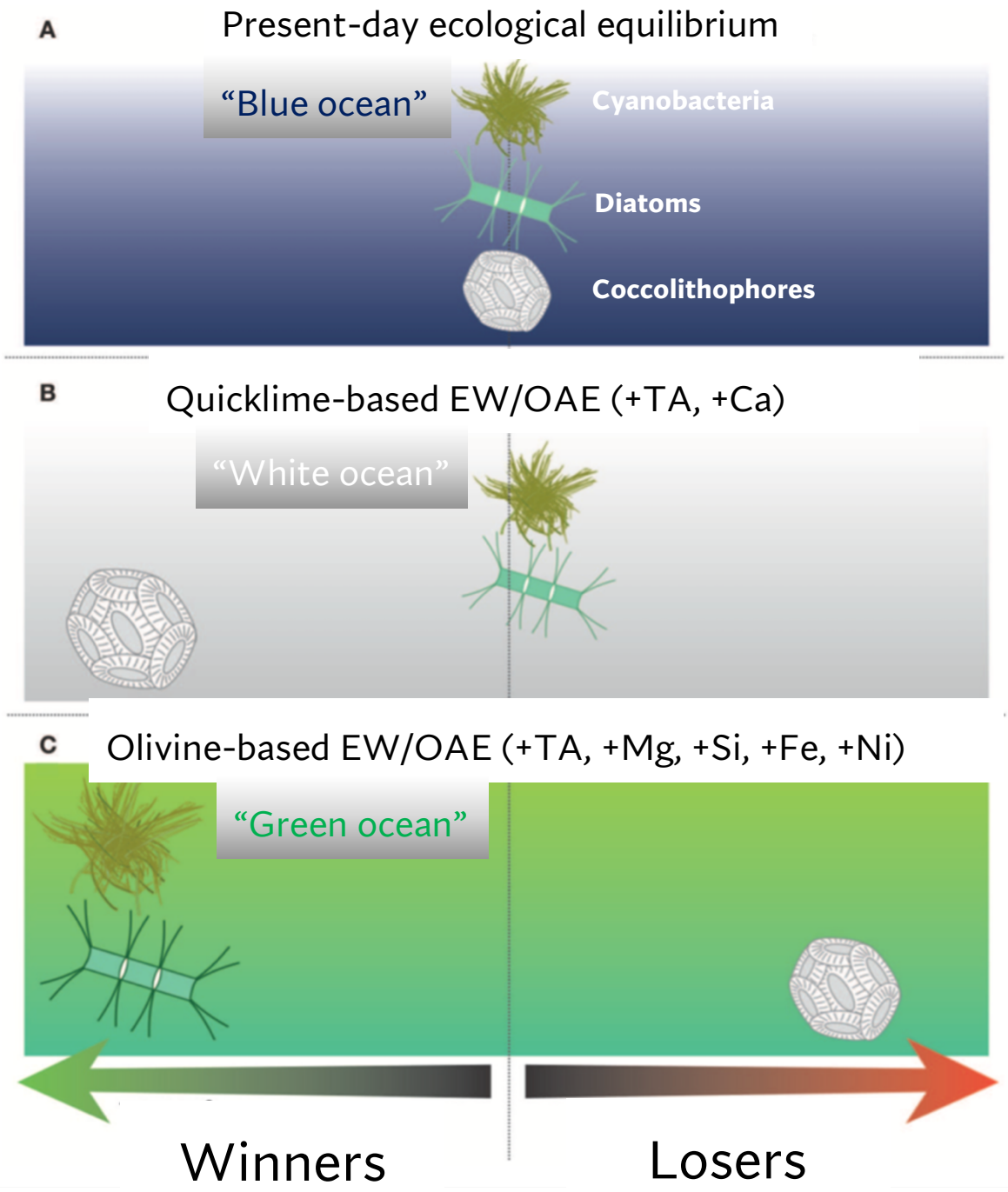

Figure 1.10: The "white or green ocean hypothesis", showing the likely relative success of three major functional groups of phytoplankton (coccolithophores, cyanobacteria (N_2-fixers) and diatoms) to OAE schemes using different source materials, as outlined in text. Original figure from Bach et al. (2019).

In Bach et al. (2019), we hypothesised that the material used for alkalinity enhancement would not just affect specific sub-groups of phytoplankton (e.g. coccolithophores, foraminifera) but could have impacts on the relative success of major phytoplankton functional groups, because they may have contrasting optima with respect to carbonate saturation and/or pH. For example, TA will increase during an EW/OAE scenario, and Ca^{2+} may be added to the surface ocean. We predicted that these carbonate chemistry conditions would be favourable for calcifiers. We conceptualised the modern-day ocean as a "blue" ocean, in ecological equilibrium between the major phytoplankton functional groups of calcifiers, silicifiers (e.g. diatoms), and nitrogen-fixers (**Figure 1.10**). In an EW/OAE scenario, the increased relative success of calcifiers could shift the ocean to a "white(r) ocean" (**Figure 1.10**). By contrast, if silicate materials (e.g. olivine) were used to enhance alkalinity in the marine environment, increasing TA would be accompanied by a rise in dissolved Si and trace metal enrichment (Fe, Ni). Silicifiers could likely benefit from an increase in dissolved Si, and nitrogen-fixers could be more successful due to Fe and Ni enrichment. These responses would result in overall increased primary productivity until macronutrients were limiting, and calcifiers could be outcompeted. This shift can be thought of as a move towards a "green(er) ocean" (**Figure 1.10**).

1.5 Thesis aims

Overall, there is a research gap for experiments that constrain the response of critical groups of pelagic calcifiers to enhanced alkalinity levels, which are representative of realistic Alkalinity Enhancement scenarios, and investigate the possibility of calcification responding in a non-linear and taxa- and/or species-specific fashion.

Specific research aims for this thesis:

1. Establish an evidence-driven approach to mCDR research strategy, and use this to inform my laboratory research.

2. Quantify the growth and calcification response of major groups of calcifiers, the coccolithophores and the planktonic foraminifera, to Alkalinity Enhancement.
3. Investigate the likelihood of "CO_2 leakage" from biotic calcium carbonate formation during Alkalinity Enhancement, based on the calcification response of coccolithophores and planktonic foraminifera measured during these experiments.
4. Examine the response of these biota to two different alkalinity-enhancing elements: Na and Ca.
5. Explore whether plankton can alter their C:N:P in response to Alkalinity Enhancement and whether this will facilitate increased POC formation, thereby providing a positive feedback on CO_2 drawdown during Alkalinity Enhancement.

References

Albright, R., Caldeira, L., Hosfelt, J., Kwiatkowski, L., Maclaren, J.K., Mason, B.M., Nebuchina, Y., Ninokawa, A., Pongratz, J., Ricke, K.L., Rivlin, T., Schneider, K., Sesboüé, M., Shamberger, K., Silverman, J., Wolfe, K., Zhu, K., Caldeira, K., 2016. Reversal of ocean acidification enhances net coral reef calcification. Nature 531, 362. https://doi.org/10.1038/nature17155

Allen, K.A., Hönisch, B., Eggins, S.M., Haynes, L.L., Rosenthal, Y., Yu, J., 2016. Trace element proxies for surface ocean conditions: A synthesis of culture calibrations with planktic foraminifera. Geochimica et Cosmochimica Acta 193, 197–221. https://doi.org/10.1016/j.gca.2016.08.015

Allen, K.A., Hönisch, B., Eggins, S.M., Yu, J., Spero, H.J., Elderfield, H., 2011. Controls on boron incorporation in cultured tests of the planktic foraminifer *Orbulina universa*. Earth and Planetary Science Letters 309, 291–301. https://doi.org/10.1016/j.epsl.2011.07.010

Aloisi, G., 2015. Covariation of metabolic rates and cell size in coccolithophores. Biogeosciences 12, 6215–6284. https://doi.org/10.5194/bg-12-4665-2015

Andersson, A.J., Mackenzie, F.T., Bates, N.R., 2008. Life on the margin: implications of ocean acidification on Mg-calcite, high latitude and cold-water marine calcifiers. Marine Ecology Progress Series 373, 265–273. https://doi.org/10.3354/meps07639

Anning, T., NA, N., Merrett, M.J., Brownlee, C., 1996. Costs and benefits of calcification in coccolithophorids. Journal of Marine Systems 9, 45–56. https://doi.org/10.1016/0924-7963(96)00015-2

AR5 Climate Change 2013: The Physical Science Basis — IPCC, URL https://www.ipcc.ch/report/ar5/wg1/ (accessed 7.19.20).

Archer, D., Eby, M., Brovkin, V., Ridgwell, A., Cao, L., Mikolajewicz, U., Caldeira, K., Matsumoto, K., Munhoven, G., Montenegro, A., Tokos, K., 2009. Atmospheric Lifetime of Fossil Fuel Carbon Dioxide. Annual Review of Earth and Planetary Sciences 37, 117–134. https://doi.org/10.1146/annurev.earth.031208.100206

Bach Lennart Thomas, Riebesell Ulf, Schulz Kai Georg, 2011. Distinguishing between the effects of ocean acidification and ocean carbonation in the coccolithophore *Emiliania huxleyi*. Limnology and Oceanography 56, 2040–2050. https://doi.org/10.4319/lo.2011.56.6.2040

Bach, L.T., 2015. Reconsidering the role of carbonate ion concentration in calcification by marine organisms. Biogeosciences 12, 4939–4951. https://doi.org/10.5194/bg-12-4939-2015

Bach, L.T., Gill, S.J., Rickaby, R.E.M., Gore, S., Renforth, P., 2019. CO_2 Removal With Enhanced Weathering and Ocean Alkalinity Enhancement: Potential Risks and Co-benefits for Marine Pelagic Ecosystems. Frontiers in Climate 1. https://doi.org/10.3389/fclim.2019.00007

Bach, L.T., Riebesell, U., Gutowska, M.A., Federwisch, L., Schulz, K.G., 2015. A unifying concept of coccolithophore sensitivity to changing carbonate chemistry embedded in an ecological framework. Progress in Oceanography 135, 125–138. https://doi.org/10.1016/j.pocean.2015.04.012

Beaufort, L., Probert, I., de Garidel-Thoron, T., Bendif, E.M., Ruiz-Pino, D., Metzl, N., Goyet, C., Buchet, N., Coupel, P., Grelaud, M., Rost, B., Rickaby, R.E.M., de Vargas, C., 2011. Sensitivity of coccolithophores to carbonate chemistry and ocean acidification. Nature 476, 80–83. https://doi.org/10.1038/nature10295

Beerling, D.J., 2019. Can plants help us avoid seeding a human-made climate catastrophe? Plants, People, Planet 0. https://doi.org/10.1002/ppp3.10066

Beerling, D.J., Leake, J.R., Long, S.P., Scholes, J.D., Ton, J., Nelson, P.N., Bird, M., Kantzas, E., Taylor, L.L., Sarkar, B., Kelland, M., DeLucia, E., Kantola, I., Müller, C., Rau, G., Hansen, J., 2018. Farming with crops and rocks to address global climate, food and soil security. Nature Plants 4, 138–147. https://doi.org/10.1038/s41477-018-0108-y

Bellamy, R., Chilvers, J., Vaughan, N.E., Lenton, T.M., 2012. A review of climate geoengineering appraisals. Wiley Interdisciplinary Reviews: Climate Change 3, 597–615. https://doi.org/10.1002/wcc.197

Bentov, S., Brownlee, C., Erez, J., 2009. The role of seawater endocytosis in the biomineralization process in calcareous foraminifera. PNAS 106, 21500–21504. https://doi.org/10.1073/pnas.0906636106

Berner, R.A., 2004. The phanerozoic carbon cycle [electronic resource]: CO_2 and O_2, Ebook central. Oxford University Press, Oxford ; New York.

Berner, R.A., 1999. A new look at the long-term carbon cycle. GSA Today 9, 2–6.

Berner, R.A., 1975. The role of magnesium in the crystal growth of calcite and aragonite from sea water. Geochimica et Cosmochimica Acta 39, 489–504. https://doi.org/10.1016/0016-7037(75)90102-7

Bijma, J., Spero, H.J., Lea, D.W., 1999. Reassessing foraminiferal stable isotope geochemistry: Impact of the oceanic carbonate system (experimental results) In: Fischer, G., Wefer, G. (eds) Use of Proxies in Paleoceanography. Springer, Berlin, Heidelberg. https://doi.org/10.1007/978-3-642-58646-0_20

Boudreau, B.P., Middelburg, J.J., Luo, Y., 2018. The role of calcification in carbonate compensation. Nature Geoscience 11, 894. https://doi.org/10.1038/s41561-018-0259-5

Brewin, R.J.W., Sathyendranath, S., Platt, T., Bouman, H., Ciavatta, S., Dall'Olmo, G., Dingle, J., Groom, S., Jönsson, B., Kostadinov, T.S., Kulk, G., Laine, M., Martínez-Vicente, V., Psarra, S., Raitsos, D.E., Richardson, K., Rio, M.-H., Rousseaux, C.S., Salisbury, J., Shutler, J.D., Walker, P., 2021. Sensing the ocean biological carbon pump from space: A review of capabilities, concepts, research gaps and future developments. Earth-Science Reviews 217. https://doi.org/10.1016/j.earscirev.2021.103604

Buitenhuis, E.T., Le Quéré, C., Bednaršek, N., Schiebel, R., 2019. Large Contribution of Pteropods to Shallow $CaCO_3$ Export. Global Biogeochemical Cycles 33, 458–468. https://doi.org/10.1029/2018GB006110

Burns, W., Corbett, C.R., 2020. Antacids for the Sea? Artificial Ocean Alkalinization and Climate Change. One Earth 3, 154–156. https://doi.org/10.1016/j.oneear.2020.07.016

Burridge, A.K., Hörnlein, C., Janssen, A.W., Hughes, M., Bush, S.L., Marlétaz, F., Gasca, R., Pierrot-Bults, A.C., Michel, E., Todd, J.A., Young, J.R., Osborn, K.J., Menken, S.B.J., Peijnenburg, K.T.C.A., 2017. Time-calibrated molecular phylogeny of pteropods. PLOS ONE 12. https://doi.org/10.1371/journal.pone.0177325

Caldeira, K., Rau, G.H., 2000. Accelerating carbonate dissolution to sequester carbon dioxide in the ocean: Geochemical implications. Geophysical Research Letters 27, 225–228. https://doi.org/10.1029/1999GL002364

Carafoli, E., 1987. Intracellular calcium homeostasis. Annual Review of Biochemistry 56, 395–433. https://doi.org/10.1146/annurev.bi.56.070187.002143

Case, R.M., Eisner, D., Gurney, A., Jones, O., Muallem, S., Verkhratsky, A., 2007. Evolution of calcium homeostasis: From birth of the first cell to an omnipresent signalling system. Cell Calcium, Calcium Channels and Transporters 42, 345–350. https://doi.org/10.1016/j.ceca.2007.05.001

Chisholm, J.R.M., Gattuso, J.-P., 1991. Validation of the alkalinity anomaly technique for investigating calcification of photosynthesis in coral reef communities. Limnology and Oceanography 36, 1232–1239. https://doi.org/10.4319/lo.1991.36.6.1232

Chou, W.-C., Gong, G.-C., Hsieh, P.-S., Chang, M.-H., Chen, H.-Y., Yang, C.-Y., Syu, R.-W., 2015. Potential impacts of effluent from accelerated weathering of limestone on seawater carbon chemistry: A case study

for the Hoping power plant in northeastern Taiwan. Marine Chemistry 168, 27–36. https://doi.org/10.1016/j.marchem.2014.10.008

Cyronak, T., Schulz, K.G., Jokiel, P.L., 2016. The Omega myth: what really drives lower calcification rates in an acidifying ocean. ICES Journal of Marine Science 73, 558–562. https://doi.org/10.1093/icesjms/fsv075

Davies, P.A., 2018. Desalination as a negative emissions technology. Environmental Science - Water Research and Technology 4, 839–850.

Davis, K.J., Dove, P.M., Yoreo, J.J.D., 2000. The Role of Mg^{2+} as an Impurity in Calcite Growth. Science 290, 1134–1137. https://doi.org/10.1126/science.290.5494.1134

de Nooijer, L.J., Toyofuku, T., Kitazato, H., 2009. Foraminifera promote calcification by elevating their intracellular pH. PNAS 106, 15374–15378. https://doi.org/10.1073/pnas.0904306106

De Vargas, C., Aubry, M.-P., Probert, I., Young, J., 2007. Origin and Evolution of Coccolithophores: From Coastal Hunters to Oceanic Farmers, in: Falkowski, P.G., Knoll, A.H. (Eds.), Evolution of Primary Producers in the Sea. Academic Press, Burlington, pp. 251–285. https://doi.org/10.1016/B978-012370518-1/50013-8

Dickson, A.G., Sabine, C.L., Christian, J.R., 2007. Guide to Best Practices for Ocean CO_2 Measurements. (Report). North Pacific Marine Science Organization.

Doney, S.C., Fabry, V.J., Feely, R.A., Kleypas, J.A., 2009. Ocean Acidification: The Other CO_2 Problem. Annual Review of Marine Science 1, 169–192. https://doi.org/10.1146/annurev.marine.010908.163834

Erez, J., Luz, B., 1983. Experimental paleotemperature equation for planktonic foraminifera. Geochimica et Cosmochimica Acta 47, 1025–1031. https://doi.org/10.1016/0016-7037(83)90232-6

Evans, D., Brierley, C., Raymo, M.E., Erez, J., Müller, W., 2016a. Planktic foraminifera shell chemistry response to seawater chemistry: Pliocene–Pleistocene seawater Mg/Ca, temperature and sea level change. Earth and Planetary Science Letters 438, 139–148. https://doi.org/10.1016/j.epsl.2016.01.013

Evans, D., Müller, W., Erez, J., 2018. Assessing foraminifera biomineralisation models through trace element data of cultures under variable seawater chemistry. Geochimica et Cosmochimica Acta, Chemistry of oceans past and present: A Special Issue in tribute to Harry Elderfield 236, 198–217. https://doi.org/10.1016/j.gca.2018.02.048

Evans, D., Wade, B., Henehan, M., Erez, J., Müller, W., 2016b. Revisiting carbonate chemistry controls on planktic foraminifera Mg/Ca: Implications for sea surface temperature and hydrology shifts over the Paleocene-Eocene Thermal Maximum and Eocene-Oligocene Transition. Climate of the Past 12, 819–835. https://doi.org/10.5194/cp-12-819-2016

Falkowski, P.G., Katz, M.E., Knoll, A.H., Quigg, A., Raven, J.A., Schofield, O., Taylor, F.J.R., 2004. The evolution of modern eukaryotic phytoplankton. Science 305, 354–360. https://doi.org/10.1126/science.1095964

Fawzy, S., Osman, A.I., Doran, J., Rooney, D.W., 2020. Strategies for mitigation of climate change: a review. Environmental Chemistry Letters. https://doi.org/10.1007/s10311-020-01059-w

Feng, E.Y., Koeve, W., Keller, D.P., Oschlies, A., 2017. Model-Based Assessment of the CO_2 Sequestration Potential of Coastal Ocean Alkalinization. Earth's Future 5, 1252–1266. https://doi.org/10.1002/2017EF000659

Findlay, H.S., Calosi, P., Crawfurd, K., 2011. Determinants of the PIC:POC response in the coccolithophore *Emiliania huxleyi* under future ocean acidification scenarios. Limnology and Oceanography 56, 1168–1178. https://doi.org/10.4319/lo.2011.56.3.1168

Fujii, M., Yeung, A.C.Y., Waite, T.D., 2015. Competitive Effects of Calcium and Magnesium Ions on the Photochemical Transformation and Associated Cellular Uptake of Iron by the Freshwater Cyanobacterial Phytoplankton Microcystis aeruginosa. Environmental Science and Technology 49, 9133–9142. https://doi.org/10.1021/acs.est.5b01583

Fuss, S., Canadell, J.G., Peters, G.P., Tavoni, M., Andrew, R.M., Ciais, P., Jackson, R.B., Jones, C.D., Kraxner, F., Nakicenovic, N., Quéré, C.L., Raupach, M.R., Sharifi, A., Smith, P., Yamagata, Y., 2014. Betting on negative emissions. Nature Climate Change. https://doi.org/10.1038/nclimate2392

Gazeau, F., Urbini, L., Cox, T., Alliouane, S., Gattuso, J.-P., 2015. Comparison of the alkalinity and calcium anomaly techniques to estimate rates of net calcification. Marine Ecology Progress Series 527, 1–12. https://doi.org/10.3354/meps11287

Geider, R., Roche, J.L., 2002. Redfield revisited: variability of C:N:P in marine microalgae and its biochemical basis. European Journal of Phycology 37, 1–17. https://doi.org/10.1017/S0967026201003456

GESAMP, 2019 “High level review of a wide range of proposed marine geoengineering techniques”. (Boyd, P.W. and Vivian, C.M.G., eds.). (IMO/FAO/UNESCO-IOC/UNIDO/WMO/IAEA/UN/UN Environment/ UNDP/ISA Joint Group of Experts on the Scientific Aspects of Marine Environmental Protection). Rep. Stud. GESAMP No. 98, 144 p.

Gim, B.-M., Hong, S., Lee, J.-S., Kim, N.-H., Kwon, E.-M., Gil, J.-W., Lim, H.-H., Jeon, E.-C., Khim, J.S., 2018. Potential ecotoxicological effects of elevated bicarbonate ion concentrations on marine organisms. Environmental Pollution 241, 194–199. https://doi.org/10.1016/j.envpol.2018.05.057

Gore, S., Renforth, P., Perkins, R., 2018. The potential environmental response to increasing ocean alkalinity for negative emissions. Mitigation and Adaptation Strategies for Global Change 24, 1191–1211. https://doi.org/10.1007/s11027-018-9830-z

Gutjahr, A., Dabringhaus, H., Lacmann, R., 1996. Studies of the growth and dissolution kinetics of the $CaCO_3$ polymorphs calcite and aragonite II. The influence of divalent cation additives on the growth and dissolution rates. Journal of Crystal Growth 158, 310–315. https://doi.org/10.1016/0022-0248(95)00447-5

Hamilton, C.P., Spero, H.J., Bijma, J., Lea, D.W., 2008. Geochemical investigation of gametogenic calcite addition in the planktonic foraminifera *Orbulina universa*. Marine Micropaleontology 68, 256–267. https://doi.org/10.1016/j.marmicro.2008.04.003

Hangx, S.J.T., Spiers, C.J., 2009. Coastal spreading of olivine to control atmospheric CO_2 concentrations: A critical analysis of viability. International Journal of Greenhouse Gas Control 3, 757–767. http://dx.doi.org/10.1016/j.ijggc.2009.07.001

Hartmann, J., West, A.J., Renforth, P., Köhler, P., De La Rocha, C.L., Wolf-Gladrow, D.A., Dürr, H.H., Scheffran, J., 2013. Enhanced chemical weathering as a geoengineering strategy to reduce atmospheric carbon dioxide, supply nutrients, and mitigate ocean acidification. Reviews of Geophysics 51, 113–149. https://doi.org/10.1002/rog.20004

Harvey, L.D.D., 2008. Mitigating the atmospheric CO_2 increase and ocean acidification by adding limestone powder to upwelling regions. Journal of Geophysical Research 113 https://doi.org/10.1029/2007JC004373

Heinze, C., Meyer, S., Goris, N., L. Anderson, Steinfeldt, R., Chang, N., Le Quéré, C., Bakker, D., 2015. The ocean carbon sink—Impacts, vulnerabilities and challenges. Earth System Dynamics 6, 327–358. https://doi.org/10.5194/esd-6-327-2015

Henderiks, J., 2008. Coccolithophore size rules — Reconstructing ancient cell geometry and cellular calcite quota from fossil coccoliths. Marine Micropaleontology 67, 143–154. https://doi.org/10.1016/j.marmicro.2008.01.005

Henderson, G., Rickaby, R., Bouman, H., 2008. Decreasing Atmosphere CO_2 By Increasing Ocean Alkalinity, The Ocean Dimension: Would The Concept Work And What Would Be The Environmental Consequences?

Hermoso, M., Godbillot, C., Minoletti, F., 2020. Enhancing Our Palaeoceanographic Toolbox Using Paired Foraminiferal and Coccolith Calcite Measurements From Pelagic Sequences. Frontiers in Earth Science 8, 38. https://doi.org/10.3389/feart.2020.00038

Hermoso, M., Horner, T.J., Minoletti, F., Rickaby, R.E.M., 2014. Constraints on the vital effect in coccolithophore and dinoflagellate calcite by oxygen isotopic modification of seawater. Geochimica et Cosmochimica Acta 141, 612–627. https://doi.org/10.1016/j.gca.2014.05.002

Hillebrand, H., Steinert, G., Boersma, M., Malzahn, A., Meunier, C.L., Plum, C., Ptacnik, R., 2013. Goldman revisited: Faster-growing phytoplankton has lower N:P and lower stoichiometric flexibility. Limnology and Oceanography 58, 2076–2088. https://doi.org/10.4319/lo.2013.58.6.2076

Holland, K., Branson, O., Haynes, L.L., Hönisch, B., Allen, K.A., Russell, A.D., Fehrenbacher, J.S., Spero, H.J., Eggins, S.M., 2020. Constraining multiple controls on planktic foraminifera Mg/Ca. Geochimica et Cosmochimica Acta 273, 116–136. https://doi.org/10.1016/j.gca.2020.01.015

Holland, K., Eggins, S.M., Hönisch, B., Haynes, L.L., Branson, O., 2017. Calcification rate and shell chemistry response of the planktic foraminifer *Orbulina universa* to changes in microenvironment seawater carbonate chemistry. Earth and Planetary Science Letters 464, 124–134. https://doi.org/10.1016/j.epsl.2017.02.018

Honegger, M., Michaelowa, A., Roy, J., 2020. Potential implications of carbon dioxide removal for the sustainable development goals. Climate Policy 0, 1–21. https://doi.org/10.1080/14693062.2020.1843388

House, K.Z., House, C.H., Schrag, D.P., Aziz, M.J., 2007. Electrochemical Acceleration of Chemical Weathering as an Energetically Feasible Approach to Mitigating Anthropogenic Climate Change. Environmental Science and Technology 41, 8464–8470. https://doi.org/10.1021/es0701816

Howes, E.L., Bednaršek, N., Büdenbender, J., Comeau, S., Doubleday, A., Gallager, S.M., Hopcroft, R.R., Lischka, S., Maas, A.E., Bijma, J., Gattuso, J.-P., 2014. Sink and swim: a status review of thecosome pteropod culture techniques. Journal of Plankton Research 36, 299–315. https://doi.org/10.1093/plankt/fbu002

Hunter, K.A., Liss, P.S., Surapipith, V., Dentener, F., Duce, R., Kanakidou, M., Kubilay, N., Mahowald, N., Okin, G., Sarin, M., Uematsu, M., Zhu, T., 2011. Impacts of anthropogenic SO_x, NO_x and NH_3 on acidification of coastal waters and shipping lanes. Geophysical Research Letters 38. https://doi.org/10.1029/2011GL047720

Iglesias-Rodriguez, M.D., Halloran, P.R., Rickaby, R.E.M., Hall, I.R., Colmenero-Hidalgo, E., Gittins, J.R., Green, D.R.H., Tyrrell, T., Gibbs, S.J., Dassow, P. von, Rehm, E., Armbrust, E.V., Boessenkool, K.P., 2008. Phytoplankton Calcification in a High-CO_2 World. Science 320, 336–340. https://doi.org/10.1126/science.1154122

Ilyina, T., Wolf-Gladrow, D., Munhoven, G., Heinze, C., 2013. Assessing the potential of calcium-based artificial ocean alkalinization to mitigate rising atmospheric CO_2 and ocean acidification. Geophysical Research Letters 40, 5909–5914. https://doi.org/10.1002/2013GL057981

IPCC, 2018: Summary for Policymakers. In: Global Warming of 1.5°C. An IPCC Special Report on the impacts of global warming of 1.5°C above pre-industrial levels and related global greenhouse gas emission pathways, in the context of strengthening the global response to the threat of climate change, sustainable development, and efforts to eradicate poverty [Masson-Delmotte, V., P. Zhai, H.-O. Pörtner, D. Roberts, J. Skea, P.R. Shukla, A. Pirani, W. Moufouma-Okia, C. Péan, R. Pidcock, S. Connors, J.B.R. Matthews, Y. Chen, X. Zhou, M.I. Gomis, E. Lonnoy, T. Maycock, M. Tignor, and T. Waterfield (eds.)].

IPCC, Masson-Delmotte, V., Zhai, P., Pirani, A., Connors, S.L., Péan, C., Berger, S., Caud, N., Chen, Y., Goldfarb, L., Gomis, M.I., Huang, M., Leitzell, K., Lonnoy, E., Matthews, J.B.R., Maycock, T.K., Waterfield, T., Yelekçi, O., Yu, R., Zhou, B., 2021. Climate Change 2021: The Physical Science Basis. Contribution of Working Group I to the Sixth Assessment Report of the Intergovernmental Panel on Climate Change. Cambridge University Press.

Jordan, R.W., 2009. Encyclopedia of Microbiology, 3rd ed.

Kheshgi, H.S., 1995. Sequestering atmospheric carbon dioxide by increasing ocean alkalinity. Energy 20, 915–922. https://doi.org/10.1016/0360-5442(95)00035-F

Kısakürek, B., Eisenhauer, A., Böhm, F., Garbe-Schönberg, D., Erez, J., 2008. Controls on shell Mg/Ca and Sr/Ca in cultured planktonic foraminiferan, *Globigerinoides ruber* (white). Earth and Planetary Science Letters 273, 260–269. https://doi.org/10.1016/j.epsl.2008.06.026

Kısakürek, B., Eisenhauer, A., Böhm, F., Hathorne, E.C., Erez, J., 2011. Controls on calcium isotope fractionation in cultured planktic foraminifera, *Globigerinoides ruber* and *Globigerinella siphonifera*. Geochimica et Cosmochimica Acta 75, 427–443. https://doi.org/10.1016/j.gca.2010.10.015

Köhler, P., Abrams, J.F., Völker, C., Hauck, J., Wolf-Gladrow, D.A., 2013. Geoengineering impact of open ocean dissolution of olivine on atmospheric CO_2 , surface ocean pH and marine biology. Environmental Research Letters 8, 014009. https://doi.org/10.1088/1748-9326/8/1/014009

Köhler, P., Hartmann, J., Wolf-Gladrow, D.A., 2010. Geoengineering potential of artificially enhanced silicate weathering of olivine. Proceedings of the National Academy of Sciences 107, 20228–20233. https://doi.org/10.1073/pnas.1000545107

Lackner, K.S., Wendt, C.H., Butt, D.P., Joyce, E.L., Sharp, D.H., 1995. Carbon dioxide disposal in carbonate minerals. Energy 20, 1153–1170. https://doi.org/10.1016/0360-5442(95)00071-N

Langer, G., Geisen, M., Baumann, K.-H., Kläs, J., Riebesell, U., Thoms, S., Young, J.R., 2006. Species-specific responses of calcifying algae to changing seawater carbonate chemistry. Geochemistry, Geophysics, Geosystems 7. https://doi.org/10.1029/2005GC001227

Langer, G., Nehrke, G., Probert, I., Ly, J., Ziveri, P., 2009. Strain-specific responses of *Emiliania huxleyi* to changing seawater carbonate chemistry. Biogeosciences 6, 2637–2646. https://doi.org/10.5194/bg-6-2637-2009

Langer, W.H., San Juan, C.A., Rau, G., Caldeira, K., 2009. Accelerated weathering of limestone for CO_2 mitigation: Opportunities for the stone and cement industries. Mining Engineering 61, 27–32.

LaRoche, J., Rost, B., Engel, A., 2010. Bioassays, batch culture and chemostat experimentation, in: Guide for Best Practices in Ocean Acidification Research and Data Reporting. Publications Office of the European Union, Brussels, pp. 81–94.

Lebrato, M., Iglesias-Rodríguez, D., Feely, R.A., Greeley, D., Jones, D.O.B., Suarez-Bosche, N., Lampitt, R.S., Cartes, J.E., Green, D.R.H., Alker, B., 2010. Global contribution of echinoderms to the marine carbon cycle: $CaCO_3$ budget and benthic compartments. Ecological Monographs 80, 441–467. https://doi.org/10.1890/09-0553.1

Lezaun, J., 2021. Hugging the Shore: Tackling Marine Carbon Dioxide Removal as a Local Governance Problem. Frontiers in Climate 3, 98. https://doi.org/10.3389/fclim.2021.684063

Lombard, F., da Rocha, R.E., Bijma, J., Gattuso, J.-P., 2010. Effect of carbonate ion concentration and irradiance on calcification in planktonic foraminifera. Biogeosciences 7, 247–255. https://doi.org/10.5194/bg-7-247-2010

Lombard, F., Erez, J., Michel, E., Labeyrie, L., 2009. Temperature effect on respiration and photosynthesis of the symbiont-bearing planktonic foraminifera *Globigerinoides ruber*, *Orbulina universa*, and *Globigerinella siphonifera*. Limnology and Oceanography 54, 210–218. https://doi.org/10.4319/lo.2009.54.1.0210

Lu, L., Huang, Z., Rau, G.H., Ren, Z.J., 2015. Microbial Electrolytic Carbon Capture for Carbon Negative and Energy Positive Wastewater Treatment. Environmental Science and Technology 49, 8193–8201. https://doi.org/10.1021/acs.est.5b00875

Manning, D.A.C., 2008. Biological enhancement of soil carbonate precipitation: passive removal of atmospheric CO_2. Mineralogical Magazine, 72(2), 639-649. doi:10.1180/minmag.2008.072.2.639

Marshall, B.J., Thunell, R.C., Spero, H.J., Henehan, M.J., Lorenzoni, L., Astor, Y., 2015. Morphometric and stable isotopic differentiation of *Orbulina universa* morphotypes from the Cariaco Basin, Venezuela. Marine Micropaleontology 120, 46–64. https://doi.org/10.1016/j.marmicro.2015.08.001

Marubini, F., Thake, B., 1999. Bicarbonate addition promotes coral growth. Limnology and Oceanography 44, 716–720. https://doi.org/10.4319/lo.1999.44.3.0716

Moel, H. de, Ganssen, G.M., Peeters, F.J.C., Jung, S.J.A., Kroon, D., Brummer, G.J.A., Zeebe, R.E., 2009. Planktic foraminiferal shell thinning in the Arabian Sea due to anthropogenic ocean acidification? Biogeosciences 6, 1917–1925. https://doi.org/10.5194/bg-6-1917-2009

Montserrat, F., Renforth, P., Hartmann, J., Leermakers, M., Knops, P., Meysman, F.J.R., 2017. Olivine Dissolution in Seawater: Implications for CO_2 Sequestration through Enhanced Weathering in Coastal Environments. Environmental Science and Technology 51, 3960–3972. https://doi.org/10.1021/acs.est.6b05942

Morse, J.W., Arvidson, R.S., 2002. The dissolution kinetics of major sedimentary carbonate minerals. Earth-Science Reviews 58, 51–84. https://doi.org/10.1016/S0012-8252(01)00083-6

Moy, A.D., Howard, W.R., Bray, S.G., Trull, T.W., 2009. Reduced calcification in modern Southern Ocean planktonic foraminifera. Nature Geoscience 2, 276–280. https://doi.org/10.1038/ngeo460

Murray, J.W., 2004. Ocean Carbonate Chemistry: The Aquatic Chemistry Fundamentals, in: Follows, M., Oguz, T. (Eds.), The Ocean Carbon Cycle and Climate, NATO Science Series. Springer Netherlands, Dordrecht, pp. 1–29. https://doi.org/10.1007/978-1-4020-2087-2_1

National Academies of Sciences, Engineering, and Medicine, 2021. A Research Strategy for Ocean-based Carbon Dioxide Removal and Sequestration. The National Academies Press, Washington D.C.

O'Dea, S.A., Gibbs, S.J., Bown, P.R., Young, J.R., Poulton, A.J., Newsam, C., Wilson, P.A., 2014. Coccolithophore calcification response to past ocean acidification and climate change. Nature Communications 5, 5363. https://doi.org/10.1038/ncomms6363

Oviedo, A.M., Langer, G., Ziveri, P., 2014. Effect of phosphorus limitation on coccolith morphology and element ratios in Mediterranean strains of the coccolithophore *Emiliania huxleyi*. Journal of Experimental Marine Biology and Ecology 459, 105–113. https://doi.org/10.1016/j.jembe.2014.04.021

Rau, G.H., 2011. CO_2 Mitigation via Capture and Chemical Conversion in Seawater. Environmental Science and Technology 45, 1088–1092. https://doi.org/10.1021/es102671x

Rau, G.H., 2008. Electrochemical Splitting of Calcium Carbonate to Increase Solution Alkalinity: Implications for Mitigation of Carbon Dioxide and Ocean Acidity. Environmental Science and Technology 42, 8935–8940. https://doi.org/10.1021/es800366q

Rau, G.H., Caldeira, K., 1999. Enhanced carbonate dissolution:: a means of sequestering waste CO_2 as ocean bicarbonate. Energy Conversion and Management 40, 1803–1813. https://doi.org/10.1016/S0196-8904(99)00071-0

Rau, G.H., Carroll, S.A., Bourcier, W.L., Singleton, M.J., Smith, M.M., Aines, R.D., 2013. Direct electrolytic dissolution of silicate minerals for air CO_2 mitigation and carbon-negative H_2 production. PNAS 110, 10095–10100. https://doi.org/10.1073/pnas.1222358110

Rau, G.H., Knauss, K.G., Langer, W.H., Caldeira, K., 2007. Reducing energy-related CO_2 emissions using accelerated weathering of limestone. Energy 32, 1471–1477. https://doi.org/10.1016/j.energy.2006.10.011

Rau, G.H., Willauer, H.D., Ren, Z.J., 2018. The global potential for converting renewable electricity to negative-CO_2-emissions hydrogen. Nature Climate Change 1. https://doi.org/10.1038/s41558-018-0203-0

Raven, J.A., Giordano, M., 2009. Biomineralization by photosynthetic organisms: evidence of coevolution of the organisms and their environment? Geobiology 7, 140–154. https://doi.org/10.1111/j.1472-4669.2008.00181.x

Renforth, P., 2019. The negative emission potential of alkaline materials. Nature Communications 10, 1401. https://doi.org/10.1038/s41467-019-09475-5

Renforth, P., Henderson, G., 2017. Assessing ocean alkalinity for carbon sequestration. Reviews of Geophysics 55, 636–674. https://doi.org/10.1002/2016RG000533

Renforth, P., Jenkins, B.G., Kruger, T., 2013. Engineering challenges of ocean liming. Energy 60, 442–452. http://dx.doi.org/10.1016/j.energy.2013.08.006

Rickaby, R.E.M., Henderiks, J., Young, J.N., 2010. Perturbing phytoplankton: response and isotopic fractionation with changing carbonate chemistry in two coccolithophore species. Climate of the Past 6, 771–785. https://doi.org/10.5194/cp-6-771-2010

Ridgwell, A., Schmidt, D.N., Turley, C., Brownlee, C., Maldonado, M.T., Tortell, P., Young, J.R., 2009. From laboratory manipulations to Earth system models: scaling calcification impacts of ocean acidification. Biogeosciences 6, 2611–2623. https://doi.org/10.5194/bg-6-2611-2009

Riebesell, U., Bellerby, R.G.J., Engel, A., Fabry, V.J., Hutchins, D.A., Reusch, T.B.H., Schulz, K.G., Morel, F.M.M., 2008. Comment on "Phytoplankton Calcification in a High-CO_2 World." Science. https://doi.org/10.1126/science.1161096

Riebesell, U., Schulz, K.G., Bellerby, R.G.J., Botros, M., Fritsche, P., Meyerhöfer, M., Neill, C., Nondal, G., Oschlies, A., Wohlers, J., Zöllner, E., 2007. Enhanced biological carbon consumption in a high CO_2 ocean. Nature 450, 545–548. https://doi.org/10.1038/nature06267

Riebesell, U., Zondervan, I., Rost, B., Tortell, P.D., Zeebe, R.E., Morel, F.M.M., 2000. Reduced calcification of marine plankton in response to increased atmospheric CO_2. Nature 407, 364–367. https://doi.org/10.1038/35030078

Ries, J.B., 2010. Review: geological and experimental evidence for secular variation in seawater Mg/Ca (calcite-aragonite seas) and its effects on marine biological calcification. Biogeosciences 7, 2795–2849. https://doi.org/10.5194/bg-7-2795-2010

Romani, A.M.P., 2011. Cellular magnesium homeostasis. Archives of Biochemistry and Biophysics 512, 1–23. https://doi.org/10.1016/j.abb.2011.05.010

Russell, A.D., Hönisch, B., Spero, H.J., Lea, D.W., 2004. Effects of seawater carbonate ion concentration and temperature on shell U, Mg, and Sr in cultured planktonic foraminifera. Geochimica et Cosmochimica Acta 68, 4347–4361. https://doi.org/10.1016/j.gca.2004.03.013

Sarmiento, J.L., Gruber, N., 2006. Ocean biogeochemical dynamics. Princeton University Press, Princeton, N.J. ; Woodstock.

Schiebel, R., 2002. Planktic foraminiferal sedimentation and the marine calcite budget. Global Biogeochemical Cycles 16, 3–1. https://doi.org/10.1029/2001GB001459

Schuiling, R.D., de Boer, P.L., 2011. Rolling stones; fast weathering of olivine in shallow seas for cost-effective CO_2 capture and mitigation of global warming and ocean acidification. Earth System Dynamics Discussion 2011, 551–568. https://doi.org/10.5194/esdd-2-551-2011

Segev, E., Erez, J., 2006. Effect of Mg/Ca ratio in seawater on shell composition in shallow benthic foraminifera. Geochemistry, Geophysics, Geosystems 7. https://doi.org/10.1029/2005GC000969

Seifritz, W., 1990. CO_2 disposal by means of silicates. Nature 345, 486. https://doi.org/10.1038/345486b0

Sheward, R.M., Poulton, A.J., Gibbs, S.J., Daniels, C.J., Bown, P.R., 2017. Physiology regulates the relationship between coccosphere geometry and growth phase in coccolithophores. Biogeosciences 14, 1493–1509. https://doi.org/10.5194/bg-14-1493-2017

Shi, D., Xu, Y.-K., M M Morel, F., 2009. Effects of the pH/pCO_2 control method on medium chemistry and phytoplankton growth. Biogeosciences 6. https://doi.org/10.5194/bg-6-1199-2009

Silverman, J., Lazar, B., Erez, J., 2007. Effect of aragonite saturation, temperature, and nutrients on the community calcification rate of a coral reef. Journal of Geophysics Research 112, C05004. https://doi.org/10.1029/2006JC003770

Smith, S.V., Key, G.S., 1975. Carbon dioxide and metabolism in marine environments. Limnology and Oceanography 20, 493–495. https://doi.org/10.4319/lo.1975.20.3.0493

Spero, H.J., Bijma, J., Lea, D.W., Bemis, B.E., 1997. Effect of seawater carbonate concentration on foraminiferal carbon and oxygen isotopes. Nature 390, 497–500. https://doi.org/10.1038/37333

Stanley, S.M., Hardie, L.A., 1998. Secular oscillations in the carbonate mineralogy of reef-building and sediment-producing organisms driven by tectonically forced shifts in seawater chemistry. Palaeogeography, Palaeoclimatology, Palaeoecology 144, 3–19. https://doi.org/10.1016/S0031-0182(98)00109-6

Stanley, S.M., Ries, J.B., Hardie, L.A., 2005. Seawater chemistry, coccolithophore population growth, and the origin of Cretaceous chalk. Geology 33, 593–596. https://doi.org/10.1130/G21405.1

Stoll, H.M., Klaas, C.M., Probert, I., Ruiz Encinar, J., Garcia Alonso, J.I., 2002. Calcification rate and temperature effects on Sr partitioning in coccoliths of multiple species of coccolithophorids in culture. Global and Planetary Change, From process studies to reconstruction of the palaeoenvironment: advances in palaeoceanography 34, 153–171. https://doi.org/10.1016/S0921-8181(02)00112-1

Taylor, A.R., Brownlee, C., Wheeler, G., 2017. Coccolithophore Cell Biology: Chalking Up Progress. Annual Review of Marine Science 9, 283–310. https://doi.org/10.1146/annurev-marine-122414-034032

Tyrrell, T., Young, J.R., 2009. Coccolithophores, in: Encyclopedia of Ocean Sciences.

UNCCS, 2019. Climate action and support trends. United Nations Climate Change Secretariat.

White, A.E., Spitz, Y.H., Karl, D.M., Letelier, R.M., 2006. Flexible elemental stoichiometry in *Trichodesmium spp*. and its ecological implications. Limnology and Oceanography 51, 1777–1790. https://doi.org/10.4319/lo.2006.51.4.1777

Wolf-Gladrow, D.A., Zeebe, R.E., Klaas, C., Körtzinger, A., Dickson, A.G., 2007. Total alkalinity: The explicit conservative expression and its application to biogeochemical processes. Marine Chemistry, Special issue: Dedicated to the memory of Professor Roland Wollast 106, 287–300. https://doi.org/10.1016/j.marchem.2007.01.006

Young, J.R., Ziveri, P., 2000. Calculation of coccolith volume and it use in calibration of carbonate flux estimates. Deep Sea Research Part II: Topical Studies in Oceanography 47, 1679–1700. https://doi.org/10.1016/S0967-0645(00)00003-5

Zeebe, R.E., Wolf-Gladrow, D.A., 2001. CO_2 in seawater: equilibrium, kinetics, isotopes, Elsevier oceanography series ; 65. Elsevier, Amsterdam ; London.

Zondervan, I., Rost, B., Riebesell, U., 2002. Effect of CO_2 concentration on the PIC/POC ratio in the coccolithophore *Emiliania huxleyi* grown under light-limiting conditions and different daylengths. Journal of Experimental Marine Biology and Ecology 272, 55–70. https://doi.org/10.1016/S0022-0981(02)00037-0

Zondervan, I., Zeebe, R.E., Rost, B., Riebesell, U., 2001. Decreasing marine biogenic calcification: A negative feedback on rising atmospheric pCO_2. Global Biogeochemical Cycles 15, 507–516. https://doi.org/10.1029/2000GB001321

Statement of Authorship for joint/multi-authored papers for PGR thesis

To appear at the end of each thesis chapter submitted as an article/paper

The statement shall describe the candidate's and co-authors' independent research contributions in the thesis publications. For each publication there should exist a complete statement that is to be filled out and signed by the candidate and supervisor **(only required where there isn't already a statement of contribution within the paper itself).**

Title of Paper	**Chapter 1, Section 1.2:** Introduction to Ocean Alkalinity Enhancement as a Carbon Dioxide Removal Technique
Publication Status	Published
Publication Details	Published as "Enhancing Ocean Alkalinity" Section 5.13, GESAMP (2019). "High level review of a wide range of proposed marine geoengineering techniques". (Boyd, P.W. and Vivian, C.M.G., eds.). (IMO/FAO/UNESCO-IOC/UNIDO/WMO/IAEA/UN/UN Environment/UNDP/ISA Joint Group of Experts on the Scientific Aspects of Marine Environmental Protection). Rep. Stud. GESAMP No. 98, 144 p.

Student Confirmation

Student Name:	Sophie Gill (SG)		
Contribution to the Paper	SG conducted the literature review and wrote Section 5.13. RR edited Section 5.13 before submission to report lead authors.		
Signature		Date	03/01/2022

Supervisor Confirmation

By signing the Statement of Authorship, you are certifying that the candidate made a substantial contribution to the publication, and that the description described above is accurate.

Supervisor name and title: Prof Rosalind E. M. Rickaby		
Supervisor comments: Sophie has stated the authorship clearly.		
Signature: 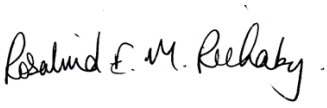	Date	03/01/2022

This completed form should be included in the thesis, at the end of the relevant chapter.

Statement of Authorship for joint/multi-authored papers for PGR thesis

To appear at the end of each thesis chapter submitted as an article/paper

The statement shall describe the candidate's and co-authors' independent research contributions in the thesis publications. For each publication there should exist a complete statement that is to be filled out and signed by the candidate and supervisor **(only required where there isn't already a statement of contribution within the paper itself).**

Title of Paper	**Chapter 1, Section 1.3:** Risks and co-benefits of increased (Earth) Alkaline metal concentrations in the marine environment
Publication Status	Published
Publication Details	Published as "Risks and co-benefits of increased (Earth) Alkaline metal concentrations in the marine environment" in Bach, Lennart T., Sophie J. Gill, Rosalind E. M. Rickaby, Sarah Gore, and Phil Renforth. 'CO2 Removal With Enhanced Weathering and Ocean Alkalinity Enhancement: Potential Risks and Co-Benefits for Marine Pelagic Ecosystems'. Frontiers in Climate 1 (2019).

Student Confirmation

Student Name:	Sophie Gill (SG)		
Contribution to the Paper	SG conducted the literature review with RR and co-wrote the paper section listed above with RR. SG compiled data and undertook calculations to contribute to Table 1.1 of the thesis (published as Table 1 in the paper listed above). SG contributed to edits of the whole paper listed above before submission and acceptance.		
Signature 		Date	03/01/2022

Supervisor Confirmation

By signing the Statement of Authorship, you are certifying that the candidate made a substantial contribution to the publication, and that the description described above is accurate.

Supervisor name and title: Prof Rosalind Rickaby		
Supervisor comments: Sophie has clearly stated the authorship contributions above.		
Signature: 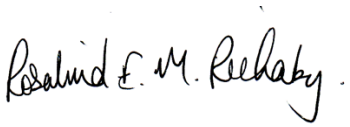	Date	03/01/2022

This completed form should be included in the thesis, at the end of the relevant chapter.

Chapter 2: Meta-analysis of Ocean Carbon Dioxide Removal literature: major focus areas for research identified using elimination criteria

Sophie J. Gill, James Gately, Wil Burns and Lydia Kapsenberg

2.1 Introduction

Achieving international climate goals increasingly relies on removing legacy emissions of carbon dioxide (CO_2) from the atmosphere (IPCC, 2021; Minx et al., 2018; Fuss et al., 2018; Nemet et al., 2018). Carbon Dioxide Removal (CDR) will be required on the order of 100-1000 Gt CO_2 before 2100 to limit global warming to 1.5 ^oC above pre-industrial levels (IPCC, 2018: Summary for Policymakers). CDR technologies may even need to be deployed in this decade to limit warming to 2 ^oC (Rogelj et al., 2015). There is thus a pressing need for robust and responsible research on all CDR approaches.

Across CDR methods, the ocean has received little attention despite its role as a major carbon sink. The ocean currently sequesters approximately a quarter of our CO_2 emissions each year, or ~2.9 Gt C/year (Watson et al., 2020; Friedlingstein et al., 2021). For context, the ocean's carbon reservoir is ~38,000 Gt C with a capacity to contain much more. In addition, seawater C concentration is approximately 45 times greater than the atmosphere (Renforth and Henderson, 2017), making seawater an attractive medium for CDR. Several natural processes, both biological and geological, draw atmospheric CO_2 into the ocean and could theoretically be boosted. Given the untapped capacity of the ocean's carbon reservoir and its potentially malleable function as a carbon sink, the ocean has recently risen as a critical component of the climate solution (Gattuso et al., 2018; Gattuso et al., 2021; National Academies of Sciences, Engineering, and Medicine, 2021; GESAMP; 2019). Funding is increasing, as philanthropy is funding research (Gagern and Kapsenberg, 2021; Gagern et al., 2019), and the public sector is investing in research projects and start-ups. Coordinated

research efforts are emerging, for example, with the advent of the OceanVisions roadmaps and the launch of the oceanCDR.net website in August 2020.

Ocean Iron Fertilization (OIF)	Adding iron (Fe) to the ocean to increase net primary production.
Macronutrient Fertilization	Ocean Macronutrient fertilization. Adding nitrate (N) or phosphate (P) to the ocean to increase net primary production.
Artificial Upwelling	Upward transport of deep nutrient-rich waters to increase net primary production.
Artificial Downwelling	Downward transport of CO_2-saturated surface waters to accelerate CO_2 equilibration with the deep ocean.
Macroalgal Cultivation	Cultivation and harvest of macroalgae as a means to remove CO_2 from surface waters.
Alkalinity Enhancement	Addition of alkaline minerals to seawater to increase alkalinity and so increase CO_2 solubility and carbon storage. Includes electrochemical production of alkalinity e.g. via electrolysis.
Electrochemical CO_2 removal	Sometimes referred to as "Indirect ocean capture", any mCDR process involving electrochemical removal of CO_2 from air by shifting the pH of seawater, with the end goal to desorb CO_2 gas.
Electrochemical $CaCO_3$ approach	Sometimes referred to as "Indirect ocean capture", any mCDR process involving electrochemical removal of CO_2 from air by shifting the pH of seawater, with the end goal to precipitate solid $CaCO_3$.
Deep storage	Use of the ocean's deep stable layers, seafloor, and sediment to store liquid CO_2, organic carbon, or other carbon rich materials.

Box 2.1: Definitions of each of the mCDR approaches analysed during this study.

Ocean-based CDR approaches, also referred to as 'marine CDR' (mCDR from hereon), includes all CDR approaches conducted in coastal and open ocean waters (National Academies of Sciences, Engineering, and Medicine, 2021). Approaches can generally be categorized into either biological or abiotic (chemical/physical) methods (see **Box 2.1**). Approaches that rely on a biological means of CDR include Ocean Iron Fertilization (OIF), Macronutrient Fertilization, Artificial Upwelling, Macroalgal Cultivation, and Blue Carbon Management (GESAMP, 2019; Energy Futures Initiative, 2020; National Academies of Sciences, Engineering, and Medicine, 2019). Approaches that rely on abiotic processes include Alkalinity Enhancement, Artificial Downwelling, Deep Storage (e.g. using the ocean's stable deep layers or seafloor), and Direct Capture (of dissolved carbon from seawater) (GESAMP, 2019; Energy Futures Initiative, 2020; National Academies of Sciences, Engineering, and Medicine, 2021). These approaches vary greatly in terms of research maturity. However, mCDR approaches have already gained considerable traction in the

private sector, and several dozen startups have emerged based on still unvetted mCDR approaches. There is an imperative need to rapidly and extensively scale research efforts on mCDR to make decisions on implementation within the coming decade (National Academies of Sciences, Engineering, and Medicine, 2021).

Several criteria must be met for any given mCDR approach to be implemented. The mCDR approach must:

(1) remove (or store) atmospheric CO_2 on a climate-relevant timescale (i.e. >100 years for sequestration (Passow and Carlson, 2012)),

(2) be quantifiable, including any relevant positive or negative feedbacks that may lead to CO_2 "leakage",

(3) keep within a, yet to be determined, acceptable level of environmental impacts,

(4) be financially viable,

(5) fit within a coherent legal/governance framework, and

(6) be accepted by society and local communities, with positive impacts on environmental justice (i.e., JEDI [Justice Equity Diversity and Inclusion]) (GESAMP, 2019; Bach, 2021; Energy Futures Initiative, 2020).

There is currently no standardized international framework to assess these criteria, despite several reviews using variations on these criteria to evaluate the state of research into mCDR (GESAMP, 2019; National Academies of Sciences, Engineering, and Medicine, 2021). To deliver a data-driven overview of the state of knowledge on these criteria, we conducted a meta-analysis on mCDR literature to assess the research maturity of the mCDR field and provide a high-level view of knowledge gaps in the context of these "elimination" criteria outlined above.

2.2 Methods

The Carbon Dioxide Removal/Negative Emissions Technologies Bibliography (https://cprclimate.org/bibliography-carbon-dioxide-removal-negative-emissions-technologies/) was used to access literature on mCDR. This is a public database hosted by the Climate Protection & Restoration Initiative and includes all CDR research publications.

The database was imported to Zotero and filtered for mCDR keywords using the Zotero advanced search function coupled with the Zotero function for complex Boolean searches. The following mCDR approaches were included: Ocean Iron Fertilization (OIF), Macronutrient (Nitrogen and Phosphorus) Fertilization, Alkalinity Enhancement (including Ocean Alkalinity Enhancement [OAE], Enhanced Weathering [EW] and Electrochemical approaches), Deep Storage, Artificial Upwelling, Artificial Downwelling, and Macroalgal Cultivation. We include Deep Storage because deep-storage approaches, such as direct injection and crop residue burial, site the marine environment as the destination of carbon removal. Many terminologies exist to describe mCDR approaches (**Box 2.1**), and a range of search terms was used to identify relevant mCDR publications in the bibliography (see **Appendix 1**). Searches and subsequent ground-truthing were conducted per guidelines set out for robust meta-analysis set out in Tawfik et al. (2019), Minx et al. (2018) and Coelho et al. (2014), full details of which can be found in **Appendix 1**. Blue carbon management was not included as an mCDR approach in our study because blue carbon management refers to the conservation and restoration of natural carbon sinks, and scalability is limited (Taillardat et al., 2018).

Only peer-reviewed publications that (i) actively contribute to advancing the field of knowledge in intentional mCDR by contributing knowledge on any of the elimination criteria, or (ii) cover natural mCDR studied with the explicit aim of application to future intentional mCDR were selected for this study (see **Appendix 1** for full details). For each publication that met these criteria, the following metadata was collected: the mCDR approach (**Box 2.1**), research topic (technology, environmental, finance, governance, social), and research type (conceptual, model, lab, field). Research types were grouped into 3 broad categories:

Meta-data	Possible tags	Description
mCDR approach	Ocean Iron Fertilization (OIF)	See **Box 2.1**.
	Macronutrient Fertilization	
	Artificial Upwelling	
	Artificial Downwelling	
	Macroalgal Cultivation	
	Alkalinity Enhancement	
	Electrochemical CO_2 removal	
	Electrochemical $CaCO_3$ approach	
	Deep storage	
Biotic or abiotic	Biotic	mCDR approach that uses the biological pump to draw down atmospheric CO_2.
	Abiotic	mCDR approach which uses the ocean's abiotic pumps, (the solubility and carbonate pumps) to draw down atmospheric CO_2.
	Both	Publication covers approaches which make use of both the biotic and abiotic ocean pumps to draw down atmospheric CO_2.
Research topic	Technology	Any technological aspect of mCDR on climate-relevant timescales, including basic research (theoretical, lab, field, modelling, etc.) and data-related topics.
	Environmental	mCDR effects on biota, and the abiotic environment.
	Environmental (biotic)	Subcategory to note when the effects discussed in the publication are on biota e.g. coral calcification, nutrient availability.
	Environmental (abiotic)	Subcategory to note when the effects discussed in the publication are on the abiotic environment e.g. pH or other physico-chemical changes.
	Governance	Any regulatory aspect of mCDR research, implementation, production, and monitoring, including policy and governing bodies.
	Governance (international)	Subcategory to note when governance issues discussed in the publication are at an international level.
	Governance (national)	Subcategory to note when governance issues discussed in the publication are at a national level.
	Governance (subnational)	Subcategory to note when governance issues discussed in the publication are at a sub-national level e.g. regional, local.
	Finance	Commercial and financial aspects, including carbon markets, associated supply chains, incentives, costs, and profits. Papers were classified as "finance" for any discussion related to economic matters listed above, and may not necessarily have provided an estimate of CDR cost.
	Social	Aspects related to societal approval of mCDR, including education, outreach, public opinion, and media communications.
	Social (public perception)	Subcategory to note when social issues discussed in the publication cover societal approval/public perception of mCDR.
	Social (JEDI)	Subcategory to note when social issues discussed in the publication cover environmental justice (Justice, Equality, Diversity and Inclusion).
Research type	Conceptual	Publications which propose an mCDR idea, including comment articles, perspectives, etc.
	Model	Publications which model the processes, outcomes and impacts of mCDR approaches.
	Field	Publications which conduct field trials to investigate the processes, outcomes and impacts of mCDR approaches.
	Lab	Publications which conduct lab experiments to investigate the processes, outcomes and impacts of mCDR approaches.
	Review	Publications which synthesise and collate data/information on mCDR approaches.
CDR potential		The carbon drawdown potential of the mCDR approach, if provided in the paper e.g. Gt C/yr or Gt CO_2/yr.
CDR cost		The financial cost of the mCDR approach, if provided in the paper e.g. USD/t CO_2 drawdown.

Table 2.1: Summary of all meta-data collected during this study.

(i) Discussion (conceptual and review papers), (ii) Empirical (papers that report lab and field observations), and (iii) modeling studies. Meta-data was also collected on the CDR drawdown potential, cost estimate, and sub-categories of research topics. See **Table 2.1** for a complete list of descriptions used in metadata collection.

The data were analyzed in R version 4.1.2, and RStudio 2021.09.0 Build 351. Given a large volume of publications on OIF, data were analyzed both in the presence and absence of publications with a sole focus on OIF. Results are presented in two groups: (i) "All" indicates publications on any mCDR study, including OIF, and (ii) "OIF only excluded" indicates the exclusion of mCDR publications in which OIF was the sole focus. The percentages calculated in this manuscript reflect the percentage of total observations, which we refer to as "counts" (N), rather than the total number of publications (n). We have made this distinction to account for publications that cover more than one mCDR approach, topic, or type: each contributing multiple observations to the overall summary count.

2.3 Results

2.3.1 Broad-scale publication trends

Between March 1977 and July 2021, a total of 349 mCDR research publications were released in peer-reviewed journals (**Figure 2.1a**). The overall publication trend for this field of research is driven by publications that cover only OIF (n=208), which make up 57.4% (*N*=234) of all counts (**Figure 2.1b**). Following OIF, the second most studied mCDR approach is Alkalinity Enhancement (14.5%, *N*=59). This is the only approach that exhibits an increasing annual observation (count) rate since 2015 (**Figure 2.2**). Alkalinity Enhancement is followed by Deep Storage (9.6% of counts, *N*=39), with a steady publication rate of 1-5 publications per year since 2015. All other mCDR approaches combined make up less than 20% (*N*=71) of mCDR counts between 1977-2021, with each approach contributing a maximum of 2 publications per year since 2015.

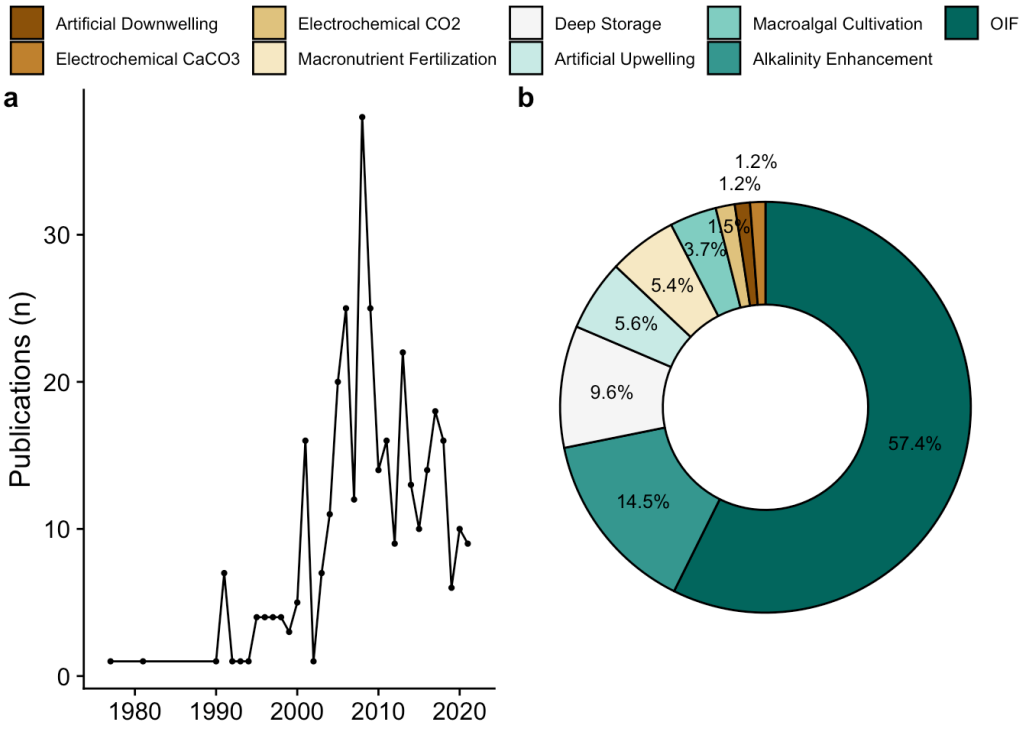

Figure 2.1: Published studies (1977-2021) that assessed – experimentally or theoretically – the use, or potential use, of mCDR approaches. (a) A time series of published studies (n) that assessed any one, or combination, of the noted mCDR approaches. (b) The percentage that each technological approach contributed to total mCDR studies over the length of the time series in Figure 2.1a. Percentages in Figure 2.1b are calculated using summary counts (*N*); as such, individual studies may contribute to the calculated percentage for multiple approaches.

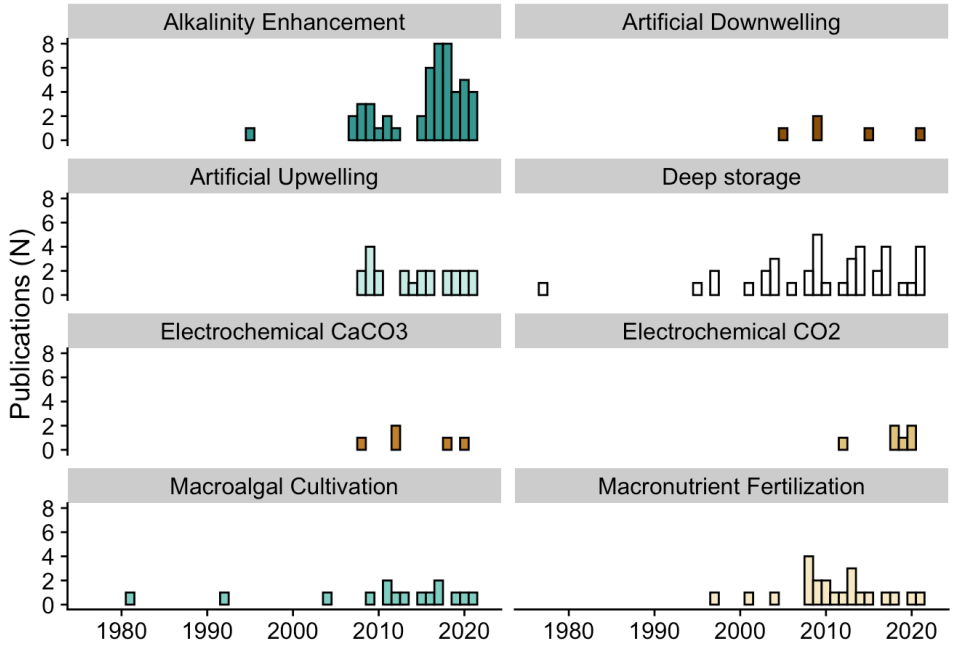

Figure 2.2: Publications (*N*) of mCDR approach publications by year (1977-2021). All OIF studies have been excluded.

Empirical studies occupy a large portion of the literature, contributing 42.7% of mCDR counts (*N*=160) (**Figure 2.3**). However, this trend is driven by the large amount of fieldwork on OIF. Excluding OIF studies, only 20.3% (*N*=31) of mCDR counts are based on empirical work (i.e., lab or field observations, primary research); this represents publications covering seven different mCDR approaches. In other words, 79.7% (*N*=122) of mCDR literature excluding OIF is based on secondary research, (i.e. discussion or modeling) rather than based on direct observation/primary research (empirical). Of this 79.7%, 42.5% (*N*=65) of counts are modeling publications, and 37.2% (*N*=57) are discussion counts.

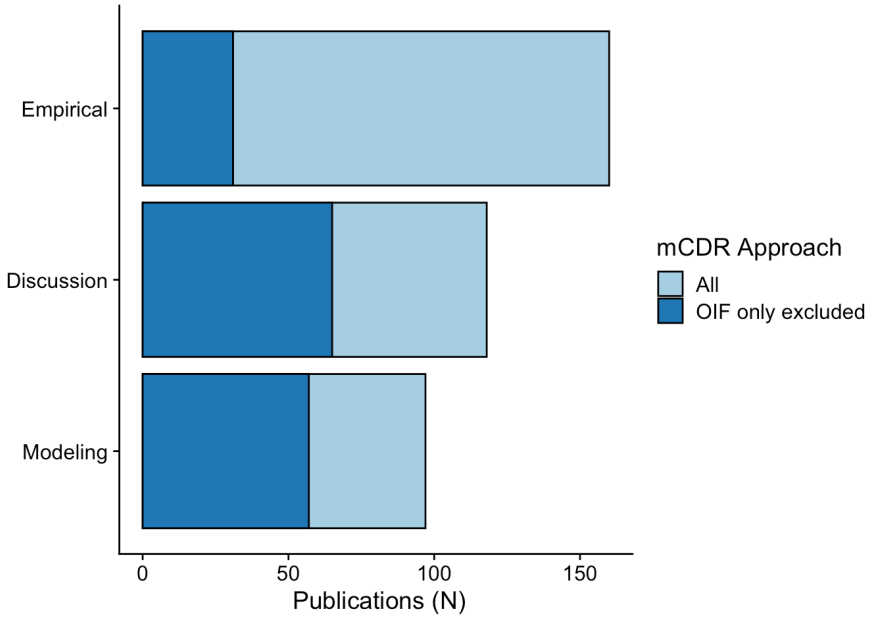

Figure 2.3: Publications (*N*) as a function of the type of data produced (1977-2021): Empirical indicates lab or field studies, Discussion indicates conceptual or review studies, Modeling indicates model-based studies. mCDR approaches are grouped in two ways: (1) **All** indicates the inclusion of any mCDR study, (2) **OIF only excluded** indicates the exclusion of studies in which OIF is the sole technology discussed.

Within modeling and empirical research, modeling counts far outweigh lab and field counts combined for all mCDR approaches when excluding OIF publications (**Figure 2.4**). Excluding counts of Discussion studies, of 37 counts (*N*) covering Alkalinity Enhancement, nearly three-quarters (73.7%) are modeling counts, compared to only 26.3% empirical counts (18.4% lab counts and 7.9% field counts). This trend of modeling outweighing empirical (lab and field) research is also emulated in data from Deep Storage, Artificial Upwelling, and Macronutrient

Fertilization publications. Still, the total number of publications for these approaches is lower than for OAE (**Figure 2.4**). Macroalgal Cultivation contrasts the other mCDR approaches in that field studies make up the majority (57.1%) of counts compared to lab and modeling counts. Notably, no field studies were found for Electrochemical CO_2 removal approaches, Electrochemical $CaCO_3$ approaches, or Artificial Downwelling.

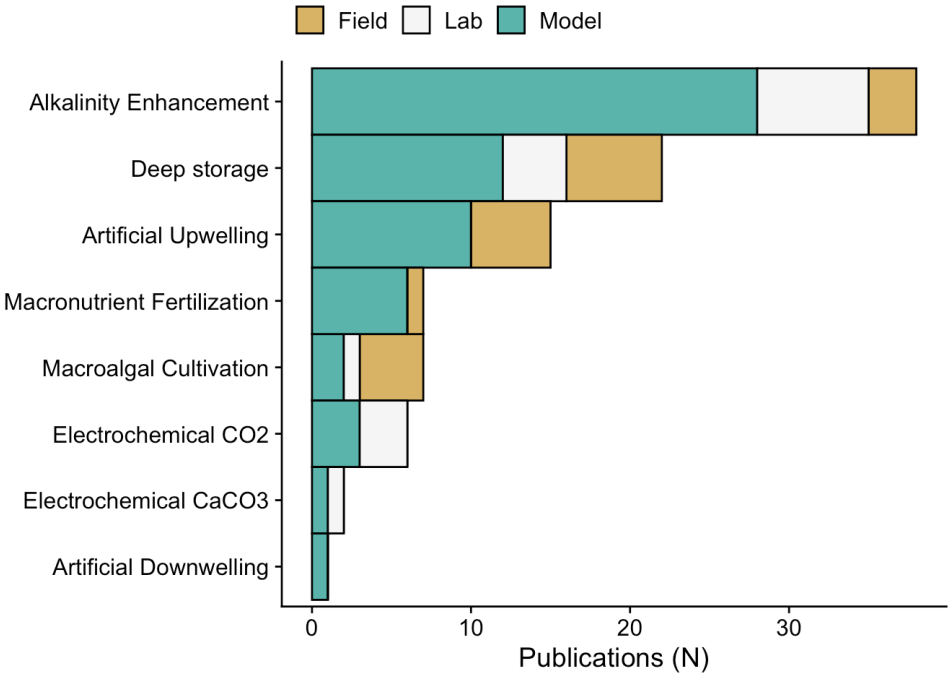

Figure 2.4: Publications (*N*) represented in the literature as a function of mCDR approach (excluding OIF studies). Any publication that was marked **exclusively** as a review and/or conceptual study was excluded. Publications that were not exclusively reviews and/or conceptual studies were included; however, the review and conceptual categories were likewise excluded from the plot.

2.3.2 Publication trends according to elimination criteria

Each of the six "elimination" criteria we have identified (see **Introduction**) can be correlated with specific meta-data we have collected, which allows us to elucidate the relative contribution of knowledge of each mCDR approach to the "elimination" criteria (**Table 2.2**). The literature covering the mCDR approaches of Electrochemical CO_2 removal, Electrochemical $CaCO_3$ and Artificial Downwelling all have <10 counts (*N*) overall contributing to the "elimination" criteria. This is notably many fewer than the rest of the mCDR approaches counts presented in **Table 2.2**.

Elimination Criteria	OIF	Alkalinity Enhancement	Deep Storage	Artificial Upwelling	Macronutrient Fertilization	Macroalgal Cultivation	Electrochemical CO2	Electrochemical CaCO3	Artificial Downwelling
Technology	191 (38%)	48 (33%)	32 (41%)	21 (40%)	20 (35%)	14 (38%)	4 (44%)	4 (40%)	4 (50%)
CDR potential	63 (13%)	37 (25%)	14 (18%)	11 (21%)	12 (21%)	10 (27%)	1 (11%)	2 (20%)	2 (25%)
Environmental	180 (36%)	31 (21%)	14 (18%)	12 (23%)	11 (19%)	8 (22%)	0 (0%)	0 (0%)	0 (0%)
CDR cost	19 (4%)	17 (12%)	5 (6%)	2 (4%)	6 (11%)	2 (5%)	4 (44%)	4 (40%)	0 (0%)
Governance	29 (6%)	7 (5%)	6 (8%)	3 (6%)	4 (7%)	2 (5%)	0 (0%)	0 (0%)	0 (0%)
Social	18 (4%)	7 (5%)	7 (9%)	3 (6%)	4 (7%)	1 (3%)	0 (0%)	0 (0%)	2 (25%)

Table 2.2: mCDR elimination criterion by mCDR approach (1977-2021). Review and conceptual papers have been included. The numbers values outside of the parentheses represent counts (n) for individual mCDR approaches; each criterion's percentage of the approaches' summary count (*N*) is shown in parentheses. Publications are not necessarily exclusive to one mCDR approach; as such, publications may contribute to multiple summary counts.

For all mCDR approaches, the portion of research covering the Technology "elimination" criteria (which indicates that a paper examines the scientific basis for climate-relevant timescales of mCDR; "elimination" criteria 1) relative to other "elimination" criteria is between 30-40% (**Table 2.2**). The share of papers examining this "elimination" criteria does not vary between approaches as much as the share of papers examining the other "elimination" criteria (**Table 2.2**).

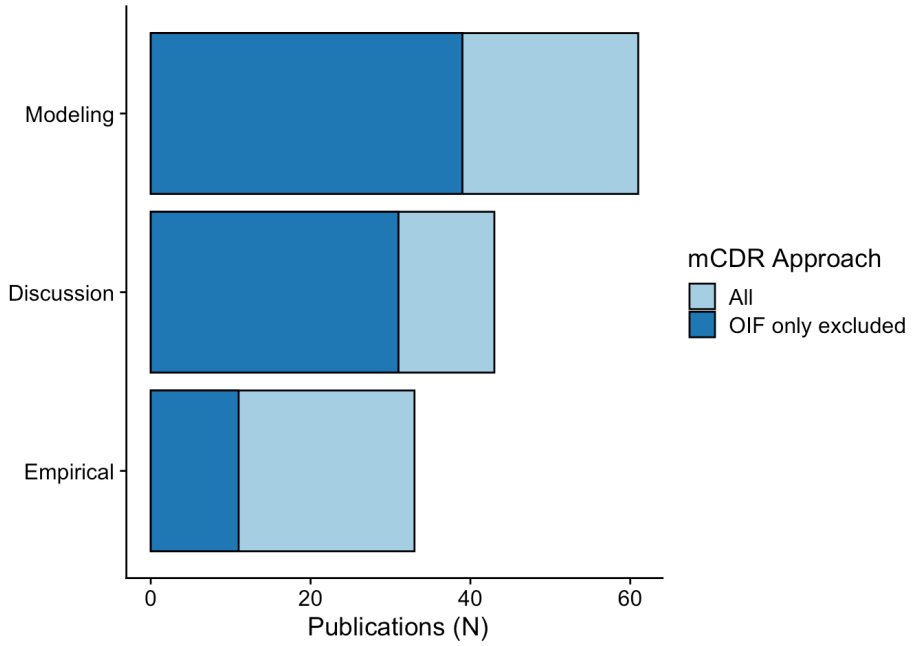

Figure 2.5: Publications (*N*) reporting CDR potentials (1977-2021). Empirical includes lab and field studies; discussion includes conceptual and review studies; modeling includes model-based studies. mCDR approaches are grouped in two ways: (1) **All** indicates the inclusion of any mCDR study, (2) **OIF only excluded** indicates the exclusion of studies in which OIF is the sole technology discussed.

Deep Storage, Alkalinity Enhancement, Artificial Upwelling, Macronutrient Fertilization and Macroalgal Cultivation all have ~20-25% coverage of quantifiable mCDR potential ("elimination" criteria 2) being provided across their respective bodies of literature (**Table 2.2**). By contrast, OIF has only 13% (*N*=63) % (*N*=5) coverage of this "elimination" criteria. However, the total number of papers covering OIF overall dwarfs the contribution of the other mCDR approaches combined. Less than half of mCDR publications overall provide quantifiable measurements or estimates on CO_2 fixation and/or storage of a given mCDR approach. 35.5% (*n*=124) of all mCDR publications report a quantitative mCDR potential (**Figure 2.5**). Of those 124 publications, 24.1% (*N*=33) are based on empirical (lab and field) data, with the remainder

consisting of discussion and modeling counts. When excluding OIF publications, only 13.5% (*N*=11) of counts reporting CDR potential are based on empirical observations (lab and field studies).

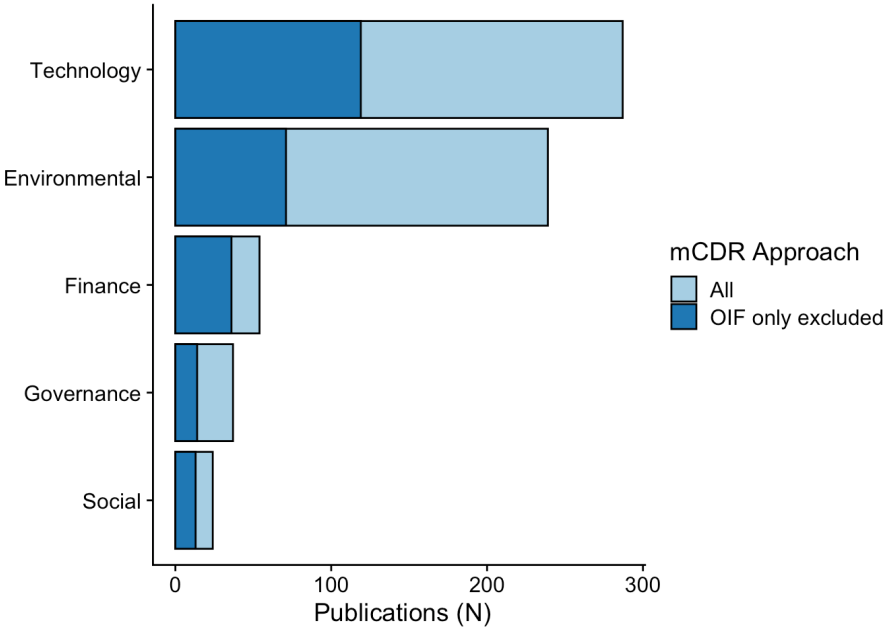

Figure 2.6: Summary counts (*N*) as a function of mCDR keyword (1977-2021). mCDR publications are grouped in two ways: (1) **All** indicates the inclusion of any mCDR study, (2) **OIF only excluded** indicates the exclusion of studies in which OIF is the sole technology discussed.

In terms of the research topics covered in the mCDR literature, most mCDR publications focus on technological and environmental topics (**Figure 2.6**), which is also reflected in the counts presented in **Table 2.2**. OIF has the highest relative contribution to environmental impacts ("elimination" criteria 3) of 36% (*N*=180) (**Table 2.2**). Alkalinity Enhancement, Deep storage, Artificial Upwelling, Macronutrient Fertilization and Macroalgal Cultivation all have comparable coverage of environmental impacts, at about 20% (**Table 2.2**). Of the total environmental impact counts however, 76.0% (*n*=152) focus on OIF, followed by Alkalinity Enhancement (11.5%, *n*=23). This shows how little overall levels of research on environmental impacts have been done on other mCDR approaches. Environmental research is generally evenly split between impacts on biota and the abiotic environment (**Figure 2.7**).

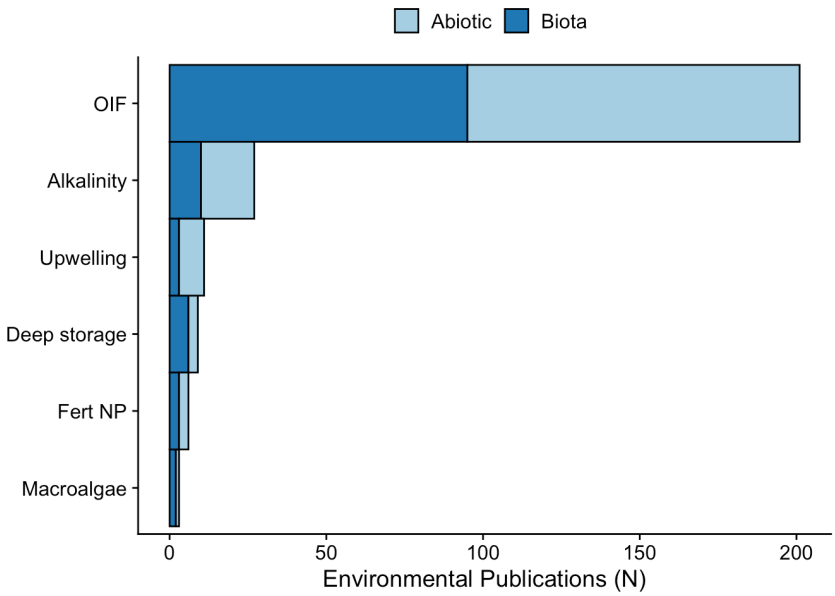

Figure 2.7: Summary counts (*N*) of mCDR environmental studies that assessed the effects, or potential effects, of technological approaches on either biota or the abiotic environment (1977-2021). Reviews and conceptual studies have been excluded. Technological approaches that are excluded here had no "keyword environmental" studies.

The count of publications covering finance, governance and social aspects are low compared to technological and environmental factors (**Figure 2.6**). This trend is similar with or without the exclusion of OIF publications.

54 publications (n) report on aspects of mCDR finance across all mCDR approaches. Despite OIF being the largest contributor of papers to the mCDR literature, only 4% (*N*=19) of literature on OIF reports a specific CDR cost ("elimination" criteria 4) (**Table 2.2**). ~10% or less of Alkalinity Enhancement (*N*=17), Deep Storage (*N*=5), Artificial Upwelling (*N*=2), Macronutrient Fertilization (*N*=6) and Macroalgal Cultivation (*N*=2) literature report a specific CDR cost (**Table 2.2**). Interestingly, despite being very small bodies of literature overall, ~40% of the literature covering Electrochemical CO_2 removal and Electrochemical $CaCO_3$ approaches reports a specific CDR cost (**Table 2.2**). It is worth noting however that this amounts to only 4 papers apiece, relative to the 19 and 17 papers for OIF and OAE, respectively. There are no specific cost estimates reported in any Artificial Downwelling papers.

Governance ("elimination" criteria 5) publications most often discuss the international (high-seas) landscape (63.6%, *N*=35), followed by national (29.1%, *N*=16), and then subnational

(regional or local) systems (7.3%, *N*=4) of governance (**Figure 2.8**). OIF dominates governance publications, but trends on primary focus at international, national, regional, and local governance systems are similar when OIF publications are excluded. Even though OIF dominates the trends in governance publications, governance publications only make up 6% (*N*=29) of the OIF literature base (**Table 2.2**). All other mCDR approaches have 5% or fewer governance papers of their total published literature, but with much lower overall total counts (i.e. $N < 10$). Electrochemical CO_2 removal, Electrochemical $CaCO_3$ approaches, and Artificial Downwelling have no governance publication record (**Table 2.2**).

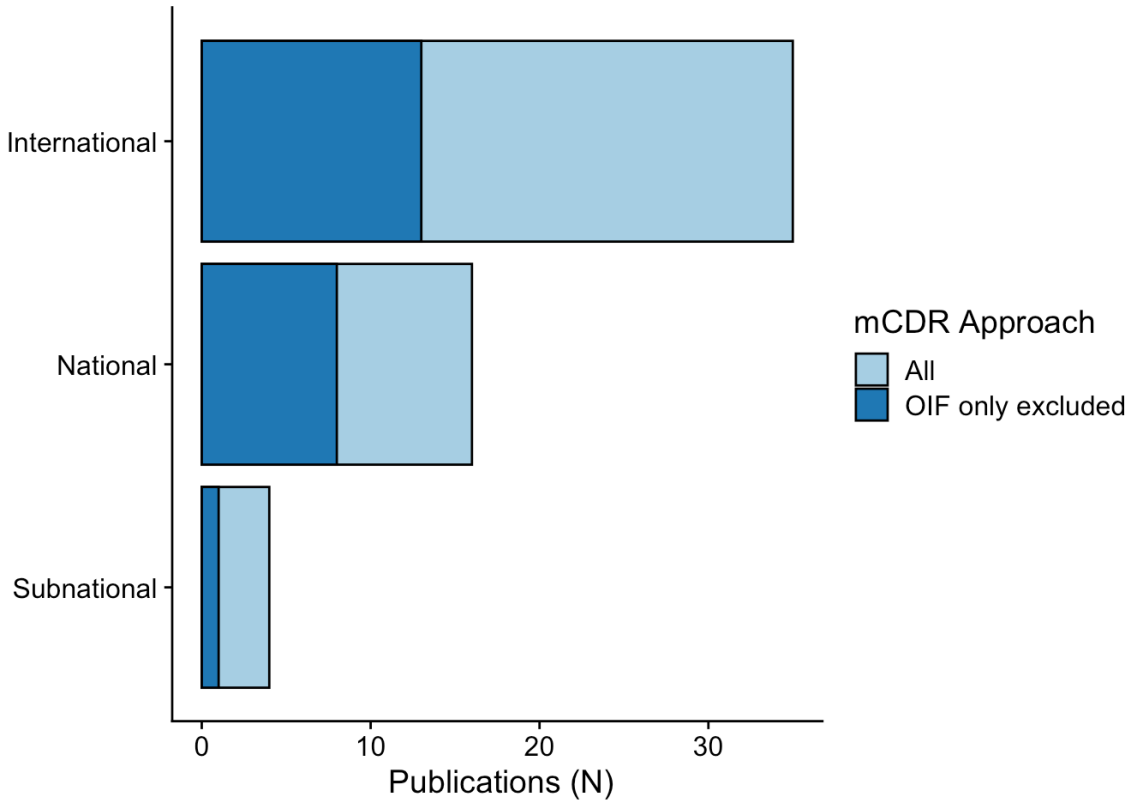

Figure 2.8: Summary counts (*N*) of mCDR governance as a function of governance level (1977-2021).

There are only 24 (n) publications that cover social issues, mainly consisting of research on public perceptions of mCDR and only a few on JEDI-related (Justice, Equity, Diversity, and Inclusion) topics (**Figure 2.9**). However, these publications do not necessarily present research on this topic, and at minimum, may only mention or speculate on social implications.

When discussion papers are excluded, only four publications contribute data on social license. Of these four, one is exclusive to OIF. All mCDR approaches only contribute publications on social aspects as <10% of their publication record, except for Artificial Upwelling, which contributes 25%, but Artificial Upwelling only has 8 counts total in **Table 2.2**.

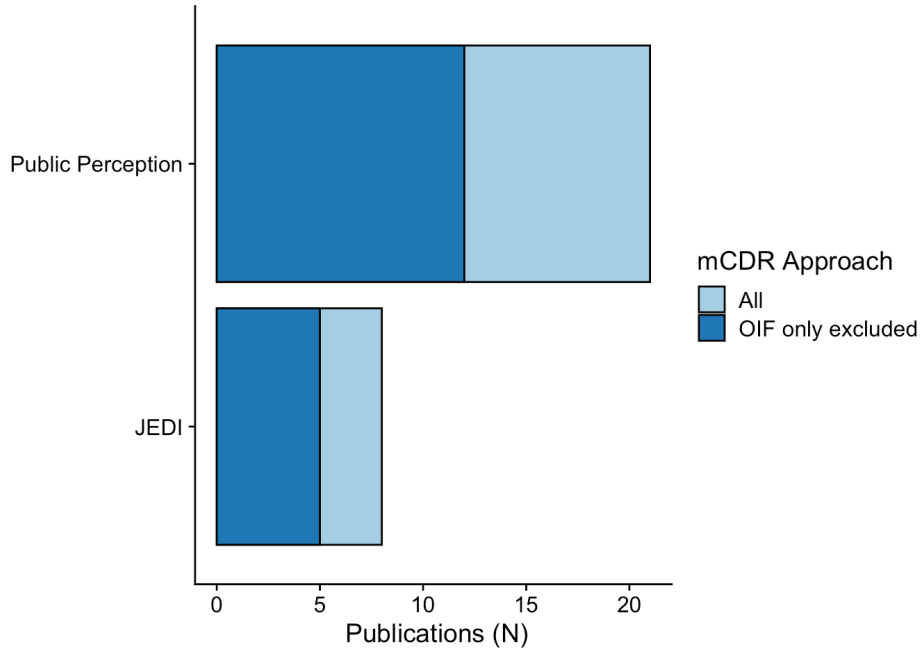

Figure 2.9: Summary counts (*N*) of mCDR social publications based on whether public perception or justice, equity, diversity and inclusion (JEDI) was the focus of study (1977-2021).

2.4 Discussion

2.4.1 The trajectory of OIF research can inform strategy for mCDR advancement

The research field on mCDR is exceptionally nascent. Most research is theoretical, highlighted by the large proportion (37.2%) of discussion papers. Additionally, all mCDR techniques other than OIF and Alkalinity Enhancement contribute overall very low counts of publications to the "elimination" criteria. To better understand the research gaps, we can turn to the progression of OIF research as the more mature mCDR pathway and interpret if/how the research strategy for the other mCDR approaches needs to be modified.

There is generally a large focus in OIF literature on "elimination" criteria 1 (Technology) and 3 (Environmental), but a proportionally small number of publications providing a quantified CDR

potential ("elimination" criteria 2) and minimal number on cost ("elimination" criteria 4), governance ("elimination" criteria 5), and finance ("elimination" criteria 6).

The lack of focus in the OIF literature on finance, governance, and social acceptability studies highlights a potentially rate-limiting step in advance towards credible deployment of mCDR approaches. The concept of "elimination" criteria for mCDR approaches dictates that even if all of the aspects of technological, environmental, and quantification of carbon drawdown were fully researched for a given mCDR approach, it would not be feasible and low-risk enough to consider larger-scale deployment if even one of the critical criteria is not satisfied. Despite the large body of research into OIF, it is still unclear whether OIF could or could not be successfully used for mCDR in a large-scale scheme (Buesseler et al., 2008; Bertram, 2011; Boyd and Vivian, 2019). We suggest that this may be partially explained by the imbalanced contribution of OIF literature to the 6 key "elimination" criteria we have identified. Therefore, it follows that a recommendation arising from our work is that future primary research into mCDR approaches should aim to fill the knowledge gaps in the "elimination" criteria. Currently, none of the mCDR techniques covered in our study shows an equal spread of published literature covering all 6 "elimination" criteria.

2.4.2 A rate-limiting step for advancement of mCDR: finance, governance and social aspects

There is an overall lack of focus on finance, governance and social aspects of research reflected in all mCDR approaches, not just OIF. To more efficiently arrive at a consensus on deployment (than OIF) while accumulating a large body of knowledge, it will be necessary to address this gap in three "elimination" criteria.

Interestingly, despite having a tiny number of publications as a whole, 44% of Electrochemical CO_2 removal publications and 40% of Electrochemical $CaCO_3$ approach papers provide an estimate of CDR cost. This could be due to a higher proportion of industrial investment in these two approaches (e.g. Stripe Fall purchasing round, 2021), indicating that cross-cutting research spanning academic and industry research may help accelerate addressing

"elimination" criteria, particularly concerning finance. It is important not to place too much weight on the low number of overall counts for these processes, however, because OIF and Alkalinity Enhancement have ~4 times as many CDR cost publications.

More broadly missing from the governance literature as a whole, across all mCDR approaches, is a focus on national and sub-national modes of governance. The international level, which currently comprises the bulk of the literature, will be necessary for effective governance strategies. However, there is still a pressing need for international legislation specific to mCDR (Wilson, 2014; Rayfuse et al., 2008; GESAMP, 2019). Additionally, it has been identified that many mCDR approaches will not operate purely on a "high-seas" scale but will work within national, regional, and local boundaries. For example, Alkalinity Enhancement may happen in discrete ocean basins or specific coastal areas.

Of particular note for social aspects is that research on climate justice and public acceptability is almost absent from the published literature across all mCDR approaches.

2.4.3 Field trials will be necessary to address elimination criteria

Only 13.5% of quantified mCDR potential estimates ("elimination" criteria 2) provided in the mCDR literature, across all approaches, are based on empirical (lab and field) data, excluding OIF. In many ways, this is the critical type of mCDR potential to allow for the advancement of a given mCDR approach. Empirical estimates provide complimentary proof in practice of predictive mCDR potential estimates provided in discussion and modeling publications. Therefore, our meta-analysis has identified an evidence-driven motivation for pursuing field trials to demonstrate the efficacy of mCDR approaches.

2.4.4 Supporting a strategic research agenda

Our meta-analysis supports recent recommendations published by the National Academies of Sciences, Engineering, and Medicine (2021) to conduct research into multiple mCDR approaches in parallel and prioritise field trials of mCDR approaches sequentially following laboratory-scale demonstrations. NASEM identify OIF, Macroalgal (seaweed) Cultivation and Alkalinity Enhancement as the most promising mCDR approaches, based on the available

evidence. Our meta-analysis confirms that Alkalinity Enhancement, in particular, occupies the largest proportion of the mCDR literature after OIF.

While Alkalinity Enhancement has relatively little field and lab data according to our analysis, it has been well-constrained during modeling studies (Köhler et al., 2010; Köhler et al., 2013; Ilyina et al., 2013; House et al., 2007; Harvey, 2008). It has a good potential for co-benefits to marine ecosystems as it draws down atmospheric CO_2 and counteracts ocean acidification (Meysman and Montserrat, 2017). A critical risk that has been identified within the Alkalinity Enhancement literature is that calcifiers (any biological organism which constructs its body using $CaCO_3$) may contribute to "leakage" of CO_2 if increased alkalinity levels drive an increase in calcification rates because calcification releases CO_2 as a by-product (Bach et al., 2019; Renforth and Henderson, 2017). This would need to be constrained as a potential negative feedback on CO_2 drawdown as part of the "elimination" criteria to accurately quantify mCDR potential including any feedbacks on atmospheric CO_2 drawdown.

Macroalgal Cultivation is gaining traction in public discourse. Numerous start-ups are pursuing the idea of Macroalgal Cultivation as a promising carbon removal approach, such as Kelp Blue and Running Tide (amongst others). It is presently unclear whether Macroalgal Cultivation has a significant impact on CO_2 drawdown, as examined recently in Bach et al. (2021) using the natural analogue of the Great Sargassum Belt. Our meta-analysis illustrates that the number of papers that quantitatively assess its CO_2-drawdown potential is low (~10). Coupling field trials with quantitative empirical estimates of mCDR potential would dramatically advance research into this particular mCDR approach to address key "elimination" criteria.

2.5 Conclusions

Our study indicates a great need for rapid and widespread empirical lab and field research on mCDR, especially considering the urgency of viable CDR pathways needed to meet international climate targets. We have determined critical knowledge gaps and future directions for mCDR research in the context of currently imbalanced contributions of published literature to a set of objective "elimination" criteria. Due to its status as the most-researched

approach in the literature, excluding OIF, Alkalinity Enhancement appears to be the focal point for the mCDR field at present. We have identified that: (i) completion of field trials, pilot studies or demonstration projects, (ii) assessment of governance/finance/social aspects, and (iii) accurate quantification of CO_2 drawdown/CDR potential are all essential conditions that must be fulfilled to efficiently address the "elimination" criteria for any given mCDR approach. In particular, governance/finance/social aspects of peer-reviewed research are not significantly contributing to the knowledge base of mCDR literature. We hope our study can provide a coherent framework to assess "elimination" criteria objectively. "Elimination" criteria ideally must be equally covered in the published literature to enable evidence-based, strategic decision-making for mCDR.

References

Bach, L.T., 2021. Ocean-based negative emissions technologies plenary panel Q&A, Ocean Carbon Biogeochemistry (OCB) Workshop 2021.

Bach, L.T., Gill, S.J., Rickaby, R.E.M., Gore, S., Renforth, P., 2019. CO_2 Removal With Enhanced Weathering and Ocean Alkalinity Enhancement: Potential Risks and Co-benefits for Marine Pelagic Ecosystems. Frontiers in Climate 1. https://doi.org/10.3389/fclim.2019.00007

Bach, L.T., Tamsitt, V., Gower, J., Hurd, C.L., Raven, J.A., Boyd, P.W., 2021. Testing the climate intervention potential of ocean afforestation using the Great Atlantic Sargassum Belt. Nature Communications 12, 2556. https://doi.org/10.1038/s41467-021-22837-2

Bertram, C., 2011. The Potential of Ocean Iron Fertilization as an Option for Mitigating Climate Change, Emissions Trading: Institutional Design, Decision Making and Corporate Strategies, Second Edition.

Boyd, P., Vivian, C., 2019. Should we fertilize oceans or seed clouds? No one knows. Nature 570, 155–156.

Buesseler, K.O., Doney, S.C., Karl, D.M., Boyd, P.W., Caldeira, K., Chai, F., Coale, K.H., Baar, H.J.W. de, Falkowski, P.G., Johnson, K.S., Lampitt, R.S., Michaels, A.F., Naqvi, S.W.A., Smetacek, V., Takeda, S., Watson, A.J., 2008. Ocean Iron Fertilization--Moving Forward in a Sea of Uncertainty. Science 319, 162–162. https://doi.org/10.1126/science.1154305

Coelho, M.S., Barbosa, F.G., Souza, M. da R.A.Z., 2014. The scientometric research on macroalgal biomass as a source of biofuel feedstock. Algal Research 6, 132–138. https://doi.org/10.1016/j.algal.2014.11.001

Energy Futures Initiative, 2020. Uncharted Waters: Expanding the Options for Carbon Dioxide Removal in Coastal and Ocean Environments.

Friedlingstein, P., Jones, M.W., O'Sullivan, M., Andrew, R.M., Bakker, D.C.E., Hauck, J., Le Quéré, C., Peters, G.P., Peters, W., Pongratz, J., Sitch, S., Canadell, J.G., Ciais, P., Jackson, R.B., Alin, S.R., Anthoni, P., Bates, N.R., Becker, M., Bellouin, N., Bopp, L., Chau, T.T.T., Chevallier, F., Chini, L.P., Cronin, M., Currie, K.I., Decharme, B., Djeutchouang, L., Dou, X., Evans, W., Feely, R.A., Feng, L., Gasser, T., Gilfillan, D., Gkritzalis, T., Grassi, G., Gregor, L., Gruber, N., Gürses, Ö., Harris, I., Houghton, R.A., Hurtt, G.C., Iida, Y., Ilyina, T., Luijkx, I.T., Jain, A.K., Jones, S.D., Kato, E., Kennedy, D., Klein Goldewijk, K., Knauer, J., Korsbakken, J.I., Körtzinger, A., Landschützer, P., Lauvset, S.K., Lefèvre, N., Lienert, S., Liu, J., Marland, G., McGuire, P.C., Melton, J.R., Munro, D.R., Nabel, J.E.M.S., Nakaoka, S.-I., Niwa, Y., Ono, T., Pierrot, D., Poulter, B., Rehder, G., Resplandy, L., Robertson, E., Rödenbeck, C., Rosan, T.M., Schwinger, J., Schwingshackl, C., Séférian, R., Sutton, A.J., Sweeney, C., Tanhua, T., Tans, P.P., Tian, H., Tilbrook, B., Tubiello, F., van der Werf, G., Vuichard, N., Wada, C., Wanninkhof, R., Watson, A., Willis, D., Wiltshire, A.J., Yuan, W., Yue, C., Yue, X., Zaehle, S., Zeng, J., 2021. Global Carbon Budget 2021. Earth System Science Data Discussions 1–191. https://doi.org/10.5194/essd-2021-386

Fuss, S., Lamb, W.F., Callaghan, M.W., Hilaire, J., Creutzig, F., Amann, T., Tim Beringer, Garcia, W. de O., Hartmann, J., Khanna, T., Luderer, G., Nemet, G.F., Joeri Rogelj, Smith, P., Vicente, J.L.V., Wilcox, J., Dominguez, M. del M.Z., Minx, J.C., 2018. Negative emissions—Part 2: Costs, potentials and side effects. Environmental Research Letters 13, 063002. https://doi.org/10.1088/1748-9326/aabf9f

Gagern, A., Kapsenberg, L., 2021. Ocean–based carbon dioxide removal: A primer for philanthropy. ClimateWorks Foundation.

Gagern, A., Rau, G., Iglesias-Rodriguez, D., Renforth, P., Burns, W., Graffy, E., 2019. Ocean Alkalinity Enhancement: Current state of knowledge and potential role of philanthropy.

Gattuso, J.-P., Magnan, A.K., Bopp, L., Cheung, W.W.L., Duarte, C.M., Hinkel, J., Mcleod, E., Micheli, F., Oschlies, A., Williamson, P., Billé, R., Chalastani, V.I., Gates, R.D., Irisson, J.-O., Middelburg, J.J., Pörtner, H.-O., Rau, G.H., 2018. Ocean Solutions to Address Climate Change and Its Effects on Marine Ecosystems. Frontiers in Marine Science 5. https://doi.org/10.3389/fmars.2018.00337

Gattuso, J.-P., Williamson, P., Duarte, C.M., Magnan, A.K., 2021. The Potential for Ocean-Based Climate Action: Negative Emissions Technologies and Beyond. Frontiers in Climate 2. https://doi.org/10.3389/fclim.2020.575716

GESAMP, 2019. “High level review of a wide range of proposed marine geoengineering techniques”. (Boyd, P.W. and Vivian, C.M.G., eds.). (IMO/FAO/UNESCO-IOC/UNIDO/WMO/IAEA/UN/UN Environment/ UNDP/ISA Joint Group of Experts on the Scientific Aspects of Marine Environmental Protection). Rep. Stud. GESAMP No. 98, 144 p.

Harvey, L.D.D., 2008. Mitigating the atmospheric CO2 increase and ocean acidification by adding limestone powder to upwelling regions. Journal of Geophysical Research 113 https://doi.org/10.1029/2007JC004373

House, K.Z., House, C.H., Schrag, D.P., Aziz, M.J., 2007. Electrochemical Acceleration of Chemical Weathering as an Energetically Feasible Approach to Mitigating Anthropogenic Climate Change. Environmental Science and Technology 41, 8464–8470. https://doi.org/10.1021/es0701816

Ilyina, T., Wolf-Gladrow, D., Munhoven, G., Heinze, C., 2013. Assessing the potential of calcium-based artificial ocean alkalinization to mitigate rising atmospheric CO_2 and ocean acidification. Geophysical Research Letters 40, 5909–5914. https://doi.org/10.1002/2013GL057981

IPCC, 2018: Summary for Policymakers, In: Global Warming of 1.5°C. An IPCC Special Report on the impacts of global warming of 1.5°C above pre-industrial levels and related global greenhouse gas emission pathways, in the context of strengthening the global response to the threat of climate change, sustainable development, and efforts to eradicate poverty [Masson-Delmotte, V., P. Zhai, H.-O. Pörtner, D. Roberts, J. Skea, P.R. Shukla, A. Pirani, W. Moufouma-Okia, C. Péan, R. Pidcock, S. Connors, J.B.R. Matthews, Y. Chen, X. Zhou, M.I. Gomis, E. Lonnoy, T. Maycock, M. Tignor, and T. Waterfield (eds.)].

IPCC, Masson-Delmotte, V., Zhai, P., Pirani, A., Connors, S.L., Péan, C., Berger, S., Caud, N., Chen, Y., Goldfarb, L., Gomis, M.I., Huang, M., Leitzell, K., Lonnoy, E., Matthews, J.B.R., Maycock, T.K., Waterfield, T., Yelekçi, O., Yu, R., Zhou, B., 2021. Climate Change 2021: The Physical Science Basis. Contribution of Working Group I to the Sixth Assessment Report of the Intergovernmental Panel on Climate Change. Cambridge University Press.

Köhler, P., Abrams, J.F., Völker, C., Hauck, J., Wolf-Gladrow, D.A., 2013. Geoengineering impact of open ocean dissolution of olivine on atmospheric CO_2, surface ocean pH and marine biology. Environmental Research Letters 8, 014009. https://doi.org/10.1088/1748-9326/8/1/014009

Köhler, P., Hartmann, J., Wolf-Gladrow, D.A., 2010. Geoengineering potential of artificially enhanced silicate weathering of olivine. PNAS 107, 20228–20233. https://doi.org/10.1073/pnas.1000545107

Meysman, F.J.R., Montserrat, F., 2017. Negative CO_2 emissions via enhanced silicate weathering in coastal environments. Biology Letters 13, 20160905. https://doi.org/10.1098/rsbl.2016.0905

Minx, J., Lamb, W., Callaghan, M., Fuss, S., Hilaire, J., Creutzig, F., Thorben Amann, Beringer, T., Garcia, W. de O., Hartmann, J., Khanna, T., Lenzi, D., Gunnar Luderer, Nemet, G.F., Rogelj, J., Smith, P., Vicente, J.L.V., Wilcox, J., Dominguez, M. del M.Z., 2018. Negative emissions—Part 1: Research landscape and synthesis. Environmental Research Letters 13. https://doi.org/10.1088/1748-9326/aabf9b

National Academies of Sciences, Engineering, and Medicine, 2021. A Research Strategy for Ocean-based Carbon Dioxide Removal and Sequestration. The National Academies Press, Washington D.C.

National Academies of Sciences, Engineering, and Medicine, 2019. Negative Emissions Technologies and Reliable Sequestration: A Research Agenda. The National Academies Press, Washington, DC. https://doi.org/10.17226/25259

Nemet, G.F., Callaghan, M.W., Creutzig, F., Fuss, S., Hartmann, J., Hilaire, J., Lamb, W.F., Minx, J.C., Rogers, S., Smith, P., 2018. Negative emissions—Part 3: Innovation and upscaling. Environmental Research Letters 13, 063003. https://doi.org/10.1088/1748-9326/aabff4

Passow, U., Carlson, C.A., 2012. The biological pump in a high CO_2 world. Marine Ecology Progress Series 470, 249–272.

Rayfuse, R., Lawrence, M., Gjerde, K.M., 2008. Ocean Fertilisation and Climate Change: The Need to Regulate Emerging High Seas Uses. International Journal of Marine and Coastal Law 23, 297–326.

Renforth, P., Henderson, G., 2017. Assessing ocean alkalinity for carbon sequestration. Reviews of Geophysics 55, 636–674. https://doi.org/10.1002/2016RG000533

Rogelj, J., Luderer, G., Pietzcker, R.C., Kriegler, E., Schaeffer, M., Krey, V., Riahi, K., 2015. Energy system transformations for limiting end-of-century warming to below 1.5 °C. Nature Climate Change 5, 519–527. https://doi.org/10.1038/nclimate2572

Taillardat, P., Friess, D.A., Lupascu, M., 2018. Mangrove blue carbon strategies for climate change mitigation are most effective at the national scale. Biology Letters 14, 20180251. https://doi.org/10.1098/rsbl.2018.0251

Tawfik, G.M., Dila, K.A.S., Mohamed, M.Y.F., Tam, D.N.H., Kien, N.D., Ahmed, A.M., Huy, N.T., 2019. A step by step guide for conducting a systematic review and meta-analysis with simulation data. Tropical Medicine and Health 47, 46. https://doi.org/10.1186/s41182-019-0165-6

Watson, A.J., Schuster, U., Shutler, J.D., Holding, T., Ashton, I.G.C., Landschützer, P., Woolf, D.K., Goddijn-Murphy, L., 2020. Revised estimates of ocean-atmosphere CO_2 flux are consistent with ocean carbon inventory. Nature Communications 11, 4422. https://doi.org/10.1038/s41467-020-18203-3

Wilson, G., 2014. Murky Waters: Ambiguous International Law for Ocean Fertilization and Other Geoengineering. Texas International Law Journal 49, 507–557.

Statement of Authorship for joint/multi-authored papers for PGR thesis

To appear at the end of each thesis chapter submitted as an article/paper

The statement shall describe the candidate's and co-authors' independent research contributions in the thesis publications. For each publication there should exist a complete statement that is to be filled out and signed by the candidate and supervisor **(only required where there isn't already a statement of contribution within the paper itself).**

Title of Paper	**Chapter 2:** Meta-analysis of Ocean Carbon Dioxide Removal literature: major focus areas for research identified using elimination criteria
Publication Status	Unpublished and unsubmitted work written in a manuscript style. Please note that this chapter is written according to US English standards, whereas the rest of the thesis is written according to UK English standards.
Publication Details	

Student Confirmation

Student Name:	Sophie Gill (SG)		
Contribution to the Paper	WB maintains the Carbon Dioxide Removal/Negative Emissions Technologies Bibliography hosted by the Climate Protection & Restoration Initiative. SG conducted the Zotero database searches. SG, JG and LK reviewed the literature to assign meta-data categories. JG visualised data. WB provided comments on interpretation of data. SG wrote the paper. LK and JG edited the draft before submission.		
Signature 		Date	03/01/2022

Supervisor Confirmation

By signing the Statement of Authorship, you are certifying that the candidate made a substantial contribution to the publication, and that the description described above is accurate.

Supervisor name and title: Prof. Rosalind Rickaby		
Supervisor comments: Sophie has stated the authorship contributions clearly above.		
Signature 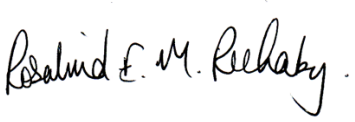	Date	03/01/2022

This completed form should be included in the thesis, at the end of the relevant chapter.

Chapter 3: The growth and calcification response of the coccolithophores *Emiliania huxleyi* and *Coccolithus braarudii* to the marine Carbon Dioxide Removal technique of Ocean Alkalinity Enhancement

Sophie J. Gill, Rosalind R. E. M. Rickaby and Gideon M. Henderson

3.1 Introduction

It is increasingly clear that to meet targets to keep global warming within 2 °C, simply reducing emissions will not be sufficient (Renforth and Henderson, 2017; Gore et al., 2018; GESAMP, 2019). There is an additional need to actively remove Carbon Dioxide (CO_2) from the atmosphere, using Carbon Dioxide Removal (CDR) technologies (IPCC AR5, 2014; Fuss et al., 2014; Fuss et al., 2018). Many of these are marine CDR (mCDR) schemes that use the ocean as the site of carbon removal (National Academies of Sciences, Engineering, and Medicine, 2021; Boettcher et al., 2021). One such proposed mCDR scheme is Ocean Alkalinity Enhancement (Hartmann et al., 2013; Kheshgi, 1995), where alkalinity is generated directly in seawater through the addition of alkalinity-enhancing materials (Bach et al., 2019). This might feasibly result in the alkalinity of the global surface ocean, currently ~ 2300 µmol kg^{-1}, being raised by 100 to >2,000 µmol kg^{-1} by the year 2100 (Bach et al., 2019; Köhler et al., 2013; Köhler et al., 2010; Ilyina et al., 2013; Feng et al., 2017; Taylor et al., 2016), which would result in a drawdown of 225-5550 Gt CO_2 (see **Appendix 2** for details of calculation).

The surface ocean carbonate buffer system would be significantly altered during OAE. In Bach et al. (2019), two different scenarios for OAE are presented (**Figure 3.1**). The first is "air-equilibrated OAE", which describes a situation in which the surface ocean and atmosphere are equilibrated with respect to pCO_2. Therefore, pCO_2 will stay constant with increasing alkalinity, but pH and $\Omega CaCO_3$ increase. It is important to consider that an air-equilibrated scenario of OAE may not occur on the initial addition of alkalinity to the surface ocean because reaching this equilibrium may take several years (Bach et al., 2019; Harvey, 2008; Feng et al.,

2017). So when alkalinity is initially added to the surface ocean, it will be added too rapidly for air-sea gas exchange to keep pace, and more extreme carbonate chemistry perturbations would occur, leading to "hotspots" of alkalinity addition (Ilyina et al., 2013; Bach et al., 2019). This could lead to locally severely decreased pCO_2 in addition to increased pH and $\Omega CaCO_3$ (**Figure 3.1**, **Panel A and B**).

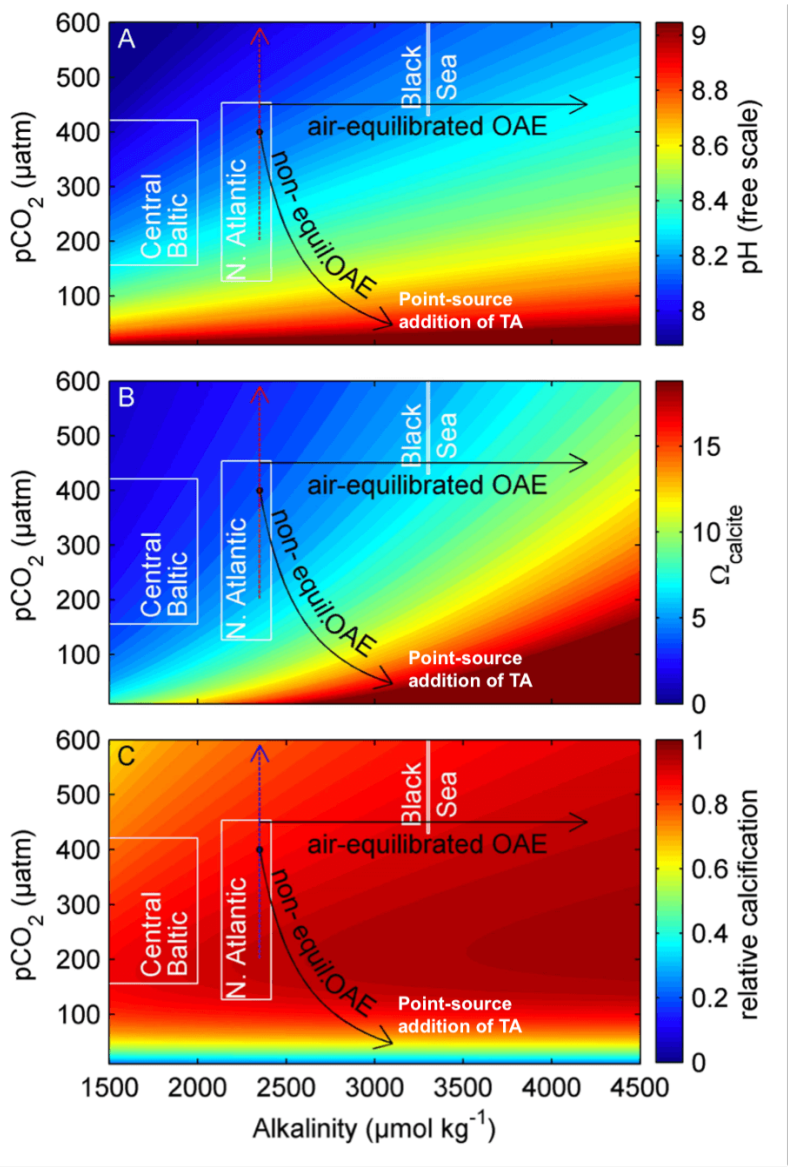

Figure 3.1: "Carbonate chemistry perturbation through EW/OAE". **(A)** pH **(B)** **Ω**$CaCO_3$ and **(C)** relative calcification rates of the coccolithophore *Gephyrocapsa oceanica* relative to Total Alkalnity and pCO_2. Arrows show the trajectory of (i) ocean acidification (dotted), (ii) air-equilibrated OAE, and (iii) non-equilibrated OAE. Label added to show extreme perturbation example of point-source addition of OAE. For more details on the construction of this figure, see original figure from Bach et al. (2019).

While there is a growing body of research on OAE (Bach et al., 2019; **Chapter 1**, **Chapter 2**), some critical unknown impacts of OAE in the marine environment, particularly on marine biota, have not yet been assessed in lab or field experiments. Calcifiers may be one of the most sensitive organisms to proposed OAE schemes (Bach et al., 2019) because they are the most sensitive organisms to the carbonate system perturbations induced by ocean acidification (Gattuso et al., 2015). Coccolithophores are one of the three major groups of calcifying plankton in the modern oceans, along with foraminifera and pteropods (Monteiro et al., 2016); (Sarmiento and Gruber, 2006). They are also estimated to be responsible for up to 10% of global carbon (inorganic + organic) fixation (Poulton et al., 2007).

E. huxleyi, a small coccolithophore from the family *Noelaerhabdaceae*, genus *Reticulofenestra* (Stevenson et al., 2014), is by far the main bloom-forming coccolithophore (Tyrrell and Merico, 2004), and is the model organism for most coccolithophore studies due to its ubiquitous presence in our surface oceans (Blanco-Ameijeiras et al., 2016); (Mayers et al., 2016). *C. braarudii*, unlike *E. huxleyi*, is a much larger coccolithophore and evolved from the *Coccolithus* genus. Despite being much less abundant in the modern surface ocean, *C. braarudii* produces a comparable amount of calcite to *E. huxleyi* globally (Poulton et al., 2007) and in some communities/regions may produce more than *E. huxleyi,* for example the Arctic Ocean (Daniels et al., 2014). These two contrasting genera of coccolithophores are often used as "endmembers" in previously published studies, e.g. Hermoso et al. (2014); Walker et al. (2018); Rickaby et al. (2010). This is because (i) the physiologies of these small and large coccolithophore genera have been inferred to differ in their control of internal pH and modes of carbon acquisition (Rickaby et al., 2010), (ii) the cellular calcite content of *C. braarudii* is often 30-80 times higher than that of *E. huxleyi* (Daniels et al., 2014), and (iii) *E. huxleyi* generally grows faster than *C. braarudii* even under identical conditions (Daniels et al., 2014). Additionally, the differing responses of *E. huxleyi* and *C. braarudii* to ocean acidification (Meyer and Riebesell, 2015) highlight the importance of examining the potential of these two

species and the genera from which they originate to differ in their response to significant shifts in carbonate chemistry, such as might occur during OAE.

Total Alkalinity (TA) in itself is not a chemical parameter that directly physiologically affects marine biota, so TA in itself will not drive physiological responses of coccolithophores during OAE. However, as outlined previously, the different components of the surface ocean carbonate system will shift their speciation as a result of TA addition to the surface ocean. These components include pH ($[H^+]$), DIC (comprised of $[CO_2](aq)$, $[HCO_3^-]$, $[CO_3^{2-}]$), pCO_2 and $\Omega CaCO_3$, which are all physiologically relevant parameters that are directly "sensed" by marine biota.

For coccolithophores, it is well-established that the main parameter of the carbonate system controlling growth responses is passive diffusion of $[CO_2](aq)$ into the cell because this directly controls photosynthesis and therefore division (growth) rate (Monteiro et al., 2016; Gafar et al., 2018; Bach et al., 2013; Sett et al., 2014). However, there is evidence that *E. huxleyi* uses Carbon Concentrating Mechanisms (CCMs) (Monteiro et al., 2016; Giordano et al., 2005; Raven et al., 1999; Kottmeier et al., 2014), to accumulate CO_2 at the active site of Rubisco to increase rates of carbon fixation (Beardall and Raven, 2013). This may be through the use of HCO_3^- ion exchange transporters, which are solute carrier family 4 (SLC4) proteins (von Dassow et al., 2009; Richier et al., 2011; Taylor et al., 2017) and/or the enzyme carbonic anhydrase (Richier et al., 2011; Bach, 2015; Rost et al., 2003; Sikes and Wheeler, 1982), which may allow this species to utilise HCO_3^- in CO_2-limiting conditions to aid growth.

There is considerably more debate about the exact species of the carbonate system which affect calcification in coccolithophores, because the transporters supplying Ca^{2+} and HCO_3^- as the base materials for $CaCO_3$ production (Bach, 2015) are poorly characterised (Tsuji and Yoshida, 2017). When pressure (P), temperature (T) and salinity (S) are constant, there is an inevitable proportionality between CO_3^{2-} and $\Omega CaCO_3$, and HCO_3^- and $[H^+]$ (Bach et al., 2015; Cyronak et al., 2016). $\Omega CaCO_3$ is not a direct physiological driver for calcification, despite

correlating well with calcification rates (Waldbusser et al., 2015), but it does control the solubility of $CaCO_3$ (Zeebe and Wolf-Gladrow, 2001) and therefore $\Omega CaCO_3$ affects how favourable the environment for calcification is (Henderson et al., 2008). The carbon species used for $CaCO_3$ formation at the calcification site could theoretically be CO_2, HCO_3^-, or CO_3^{2-}, because these species are in constant exchange with one another in the carbonate buffer system and may be transformed to CO_3^{2-} before reacting with Ca^{2+} (Bach, 2015). The exact seawater DIC substrate for calcification is still unknown, but it is generally assumed that HCO_3^- is the substrate that has to be supplied from bulk seawater to the site of calcification and $[H^+]$ is the waste product that has to be removed from the site of calcification to bulk seawater during the production of $CaCO_3$ (Cyronak et al., 2016).

Photosynthesis and calcification proceed in parallel as cellular processes (Tsuji and Yoshida, 2017) and as such are coupled (Paasche, 2002; Allemand et al., 2004). There is a possibility intracellular CO_2 from respired biomass could react with H_2O to form HCO_3^- and H^+ (catalysed by carbonic anhydrase), which could be an alternative inorganic carbon source for calcification (Bach, 2015). It has even been suggested that calcification may act as a CCM by supplying a source of CO_2 for photosynthesis (Reinfelder, 2011), but experimental evidence examining the lack of dependence of photosynthesis on calcification suggests that this is not the case for *E. huxleyi* (Bach et al., 2013; Leonardos et al., 2009) or *C. braarudii* (Walker et al., 2018).

In 2015, Bach et al. presented the latest synthesis to understanding the drivers of coccolithophore calcification: the substrate-inhibitor concept, which describes the dependence of coccolithophore calcification rates on the physiologically relevant species of the carbonate system. In this hypothesis, calcification is facilitated by the primary substrate for calcification, bicarbonate (HCO_3^-), and CO_2, which is required for cell growth. Calcification is inhibited by protons (H^+), i.e. low pH.

The substrate-inhibitor concept allows us to predict what might happen during air-equilibrated and non-equilibrated scenarios. During air-equilibrated OAE scenarios, we can expect calcification to increase because there will be higher pH coupled with higher available HCO_3^-,

in conjunction with a constant level of pCO_2, so no risk to limitation of growth rate. Data from Bach et al. (2015), based on *Gephyrocapsa oceanica* (*G. oceanica*, an abundant, bloom-forming coccolithophore in the modern oceans) calcification rates in response to carbonate chemistry perturbations, predicts that relative calcification will increase in an air-equilibrated OAE scenario (**Figure 3.1**, **Panel C**).

During non-equilibrated OAE scenarios, pH and HCO_3^- will increase, but pCO_2 will decrease. pCO_2 may be driven low enough at these hotspots to induce phytoplankton growth limitation, for example, if pCO_2 levels went below ~100 µatm, dependent on species and genotype (Riebesell et al., 1993; Sett et al., 2014; Bach et al., 2011; Goldman, 1999; Hansen, 2002). For coccolithophores specifically, the growth rate of model organism *Emiliania huxleyi* (*E. huxleyi*) starts to decline at CO_2 levels below 8-10 µmol CO_2 kg^{-1} and becomes strongly CO_2-limited at levels below 5 µmol CO_2 kg^{-1} (Bach et al., 2013; Sett et al., 2014). Therefore, we can predict that the growth of phytoplankton may decrease if the threshold for CO_2 limitation is crossed, and calcification may decrease (shown in **Figure 3.1, Panel C**).

Another crucial aspect of proposed OAE schemes to examine is that many of them would employ Ca-containing materials to raise ocean alkalinity (GESAMP, 2019); (Ilyina et al., 2013). Due to the high concentration (10mM) of Ca in the global oceans, the addition of Ca at the amounts representative of OAE is relatively small, i.e. <11mM final concentration (Bach et al., 2019). The growth of the coccolithophores *E. huxleyi* and *G. oceanica* in response to up to 50 mM Ca was examined in Müller et al. (2015), and no significant changes were observed in cellular parameters until Ca concentrations approached 50 mM, much higher than the modern ocean concentration of 10 mM. Therefore, it is reasonable to predict that Ca concentration increases due to OAE are unlikely to result in detectable growth and calcification responses in coccolithophores. However, it has been identified in Bach et al. (2019) (see **Chapter 1**) that examining the response to increased Ca levels expected during OAE is crucial due to the pressing nature of the climate crisis and the likelihood of mCDR technology deployment.

In this study, we examine the growth and calcification response of the two key "endmember" species of coccolithophore (*Emiliania huxleyi* and *Coccolithus braarudii*) to OAE scenarios in both CO_2-replete (air-equilibrated OAE) and CO_2-limited (non-equilibrated OAE) conditions using in-vitro laboratory culture experiments. We also compare how the addition of the monovalent cation Na^+ and divalent cation Ca^{2+} to raise Total Alkalinity affects growth and calcification responses.

There are three main strands of inquiry for these experimental manipulations:

1. Does Alkalinity Enhancement from control TA to high TA values drive a significant growth and calcification response?
    - If so, are these responses different between *E. huxleyi* and *C. braarudii*?
2. What influence does Alkalinity Enhancement exert on growth and calcification in CO_2-replete vs CO_2-limited conditions?
3. Is there any difference observed in the growth and calcification of *E. huxleyi* and *C. braarudii* when the cation used to raise TA is different? (Na^+ vs Ca^{2+})

3.2 Methods

3.2.1 Simulation of air-equilibrated OAE

Batch culture experiments on *E. huxleyi* and *C. braarudii* response to enhanced alkalinity were conducted at the University of Oxford Department of Earth Sciences. Culture medium was prepared using Synthetic Ocean Water (SOW), enriched with 882 µmol L^{-1} nitrate, 36.2 µmol L^{-1} (37.286µmol kg SW^{-1}) phosphate and 106 µmol L^{-1} silicate (109.18 µmol kg SW^{-1}), with trace metals and vitamins according to L1 (Guillard and Hargraves, 1993).

Two different pathways to simulate OAE were used: (i) adding $NaHCO_3$ to Synthetic Ocean Water (SOW), and (ii) adding Na_2CO_3 + $CaCl_2$ to SOW. These pathways compare the effect of alkalinity added as Na^+ vs added as Ca^{2+}. Calcium bicarbonate, $Ca(HCO_3)_2$, does not exist in solid-state, so Na_2CO_3 + $CaCl_2$ simulates $Ca(HCO_3)_2$ addition to SOW to make it comparable to the SOW + $NaHCO_3$ pathway.

Before conducting experiments with enhanced alkalinity treatments, the length of time it would take for culture media to equilibrate with atmospheric CO_2, to simulate an air-equilibrated scenario of OAE, was tested using ~4000 μmol kg^{-1} treatments for both Pathway 1: adding $NaHCO_3$ to Synthetic Ocean Water (SOW), and Pathway 2: adding Na_2CO_3 + $CaCl_2$ to SOW. This was tested using solutions of TA ~ 4000 μmol kg^{-1} because this was the highest level of TA which experimental manipulations would cover, and so out of the enhanced alkalinity treatments could be safely assumed to take the longest amount of time to equilibrate. The identical 2L flasks were used for bubbling these solutions to prepare experimental media, so the size of the flask/surface area of the solution available to exchange with the air was identical between test and experimental conditions.

Pathway 1 and Pathway 2 solutions were made by adding amounts of $NaHCO_3$ and Na_2CO_3 + $CaCl_2$ respectively for each pathway to SOW to achieve a rise in TA of ~1500 μmol kg^{-1} above control SOW values (~2500 μmol kg^{-1}). Solutions were then bubbled with ambient air for 72 hours and samples for TA were taken at Time (T, hours) = 0, T = 0.5, T = 1, T = 2, T = 17, T = 20, T = 24, T = 48 and T = 72. TA of the solutions at each time-stamp was measured with an average precision of ~ 9 μmol kg^{-1} on duplicate samples by Gran titration using a Metrohm Ti-touch 916. The 9ml samples were split into 3ml triplicate samples to analyse on the autotitrator. The autotitrator is calibrated daily against a certified seawater reference material (Dickson Batch 174, Scripps Institute of Oceanography, measured at ~21 μmol kg^{-1} precision). The pH of each solution was also measured using the 867 pH module, which is calibrated daily against standard NBS buffers. Subsequent calculation of the rest of the carbonate system was completed using CO2SYS v2.1 (Pierrot et al., 2006), with inputs of Total Alkalinity and pH, K1 and K2 constants from (Roy et al., 1993), KHSO4 values from Dickson, pH on the NBS scale and $[B]_T$ value from (Lee et al., 2010).

$[CO_2]$ evolution over time in the Pathway 1 and Pathway 2 solutions is shown in **Figure 3.2** for Pathway 1 and 2. In both pathways, $[CO_2]$ did not change after 120 minutes, and so equilibration with the atmosphere was complete by this time.

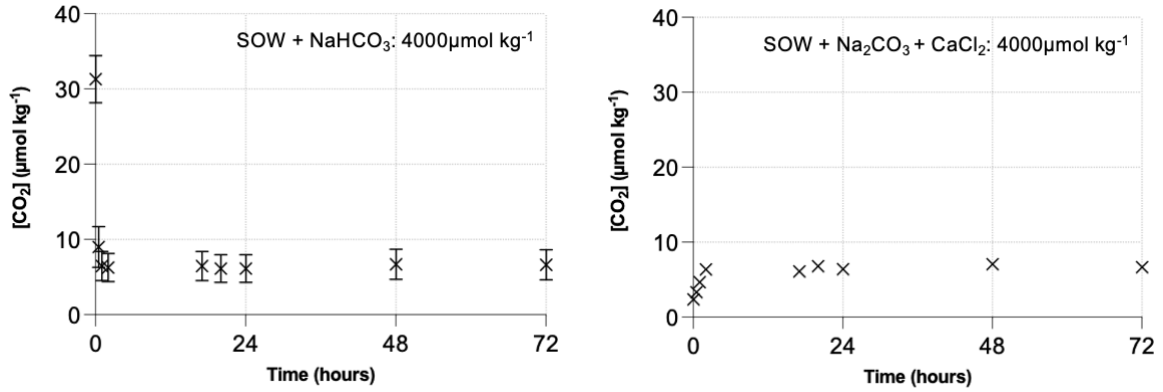

Figure 3.2: Equilibration tests for Pathway 1 (SOW + $NaHCO_3$) and Pathway 2 (SOW + Na_2CO_3 + $CaCl_2$), both at Total Alkalinity (TA) = 4000µmol kg^{-1}. Equilibration trajectory shown using [CO_2] over a 72-hour period in enhanced alkalinity media. Crosses represent each sample measurement, error bars represent error added in quadrature from *CO2sys* upper and lower bound coupled with analytical error. In the case of no error bars, this is because the size of the symbol obscures the error bar.

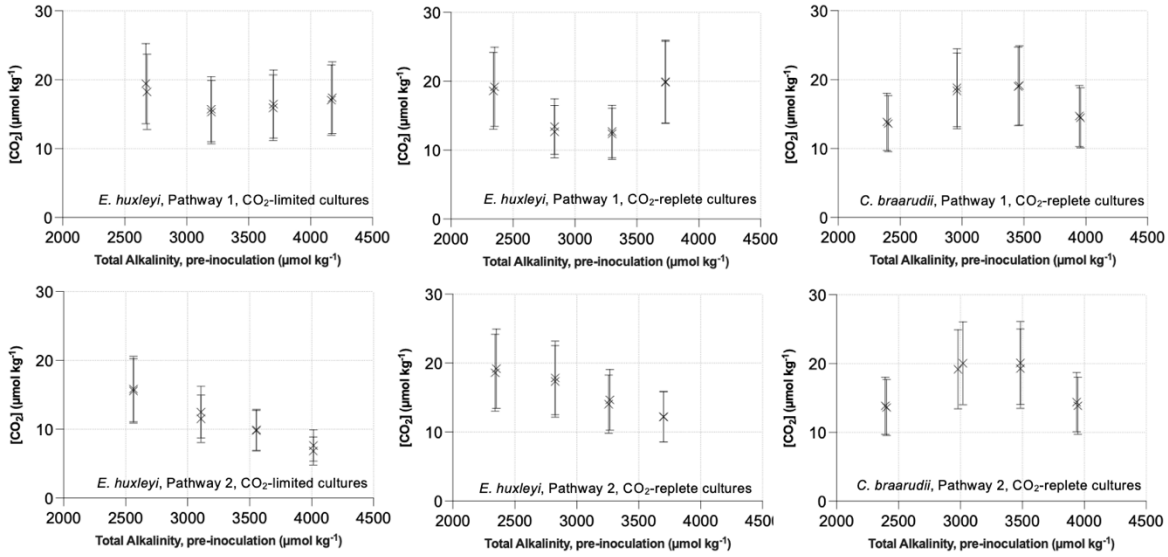

Figure 3.3: [CO_2] concentrations at cell inoculation in experimental enhanced alkalinity culture media. After bubbling, before any cultures inoculated. Pathway 1 = (SOW + $NaHCO_3$), Pathway 2 = (SOW + Na_2CO_3 + $CaCl_2$). Crosses represent each duplicate sample measurement, error bars represent error added in quadrature from *CO2sys* upper and lower bound coupled with analytical error.

In the culture media used in the actual experiments, after Total Alkalinity (TA) was raised in the culture media, the media was bubbled with ambient air for 120 minutes to equilibrate the seawater carbonate system with atmospheric CO_2. The aim of this was to simulate air-equilibrated scenarios of OAE, with constant [CO_2] with increasing TA. However, as shown in **Figure 3.3**, [CO_2] is not perfectly constant with increasing TA for any of the experimental culture media manipulations. The amount of time for equilibration was tested thoroughly

beforehand, as outlined above, so it can be safely assumed that these solutions all equilibrated with atmospheric CO_2. It is possible that the variations in [CO_2] between control and enhanced alkalinity solutions are smaller than the sensitivity of the calculation of [CO_2] using TA and pH in CO2SYS following Gran titration. Therefore, [CO_2] may likely be constant with increasing TA, but noise in our measurement of [CO_2] at the beginning of all cell incubations obscures this signal.

Before inoculating the experimental cultures, the media was then 0.22µm filter-sterilised and sealed in parafilmed 2L polycarbonate bottles. Samples for initial TA for the culture media were taken from this 0.22µm filter-sterilised culture media, parafilmed to prevent any evaporation which would affect alkalinity levels, and stored at 4 °C before analysis. The starting carbonate chemistry of all experimental manipulations relative to increasing TA is shown in **Figure 3.4**.

3.2.2 CO_2-replete vs CO_2-limited cultures

CO_2-replete experiments were carried out on *E. huxleyi* strain RCC911 (morphotype A) and *C. braarudii* strain RCC1198 following best practices decided by the community (LaRoche et al., 2010) for dilute culturing. In these experiments, Dissolved Inorganic Carbon (DIC) drawdown over the course of culturing was <5% (**Figure 3.5**), meaning that there was no significant drift in the carbonate chemistry of the media, and so [CO_2] was replete throughout the experimental incubations, meaning that these experiments are representative of an air-equilibrated OAE scenario.

CO_2-limited OAE experiments were carried out on *E. huxleyi* strain SO 14-2 (morphotype A). The strains for CO_2-replete and CO_2-limited *E. huxleyi* experiments are different due to constraints on strains available to culture in the lab before and after the COVID-19 pandemic. Both RCC911 and SO 14-2 are morphotype A. Morphotypes of *E. huxleyi* commonly show similarities in growth, calcification, morphology and share similar genetic material (Cook et al., 2011; Rigual-Hernández et al., 2020). Therefore, the results from both strains can be robustly compared.

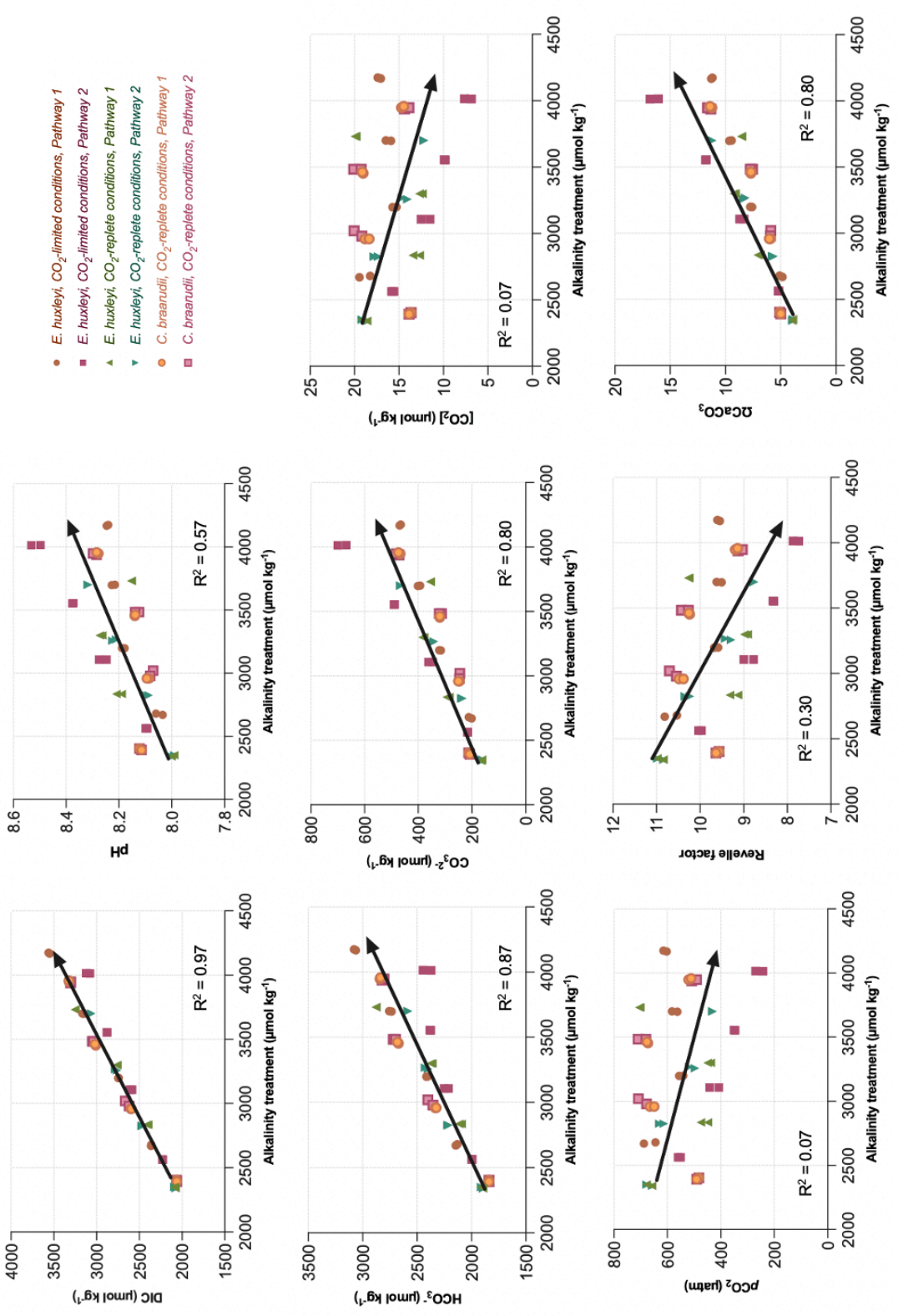

Figure 3.4: Initial alkalinity treatment (pre-inoculation) conditions vs. initial carbonate system parameters in culture media i.e. after equilibration, before inoculation of cultures. Total Alkalinity and pH were measured via Gran titration and pH probe respectively (as outlined in text), and then used as inputs for calculation of the rest of the carbonate system in CO2SYS v2.1 (Pierrot et al. 2016), with K1 and K2 constants from Roy, et al. (1993), $KHSO_4$ values from Dickson, pH on the NBS scale and $[B]_T$ value from Lee et al. (2010). Black arrow represents the regression line calculated using simple linear regression performed in GraphPad Prism 9, with the direction of the arrow showing the direction of the general trendline.

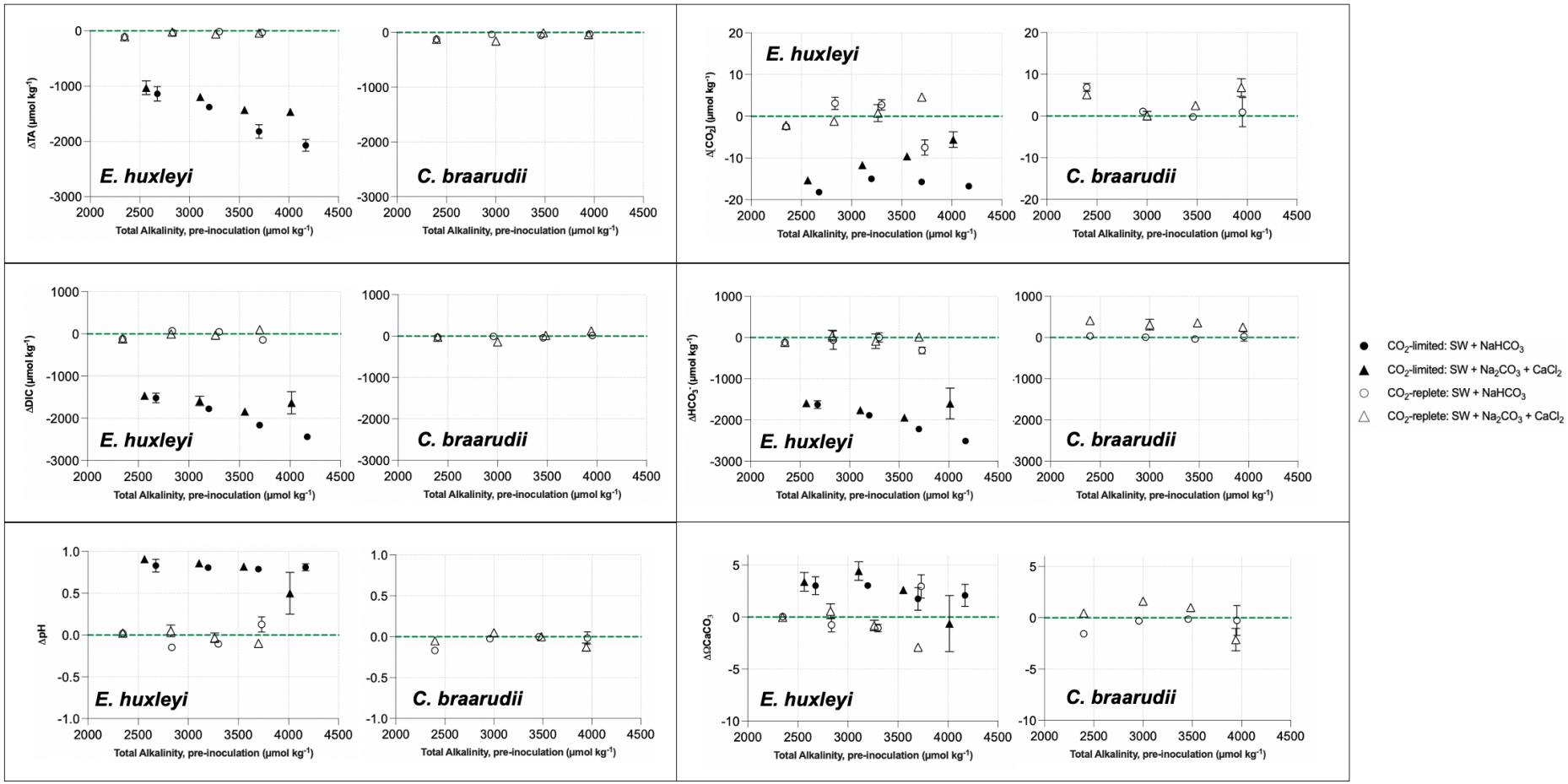

Figure 3.5: Drifts in carbonate system parameters in CO_2-replete and CO_2-limited cultures (legend on right-hand side) between pre-inoculation and cell harvest. Total Alkalinity and pH were measured via Gran titration and pH probe respectively (as outlined in text), and then used as inputs for calculation of the rest of the carbonate system in CO2SYS v2.1 (Pierrot et al. 2016), with K1 and K2 constants from Roy, et al. (1993), $KHSO_4$ values from Dickson, pH on the NBS scale and $[B]_T$ value from Lee et al. (2010).

Emiliania huxleyi (RCC911) – CO_2-replete conditions											
	Initial alkalinity treatment	Total alkalinity ($\mu molkg^{-1}$)	DIC ($\mu molkg^{-1}$)	pH (NBS scale)	pCO_2 (μatm)	$[CO_2]$ ($\mu molkg^{-1}$)	HCO_3^- ($\mu molkg^{-1}$)	CO_3^{2-} ($\mu molkg^{-1}$)	$\Omega CaCO_3$	Ca (mM)	Increase in Ca relative to control (%)
Pathway 1 – SOW + $NaHCO_3$	Control (SOW)	2346	2086	7.996	668	18.9	1904	164	3.9	10.5	N/A
	E1 (Control + ~500 $\mu molkg^{-1}$)	2835	2406	8.200	462	13.1	2104	289	7.0	10.5	N/A
	E2 (Control + ~1000 $\mu molkg^{-1}$)	3299	2762	8.269	444	12.6	2368	381	9.2	10.5	N/A
	E3 (Control + ~1500 $\mu molkg^{-1}$)	3732	3253	8.153	703	19.9	2878	355	8.5	10.5	N/A
Pathway 2 – SOW + Na_2CO_3 +$CaCl_2$	Control (SOW)	2346	2086	7.996	668	18.9	1904	164	3.9	10.5	N/A
	E1 (Control + ~500 $\mu molkg^{-1}$)	2825	2473	8.093	662	17.6	2217	238	5.7	10.8	2.8
	E2 (Control + ~1000 $\mu molkg^{-1}$)	3263	2775	8.218	508	14.4	2414	346	8.3	11.0	5.1
	E3 (Control + ~1500 $\mu molkg^{-1}$)	3701	3066	8.319	432	12.2	2586	467	11.2	11.3	7.4
Emiliania huxleyi (OA15) – CO_2-limited conditions											
	Initial alkalinity treatment	Total alkalinity ($\mu molkg^{-1}$)	DIC ($\mu molkg^{-1}$)	pH (NBS scale)	pCO_2 (μatm)	$[CO_2]$ ($\mu molkg^{-1}$)	HCO_3^- ($\mu molkg^{-1}$)	CO_3^{2-} ($\mu molkg^{-1}$)	$\Omega CaCO_3$	Ca (mM)	Increase in Ca relative to control (%)
Pathway 1 – SOW + $NaHCO_3$	Control (SOW)	1537	844	8.879	24.2	0.685	511	333	8.0	10.5	N/A
	E1 (Control + ~500 $\mu molkg^{-1}$)	1819	971	8.990	18.7	0.530	525	445	10.7	10.5	N/A
	E2 (Control + ~1000 $\mu molkg^{-1}$)	1881	999	9.011	18.0	0.509	528	471	11.3	10.5	N/A
	E3 (Control + ~1500 $\mu molkg^{-1}$)	2100	1118	9.054	17.4	0.493	563	554	13.3	10.5	N/A
Pathway 2 – SOW + Na_2CO_3 +$CaCl_2$	Control (SOW)	1534	767	9.005	14.1	0.398	408	358	8.6	10.5	N/A
	E1 (Control + ~500 $\mu molkg^{-1}$)	1997	1025	9.115	13.0	0.369	483	542	13.0	10.8	2.8
	E2 (Control + ~1000 $\mu molkg^{-1}$)	2125	1040	9.194	9.8	0.277	441	599	14.4	11.0	5.1
	E3 (Control + ~1500 $\mu molkg^{-1}$)	2550	1283	9.208	11.5	0.326	534	748	15.2	11.3	7.4
Coccolithus braarudii (RCC1198) – CO_2-replete conditions											
	Initial alkalinity treatment	Total alkalinity ($\mu molkg^{-1}$)	DIC ($\mu molkg^{-1}$)	pH (NBS scale)	pCO_2 (μatm)	$[CO_2]$ ($\mu molkg^{-1}$)	HCO_3^- ($\mu molkg^{-1}$)	CO_3^{2-} ($\mu molkg^{-1}$)	$\Omega CaCO_3$	Ca (mM)	Increase in Ca relative to control (%)
Pathway 1 – SOW + $NaHCO_3$	Control (SOW)	2398	2065	8.119	487	13.8	1841	210	5.1	10.5	N/A
	E1 (Control + ~500 $\mu molkg^{-1}$)	2959	2598	8.091	658	18.6	2330	249	6.0	10.5	N/A
	E2 (Control + ~1000 $\mu molkg^{-1}$)	3459	3017	8.140	675	19.1	2678	320	7.7	10.5	N/A
	E3 (Control + ~1500 $\mu molkg^{-1}$)	3953	3325	8.282	516	14.6	2840	471	11.3	10.5	N/A
Pathway 2 – SOW + Na_2CO_3 +$CaCl_2$	Control (SOW)	2398	2065	8.119	487	13.8	1841	210	5.1	10.5	N/A
	E1 (Control + ~500 $\mu molkg^{-1}$)	3000	2645	8.077	694	19.6	2379	246	5.9	10.8	2.8
	E2 (Control + ~1000 $\mu molkg^{-1}$)	3484	3047	8.132	696	19.7	2709	318	7.7	11.0	5.1
	E3 (Control + ~1500 $\mu molkg^{-1}$)	3943	3306	8.292	500	14.2	2814	478	11.5	11.3	7.4

Table 3.1: Carbonate chemistry for CO_2-replete and CO_2-limited conditions at harvest. Total Alkalinity and pH were measured via Gran titration and pH probe respectively (as outlined in text), and then used as inputs for calculation of the rest of the carbonate system in CO2SYS v2.1 (Pierrot et al. 2016), with K1 and K2 constants from Roy, et al. (1993), $KHSO_4$ values from Dickson, pH on the NBS scale and $[B]_T$ value from Lee et al. (2010). Ca levels in solution are calculated using the molar amounts of Ca^{2+} in the volume of $CaCl_2$ added to the enhanced alkalinity treatments.

CO_2-limited cultures were achieved by using the same alkalinity addition pathways and equilibration methods as in the CO_2-replete, dilute cultures, but inoculating at higher cell culture densities and then allowing the cultures to grow to very high cell culture densities (2 - 3 x 10^6 cells ml^{-1}) before the point of harvest. This drives the [CO_2] to <1µmol kg^{-1} by the time of harvest, below *E. huxleyi*'s threshold for CO_2-limitation (Sett et al., 2014) so the cells were severely CO_2-limited during much of the experimental incubations. Therefore, the CO_2-limited experimental incubations are representative of a non-equilibrated OAE scenario. As shown in **Figure 3.5**, the carbonate system drifts in the CO_2-limited cultures compared to the CO_2-replete cultures over the course of the experimental incubations are significantly larger.

See **Table 3.1** for a full summary of the carbonate chemistry conditions of CO_2-replete and CO_2-limited experiments at harvest of cultures.

3.2.3 Experimental protocol in CO_2-replete conditions

Before inoculation of the experiments, all cultures were pre-acclimated to the control or enhanced alkalinity conditions in small-volume, dilute cultures for a minimum of 5 generations, to ensure that growth and calcification responses measured in the final experiments were adapted growth responses (LaRoche et al., 2010). These small-volume acclimated cultures were manually agitated during pre-acclimation by daily gentle inversion and subsampled on at dilute culture densities in the exponential phase for inoculating the experimental cultures to avoid significant drift in the carbonate system.

At the beginning of the CO_2-replete experiments, ~100 cells ml^{-1} of RCC911 (recommended by LaRoche et al. (2010)) and ~400 cells ml^{-1} of RCC1198 (after Hermoso (2015)) in each experimental alkalinity treatment were inoculated in 600ml triplicates, to ensure reproducibility of results. In addition, for each set of triplicates, an additional large-volume 2L culture was run alongside to harvest PIC:POC samples at the required cell biomass. These large 2L cultures had near-identical growth rates to the 600ml triplicates, which were checked following methods for running simultaneous cultures outlined in Hermoso et al. (2014).

The polycarbonate culture flasks included vented lids, allowing for atmospheric exchange. Cultures were grown at 17 ^{o}C (optimum temperature for RCC911 and RCC1198) on a 14h:10h light:dark cycle, under a light intensity of between ~90-105 µmol photons m^{-2} s^{-1}. A range is provided because light intensity was lower at the sides of the incubator compared to the centre. Each day, culture flasks were manually agitated to ensure that the cells were kept in suspension. Cell count (cells ml^{-1}) and coccosphere size (µm) were measured every day using a Beckman Coulter Counter Z2 analyser. Specific growth rate, µ (d^{-1}), was calculated (**Equation 3.1**) using the cell abundances at the start of the experiment (c_0) and at harvest (c_1), as well as the length of the experimental incubation period (Δt, incubation time in days):

$$\mu = \frac{\ln c_1 - \ln c_2}{\Delta t} \quad \textbf{(3.1)}$$

Growth rate data were tested for significant difference using one-way ANOVA and the post-hoc Tukey-Kramer test in GraphPad Prism 9. Before these statistical analyses, data were tested for normality using the Shapiro-Wilks test (Gore et al., 2018) (Shafiee et al., 2021). If data did not pass the test for normality using Shapiro-Wilks, the Kruskal-Wallis test for significant difference and Dunn's multiple comparison test were used following best practice guidelines for statistical analysis (Motulsky, GraphPad Statistics Guide).

9ml alkalinity samples were collected each day by 0.22µm syringe-filtering the culture medium. These were stored identically to the initial alkalinity samples before they were analysed. The cultures were harvested after growing for a minimum of 5 generations in the exponential phase (recommended by LaRoche et al. (2010)) when cell densities reached a maximum of 60,000-100,000 cells ml^{-1} for *E. huxleyi* (recommended by LaRoche et al. (2010) and Bach et al. (2013)), and 5,000-6,000 cells ml^{-1} for *C. braarudii* (after Hermoso (2015)).

Analysis of alkalinity samples was completed at the Department of Earth Sciences, University of Oxford, as outlined in **Section 3.2.1**, (**p.77**).

Calcification rate (RCa) for the cultures is calculated using the change in Total Alkalinity (ΔTA) in the final culture medium compared to the initial culture medium (**Equation 3.2**):

$$\Delta TA = TA_{initial} - TA_{final} \quad \textbf{(3.2)}$$

This is because coccolithophores extract alkalinity from the culture medium as they calcify. This method of calculating calcification rate is known as the alkalinity anomaly technique (Chisholm and Gattuso, 1991; Cohen et al., 2017). This technique assumes that uptake of nutrients which are conservative ions e.g. NO_3^-, PO_4^{3-}, which contribute to ΔTA by biota, negligibly affects ΔTA, and that the processes of respiration and photosynthesis do not affect ΔTA. Chisholm and Gattuso (1991) confirmed that all underlying assumptions of the alkalinity anomaly technique are correct, and no correction for nutrient changes are required in the calculation of calcification because these changes are smaller than the variation in actual calcification values.

The drift in alkalinity can then be converted into a calcification rate as follows. First, we divide ΔTA by 2 because the formation of 1 mole of $CaCO_3$ reduces alkalinity in the culture medium by 2 moles (Wolf-Gladrow et al., 2007); (Bach et al., 2019). This can be converted into mass using the molar mass of $CaCO_3$. Then we divide by the change in cell number over the duration of the experiment (Δcells ml^{-1}) and the number of days (d) to provide RCa (pg $CaCO_3$ $cell^{-1}$ day^{-1}), shown in **Equation 3.3**:

$$RCa\ (pg\ cell^{-1}d^{-1}) = \left(\frac{1}{2} \cdot \frac{\Delta TA}{\Delta cells\ ml^{-1}}\right) \cdot\ d^{-1} \quad \textbf{(3.3)}$$

The calcite quota ($CaCO_3$ $cell^{-1}$) is simply calculated using the same equation without the inclusion of a term for the duration of the experiment (**Equation 3.4**):

$$CaCO_3\ (pg\ cell^{-1}) = \left(\frac{1}{2} \cdot \frac{\Delta TA}{\Delta cells\ ml^{-1}}\right) \quad \textbf{(3.4)}$$

Samples for total particulate carbon (TPC) and Particulate Organic Carbon (POC) were taken in duplicate at harvest from the large-volume 2L cultures. These were filtered onto pre-combusted (12 h, 500 °C) GF/F filters (pore size 0.6µm), dried overnight at 40 °C and then stored at -20 °C before analysis. When ready to undergo analysis, POC filters were treated with 230µl of HCl (0.1M) to remove the inorganic carbon and oven-dried overnight at 40 °C

again, after the methods of Oviedo et al. (2014). TPC and POC were subsequently measured via CHN analyser at Pennine Analytical Laboratories, UK. PIC (Particulate Inorganic Carbon) was then determined from the difference between TPC and POC.

SEM samples were taken at harvest from the triplicate 600ml cultures by pipetting 10ml of culture onto a 47mm polycarbonate filter (0.6µm pore size) and filtering gently using a Whatman filter pump. Cells on the filter were alternately washed with 10mM $CaCl_2$ solution and 100% Ethanol 3-5 times before drying in a laminar flow hood overnight. Samples were then gold-coated and imaged on a Zeiss Sigma 300 Field Emission Gun Scanning Electron Microscope (FEG-SEM) at the William Dunn School of Pathology, University of Oxford.

Malformation statistics were generated from a collection of SEM images using a combination of manual observations and ImageJ. For each image of either coccospheres or free liths from each experimental condition, every individual lith was categorised as follows: (i) not malformed if there was no evidence of malformation, (ii) mildly malformed if <50% of the total lith was malformed, or (iii) severely malformed if ≥50% of the total lith was malformed. Examples of liths that fit into each of these categories for *E. huxleyi* and *C. braarudii* and the total number of liths analysed for each experimental treatment are included in full in **Appendix 2**.

3.2.4 Experimental protocol in CO_2-limited conditions

Before inoculation of the experiments, all CO_2-limited cultures were pre-acclimated to the control or enhanced alkalinity conditions in the same way as the CO_2-replete cultures. At the beginning of the CO_2-limited experiments, ~1000 cells ml^{-1} SO 14-2 were inoculated in triplicate (~10 times higher cell culture density than recommended by LaRoche et al. (2010), the same inoculation density reported in Kottmeier et al. (2016)).

The CO_2-limited cultures were grown at 15 ^oC (optimum temperature for SO 14-2), on a 14h:10h light:dark cycle, under a light intensity of ~75 – 95 µmol photons m^{-2} s^{-1}. A range is provided because light intensity will not be the same at the sides of the incubator as in the centre. As explained above, cultures were harvested at cell culture densities of 2 - 3 x 10^6 cells ml^{-1}. All other aspects of culturing practice carried out, and samples harvested, were the

same as for the CO_2-replete experiments. The only elements of analysis that were different for the CO_2-limited cultures were that (i) TPC and POC were measured on a SERCON 20/22 Isotope ratio mass spectrometer (IRMS) coupled to a SERCON GSL elemental analyser in the School of Archaeology, University of Oxford and (ii) analysis of alkalinity samples was completed at the National Oceanography Centre, Southampton. The alkalinity of the solutions was measured with a precision of ~2 μmol kg^{-1} on duplicate samples by Gran titration using a Metrohm Ti-touch 916. The titrator is calibrated daily against a certified seawater reference material (Dickson Batch 180, Scripps Institute of Oceanography). The pH of each solution was also measured using the 867 pH module, which is regularly calibrated against standard NBS buffers.

3.3 Results and Discussion

3.3.1 Growth and calcification response of coccolithophores

Growth rates in *E. huxleyi* are ~3 times lower in CO_2-limited conditions compared to CO_2-replete conditions (**Figure 3.6**), both in like-for-like control and enhanced alkalinity culture media. There are no significant differences in growth rate with increasing TA compared to control in CO_2-limited conditions, but growth rates increase with statistically significant difference with increasing TA compared to control in CO_2-replete conditions (**Figure 3.6**, **Panel A**). Also shown in **Figure 3.6** are the other carbonate system parameters which are physiologically relevant for coccolithophores (outlined in the **Introduction**) plotted relative to the growth rates observed in the experimental manipulations.

There are four independent variables (*x*-axis) where the range of culture media values do not overlap for the CO_2-limited and CO_2-replete systems: DIC (**Figure 3.6**, **Panel D**), pH (**Figure 3.6**, **Panel F**), HCO_3^- (**Figure 3.6**, **Panel E**), and [CO_2] (**Figure 3.6**, **Panel G**). Here, we can examine the clustering of points on the plots to identify distinct sample groups relative to the independent variables (McCammon, 1968; Motulsky, GraphPad Statistics Guide). The lack of overlap indicates that those independent variables, either alone or in an interactive fashion,

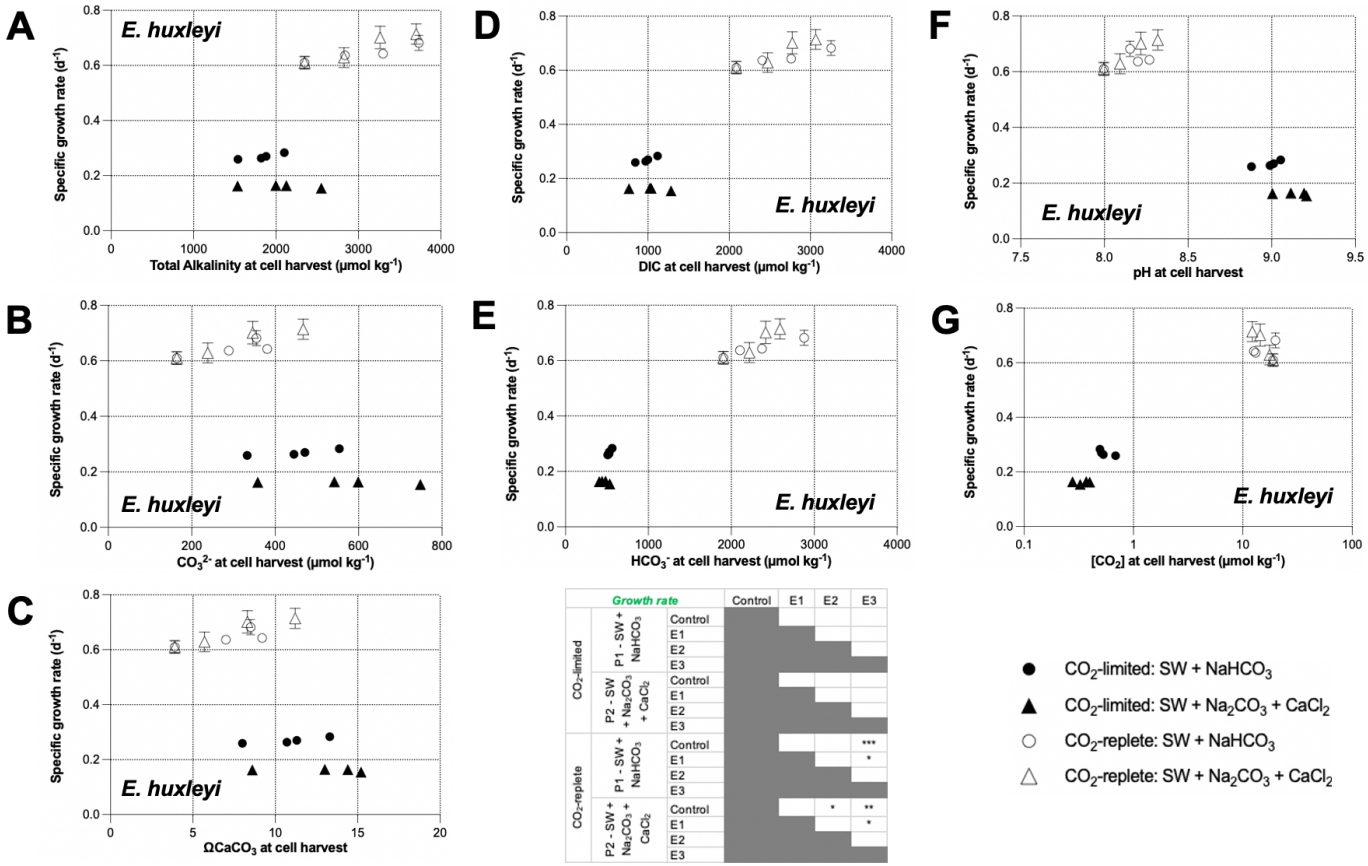

Figure 3.6: *E. huxleyi* specific growth rate response to individual carbonate system parameters in culture media at cell harvest: (A) Total Alkalinity, (B) CO_3^{2-}, (C) $\Omega CaCO_3$, (D) Dissolved Inorganic Carbon (DIC), (E) HCO_3^-, (F) pH, (G) $[CO_2]$. Shown with accompanying table showing statistical significance. * = $P \leq 0.05$, ** = $P \leq 0.01$, *** = $P \leq 0.001$, **** = $P \leq 0.0001$. As outlined in text, Control = Synthetic Ocean Water (SOW), E1 (Control + ~500 µmol kg^{-1}), E2 (Control + ~1000 µmol kg^{-1}), E3 (Control + ~1500 µmol kg^{-1}). In cases where no error bar is shown, this is because the size of the symbol obscures the error bar. Error bars shown are triplicate values from biological triplicate cultures. Note that the *x*-axis for $[CO_2]$ is on $\log_{10}$ scale.

are likely to be driving the difference in growth rates between the CO_2-limited and CO_2-replete systems.

It is not altogether surprising that [CO_2] exerts a large depression on *E. huxleyi* growth rates in the CO_2-limited cultures compared to the CO_2-replete cultures because it is well-established that low [CO_2] suppresses phytoplankton growth (Riebesell et al., 1993; Bach et al., 2011; Sett et al., 2014). High pH (>8.5) has been shown to depress phytoplankton growth in several studies (Durbin and Chen, 1994; Taraldsvik and Myklestad, 2000; Hansen, 2002; Soderberg and Hansen, 2007), although some evidence suggests that phytoplankton growth may be stimulated by pH ~9 (Pedersen and Hansen, 2003; Hinga, 2002), which accurately covers the pH values in the CO_2-limited cultures of this study (**Figure 3.6**, **Panel F**). Therefore, pH could at least partially be driving the growth rate responses observed in this study, although the exact physiological mechanism for this is unclear. DIC is composed of HCO_3^-, CO_2 and CO_3^{2-},

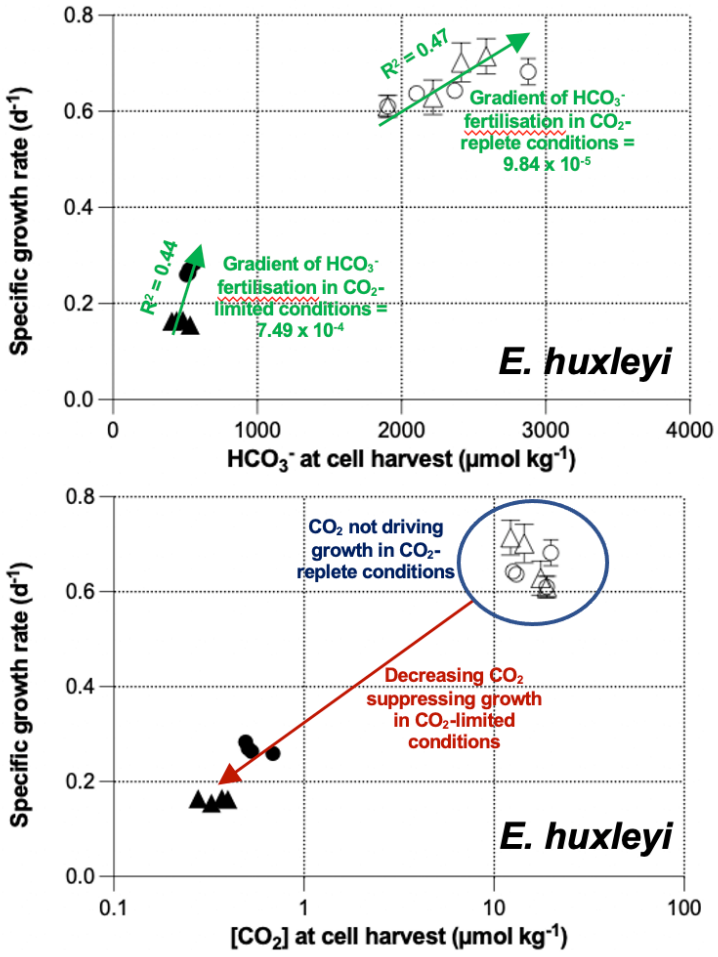

Figure 3.7: *E. huxleyi* specific growth rate response to (A) HCO_3^- and (B) [CO_2] in culture media at cell harvest. Gradient and R^2 values calculated by performing simple linear regression in GraphPad Prism 9. In cases where no error bar is shown, this is because the size of the symbol obscures the error bar. Error bars shown are triplicate values from biological triplicate cultures. Note that the *x*-axis for [CO_2] is on $\log_{10}$ scale.

so it is more useful to focus on HCO_3^- and CO_2 as the specific physiological drivers to explain the observed responses rather than DIC as a whole component.

Figure 3.7, **Panel A** shows the strength of the positive relationship between [HCO_3^-] and growth rate in *E. huxleyi* both in CO_2-limited (R^2 = 0.4437) and CO_2-replete (R^2 = 0.4740) regimes. Even when *E. huxleyi* growth rate is severely limited by [CO_2] in CO_2-limited conditions (**Figure 3.7**, **Panel B**), there is a clear influence of HCO_3^- fertilising growth (**Figure 3.7**, **Panel A**). As outlined in the **Introduction**, a range of evidence suggests that *E. huxleyi* may use Carbon Concentrating Mechanisms (CCMs) under CO_2-limited conditions (Monteiro et al., 2016; Giordano et al., 2005; Raven et al., 1999; Kottmeier et al., 2014), which allows this species to utilise HCO_3^- to facilitate growth. This is likely to be the case in our experiments.

In CO_2-replete conditions, there is no correlation between increasing [CO_2] and increasing growth rates in *E. huxleyi* (**Figure 3.7**, **Panel B**). There is, however, clear evidence of HCO_3^- fertilising growth in CO_2-replete conditions, although the gradient of HCO_3^- fertilisation is one order of magnitude lower in CO_2-replete conditions compared to CO_2-limited conditions (**Figure 3.7**, **Panel A**). This indicates that an increase [HCO_3^-] exerts a weaker influence on growth rates when [CO_2] is not limiting compared to when [CO_2] is limiting. DIC is present in seawater at concentrations 2-3 orders of magnitude higher than the major limiting macronutrients N and P, and 5-6 orders of magnitude higher than the limiting micronutrient Fe (Herfort et al., 2002), and is not viewed as a limiting component of the carbonate system for the growth of phytoplankton (Redfield, 1958). However, our study suggests that even if *E. huxleyi* is not CO_2-limited, it can be significantly fertilised if the availability of HCO_3^- increases, indicating that *E. huxleyi* growth, and therefore photosynthesis, may be limited by the availability of HCO_3^- in the modern ocean. This is supported by prior work showing that photosynthesis in *E. huxleyi* is not saturated at 2mM DIC (Herfort et al., 2002) and may require 15 times modern-day seawater concentrations to achieve saturation (Paasche, 1964).

The response of *E. huxleyi* calcification to enhanced TA, both in terms of cellular calcification rate (**Panel A**) and cellular calcite quota, $CaCO_3$ $cell^{-1}$ (**Panel B**), is shown in **Figure 3.8**.

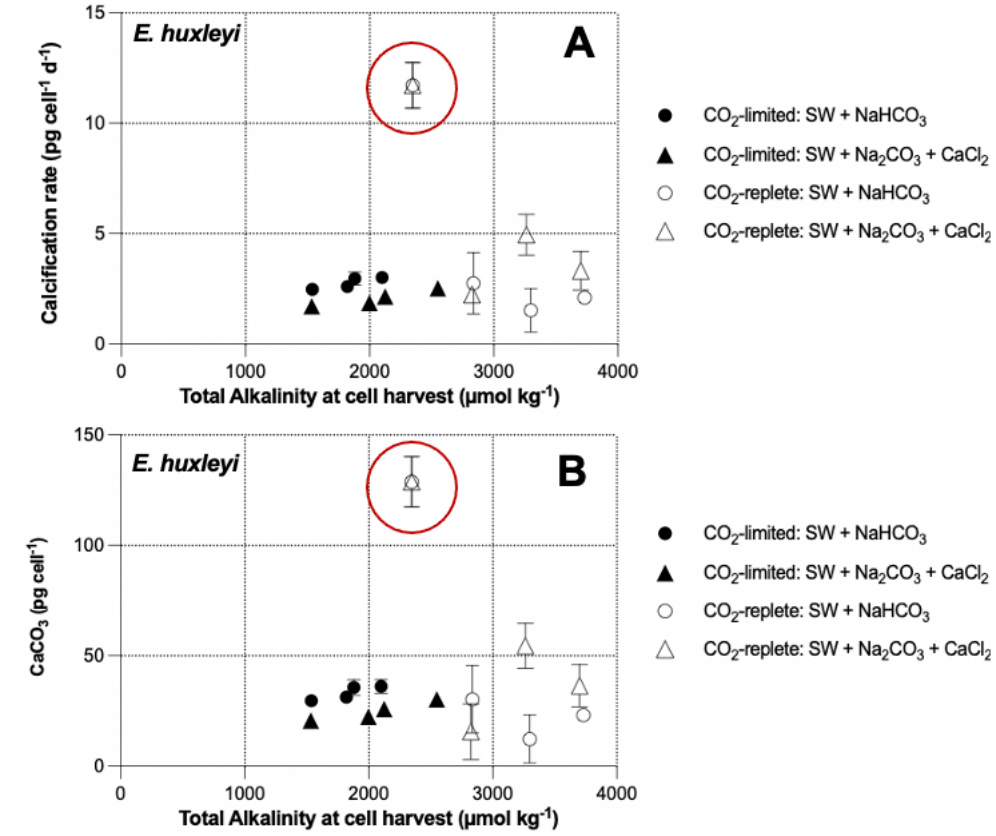

Figure 3.8: *E. huxleyi* (A) Celullar calcification rate and (B) cellular calcite quota vs Total Alkalinity in culture media at cell harvest. In cases where no error bar is shown, this is because the size of the symbol obscures the error bar. Error bars shown are triplicate values from biological triplicate cultures. Outlier discussed in text circled in red.

Circled are the control (SOW) values for *E. huxleyi* in CO_2-replete conditions. Prima facie, it appears that cellular calcification rate and cellular calcite quota decreases by ~5.8 times in CO_2-limited control SOW compared to CO_2-replete control SOW. However, this value is vastly different from all other data, and ROUT analysis (Motulsky and Brown, 2006), Q = 0.1%, returned that this value is an outlier. The data for cellular calcification rate and cellular calcite quota in enhanced alkalinity do not show consistent trends either, indicating that there could be a problem with the reliability of the alkalinity drift method for calculating cellular calcification rate and cellular calcite quota in CO_2-replete conditions (see **3.2 Methods**). CO_2-limited values are subject to a significantly smaller amount of error in measurement (**Figure 3.8**). This could be because the alkalinity drift in CO_2-replete conditions was an order of magnitude smaller than the alkalinity drift in CO_2-limited conditions (see **Figure 3.5**). This could add a significantly higher likelihood of noise and occurrence of spurious values.

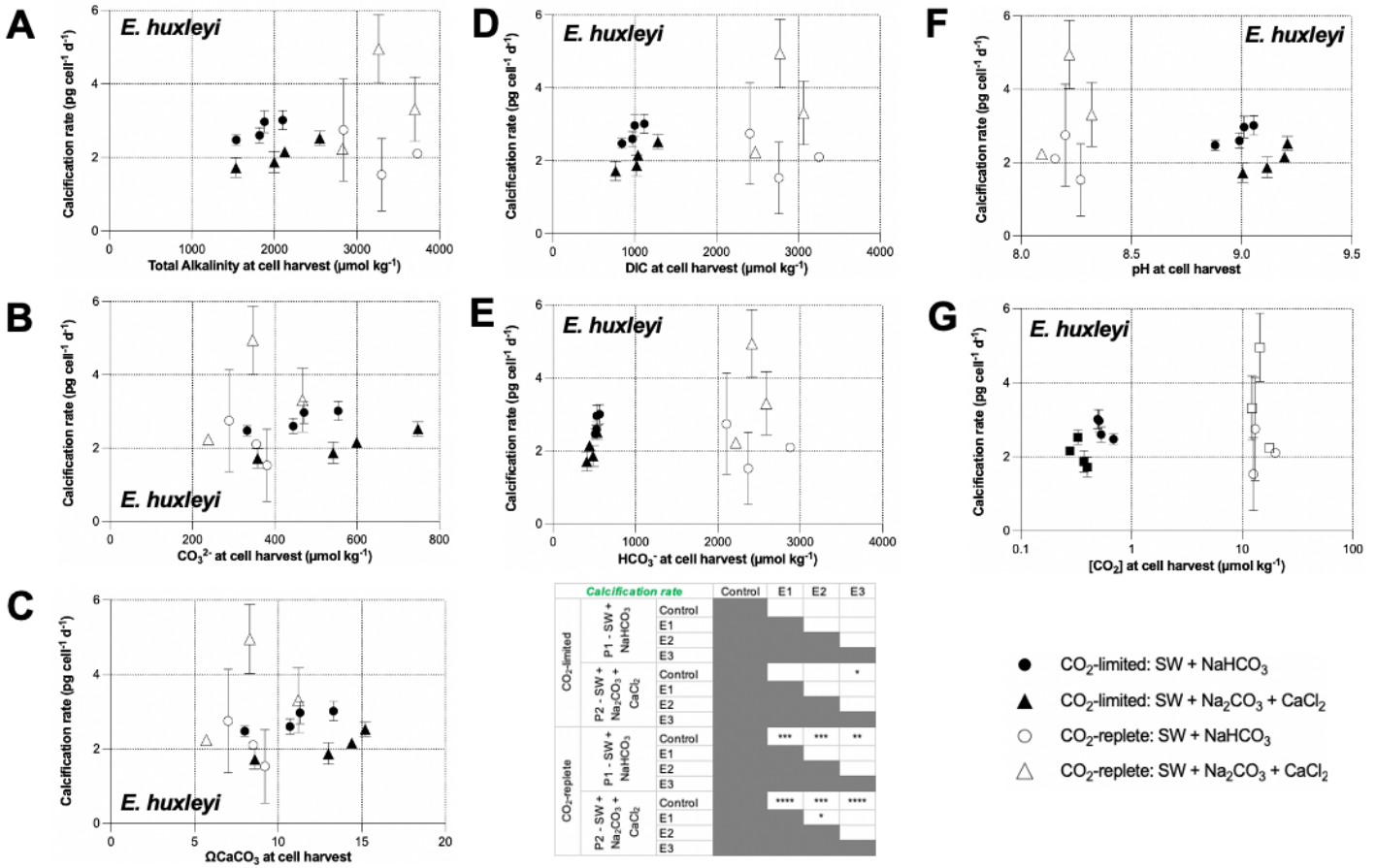

Figure 3.9: *E. huxleyi* cellular calcification rate response to individual carbonate system parameters in culture media at cell harvest: (A) Total Alkalinity, (B) CO_3^{2-}, (C) $\Omega CaCO_3$, (D) Dissolved Inorganic Carbon (DIC), (E) HCO_3^-, (F) pH, (G) $[CO_2]$. Shown with accompanying table showing statistical significance. * = $P \leq 0.05$, ** = $P \leq 0.01$, *** = $P \leq 0.001$, **** = $P \leq 0.0001$. As outlined in text, Control = Synthetic Ocean Water (SOW), E1 (Control + ~500 µmol kg^{-1}), E2 (Control + ~1000 µmol kg^{-1}), E3 (Control + ~1500 µmol kg^{-1}). In cases where no error bar is shown, this is because the size of the symbol obscures the error bar. Error bars shown are triplicate values from biological triplicate cultures. Note that the *x*-axis for $[CO_2]$ is on $\log_{10}$ scale.

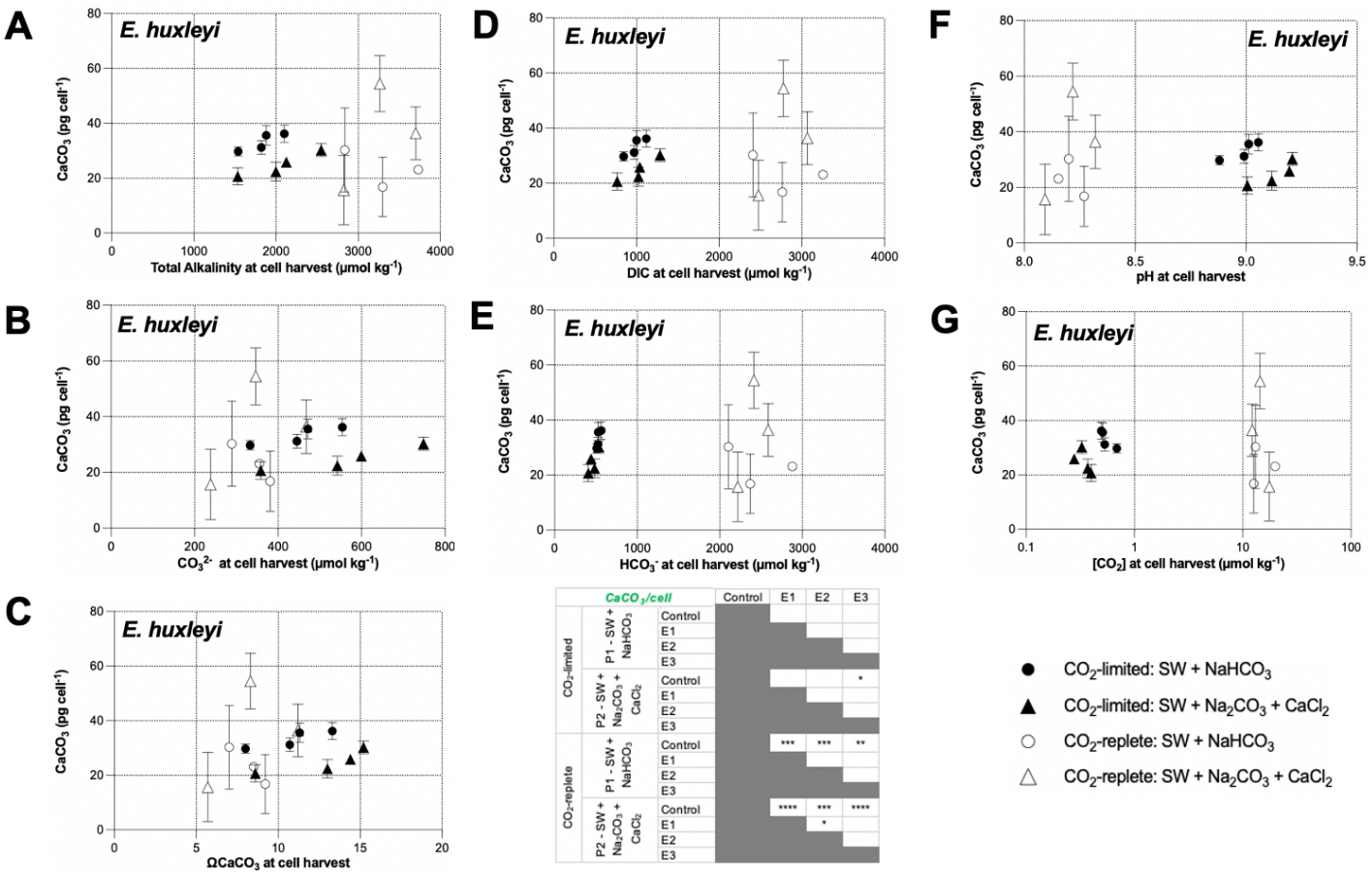

Figure 3.10: *E. huxleyi* cellular calcite quota response to individual carbonate system parameters in culture media at cell harvest: (A) Total Alkalinity, (B) CO_3^{2-}, (C) $\Omega CaCO_3$, (D) Dissolved Inorganic Carbon (DIC), (E) HCO_3^-, (F) pH, (G) $[CO_2]$. Shown with accompanying table showing statistical significance. * = P ≤ 0.05, ** = P ≤ 0.01, *** = P ≤ 0.001, **** = P ≤ 0.0001. As outlined in text, Control = Synthetic Ocean Water (SOW), E1 (Control + ~500 µmol kg^{-1}), E2 (Control + ~1000 µmol kg^{-1}), E3 (Control + ~1500 µmol kg^{-1}). In cases where no error bar is shown, this is because the size of the symbol obscures the error bar. Error bars shown are triplicate values from biological triplicate cultures. Note that the *x*-axis for $[CO_2]$ is on $\log_{10}$ scale.

In **Figure 3.9**, the likely outlier has been removed from the dataset for cellular calcification rate. There is no significant difference between calcification rates in CO_2-limited and CO_2-replete conditions. There are no clear trends in cellular calcification rates with increasing TA in CO_2-replete conditions. As explained in the preceding paragraph, this could be due to the margin of error when working with the alkalinity drift in these dilute cultures. Within the CO_2-limited system, there is a clear increase in cellular calcification rate with increasing Total Alkalinity (**Figure 3.9**, **Panel A**). A positive relationship between DIC (**Figure 3.9**, **Panel D**), pH (**Figure 3.9**, **Panel F**) and HCO_3^- (**Figure 3.9**, **Panel E**) and calcification rates are also observed. **Figure 3.10** plots cellular calcite quota against the carbonate system, and these exhibit exactly the same trends as **Figure 3.9**. This is expected because as outlined in the **Methods**, cellular calcite quota and cellular calcification rate are both calculated using TA drift.

The relationship between cellular calcification and DIC, pH and HCO_3^- under CO_2-limited conditions only are plotted in **Figure 3.11** (cellular calcification rate) and **Figure 3.12** (cellular calcite quota). For both cellular calcification rate (**Figure 3.11**) and cellular calcite quota (**Figure 3.12**) there are relatively strong positive correlations between TA (**Panel A**), CO_3^{2-} (**Panel B**), $\Omega CaCO_3$ (**Panel C**), DIC (**Panel D**), HCO_3^- (**Panel E**), and pH (**Panel F**) within Pathway 1 and Pathway 2 separately. There is also a reasonably strong trend of decreasing cellular calcification rate (**Figure 3.11**, **Panel G**) with increasing [CO_2] for both pathways and decreasing cellular calcite quota (**Figure 3.12**, **Panel G**) with increasing [CO_2] for both pathways. Perhaps the most striking trend, however, is one that unites the two pathways; that of increasing cellular calcification rate with increasing HCO_3^- (**Figure 3.11**, **Panel E**) and increasing cellular calcite quota with increasing HCO_3^- (**Figure 3.12**, **Panel E**). The influence of a carbonate chemistry parameter overriding any influence of an individual experimental trajectory indicates a fundamental physiological control of HCO_3^- on calcification (rate and quota), regardless of the mode of chemical alkalinity manipulation. This aligns with the most recent updates to our understanding of calcification (see **Introduction**), where HCO_3^- is the

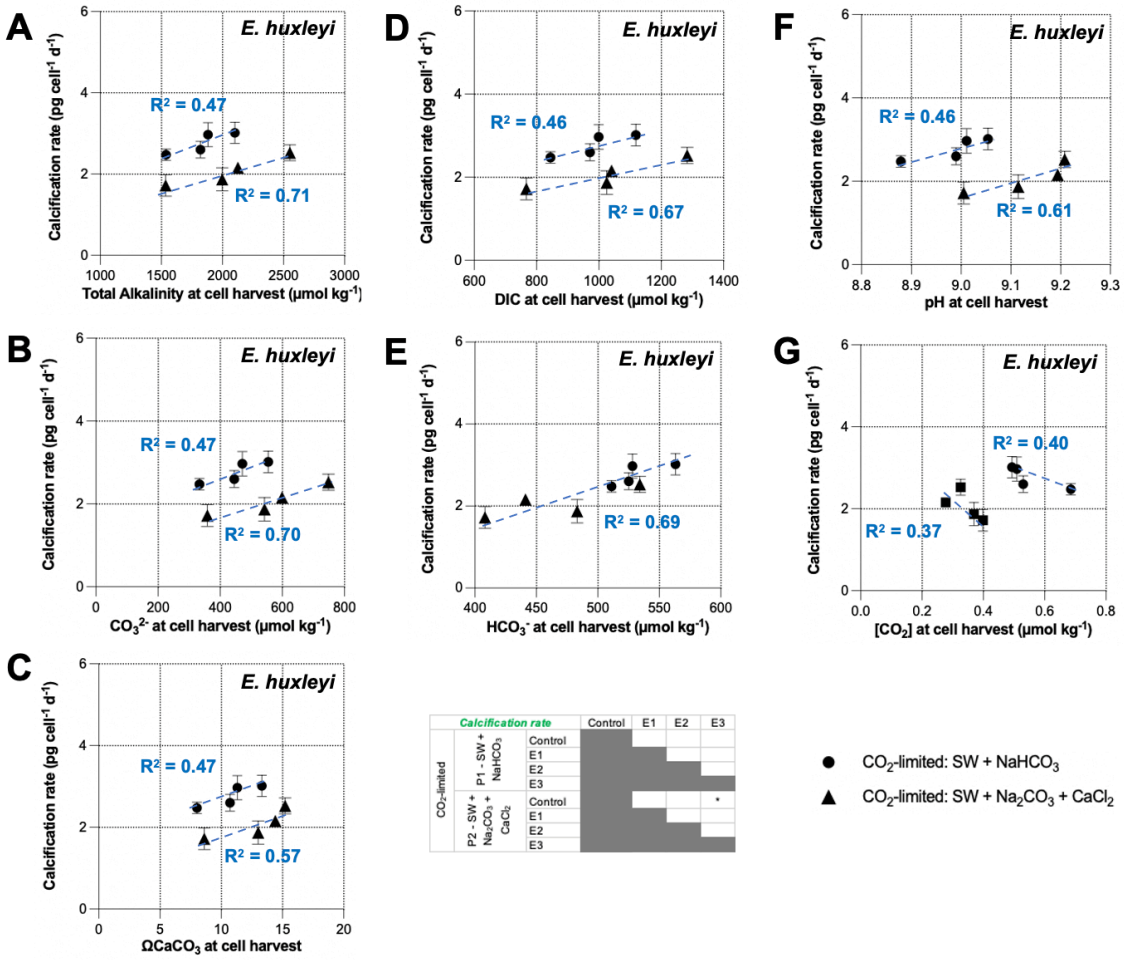

Figure 3.11: *E. huxleyi* cellular calcification rate response to individual carbonate system parameters in culture media at cell harvest, in the CO_2-limited system only: (A) Total Alkalinity, (B) CO_3^{2-}, (C) $\Omega CaCO_3$, (D) Dissolved Inorganic Carbon (DIC), (E) HCO_3^-, (F) pH, (G) $[CO_2]$. Shown with accompanying table showing statistical significance. * = P ≤ 0.05, ** = P ≤ 0.01, *** = P ≤ 0.001, **** = P ≤ 0.0001. As outlined in text, Control = Synthetic Ocean Water (SOW), E1 (Control + ~500 µmol kg^{-1}), E2 (Control + ~1000 µmol kg^{-1}), E3 (Control + ~1500 µmol kg^{-1}). In cases where no error bar is shown, this is because the size of the symbol obscures the error bar. Error bars shown are triplicate values from biological triplicate cultures. Note that the *x*-axis for $[CO_2]$ is **NOT** on $\log_{10}$ scale. Regression performed using simple linear regression in GraphPad Prism 9.

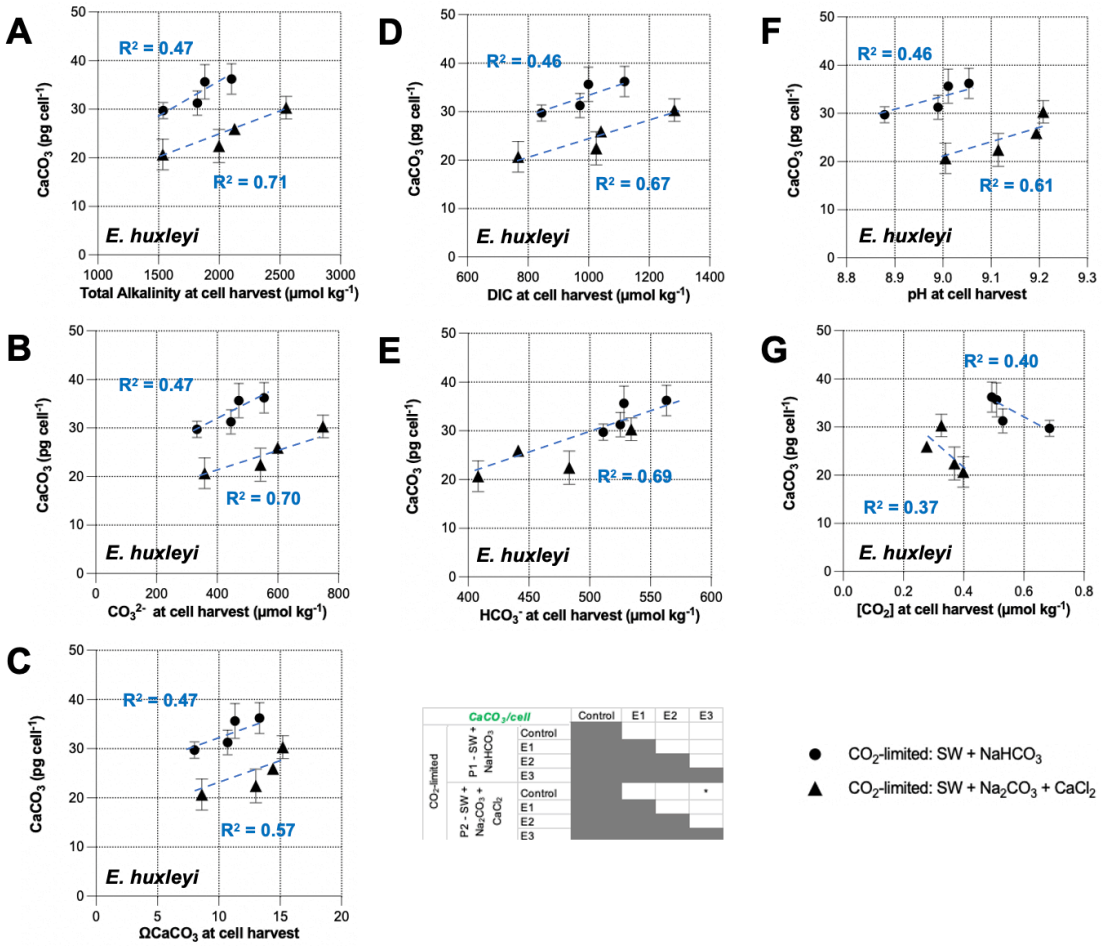

Figure 3.12: *E. huxleyi* cellular calcification quota response to individual carbonate system parameters in culture media at cell harvest, in the CO_2-limited system only: (A) Total Alkalinity, (B) CO_3^{2-}, (C) $\Omega CaCO_3$, (D) Dissolved Inorganic Carbon (DIC), (E) HCO_3^-, (F) pH, (G) $[CO_2]$. Shown with accompanying table showing statistical significance. * = P ≤ 0.05, ** = P ≤ 0.01, *** = P ≤ 0.001, **** = P ≤ 0.0001. As outlined in text, Control = Synthetic Ocean Water (SOW), E1 (Control + ~500 µmol kg^{-1}), E2 (Control + ~1000 µmol kg^{-1}), E3 (Control + ~1500 µmol kg^{-1}). In cases where no error bar is shown, this is because the size of the symbol obscures the error bar. Error bars shown are triplicate values from biological triplicate cultures. Note that the *x*-axis for $[CO_2]$ is **NOT** on $\log_{10}$ scale. Regression performed using simple linear regression in GraphPad Prism 9.

primary substrate for calcification (Bach et al., 2015; Cyronak et al., 2016; Taylor et al., 2017) and as such exerts a first-order control on cellular calcification rate (and as observed in this study, cellular calcite quota, too).

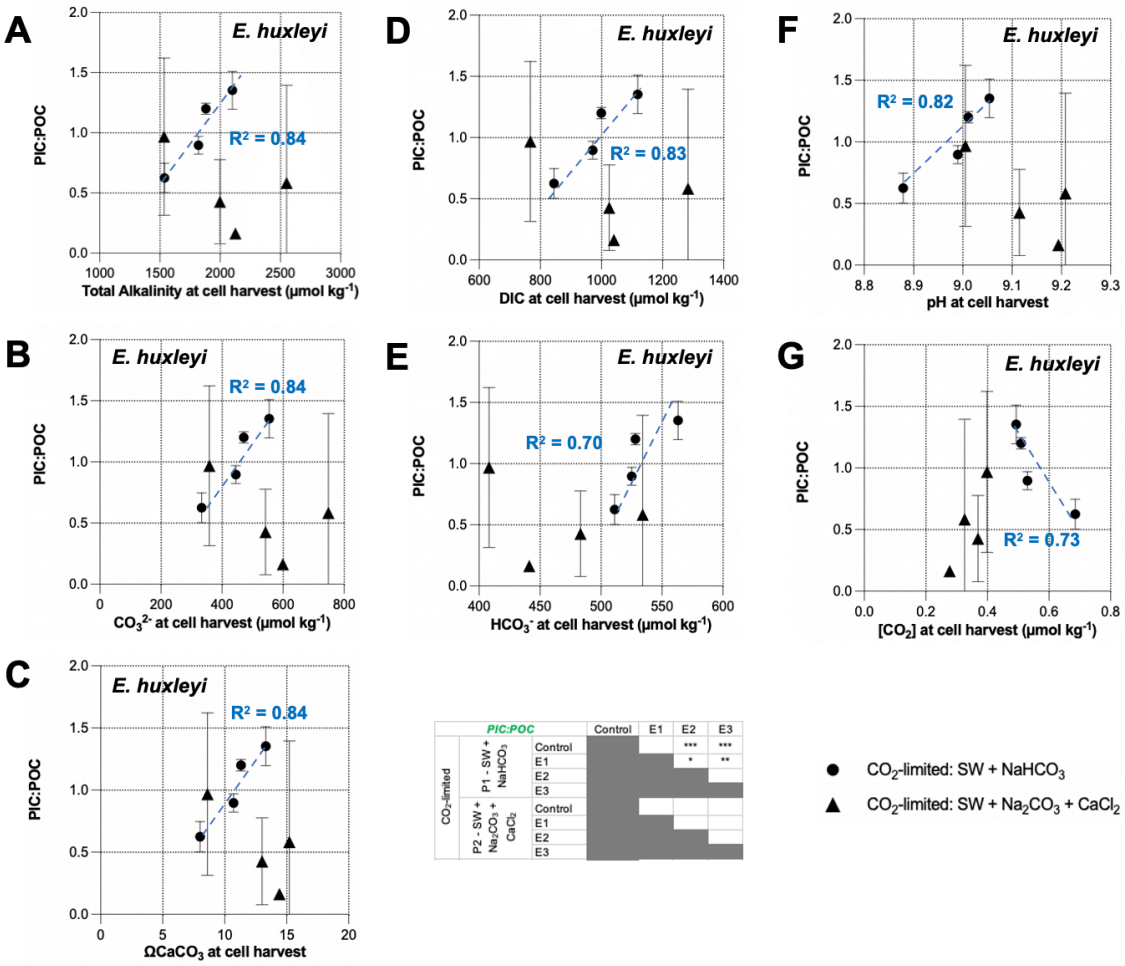

Figure 3.13: *E. huxleyi* PIC:POC response to individual carbonate system parameters in culture media at cell harvest, in the CO_2-limited system only: (A) Total Alkalinity, (B) CO_3^{2-}, (C) $\Omega CaCO_3$, (D) Dissolved Inorganic Carbon (DIC), (E) HCO_3^-, (F) pH, (G) $[CO_2]$. Shown with accompanying table showing statistical significance. * = P ≤ 0.05, ** = P ≤ 0.01, *** = P ≤ 0.001, **** = P ≤ 0.0001. As outlined in text, Control = Synthetic Ocean Water (SOW), E1 (Control + ~500 µmol kg^{-1}), E2 (Control + ~1000 µmol kg^{-1}), E3 (Control + ~1500 µmol kg^{-1}). In cases where no error bar is shown, this is because the size of the symbol obscures the error bar. Error bars shown are technical replicate values measured on duplicate filters taken from 2L large-volume cultures run alongside biological triplicate cultures combined with analytical uncertainty (added in quadrature). Note that the *x*-axis for $[CO_2]$ is on $\log_{10}$ scale. Regression performed using simple linear regression in GraphPad Prism 9.

The relationships between PIC:POC and the carbonate system parameters in the CO_2-limited system are similar to those with cellular calcification rate and calcite quota (**Figure 3.13**), at least with Pathway 1, where linear correlations between all carbonate system parameters are of high strength. Pathway 2 does not show any conclusive trends with any of the carbonate system parameters (**Figure 3.13**). This is mainly due to the large error of measurement evident

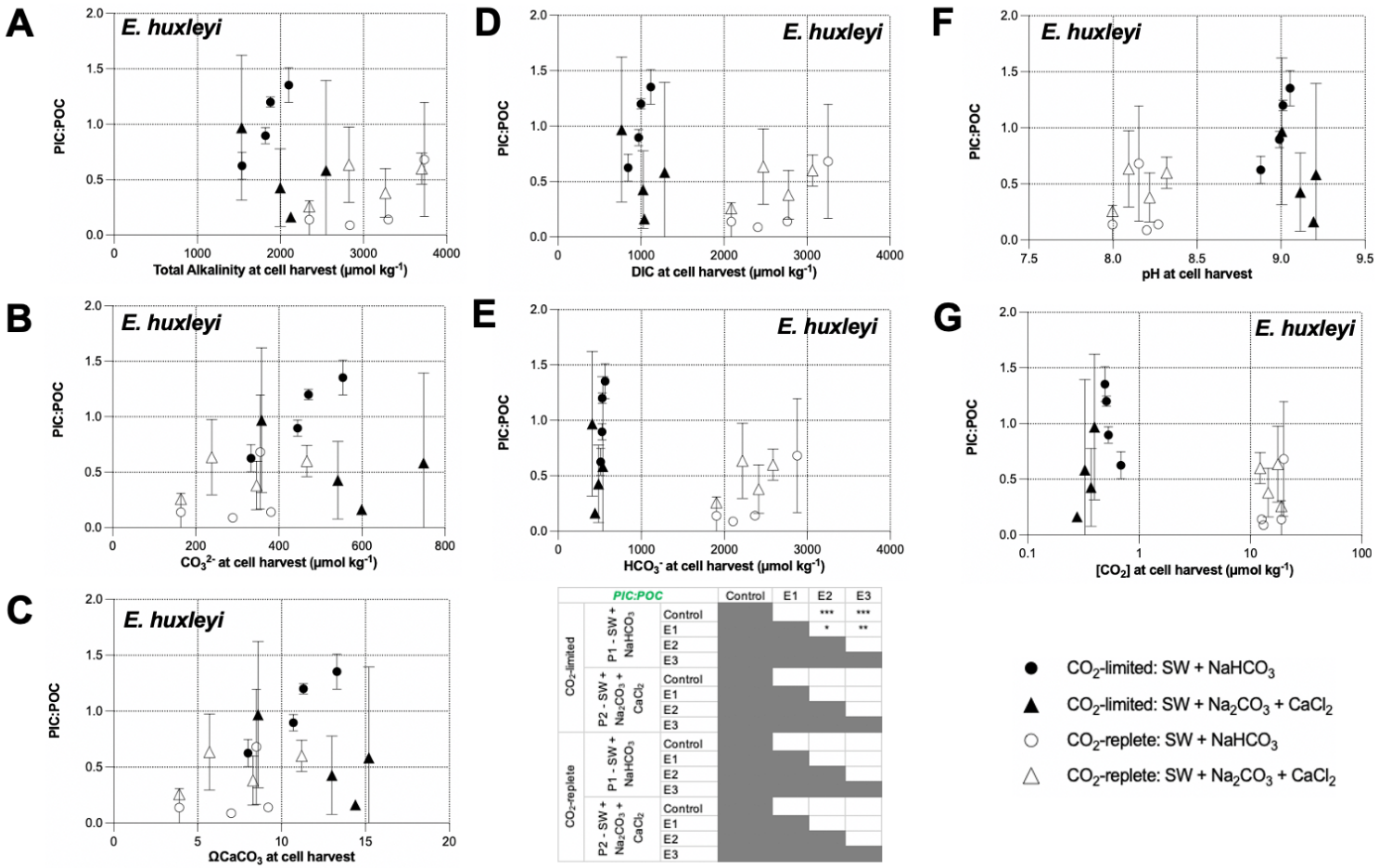

Figure 3.14: *E. huxleyi* PIC:POC response to individual carbonate system parameters in culture media at cell harvest, in the CO_2-limited and CO_2-replete system: (A) Total Alkalinity, (B) CO_3^{2-}, (C) $\Omega CaCO_3$, (D) Dissolved Inorganic Carbon (DIC), (E) HCO_3^-, (F) pH, (G) $[CO_2]$. Shown with accompanying table showing statistical significance. * = P ≤ 0.05, ** = P ≤ 0.01, *** = P ≤ 0.001, **** = P ≤ 0.0001. As outlined in text, Control = Synthetic Ocean Water (SOW), E1 (Control + ~500 µmol kg^{-1}), E2 (Control + ~1000 µmol kg^{-1}), E3 (Control + ~1500 µmol kg^{-1}). In cases where no error bar is shown, this is because the size of the symbol obscures the error bar. Error bars shown are technical replicate values measured on duplicate filters taken from 2L large-volume cultures run alongside biological triplicate cultures combined with analytical uncertainty (added in quadrature). Note that the *x*-axis for $[CO_2]$ is on $\log_{10}$ scale. Regression performed using simple linear regression in GraphPad Prism 9.

in these samples. The lack of precision in these measurements could be due to analytical problems with the PIC:POC measurement, but there is nothing recorded in laboratory notebooks which would point to a known source of error on these samples. PIC:POC values in both the CO_2-replete and CO_2-limited systems are shown in **Figure 3.14**. No regression lines shown for the CO_2-limited systems are shown on **Figure 3.14**, unlike in **Figure 3.13**. It appears that as in the CO_2-limited system, there is a possible positive trend in CO_2-replete Pathway 1, but no statistically significant differences between these treatments were returned by ANOVA analysis (**Figure 3.14**).

There is strong evidence (R^2 = 0.7532) that coccosphere size increases with increasing TA for CO_2-limited cultures of *E. huxleyi*, whereas coccosphere size does not change with increasing TA in CO_2-replete conditions (**Figure 3.15**, **Panel A**). As outlined previously, cellular calcification rate and quota increased with increasing TA under CO_2-limited conditions. Therefore, a larger coccosphere could be explained by the increasing amount of calcification at higher TA. Indeed, coccosphere size correlates with cellular calcite quota (**Figure 3.15**, **Panel B**), and the relationship is moderately strong (R^2 = 0.4176).

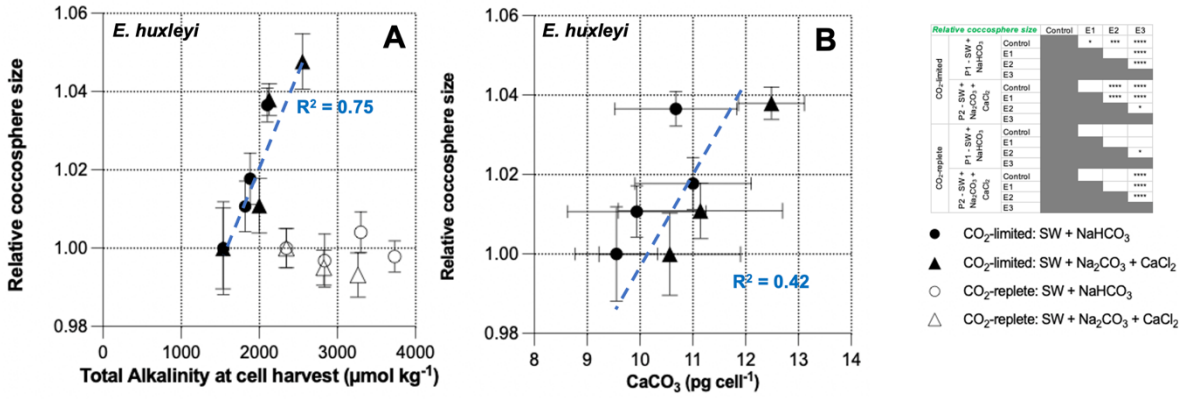

Figure 3.15: Trends in *E. huxleyi* relative coccosphere size (A) vs Total Alkalinity at cell harvest in both CO_2-replete and CO_2-limited conditions and (B) vs cellular calcite quota in CO_2-limited conditions. Shown with accompanying table showing statistical significance. * = P ≤ 0.05, ** = P ≤ 0.01, *** = P ≤ 0.001, **** = P ≤ 0.0001. As outlined in text, Control = Synthetic Ocean Water (SOW), E1 (Control + ~500 µmol kg^{-1}), E2 (Control + ~1000 µmol kg^{-1}), E3 (Control + ~1500 µmol kg^{-1}). In cases where no error bar is shown, this is because the size of the symbol obscures the error bar. Error bars (horizontal and vertical) shown are triplicate values from biological triplicate cultures. Note that the *x*-axis for [CO_2] is on $\log_{10}$ scale. Regression performed using simple linear regression in GraphPad Prism 9.

E. huxleyi shows an increased tendency towards malformed liths with increasing TA both in CO_2-replete and CO_2-limited conditions (**Figure 3.16**). The baseline level of malformation in control conditions is higher for RCC911 (the strain used for *E. huxleyi* CO_2-replete experiments) than for SO 14-2 (the strain used for *E. huxleyi* CO_2-limited experiments).

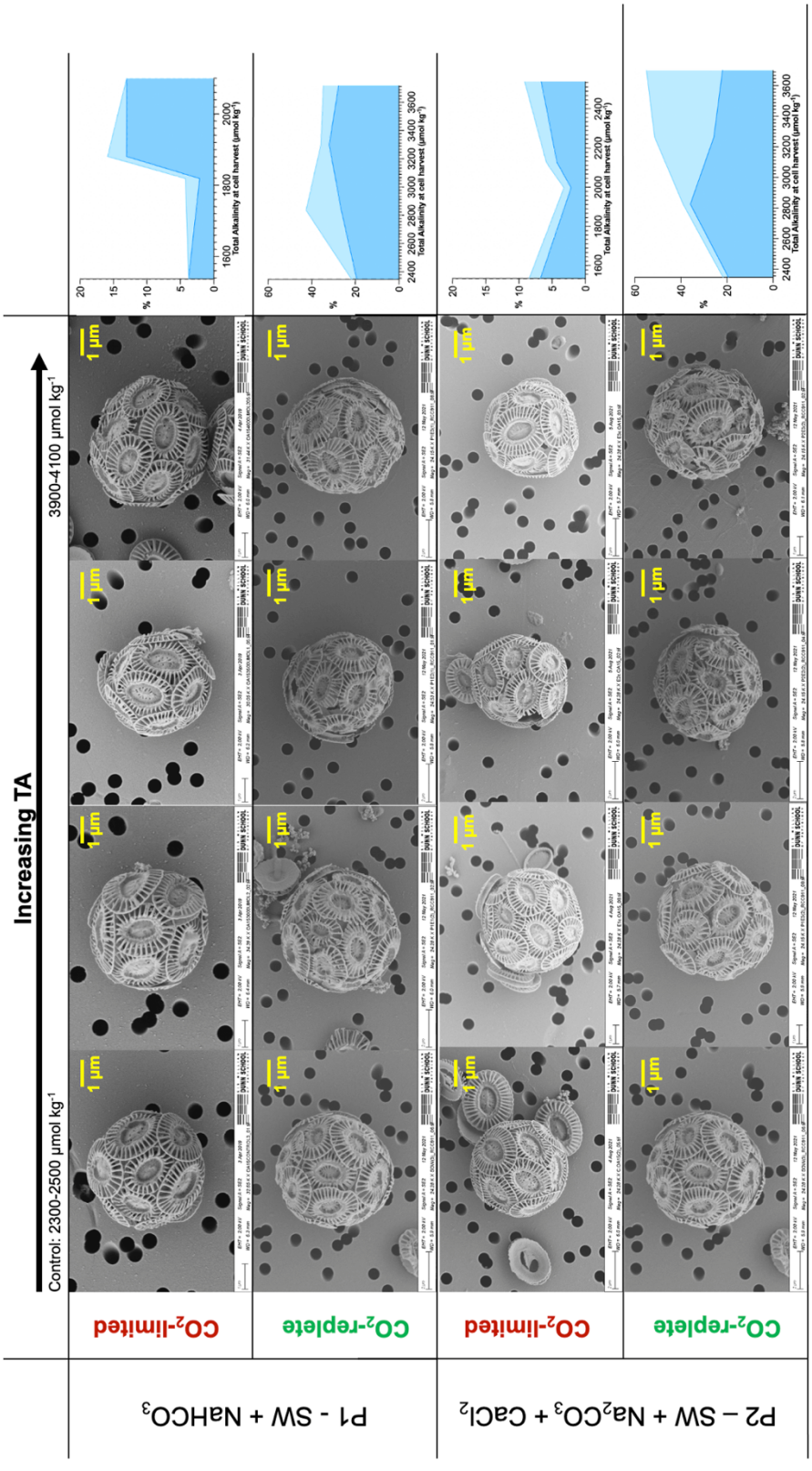

Figure 3.16: SEM images taken of *E. huxleyi* at cell harvest from CO_2-replete and CO_2-limited cultures. Trendline shown for increasing TA. Accompanying graphs show Total Alkalinity at cell harvest on x axis vs. % malformation on y axis. Upper line on each graph = total % of lith malformation observed. Lighter blue area = % of liths exhibiting severe malformation. Darker blue area = % of liths exhibiting mild malformation. For full details of these categorisations, please see section **3.2.3.**

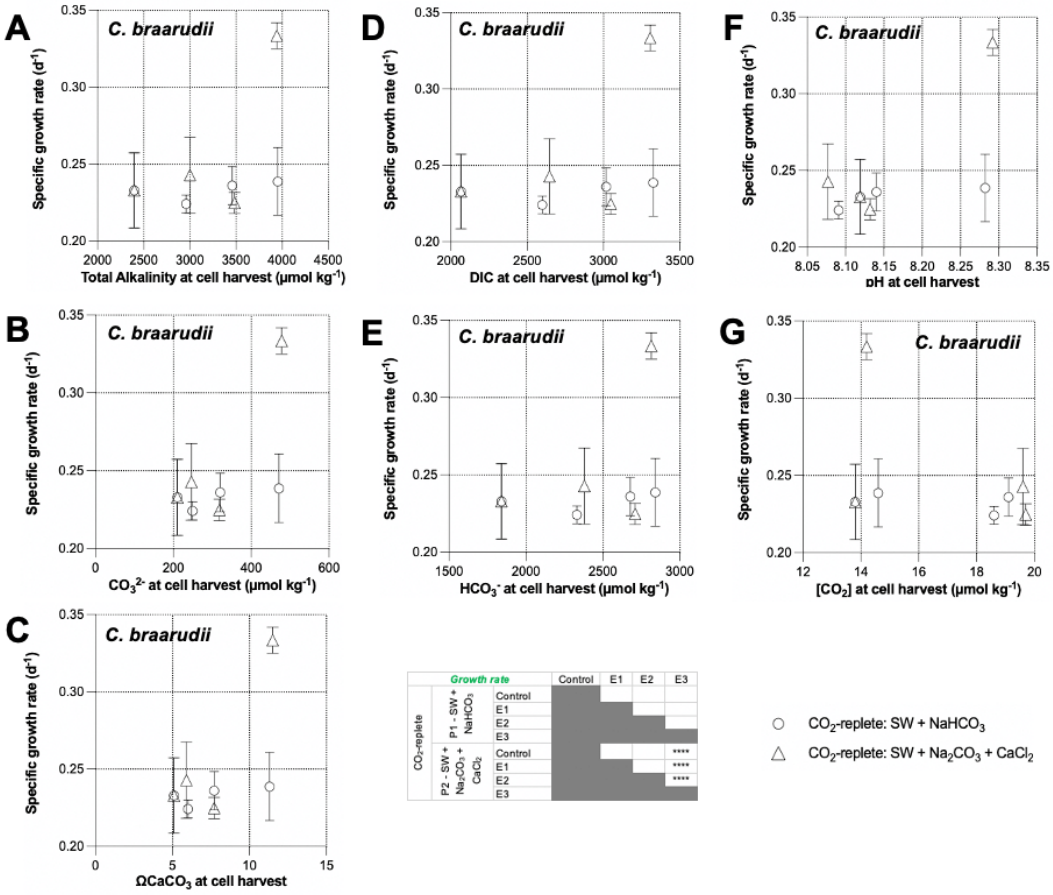

Figure 3.17: *C. braarudii* specific growth rate response to individual carbonate system parameters in culture media at cell harvest: (A) Total Alkalinity, (B) CO_3^{2-}, (C) $\Omega CaCO_3$, (D) Dissolved Inorganic Carbon (DIC), (E) HCO_3^-, (F) pH, (G) $[CO_2]$. Shown with accompanying table showing statistical significance. * = P ≤ 0.05, ** = P ≤ 0.01, *** = P ≤ 0.001, **** = P ≤ 0.0001. As outlined in text, Control = Synthetic Ocean Water (SOW), E1 (Control + ~500 µmol kg^{-1}), E2 (Control + ~1000 µmol kg^{-1}), E3 (Control + ~1500 µmol kg^{-1}). In cases where no error bar is shown, this is because the size of the symbol obscures the error bar. Error bars shown are triplicate values from biological triplicate cultures.

Coccolithus braarudii (C. braarudii), in contrast to E. huxleyi, generally does not change its growth rate with increasing TA or any of the other carbonate system parameters which co-vary with increasing TA (**Figure 3.17**). The only exception is for the highest TA treatment (TA = 3953 µmol kg^{-1}, see **Table 3.1**) for Pathway 2, where growth rate is significantly increased compared to all other values. The only difference between culture media for this culture and the corresponding level of TA in Pathway 1 culture (TA = 3943 µmol kg^{-1}, see **Table 3.1**) is that alkalinity has been added as Ca^{2+} rather than Na^+. The concentration of Ca^{2+} in Pathway 2, where TA = 3953 µmol kg^{-1}, is 7.4% higher ($[Ca^{2+}]$ = 11.3mM) than in the corresponding Pathway 1 treatment, where TA = 3943 µmol kg^{-1} and $[Ca^{2+}]$ = 10.5mM (see **Table 3.1**). It is

unlikely that an increase in Ca^{2+} of this magnitude would physiologically impact *C. braarudii* in a significant fashion, based on past work with *C. braarudii* response to raised concentrations of Ca^{2+} in solution. No significant response of the coccolithophores *E. huxleyi* or *G. oceanica* to increased Ca^{2+} was observed until [Ca^{2+}] = 50mM (Müller et al., 2015), and *C. braarudii* has been shown to be tolerant to higher [Ca^{2+}] than *E. huxleyi* (Müller et al., 2011). Additionally, ROUT analysis (Q = 0.1%) returned that this value is an outlier compared to the rest of the dataset. Therefore, we conclude that there is no significant impact on *C. braarudii* growth rate from the OAE treatments in our study.

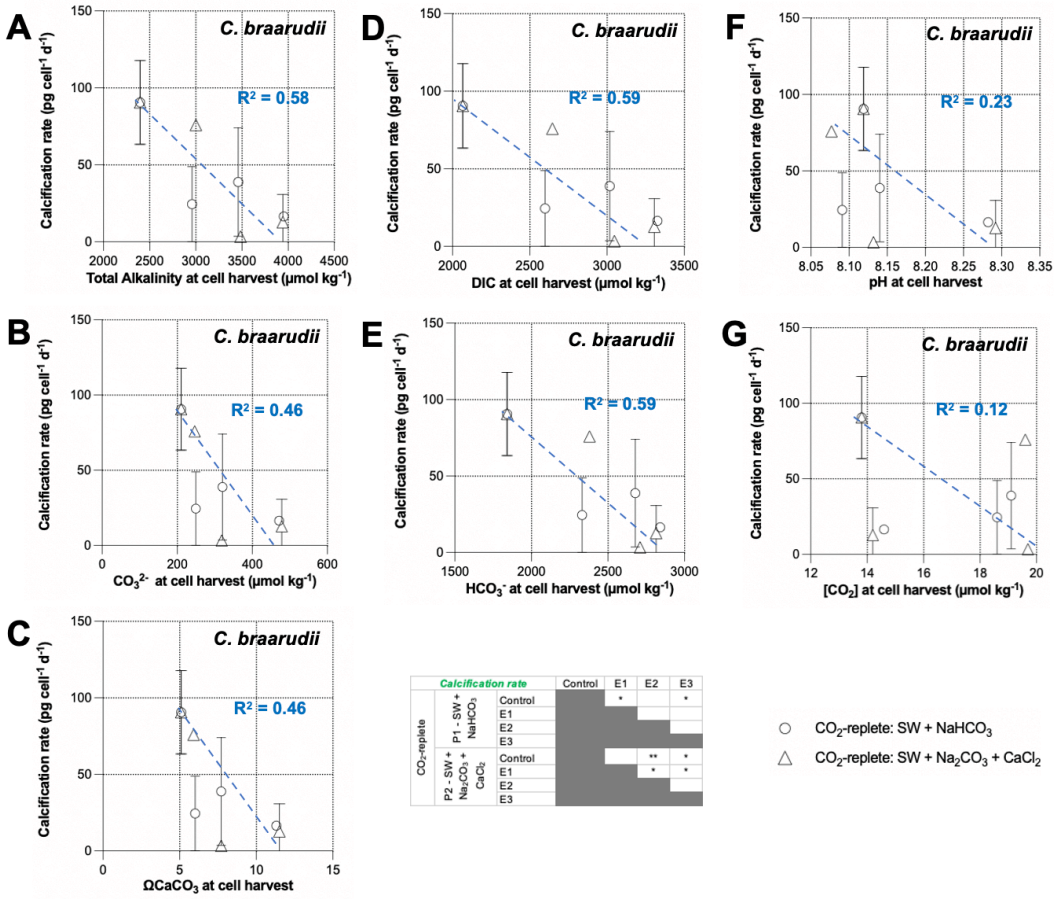

Figure 3.18: *C. braarudii* cellular calcification rate response to individual carbonate system parameters in culture media at cell harvest: (A) Total Alkalinity, (B) CO_3^{2-}, (C) $\Omega CaCO_3$, (D) Dissolved Inorganic Carbon (DIC), (E) HCO_3^-, (F) pH, (G) [CO_2]. Shown with accompanying table showing statistical significance. * = P ≤ 0.05, ** = P ≤ 0.01, *** = P ≤ 0.001, **** = P ≤ 0.0001. As outlined in text, Control = Synthetic Ocean Water (SOW), E1 (Control + ~500 µmol kg^{-1}), E2 (Control + ~1000 µmol kg^{-1}), E3 (Control + ~1500 µmol kg^{-1}). In cases where no error bar is shown, this is because the size of the symbol obscures the error bar. Error bars shown are triplicate values from biological triplicate cultures. Regression performed using simple linear regression in GraphPad Prism 9.

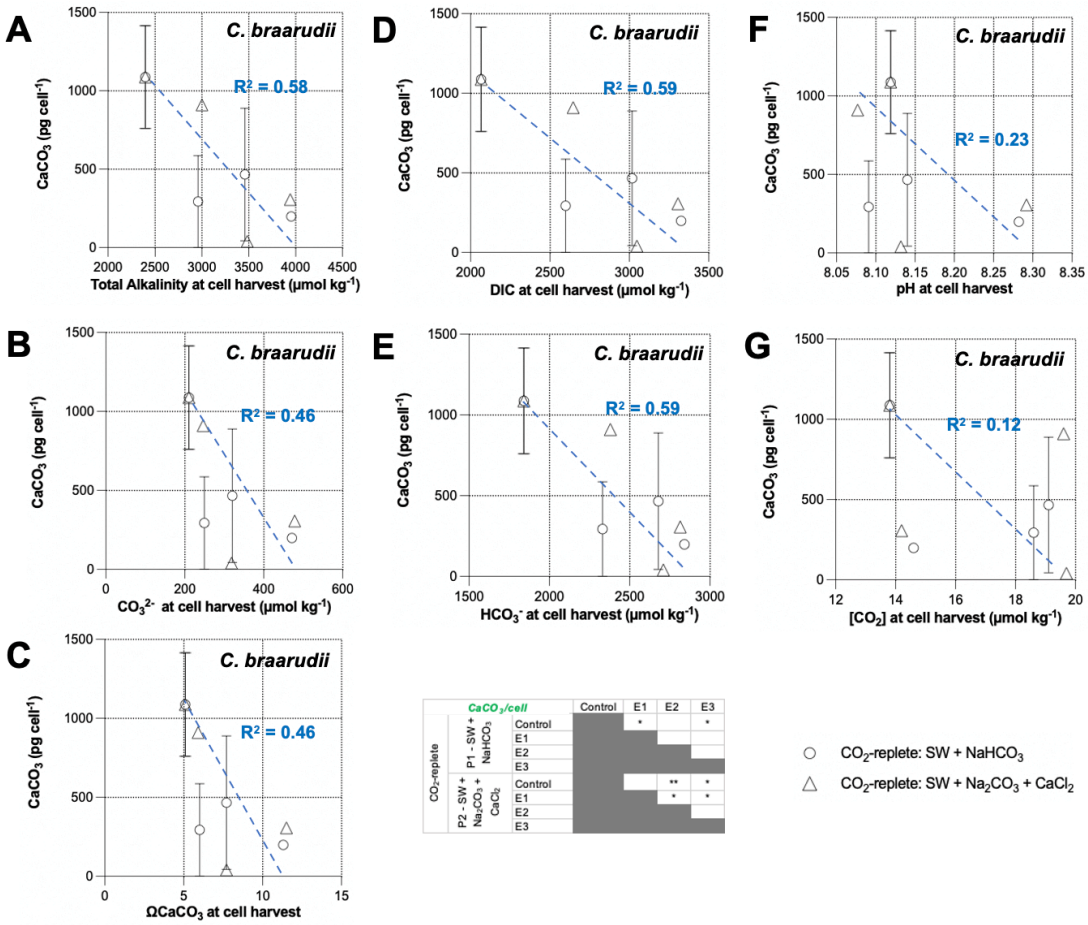

Figure 3.19: *C. braarudii* cellular calcite quota response to individual carbonate system parameters in culture media at cell harvest: (A) Total Alkalinity, (B) CO_3^{2-}, (C) $\Omega CaCO_3$, (D) Dissolved Inorganic Carbon (DIC), (E) HCO_3^-, (F) pH, (G) $[CO_2]$. Shown with accompanying table showing statistical significance. * = P ≤ 0.05, ** = P ≤ 0.01, *** = P ≤ 0.001, **** = P ≤ 0.0001. As outlined in text, Control = Synthetic Ocean Water (SOW), E1 (Control + ~500 µmol kg^{-1}), E2 (Control + ~1000 µmol kg^{-1}), E3 (Control + ~1500 µmol kg^{-1}). In cases where no error bar is shown, this is because the size of the symbol obscures the error bar. Error bars shown are triplicate values from biological triplicate cultures. Regression performed using simple linear regression in GraphPad Prism 9.

By contrast, for *C. braarudii*, there appears to be a convincing trend of decreasing cellular calcification rate (**Figure 3.18**) and cellular calcite quota (**Figure 3.19**) with increasing TA and the other co-varying parameters: DIC, pH, CO_3^{2-}, $\Omega CaCO_3$, HCO_3^- and $[CO_2](aq)$. As explained for E. huxleyi, the same trends and correlations with cellular calcification rate and cellular calcite quota are to be expected due to the fact both these measures are calculated using TA drift (see **Methods**). The correlations with $[CO_2]$ are likely poor (R^2 = 0.1236) due to the variation in $[CO_2]$ values with increasing TA in the culture media prior to inoculation (see **Figure 3.3**). Nevertheless, explanations invoking changes in $[CO_2]$ cannot be used for

calcification rate or quota in *C. braarudii* because there is no robust trend in [CO_2] with increasing TA in culture media. Physiologically, therefore, the only parameter which could feasibly drive a decrease in calcification (rate and quota) in *C. braarudii* is pH. Increasing $\Omega CaCO_3$ should promote a more favourable environment for calcification. Increasing DIC/HCO_3^-, as the substrate for calcification, should promote more calcification. TA and CO_3^{2-} are not physiologically relevant parameters for coccolithophores. Increasing pH should in theory provide an easier environment in which to carry out calcification, because the high external pH has low [H^+] and therefore it should be easier to expel H^+ produced during calcification. This is not what is observed in our experimental manipulations. One of the only similar culturing studies which has been conducted with *C. braarudii* found that average PIC quota was shown to decrease with increasing pH (>8.1) and decreasing [CO_2](aq) (Langer et al., 2006). We tentatively suggest that if it weren't for the lack of trend in [CO_2] with increasing TA in our culture media data, this might be the same trend we would observe in our data, in light of an alternative credible physiological explanation. If this were true, it would suggest that *C. braarudii* is most sensitive to [CO_2] as the source of DIC for calcification.

There are no trends in PIC:POC of *C. braarudii* with increasing TA or any of the other co-varying carbonate system parameters (**Figure 3.20**), although this is mainly due to the large error associated with these measurements. There are also no trends in coccosphere size of *C. braarudii* linked to either increasing TA or cellular calcite quota (**Figure 3.21**). *C. braarudii* cultures show no particularly clear trends in malformation with increasing TA, but can generally be said to be more malformed with increasing TA relative to control conditions (**Figure 3.22**).

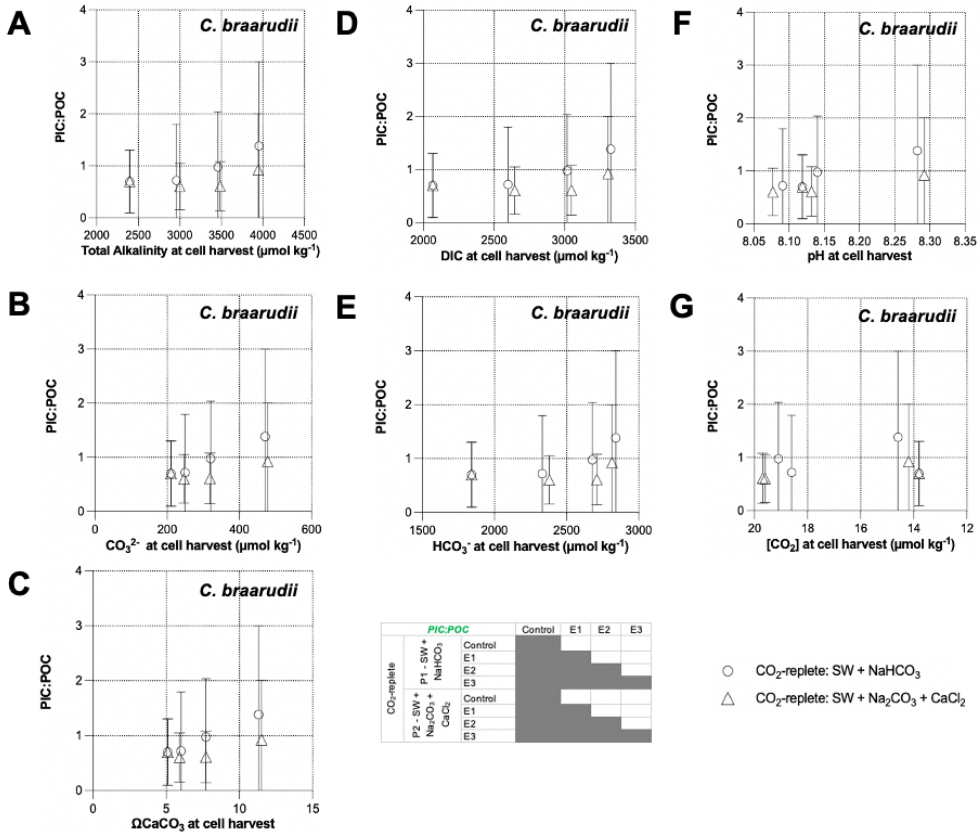

Figure 3.20: *C. braarudii* PIC:POC response to individual carbonate system parameters in culture media at cell harvest: (A) Total Alkalinity, (B) CO_3^{2-}, (C) $\Omega CaCO_3$, (D) Dissolved Inorganic Carbon (DIC), (E) HCO_3^-, (F) pH, (G) $[CO_2]$. Shown with accompanying table showing statistical significance. * = P ≤ 0.05, ** = P ≤ 0.01, *** = P ≤ 0.001, **** = P ≤ 0.0001. As outlined in text, Control = Synthetic Ocean Water (SOW), E1 (Control + ~500 µmol kg^{-1}), E2 (Control + ~1000 µmol kg^{-1}), E3 (Control + ~1500 µmol kg^{-1}). In cases where no error bar is shown, this is because the size of the symbol obscures the error bar. Error bars shown are technical replicate values measured on duplicate filters taken from 2L large-volume cultures run alongside biological triplicate cultures combined with analytical uncertainty (added in quadrature).

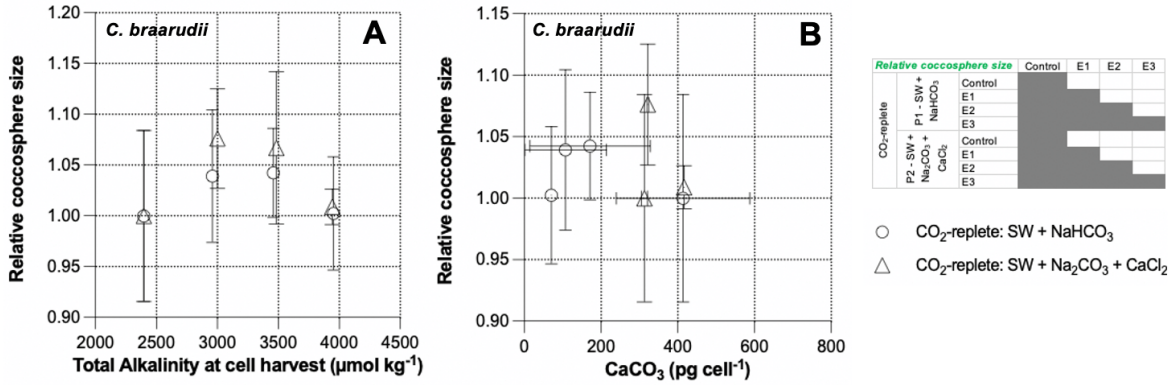

Figure 3.21: Trends in *C. braarudii* relative coccosphere size in both CO_2-replete and CO_2-limited conditions (A) vs Total Alkalinity at cell harvest and (B) vs cellular calcite quota. Shown with accompanying table showing statistical significance. * = P ≤ 0.05, ** = P ≤ 0.01, *** = P ≤ 0.001, **** = P ≤ 0.0001. As outlined in text, Control = Synthetic Ocean Water (SOW), E1 (Control + ~500 µmol kg^{-1}), E2 (Control + ~1000 µmol kg^{-1}), E3 (Control + ~1500 µmol kg^{-1}). In cases where no error bar is shown, this is because the size of the symbol obscures the error bar. Error bars (horizontal and vertical) shown are triplicate values from biological triplicate cultures. Note that the *x*-axis for $[CO_2]$ is on $\log_{10}$ scale.

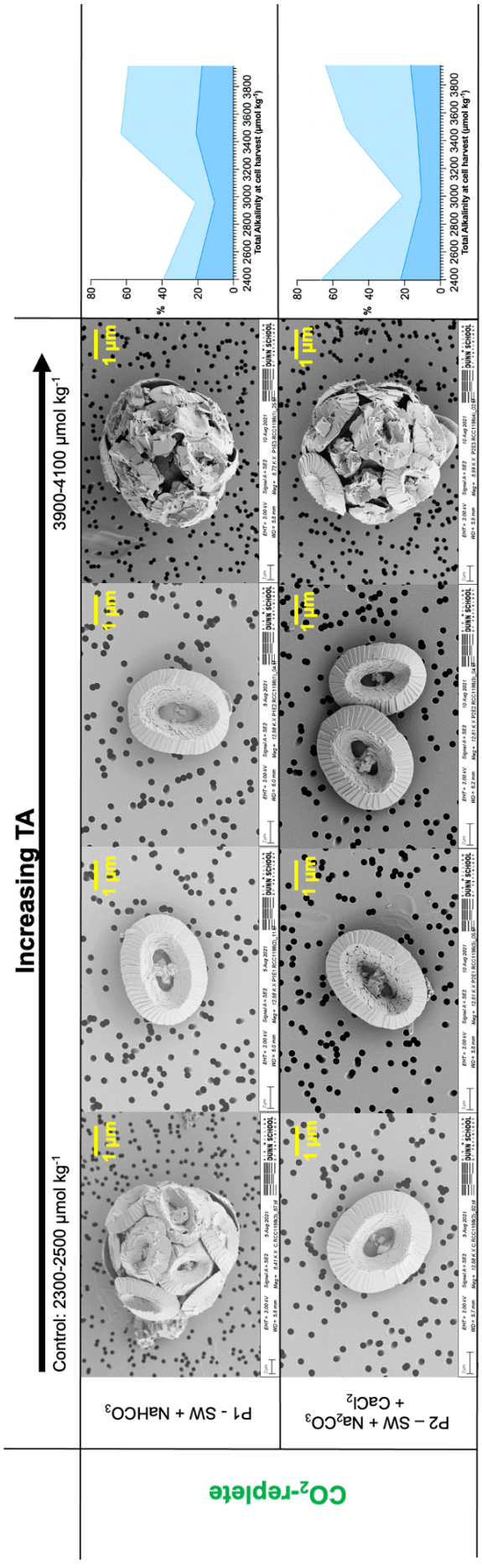

Figure 3.22: SEM images taken of *C. braarudii* at cell harvest from CO_2-replete cultures. Trendline shown for increasing TA. Accompanying graphs show Total Alkalinity at cell harvest on x axis vs. % malformation on y axis. Upper line on each graph = total % of lith malformation observed. Lighter blue area = % of liths exhibiting severe malformation. Darker blue area = % of liths exhibiting mild malformation. For full details of these categorisations, please see section **3.2.3.**

The increased tendency towards malformation in all cultures of *E. huxleyi* and *C. braarudii*, whether CO_2-limited or CO_2-replete, with increasing TA indicates that the intracellular process of coccolithogenesis has been disrupted. Morphological abnormalities in *E. huxleyi* have been observed under environmental stress due to ocean acidification (De Bodt et al., 2010; Riebesell et al., 2000; Beaufort et al., 2011; Zondervan et al., 2001), and are indicative of adverse carbonate chemistry conditions (Faucher et al., 2020). Morphological abnormalities have also been observed in C. braarudii in response to high [DIC] (up to 7800 µmol kg^{-1}) (Rickaby et al., 2010). We surmise that the OAE treatments exert an environmental stress on the coccolithophores in our study, evidenced by the fact that they alter their growth and/or calcification in response to OAE, and therefore the morphological

abnormalities we observe reflect these adverse carbonate chemistry conditions. We suggest that because morphological control is of secondary importance to cellular function (Müller, 2019), under carbonate chemistry conditions where essential functions (i.e. growth, calcification) are perturbed, morphological abnormalities may reflect a diversion of cellular energy from extraneous functions to core cellular functions.

3.3.2 Implications for coccolithophore physiology

It is clear from the discussion so far that it is difficult to pin down the exact physiological mechanisms behind the growth and calcification of coccolithophores in response to OAE because so many parameters of the carbonate system are physiologically relevant for coccolithophore cell biology that co-vary during a realistic OAE scenario. This will be a non-trivial problem for the community going forward.

As predicted in the **Introduction**, our data support the hypothesis that the addition of TA as Ca^{2+} is unlikely to result in physiological or calcification responses in coccolithophores at the [Ca^{2+}] expected to result from OAE. For both *E. huxleyi* and *C. braarudii*, there is no real difference in the growth and calcification responses for Pathway 1 (no Ca) vs Pathway 2 (+Ca) in CO_2-replete conditions. There is some evidence that the growth rate, cellular calcification rate and cellular calcite quota for Pathway 1 and Pathway 2 lie on different trendlines *for E. huxleyi* in CO_2-limited conditions. However, these differing trendlines disappear when growth rate, cellular calcification rate and cellular calcite quota are plotted against the driving physiological parameter for growth and calcification in coccolithophores; [HCO_3^-]. Therefore, we can conclude that there is no significant impact on coccolithophores of adding TA to the surface ocean using Na^+ or Ca^{2+}.

In CO_2-limited conditions, *E. huxleyi* growth rate increases by a factor of 1.74 between control and the highest TA conditions (control + 1500 µmol kg^{-1}). Cellular calcification rate and cellular calcite quota increase by a factor of 1.76 over the same range of TA. The fact that growth rate and cellular calcification rate increase by approximately the same factor with enhanced TA, coupled with the fact that both processes are most strongly linked with HCO_3^- out of all the

carbonate system parameters, supports prior work which suggests that these processes are tightly coupled in *E. huxleyi* (Rickaby et al., 2016; Tsuji and Yoshida, 2017; Paasche, 2002).

In addition, evidence of HCO_3^- fertilisation in *E. huxleyi* under CO_2-limited conditions supports a growing body of evidence that expression of HCO_3^- transporters, or some other CCM such as Carbonic Anhydrase (CA), is dependent on CO_2 availability (Reinfelder, 2011). However, the strong evidence shown in our study that *E. huxleyi* is fertilised in a linear fashion by HCO_3^- both in CO_2-limited and CO_2-replete conditions, suggests that expression of HCO_3^- transporters may be proportional to HCO_3^- availability, in addition to CO_2 availability. There appears to be a complex interplay between the influence of these two carbonate system parameters on growth of *E. huxleyi* in our experimental manipulations.

Our data suggest that both HCO_3^- and CO_2 exert influence on *E. huxleyi* growth. Our data also support prior work concluding that HCO_3^- is the primary substrate for calcification. We assert that *E. huxleyi* is an opportunist that is able to switch between HCO_3^- and CO_2 as its primary carbon source for growth (Kottmeier et al., 2016; Krug et al., 2011) and the extent to which these individual parameters affect growth rates is dependent on their availability in the culture media.

It is beyond the scope of our study to identify what kind of CCM is activated in *E. huxleyi* to facilitate HCO_3^- transport; this would require work with transcriptomics, such as Quantitative reverse-transcriptase polymerase chain reaction (qRT-PCR) to identify the gene expression of HCO_3^- transporters or the presence of CA (Bach et al., 2013; Mackinder et al., 2011; Zhang et al., 2021). However, we can conclusively say that our data shows that *E. huxleyi* is utilising a CCM.

In contrast with *E. huxleyi*, it appears that *C. braarudii* growth is overall less responsive to changing carbonate chemistry in our experimental conditions. Unlike *E. huxleyi* which is able to alter its mode of carbon acquisition dependent on the availability of carbon species in the culture media, *C. braarudii* appears to be more static in its mode of carbon acquisition for growth. There is no evidence for the limitation of *C. braarudii* by HCO_3^- in the modern surface

ocean because growth rates of *C. braarudii* do not increase despite the increased supply of HCO_3^- in OAE treatments. Calcification is clearly not acting as a CCM for *C. braarudii* because growth rates are not impacted when calcification rates and quota decrease, which supports work completed by Walker et al. (2018) with the same species. Calcification in *C. braarudii* does not increase with increasing HCO_3^- as a result of elevated TA, in contrast to *E. huxleyi* in CO_2-limited conditions. It has been suggested that the *Coccolithus* lineage of coccolithophores has always been able to utilise an active HCO_3^- uptake pathway to a common internal pool (Rickaby et al., 2010) to maintain pH stability in the cell to balance the processes of photosynthesis and calcification. This could explain why *C. braarudii* is so static in its mode of carbon acquisition compared to *E. huxleyi*, which is of the *Reticulofenestra* lineage. This is also supported by work by Claxton et al. (unpub.) that *C. braarudii* is more permeable to HCO_3^- than *G. oceanica* (genetically a very similar coccolithophore to *E. huxleyi*), likely due to its larger carbon demand as a much larger coccosphere than *G. oceanica*. *G. oceanica* conversely has a scaleable permeability to HCO_3^- resulting from the upregulation of HCO_3^- transporters at lower external CO_2(aq).

Decreasing cellular calcification rate and quota in *C. braarudii* with increasing TA show that calcification, like growth, in *C. braarudii* is less able to take advantage of alternative carbon species that are readily available in the culture media as a result of alkalinity enhancement. By extension, carbon acquisition mechanisms in *C. braarudii* must therefore be less adaptable than *E. huxleyi*, As outlined previously, it may be that decreasing [CO_2] is the true physiological driver of decreasing calcification in *C. braarudii*, in contrast with our data signifying that [HCO_3^-] is the main driver of calcification in *E. huxleyi*. However, trends in [CO_2] with increasing TA as a result of equilibration (**Figure 3.3**) preclude a definitive answer on this.

In summary, our results support a growing body of evidence that suggests there is a very different fundamental physiology of the *Coccolithus* and *Reticulofenestra* genii (Rickaby et al., 2010; Walker et al., 2018) of coccolithophores. *E. huxleyi* (*Reticulofenestra*) growth and calcification appear to proceed in a coupled way that allows the cells to act as opportunists to

make use of different carbon species as fuel, whereas *C. braarudii* (*Coccolithus*) growth and calcification are much more static processes that do not adjust to changing availability of carbon species in the environment.

3.3.3 Implications for Ocean Alkalinity Enhancement

As outlined previously, the CO_2-replete culturing experiments with *E. huxleyi* and *C. braarudii* are analogous to an air-equilibrated OAE scenario, and the CO_2-limited culturing experiments with *E. huxleyi* are analogous to a non-equilibrated OAE scenario (see Figure 3.1). Under CO_2-replete conditions, *E. huxleyi* does not change its cellular calcification rate or quota in response to raised TA (although if the outlier removed in **Figure 3.8** is not an outlier, then it may decrease its calcification rate), and *C. braarudii* decreases both its cellular calcification rate and quota. This indicates that in air-equilibrated OAE scenarios, there is unlikely to be any "CO_2 leakage" from enhanced coccolithophore calcification when alkalinity is added to the surface ocean. This study suggests that there may be less CO_2 re-emitted into the atmosphere per cell, from the aggregate effect of *C. braarudii* decreasing cellular calcification and *E. huxleyi* constant cellular calcification. However, even if *E. huxleyi* calcification per cell doesn't change, the growth rate of *E. huxleyi* significantly increases with the increased supply of HCO_3^-. A larger population size of *E. huxleyi* would result from this, and so by virtue of there being a higher number of cells calcifying, the overall amount of calcification from the *E. huxleyi* population would be significantly increased. This situation would be analogous to the high alkalinity (~3300 μmol kg^{-1}) Black Sea (Sorokin, 2002) where blooms of *E. huxleyi* are ubiquitous (Kopelevich et al., 2014; Kopelevich et al., 2020) and population levels of calcification are extremely high, as evidenced by the thick layers of calcareous ooze overlying bottom sediments (Hay, 1988).

E. huxleyi cellular calcification rates and quota may however increase in non-equilibrated OAE scenarios, resulting in CO_2 re-release after drawdown into the surface ocean from alkalinity addition. However, probably, non-equilibrated OAE scenarios will only occur on initial point-source additions of alkalinity, so any possible re-release of CO_2 would be short-lived, and it is

likely that once the surface ocean and atmosphere have equilibrated that coccolithophore calcification would then decrease or remain the same relative to control conditions. Additionally, our laboratory experiments were conducted under nutrient-replete conditions, and at some point in the natural environment, calcification response to OAE will be limited by lack of available nutrients.

However, in the global ocean, it is not just the process of calcification that induces changes in the carbon cycle. What if PIC:POC values of coccolithophores change? What would happen to global organic carbon fixation? Renforth and Henderson (2017) predict that if PIC:POC < 1, organic carbon export would offset the CO_2 emission from the counter carbonate pump. In our study, it is difficult to conclusively say if PIC:POC values will remain <1 for both *E. huxleyi* and *C. braarudii* in an OAE scenario because errors on the measurements of TPC and POC were high. However, our results do tentatively indicate that it is possible that PIC:POC may increase under OAE scenarios, and therefore it is still an unanswered question to what extent the interaction between PIC and POC formation will impact overall carbon drawdown during OAE.

Prima facie, a small risk of CO_2 re-release by coccolithophore calcification during OAE is good news for the future development of OAE schemes because the efficacy of CO_2 drawdown through alkalinity addition will not be reduced if CO_2 is not re-released from enhanced calcification. However, there may also be risks associated with decreased pelagic calcification in our oceans. Calcium carbonate formation by biota contributes to the ballasting of organic carbon particulate matter to the deep ocean (Rost and Riebesell, 2004; Honjo et al., 2008; Ziveri et al., 2007). Therefore, it follows that less calcite formation could lead to less ballasting and less organic carbon export to the deep ocean. This could have wide-ranging impacts on global carbon cycling. Again, while showing strong evidence for calcification responses in coccolithophores, we reiterate that our study still leaves unanswered questions concerning the interaction between biotic organic and inorganic carbon formation during OAE.

3.4 Conclusions

This study is the first to examine the response of two key "endmember" species of coccolithophores, *E. huxleyi* and *C. braarudii*, to the carbonate chemistries specific to Ocean Alkalinity Enhancement (OAE) as an mCDR technique. We have shown that the addition of Total Alkalinity using Ca^{2+} compared to Na^{+} does not result in notable differences in coccolithophore growth and/or calcification response. Under non-equilibrated OAE scenarios, cellular calcification rates and calcite quota of *E. huxleyi* may increase. Under air-equilibrated OAE scenarios, cellular calcification rates and calcite quota of *E. huxleyi* likely do not change, although our study shows strong evidence that this major bloom-forming coccolithophore in our oceans may be limited by [HCO_3^-] at modern surface ocean concentrations. An increase in *E. huxleyi* growth rates stimulated by supply of HCO_3^- during OAE may mean that *E. huxleyi* population levels of calcification will increase during air-equilibrated OAE scenarios, thereby increasing re-release of CO_2 to the atmosphere following OAE. By contrast, *C. braarudii* decreases its cellular calcification rate and quota in response to air-equilibrated OAE. Therefore, the possibility of "CO_2 leakage" during OAE from the calcification feedback in the surface ocean is dependent on (i) the equilibration conditions and (ii) coccolithophore species. The differing growth and calcification responses of *E. huxleyi* and *C. braarudii* to the carbonate chemistries resulting from OAE indicate that these two species differ in their mode of carbon acquisition ("opportunist" vs "static") for these cellular processes, supporting prior work that indicates that the coccolithophore *Coccolithus* and *Reticulofenestra* genii do not have the same cellular carbon utilisation mechanisms.

References

Allemand, D., Ferrier-Pagès, C., Furla, P., Houlbrèque, F., Puverel, S., Reynaud, S., Tambutté, É., Tambutté, S., Zoccola, D., 2004. Biomineralisation in reef-building corals: from molecular mechanisms to environmental control. Comptes Rendus Palevol 3, 453–467. https://doi.org/10.1016/j.crpv.2004.07.011

Bach L. T., Riebesell U., Schulz K. G., 2011. Distinguishing between the effects of ocean acidification and ocean carbonation in the coccolithophore *Emiliania huxleyi*. Limnology and Oceanography 56, 2040–2050. https://doi.org/10.4319/lo.2011.56.6.2040

Bach, L.T., 2015. Reconsidering the role of carbonate ion concentration in calcification by marine organisms. Biogeosciences 12, 4939–4951. https://doi.org/10.5194/bg-12-4939-2015

Bach, L.T., Gill, S.J., Rickaby, R.E.M., Gore, S., Renforth, P., 2019. CO_2 Removal With Enhanced Weathering and Ocean Alkalinity Enhancement: Potential Risks and Co-benefits for Marine Pelagic Ecosystems. Frontiers in Climate 1. https://doi.org/10.3389/fclim.2019.00007

Bach, L.T., Mackinder, L.C.M., Schulz, K.G., Wheeler, G., Schroeder, D.C., Brownlee, C., Riebesell, U., 2013. Dissecting the impact of CO_2 and pH on the mechanisms of photosynthesis and calcification in the coccolithophore *Emiliania huxleyi*. New Phytologist 199, 121–134. https://doi.org/10.1111/nph.12225

Bach, L.T., Riebesell, U., Gutowska, M.A., Federwisch, L., Schulz, K.G., 2015. A unifying concept of coccolithophore sensitivity to changing carbonate chemistry embedded in an ecological framework. Progress in Oceanography 135, 125–138. https://doi.org/10.1016/j.pocean.2015.04.012

Beardall, J., Raven, J.A., 2013. Calcification and ocean acidification: new insights from the coccolithophore *Emiliania huxleyi*. New Phytologist 199, 1–3. https://doi.org/10.1111/nph.12297

Beaufort, L., Probert, I., de Garidel-Thoron, T., Bendif, E.M., Ruiz-Pino, D., Metzl, N., Goyet, C., Buchet, N., Coupel, P., Grelaud, M., Rost, B., Rickaby, R.E.M., de Vargas, C., 2011. Sensitivity of coccolithophores to carbonate chemistry and ocean acidification. Nature 476, 80–83. https://doi.org/10.1038/nature10295

Blanco-Ameijeiras, S., Lebrato, M., Stoll, H.M., Iglesias-Rodriguez, D., Müller, M.N., Méndez-Vicente, A., Oschlies, A., 2016. Phenotypic Variability in the Coccolithophore *Emiliania huxleyi*. PLOS One 11. https://doi.org/10.1371/journal.pone.0157697

Boettcher, M., Brent, K., Buck, H.J., Low, S., McLaren, D., Mengis, N., 2021. Navigating Potential Hype and Opportunity in Governing Marine Carbon Removal. Frontiers in Climate 3. https://doi.org/10.3389/fclim.2021.664456

Chisholm, J.R.M., Gattuso, J.-P., 1991. Validation of the alkalinity anomaly technique for investigating calcification of photosynthesis in coral reef communities. Limnology and Oceanography 36, 1232–1239. https://doi.org/10.4319/lo.1991.36.6.1232

Cohen, S., Krueger, T., Fine, M., 2017. Measuring coral calcification under ocean acidification: methodological considerations for the ^{45}Ca-uptake and total alkalinity anomaly technique. PeerJ 5, e3749. https://doi.org/10.7717/peerj.3749

Cook, S.S., Whittock, L., Wright, S.W., Hallegraeff, G.M., 2011. Photosynthetic Pigment and Genetic Differences Between Two Southern Ocean Morphotypes of *Emiliania Huxleyi* (haptophyta). Journal of Phycology 47, 615–626. https://doi.org/10.1111/j.1529-8817.2011.00992.x

Cyronak, T., Schulz, K.G., Jokiel, P.L., 2016. The Omega myth: what really drives lower calcification rates in an acidifying ocean. ICES Journal of Marine Science 73, 558–562. https://doi.org/10.1093/icesjms/fsv075

Daniels, C.J., Sheward, R.M., Poulton, A.J., 2014. Biogeochemical implications of comparative growth rates of *Emiliania huxleyi* and *Coccolithus* species. Biogeosciences 11, 6915–6925. https://doi.org/10.5194/bg-11-6915-2014

De Bodt, C., Van Oostende, N., Harlay, J., Sabbe, K., Chou, L., 2010. Individual and interacting effects of pCO_2 and temperature on *Emiliania huxleyi* calcification: Study of the calcite production, the coccolith

morphology and the coccosphere size. Biogeosciences 7, 1401–1412. https://doi.org/10.5194/bg-7-1401-2010

Durbin, E.G., Chen, C.Y., 1994. Effects of pH on the growth and carbon uptake of marine phytoplankton. Marine ecology progress series 109, 83-94. https://doi.org/10.3354/meps109083

Faucher, G., Riebesell, U., Bach, L.T., 2020. Can morphological features of coccolithophores serve as a reliable proxy to reconstruct environmental conditions of the past? Climate of the Past 16, 1007–1025. https://doi.org/10.5194/cp-16-1007-2020

Feng, E.Y., Koeve, W., Keller, D.P., Oschlies, A., 2017. Model-Based Assessment of the CO_2 Sequestration Potential of Coastal Ocean Alkalinization. Earth's Future 5, 1252–1266. https://doi.org/10.1002/2017EF000659

Fuss, S., Canadell, J.G., Peters, G.P., Tavoni, M., Andrew, R.M., Ciais, P., Jackson, R.B., Jones, C.D., Kraxner, F., Nakicenovic, N., Quéré, C.L., Raupach, M.R., Sharifi, A., Smith, P., Yamagata, Y., 2014. Betting on negative emissions. Nature Climate Change 4, 850–853. https://doi.org/10.1038/nclimate2392

Fuss, S., Lamb, W.F., Callaghan, M.W., Hilaire, J., Creutzig, F., Amann, T., Tim Beringer, Garcia, W. de O., Hartmann, J., Khanna, T., Luderer, G., Nemet, G.F., Joeri Rogelj, Smith, P., Vicente, J.L.V., Wilcox, J., Dominguez, M. del M.Z., Minx, J.C., 2018. Negative emissions—Part 2: Costs, potentials and side effects. Environmental Research Letters 13, 063002. https://doi.org/10.1088/1748-9326/aabf9f

Gafar, N.A., Eyre, B.D., Schulz, K.G., 2018. A Conceptual Model for Projecting Coccolithophorid Growth, Calcification and Photosynthetic Carbon Fixation Rates in Response to Global Ocean Change. Frontiers in Marine Science 4, 433. https://doi.org/10.3389/fmars.2017.00433

Gattuso, J.-P., Magnan, A., Billé, R., Cheung, W.W.L., Howes, E.L., Joos, F., Allemand, D., Bopp, L., Cooley, S.R., Eakin, C.M., Hoegh-Guldberg, O., Kelly, R.P., Pörtner, H.-O., Rogers, A.D., Baxter, J.M., Laffoley, D., Osborn, D., Rankovic, A., Rochette, J., Sumaila, U.R., Treyer, S., Turley, C., 2015. Contrasting futures for ocean and society from different anthropogenic CO_2 emissions scenarios. Science 349, aac4722. https://doi.org/10.1126/science.aac4722

GESAMP, 2019. "High level review of a wide range of proposed marine geoengineering techniques". (Boyd, P.W. and Vivian, C.M.G., eds.). (IMO/FAO/UNESCO-IOC/UNIDO/WMO/IAEA/UN/UN Environment/ UNDP/ISA Joint Group of Experts on the Scientific Aspects of Marine Environmental Protection). Rep. Stud. GESAMP No. 98, 144 p.

Giordano, M., Beardall, J., Raven, J.A., 2005. CO_2 concentrating mechanisms in algae: mechanisms, environmental modulation, and evolution. Annual Review of Plant Biology 56, 99–131. https://doi.org/10.1146/annurev.arplant.56.032604.144052

Goldman, J.C., 1999. Inorganic carbon availability and the growth of large marine diatoms. Marine Ecology Progress Series 180, 81–91. https://doi.org/10.3354/meps180081

Gore, S., Renforth, P., Perkins, R., 2018. The potential environmental response to increasing ocean alkalinity for negative emissions. Mitigation and Adaptation Strategies for Global Change, 24, 1191–1211. https://doi.org/10.1007/s11027-018-9830-z

Guillard, R.R.L., Hargraves, P.E., 1993. *Stichochrysis immobilis* is a diatom, not a chrysophyte. Phycologia 32, 234–236. https://doi.org/10.2216/i0031-8884-32-3-234.1

Hansen, P.J., 2002. Effect of high pH on the growth and survival of marine phytoplankton: implications for species succession. Aquatic Microbial Ecology 28, 279–288. https://doi.org/10.3354/ame028279

Hartmann, J., West, A.J., Renforth, P., Köhler, P., De La Rocha, C.L., Wolf-Gladrow, D.A., Dürr, H.H., Scheffran, J., 2013. Enhanced chemical weathering as a geoengineering strategy to reduce atmospheric carbon dioxide, supply nutrients, and mitigate ocean acidification. Reviews of Geophysics 51, 113–149. https://doi.org/10.1002/rog.20004

Harvey, L.D.D., 2008. Mitigating the atmospheric CO_2 increase and ocean acidification by adding limestone powder to upwelling regions. Journal of Geophysical Research 113, C04028. https://doi.org/10.1029/2007JC004373

Hay, B.J., 1988. Sediment accumulation in the central western Black Sea over the past 5100 years. Paleoceanography 3, 491–508. https://doi.org/10.1029/PA003i004p00491

Henderson, G., Rickaby, R., Bouman, H., 2008. Decreasing Atmosphere CO2 By Increasing Ocean Alkalinity, The Ocean Dimension: Would The Concept Work And What Would Be The Environmental Consequences?

Herfort, L., Thake, B., Roberts, J., 2002. Acquisition and use of bicarbonate by *Emiliania huxleyi*. New Phytologist 156, 427–436. https://doi.org/10.1046/j.1469-8137.2002.00523.x

Hermoso, M., 2015. Control of ambient pH on growth and stable isotopes in phytoplanktonic calcifying algae. Paleoceanography 30, 2015PA002844. https://doi.org/10.1002/2015PA002844

Hermoso, M., Horner, T.J., Minoletti, F., Rickaby, R.E.M., 2014. Constraints on the vital effect in coccolithophore and dinoflagellate calcite by oxygen isotopic modification of seawater. Geochimica et Cosmochimica Acta 141, 612–627. https://doi.org/10.1016/j.gca.2014.05.002

Hinga, K.R., 2002. Effects of pH on coastal marine phytoplankton. Mar Ecol Prog Ser 238, 281–300. https://doi.org/10.3354/meps238281

Honjo, S., Manganini, S.J., Krishfield, R.A., Francois, R., 2008. Particulate organic carbon fluxes to the ocean interior and factors controlling the biological pump: A synthesis of global sediment trap programs since 1983. Progress in Oceanography 76, 217–285. https://doi.org/10.1016/j.pocean.2007.11.003

Ilyina, T., Wolf-Gladrow, D., Munhoven, G., Heinze, C., 2013. Assessing the potential of calcium-based artificial ocean alkalinization to mitigate rising atmospheric CO_2 and ocean acidification. Geophysical Research Letters 40, 5909–5914. https://doi.org/10.1002/2013GL057981

IPCC AR5, 2014. Fifth Assessment Report - Mitigation of Climate Change [WWW Document]. URL https://www.ipcc.ch/report/ar5/wg3/mindex.shtml (accessed 10.18.17).

Kheshgi, H.S., 1995. Sequestering atmospheric carbon dioxide by increasing ocean alkalinity. Energy 20, 915–922. https://doi.org/10.1016/0360-5442(95)00035-F

Köhler, P., Abrams, J.F., Völker, C., Hauck, J., Wolf-Gladrow, D.A., 2013. Geoengineering impact of open ocean dissolution of olivine on atmospheric CO_2, surface ocean pH and marine biology. Environmental Research Letters. 8, 014009. https://doi.org/10.1088/1748-9326/8/1/014009

Köhler, P., Hartmann, J., Wolf-Gladrow, D.A., 2010. Geoengineering potential of artificially enhanced silicate weathering of olivine. PNAS 107, 20228–20233. https://doi.org/10.1073/pnas.1000545107

Kopelevich, O., Burenkov, V.I., Шеберстов, C., Vazyulya, S., Kravchishina, M., Pautova, L., Silkin, V., Artemiev, V., Григорьев, A.B., 2014. Satellite monitoring of coccolithophore blooms in the Black Sea from ocean color data. Remote Sensing of Environment 146, 113–123. https://doi.org/10.1016/j.rse.2013.09.009

Kopelevich, O., Sheberstov, S., Vazyulya, S., 2020. Effect of a Coccolithophore Bloom on the Underwater Light Field and the Albedo of the Water Column. Journal of Marine Science and Engineering 8, 456. https://doi.org/10.3390/jmse8060456

Kottmeier, D., Rokitta, S., Tortell, P., Rost, B., 2014. Strong shift from HCO_3^- to CO_2 uptake in *Emiliania huxleyi* with acidification: new approach unravels acclimation versus short-term pH effects. Photosynthesis Research 121, 265–275 (2014). https://doi.org/10.1007/s11120-014-9984-9

Kottmeier, D.M., Rokitta, S.D., Rost, B., 2016. H^+-driven increase in CO_2 uptake and decrease in uptake explain coccolithophores' acclimation responses to ocean acidification. Limnology and Oceanography 61, 2045–2057. https://doi.org/10.1002/lno.10352

Krug, S.A., Schulz, K.G., Riebesell, U., 2011. Effects of changes in carbonate chemistry speciation on *Coccolithus braarudii*: a discussion of coccolithophorid sensitivities. Biogeosciences 8, 771–777. https://doi.org/10.5194/bg-8-771-2011

Langer, G., Geisen, M., Baumann, K.-H., Kläs, J., Riebesell, U., Thoms, S., Young, J.R., 2006. Species-specific responses of calcifying algae to changing seawater carbonate chemistry. Geochemistry, Geophysics, Geosystems 7, Q09006. https://doi.org/10.1029/2005GC001227

LaRoche, J., Rost, B., Engel, A., 2010. Bioassays, batch culture and chemostat experimentation, in: Guide for Best Practices in Ocean Acidification Research and Data Reporting. Publications Office of the European Union, Brussels, pp. 81–94.

Lee, K., Kim, T.-W., Byrne, R.H., Millero, F.J., Feely, R.A., Liu, Y.-M., 2010. The universal ratio of boron to chlorinity for the North Pacific and North Atlantic oceans. Geochimica et Cosmochimica Acta 74, 1801–1811. https://doi.org/10.1016/j.gca.2009.12.027

Leonardos, N., Read, B., Thake, B., Young, J.R., 2009. No Mechanistic Dependence Of Photosynthesis On Calcification In The Coccolithophorid *Emiliania Huxleyi* (Haptophyta). Journal of Phycology 45, 1046–1051. https://doi.org/10.1111/j.1529-8817.2009.00726.x

Mackinder, L., Wheeler, G., Schroeder, D., von Dassow, P., Riebesell, U., Brownlee, C., 2011. Expression of biomineralization-related ion transport genes in *Emiliania huxleyi*. Environmental Microbiology 13, 3250–3265. https://doi.org/10.1111/j.1462-2920.2011.02561.x

Mayers, T.J., Bramucci, A.R., Yakimovich, K.M., Case, R.J., 2016. A Bacterial Pathogen Displaying Temperature-Enhanced Virulence of the Microalga *Emiliania huxleyi*. Frontiers in Microbiology 7. https://doi.org/10.3389/fmicb.2016.00892

McCammon, R.B., 1968. Multiple Component Analysis and Its Application in Classification of Environments. AAPG Bulletin 52, 2178–2196. https://doi.org/10.1306/5D25C55D-16C1-11D7-8645000102C1865D

Meyer, J., Riebesell, U., 2015. Reviews and Syntheses: Responses of coccolithophores to ocean acidification: a meta-analysis. Biogeosciences 12, 1671–1682. https://doi.org/10.5194/bg-12-1671-2015

Monteiro, F.M., Bach, L.T., Brownlee, C., Bown, P., Rickaby, R.E.M., Poulton, A.J., Tyrrell, T., Beaufort, L., Dutkiewicz, S., Gibbs, S., Gutowska, M.A., Lee, R., Riebesell, U., Young, J., Ridgwell, A., 2016. Why marine phytoplankton calcify. Science Advances 2, e1501822. https://doi.org/10.1126/sciadv.1501822

Motulsky, H.J., GraphPad Statistics Guide. URL http://www.graphpad.com/guides/prism/7/statistics/index.htm (accessed 12.7.21).

Motulsky, H.J., Brown, R.E., 2006. Detecting outliers when fitting data with nonlinear regression - a new method based on robust nonlinear regression and the false discovery rate. BMC Bioinformatics 7, 123. https://doi.org/10.1186/1471-2105-7-123

Müller, M.N., 2019. On the genesis and function of coccolithophore calcification. Frontiers in Marine Science 6. https://doi.org/10.3389/fmars.2019.00049

Müller, M.N., Barcelos e Ramos, J., Schulz, K.G., Riebesell, U., Kaźmierczak, J., Gallo, F., Mackinder, L., Li, Y., Nesterenko, P.N., Trull, T.W., Hallegraeff, G.M., 2015. Phytoplankton calcification as an effective mechanism to alleviate cellular calcium poisoning. Biogeosciences 12, 6493–6501. https://doi.org/10.5194/bg-12-6493-2015

Müller, M.N., Kisakurek, B., Buhl, D., Gutperlet, R., Kolevica, A., Riebesell, U., Stoll, H., Eisenhauer, A., 2011. Response of the coccolithophores *Emiliania huxleyi* and *Coccolithus braarudii* to changing seawater Mg^{2+} and Ca^{2+} concentrations: Mg/Ca, Sr/Ca ratios and $\delta^{44/40}Ca$, $\delta^{26/24}Mg$ of coccolith calcite. https://doi.org/10.1016/J.GCA.2011.01.035

National Academies of Sciences, Engineering, and Medicine, 2021. A Research Strategy for Ocean-based Carbon Dioxide Removal and Sequestration. The National Academies Press, Washington D.C.

Oviedo, A.M., Langer, G., Ziveri, P., 2014. Effect of phosphorus limitation on coccolith morphology and element ratios in Mediterranean strains of the coccolithophore *Emiliania huxleyi*. Journal of Experimental Marine Biology and Ecology 459, 105–113. https://doi.org/10.1016/j.jembe.2014.04.021

Paasche, E., 2002. A review of the coccolithophorid *Emiliania huxleyi* (Prymnesiophyceae), with particular reference to growth, coccolith formation, and calcification-photosynthesis interactions. Phycologia 40, 503–529. https://doi.org/10.2216/i0031-8884-40-6-503.1

Paasche, E., 1964. A tracer study of the inorganic carbon uptake during coccolith formation and photosynthesis in the coccolithophorid *Coccolithus huxleyi*. Chemistry.

Pedersen, M.F., Hansen, P.J., 2003. Effects of high pH on a natural marine planktonic community. Marine Ecology Progress Series 260, 19–31. https://doi.org/10.3354/MEPS260019

Pierrot, D., Lewis, E., Wallace, D.W.R., 2006. MS Excel Program Developed for CO_2 System Calculations, in: Tech. Rep. Presented at the Carbon Dioxide Inf. Anal. Cent., Oak Ridge Natl. Lab., US DOE, Oak Ridge, Tennessee.

Poulton, A.J., Adey, T.R., Balch, W.M., Holligan, P.M., 2007. Relating coccolithophore calcification rates to phytoplankton community dynamics: Regional differences and implications for carbon export. Deep-Sea Research Part II: Topical Studies in Oceanography 54, 538–557. https://doi.org/10.1016/j.dsr2.2006.12.003

Raven, J.A., Evans, M.C.W., Korb, R.E., 1999. The role of trace metals in photosynthetic electron transport in O_2-evolving organisms. Photosynthesis Research 60, 111–150. https://doi.org/10.1023/A:1006282714942

Redfield, A.C., 1958. The Biological Control Of Chemical Factors In The Environment. American Scientist 46, 230A–221.

Reinfelder, J.R., 2011. Carbon Concentrating Mechanisms in Eukaryotic Marine Phytoplankton. Annual Review of Marine Science 3, 291–315. https://doi.org/10.1146/annurev-marine-120709-142720

Renforth, P., Henderson, G., 2017. Assessing ocean alkalinity for carbon sequestration. Reviews of Geophysics 55, 636–674. https://doi.org/10.1002/2016RG000533

Richier, S., Fiorini, S., Kerros, M.-E., von Dassow, P., Gattuso, J.-P., 2011. Response of the calcifying coccolithophore *Emiliania huxleyi* to low pH/high pCO_2: from physiology to molecular level. Marine Biology 158, 551–560. https://doi.org/10.1007/s00227-010-1580-8

Rickaby, R.E.M., Henderiks, J., Young, J.N., 2010. Perturbing phytoplankton: response and isotopic fractionation with changing carbonate chemistry in two coccolithophore species. Climate of the Past 6, 771–785. https://doi.org/10.5194/cp-6-771-2010

Rickaby, R.E.M., Hermoso, M., Lee, R.B.Y., Rae, B.D., Heureux, A.M.C., Balestreri, C., Chakravarti, L., Schroeder, D.C., Brownlee, C., 2016. Environmental carbonate chemistry selects for phenotype of recently isolated strains of *Emiliania huxleyi*. Deep Sea Research Part II: Topical Studies in Oceanography, Impacts of surface ocean acidification in polar seas and globally: a field-based approach 127, 28–40. https://doi.org/10.1016/j.dsr2.2016.02.010

Riebesell, U., Wolf-Gladrow, D.A., Smetacek, V., 1993. Carbon dioxide limitation of marine phytoplankton growth rates. Nature 361, 249–251. https://doi.org/10.1038/361249a0

Riebesell, U., Zondervan, I., Rost, B., Tortell, P.D., Zeebe, R.E., Morel, F.M.M., 2000. Reduced calcification of marine plankton in response to increased atmospheric CO_2. Nature 407, 364–367. https://doi.org/10.1038/35030078

Rigual-Hernández, A.S., Trull, T.W., Flores, J.A., Nodder, S.D., Eriksen, R., Davies, D.M., Hallegraeff, G.M., Sierro, F.J., Patil, S.M., Cortina, A., Ballegeer, A.M., Northcote, L.C., Abrantes, F., Rufino, M.M., 2020. Full annual monitoring of Subantarctic *Emiliania huxleyi* populations reveals highly calcified morphotypes in high-CO_2 winter conditions. Scientific Reports 10, 2594. https://doi.org/10.1038/s41598-020-59375-8

Rost, B., Riebesell, U., 2004. Coccolithophores and the biological pump: responses to environmental changes, in: Thierstein, H.R., Young, J.R. (Eds.), Coccolithophores: From Molecular Processes to Global Impact. Springer, Berlin, Heidelberg, pp. 99–125. https://doi.org/10.1007/978-3-662-06278-4_5

Rost, B., Riebesell, U., Burkhardt, S., Sültemeyer, D., 2003. Carbon acquisition of bloom-forming marine phytoplankton. Limnology and Oceanography 48, 55–67. https://doi.org/10.4319/lo.2003.48.1.0055

Roy, R.N., Roy, L.N., Lawson, M., Vogel, K.M., Porter Moore, C., Davis, W., Millero, F.J., 1993. Thermodynamics of the dissociation of boric acid in seawater at S = 35 from 0 to 55°C. Marine Chemistry 44, 243–248. https://doi.org/10.1016/0304-4203(93)90206-4

Sarmiento, J.L., Gruber, N., 2006. Ocean biogeochemical dynamics. Princeton University Press, Princeton, N.J. ; Woodstock.

Sett, S., Bach, L.T., Schulz, K.G., Koch-Klavsen, S., Lebrato, M., Riebesell, U., 2014. Temperature Modulates Coccolithophorid Sensitivity of Growth, Photosynthesis and Calcification to Increasing Seawater pCO_2. PLOS ONE 9, e88308. https://doi.org/10.1371/journal.pone.0088308

Shafiee, R.T., Diver, P.J., Snow, J.T., Zhang, Q., Rickaby, R.E.M., 2021. Marine ammonia-oxidising archaea and bacteria occupy distinct iron and copper niches. ISME Communications. 1, 1–12. https://doi.org/10.1038/s43705-021-00001-7

Sikes, C.S., Wheeler, A.P., 1982. Carbonic Anhydrase and Carbon Fixation in Coccolithophorids. Journal of Phycology 18, 423–426. https://doi.org/10.1111/j.1529-8817.1982.tb03205.x

Soderberg, L.M., Hansen, P.J., 2007. Growth limitation due to high pH and low inorganic carbon concentrations in temperate species of the dinoflagellate genus *Ceratium*. https://doi.org/10.3354/MEPS07146

Sorokin, Y.I., 2002. The Black Sea: Ecology and Oceanography. Backhuys Publisher, Leiden.

Stevenson, E.I., Hermoso, M., Rickaby, R.E.M., Tyler, J.J., Minoletti, F., Parkinson, I.J., Mokadem, F., Burton, K.W., 2014. Controls on stable strontium isotope fractionation in coccolithophores with implications for the marine Sr cycle. Geochimica et Cosmochimica Acta 128, 225–235. https://doi.org/10.1016/j.gca.2013.11.043

Taraldsvik, M., Myklestad, S., 2000. The effect of pH on growth rate, biochemical composition and extracellular carbohydrate production of the marine diatom *Skeletonema costatum*. https://doi.org/10.1080/09670260010001735781

Taylor, A.R., Brownlee, C., Wheeler, G., 2017. Coccolithophore Cell Biology: Chalking Up Progress. Annual Review of Marine Science 9, 283–310. https://doi.org/10.1146/annurev-marine-122414-034032

Taylor, L.L., Quirk, J., Thorley, R.M.S., Kharecha, P.A., Hansen, J., Ridgwell, A., Lomas, M.R., Banwart, S.A., Beerling, D.J., 2016. Enhanced weathering strategies for stabilizing climate and averting ocean acidification. Nature Climate Change 6, 402–406. https://doi.org/10.1038/nclimate2882 http://www.nature.com/nclimate/journal/v6/n4/abs/nclimate2882.html#supplementary-information

Tsuji, Y., Yoshida, M., 2017. Chapter Seven - Biology of Haptophytes: Complicated Cellular Processes Driving the Global Carbon Cycle, in: Hirakawa, Y. (Ed.), Advances in Botanical Research, Secondary Endosymbioses. Academic Press, pp. 219–261. https://doi.org/10.1016/bs.abr.2017.07.002

Tyrrell, T., Merico, A., 2004. *Emiliania huxleyi*: bloom observations and the conditions that induce them, in: Thierstein, H.R., Young, J.R. (Eds.), Coccolithophores: From Molecular Processes to Global Impact. Springer, Berlin, Heidelberg, pp. 75–97. https://doi.org/10.1007/978-3-662-06278-4_4

von Dassow, P., Ogata, H., Probert, I., Wincker, P., Da Silva, C., Audic, S., Claverie, J.-M., de Vargas, C., 2009. Transcriptome analysis of functional differentiation between haploid and diploid cells of *Emiliania*

huxleyi, a globally significant photosynthetic calcifying cell. Genome Biology 10, R114. https://doi.org/10.1186/gb-2009-10-10-r114

Waldbusser, G.G., Hales, B., Langdon, C.J., Haley, B.A., Schrader, P., Brunner, E.L., Gray, M.W., Miller, C.A., Gimenez, I., 2015. Saturation-state sensitivity of marine bivalve larvae to ocean acidification. Nature Climate Change 5, 273–280. https://doi.org/10.1038/nclimate2479

Walker, C.E., Taylor, A.R., Langer, G., Durak, G.M., Heath, S., Probert, I., Tyrrell, T., Brownlee, C., Wheeler, G.L., 2018. The requirement for calcification differs between ecologically important coccolithophore species. New Phytologist 0. https://doi.org/10.1111/nph.15272

Wolf-Gladrow, D.A., Zeebe, R.E., Klaas, C., Körtzinger, A., Dickson, A.G., 2007. Total alkalinity: The explicit conservative expression and its application to biogeochemical processes. Marine Chemistry, Special issue: Dedicated to the memory of Professor Roland Wollast 106, 287–300. https://doi.org/10.1016/j.marchem.2007.01.006

Zeebe, R.E., Wolf-Gladrow, D.A., 2001. CO_2 in seawater: equilibrium, kinetics, isotopes, Elsevier oceanography series ; 65. Elsevier, Amsterdam ; London.

Zhang, E., Wu, S., Cai, W., Zeng, J., Li, J., Li, G., Liu, J., 2021. Validation of superior reference genes for qRT-PCR and Western blot analyses in marine *Emiliania huxleyi*–virus model system. Journal of Applied Microbiology 131, 257–271. https://doi.org/10.1111/jam.14958

Ziveri, P., de Bernardi, B., Baumann, K.-H., Stoll, H.M., Mortyn, P.G., 2007. Sinking of coccolith carbonate and potential contribution to organic carbon ballasting in the deep ocean. Deep Sea Research Part II: Topical Studies in Oceanography, The Role of Marine Organic Carbon and Calcite Fluxes in Driving Global Climate Change, Past and Future 54, 659–675. https://doi.org/10.1016/j.dsr2.2007.01.006

Zondervan, I., Zeebe, R.E., Rost, B., Riebesell, U., 2001. Decreasing marine biogenic calcification: A negative feedback on rising atmospheric pCO_2. Global Biogeochemical Cycles 15, 507–516. https://doi.org/10.1029/2000GB001321

Statement of Authorship for joint/multi-authored papers for PGR thesis

To appear at the end of each thesis chapter submitted as an article/paper

The statement shall describe the candidate's and co-authors' independent research contributions in the thesis publications. For each publication there should exist a complete statement that is to be filled out and signed by the candidate and supervisor **(only required where there isn't already a statement of contribution within the paper itself).**

Title of Paper	**Chapter 3:** The growth and calcification response of the coccolithophores *Emiliania huxleyi* and *Coccolithus braarudii* to the marine Carbon Dioxide Removal technique of Ocean Alkalinity Enhancement
Publication Status	Unpublished and unsubmitted work written in a manuscript style.
Publication Details	

Student Confirmation

Student Name:	Sophie Gill (SG)		
Contribution to the Paper	SG designed experiments with input from RR and GH. SG conducted all experimental work. SG analysed all data. SG wrote the chapter. RR provided comments on the chapter that SG used to redraft before thesis submission.		
Signature 		Date	03/01/2022

Supervisor Confirmation

By signing the Statement of Authorship, you are certifying that the candidate made a substantial contribution to the publication, and that the description described above is accurate.

Supervisor name and title: Prof. Rosalind Rickaby		
Supervisor comments: Sophie has stated the authorship clearly above.		
Signature 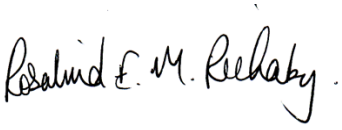	Date	03/01/2022

This completed form should be included in the thesis, at the end of the relevant chapter.

Chapter 4: Changing Redfield ratio of the coccolithophores *Emiliania huxleyi* and *Coccolithus braarudii* in response to Ocean Alkalinity Enhancement: a potential positive feedback for CO_2 drawdown?

Sophie J. Gill, Rosalind R. E. M. Rickaby and Gideon M. Henderson

4.1 Introduction

The elemental composition of marine organic matter is a fundamental parameter in the global ocean. It exerts control on the competitive advantage of marine plankton over one another and governs interactions between the global carbon, nitrogen, phosphorus and oxygen cycles (DeVries and Deutsch, 2014; Arrigo, 2005). The proposed marine Carbon Dioxide Removal (mCDR) scheme of Ocean Alkalinity Enhancement (OAE) raises surface ocean Total Alkalinity (TA) to increase CO_2 drawdown via air-sea gas exchange (Renforth and Henderson, 2017; GESAMP, 2019; Bach et al., 2019). Raising TA also raises Dissolved Inorganic Carbon (DIC) concentration. DIC is a necessary component for the production of Particulate Organic Carbon (POC) by marine biota. Therefore, if DIC increases in the surface ocean, increased POC formation may occur in OAE scenarios (Riebesell et al., 2007). Henderson et al. (2008) posit that any additional POC export from the ocean's surface layer could remove additional carbon from the surface ocean, therefore reducing atmospheric CO_2 even further, shown schematically in **Figure 4.1**.

The canonical Redfield ratio (106 C: 16 N: 1 P) of marine phytoplankton is a crucial control on this process. If C:N:P of marine phytoplankton is fixed, then the extent of additional POC production following OAE is likely to be small because, in the modern ocean, POC production is limited by phosphate and nitrate rather than by the availability of DIC (Redfield, 1958; Lenton and Watson, 2000). Conversely, suppose organisms like coccolithophores can alter their C:N:P in response to external seawater chemistry perturbations. In that case, this mechanism of additional POC export could be a potential positive feedback of enhancing ocean alkalinity

to draw down atmospheric CO_2 (Henderson et al., 2008). Any shift in the elemental stoichiometry of phytoplankton such that there would be increases in carbon relative to elements that limit growth (e.g. N, P, Si, Fe) could increase the amount of carbon exported relative to the amount of limiting nutrient (Finkel et al., 2010; Falkowski et al., 2000; Sigman and Boyle, 2000). For example, C:N in excess of the Redfield C:N ratio would push the oceans into a regime of "carbon over-consumption" (Broecker, 1982; Riebesell et al., 2007). This potential for a positive feedback on carbon drawdown could be important to quantify as part of the ocean's response to an OAE scheme.

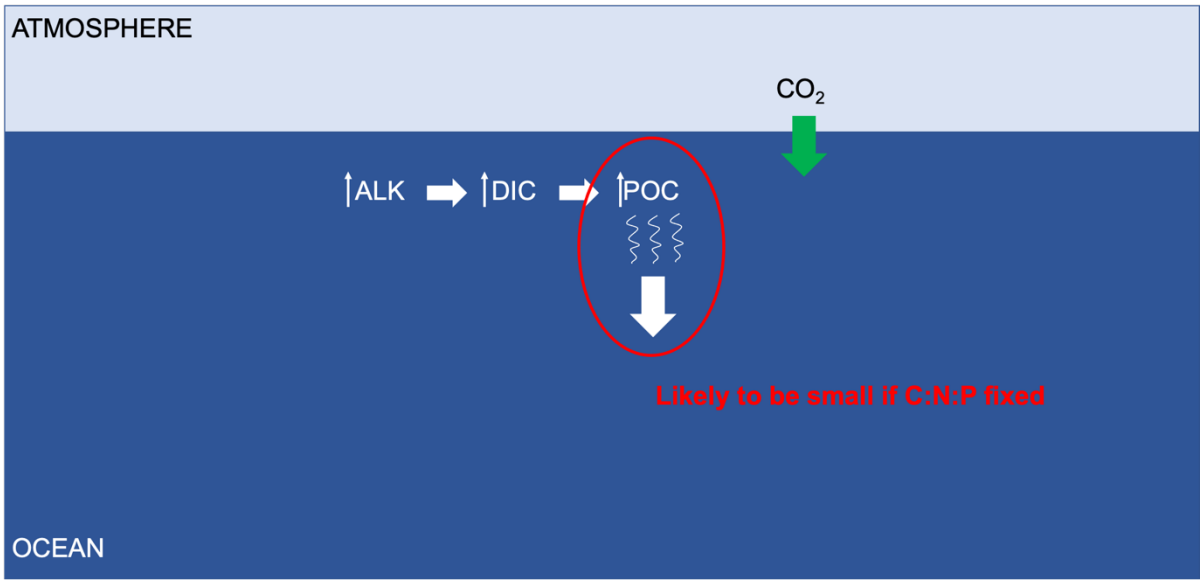

Figure 4.1: Diagram showing the potential for a positive feedback for carbon drawdown during Ocean Alkalinity Enhancement (OAE) if C:N:P of marine phytoplankton is not fixed. ALK = Total Alkalinity, DIC = Dissolved Inorganic Carbon, POC = Particulate Organic Carbon.

A large body of evidence suggests that the Redfield ratio in marine phytoplankton species is not uniform, despite holding a remarkably constant global average (Arrigo, 2005; Galbraith and Martiny, 2015; Klausmeier et al., 2008). Quigg et al. (2013) and Geider and Roche (2002) observed variability of C:N:P in and between species of marine microalgae, and Weber and Deutsch (2010) found using a Global Circulation Model that different phytoplankton in different areas of the global ocean have different C:N:P. The consensus is that the canonical Redfield ratio is not a "universally optimal value", but is instead an average of the different Redfield

ratio values of diverse oceanic plankton (Geider and Roche, 2002; Arrigo, 2005; Ptacnik et al., 2010; They et al., 2017).

A growing body of evidence suggests that phytoplankton C:N:P may alter in response to external environmental perturbations and cellular processes, in particular growth rate (They et al., 2017; Schulhof et al., 2019; Tanioka and Matsumoto, 2017; Tanioka and Matsumoto, 2020). For example, Hillebrand et al. (2013) found that faster-growing phytoplankton have lower stoichiometric flexibility and lower N:P, and Riebesell et al. (2007) observed increased C:N and C:P in response to high dissolved CO_2 conditions exerted by ocean acidification.

This study quantifies the Redfield ratio (C:N:P) of the coccolithophores *Emiliania huxleyi* and *Coccolithus braarudii* under OAE scenarios in CO_2-replete and CO_2-limited conditions.

4.2 Methods

4.2.1 Batch culturing

This study uses the same methods of acclimated batch culturing as **Chapter 3**, with the same CO_2-replete and CO_2-limited conditions examined for OAE scenarios with both *E. huxleyi* and *C. braarudii*. See **Chapter 3.2** for details of the experimental framework. Samples for N and P analysis were taken in duplicate from each 2L large-volume culture run alongside triplicate cultures for each enhanced alkalinity treatment, as outlined in **Chapter 3.2** for TPC and POC samples.

4.2.2 C:N:P sampling and analysis

C values are obtained from POC measurements; PIC:POC values presented in **Chapter 3** use the same POC values presented as C:N and C:P values in this chapter. Particulate Organic Carbon (POC) samples were taken in duplicate at harvest from the large-volume 2L cultures. These were filtered onto pre-combusted (12 h, 500 ^{o}C) GF/F filters (pore width 0.6µm), dried overnight at 40 ^{o}C and then stored at -20 ^{o}C before analysis. When ready to undergo analysis, POC filters were treated with 230µl of HCl (0.1 M) to remove the inorganic carbon and oven-dried overnight at 40 ^{o}C again, after the methods of Oviedo et al. (2014).

POC samples from CO_2-replete batch cultures (*E. huxleyi* strain RCC911 and *C. braarudii* strain RCC1198) were measured via CHN analyser at Pennine Analytical Laboratories, UK, and CO_2-limited batch cultures (*E. huxleyi* strain SO 14-2) were measured using a SERCON 20/22 Isotope ratio mass spectrometer (IRMS) coupled to a SERCON GSL elemental analyser in the School of Archaeology, University of Oxford.

PON and POP values are obtained using a wet chemistry oxidation method adapted from Raimbault et al. (1999). Samples for PON and POP are filtered in duplicate from the 2L large-volume cultures onto pre-ashed (450 ^oC, 12h) GF/F filters (pore width 0.6µm). After collection, GF/F filters were curled into the inside of 15ml Falcon tubes and dried at 40-60 ^oC overnight, then transferred to a -20 ^oC freezer for storage before analysis.

When ready to analyse, each sample GF/F filter was added to a Pyrex tube containing 8ml oxidising reagent. The oxidising reagent for the wet chemistry process consists of 1.5g sodium tetraborate and 0.75g potassium peroxodisulfate dissolved in 100ml MilliQ. The Pyrex tubes in which samples are placed were cleaned for 24 hours in 10% HCl to remove any P and then underwent one blank autoclave digestion to remove any trace of organic material.

Each Pyrex tube containing oxidising reagent and GF/F filter sample was sealed and transferred to the autoclave for digestion (T = 121 ^oC). This wet-oxidation method converts PON and POP to nitrite and soluble reactive phosphate, respectively, by performing a persulfate wet-oxidation in slightly alkaline conditions (Raimbault et al., 1999). After samples were cooled, they were removed from the autoclave, and the N and P spectrophotometric assays were carried out.

See Doane and Horwáth (2003) for full details of the method for preparation and execution of the N assay. Reagents required were prepared as follows. 400mg VCl_3 was dissolved in 50ml 1M HCl and vortexed thoroughly until all dissolved. 200mg sulfanilamide and 10mg N-(1-naphthyl)ethylenediamine dihydrochloride (NEDD) were dissolved in 400ml MilliQ. The VCl_3 solution was combined carefully with the sulfanilamide + NEDD to make a Griess reagent. Standards for N were made by creating a dilution curve by diluting a working 1000µM $NaNO_3$

solution with the oxidising reagent. In 1.5ml centrifuge tubes, 50µL sample, standard or blank, was combined with 950µL Greiss reagent. The samples were vortexed well and left to react for 60 minutes. In this time, the samples turn a shade of Fuschia pink. The Griess reagent reacts with nitrite ion to form a red-pink azo dye (Irandoust et al., 2013). 150µL of each sample was then loaded into a 96-well plate in duplicate and measured on a Tecan SparkControl plate reader at 540nm. The standard curve for this nitrate assay is shown in **Figure 4.2**.

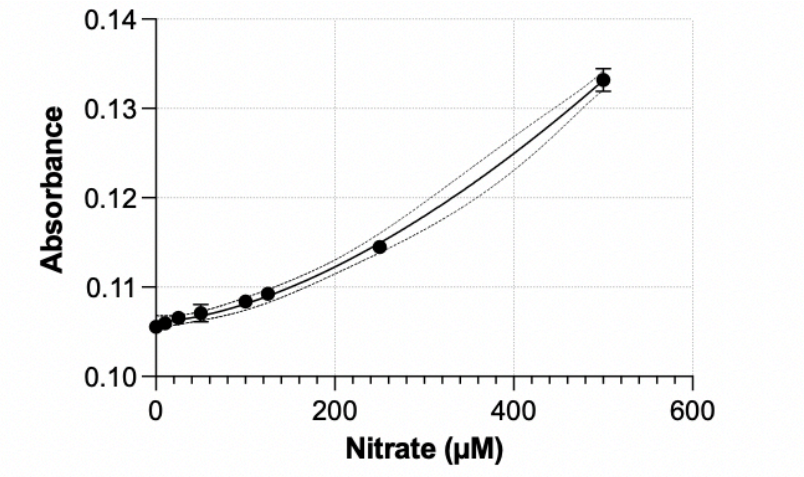

Figure 4.2: Standard curve for nitrate assay. Curve fitted using Sigmoidal Least Squares Fit, in GraphPad Prism 9, plotted here with 95% confidence bands. Standards measured in duplicate; points plotted are average values with standard error. In cases where no error bar is shown, this is because the size of the point obscures the error bar. Values for samples presented in **Chapter 4** interpolated from this standard curve.

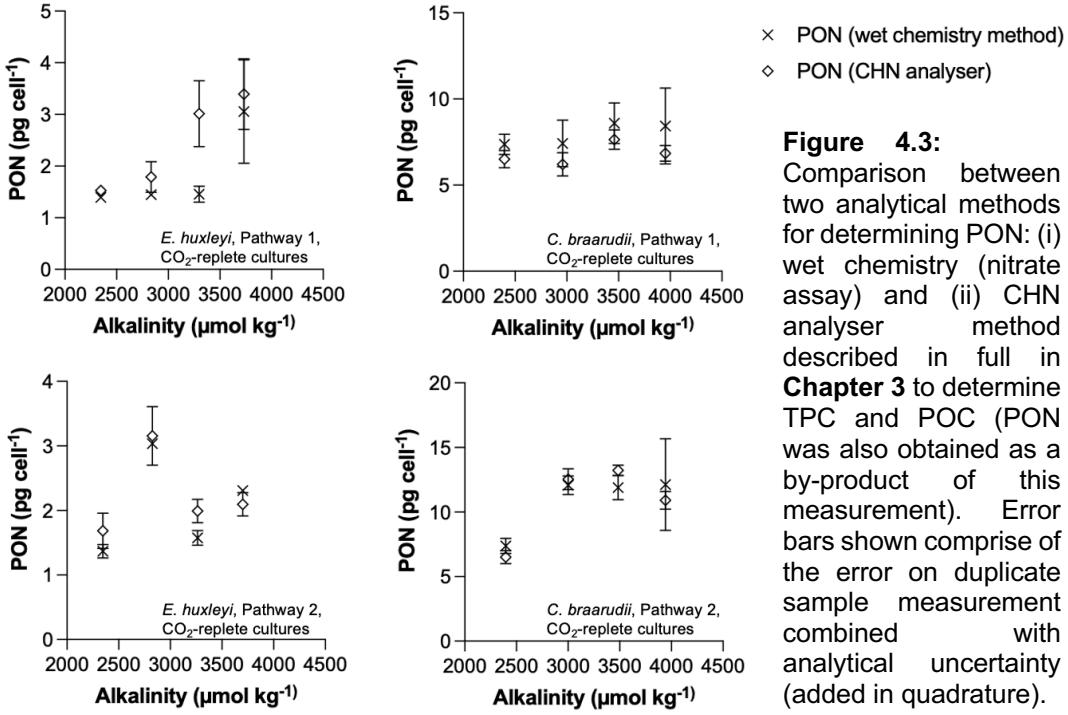

Figure 4.3: Comparison between two analytical methods for determining PON: (i) wet chemistry (nitrate assay) and (ii) CHN analyser method described in full in **Chapter 3** to determine TPC and POC (PON was also obtained as a by-product of this measurement). Error bars shown comprise of the error on duplicate sample measurement combined with analytical uncertainty (added in quadrature).

Figure 4.3 shows the good agreement between PON measured via the wet chemistry method described here, and the CHN analyser measurements described to obtain TPC and POC measurements in **Chapter 3**. This indicates that PON measurements presented in this chapter from the nitrate assay obtained are highly accurate due to the numerical agreement between two independent analytical methods of determining PON.

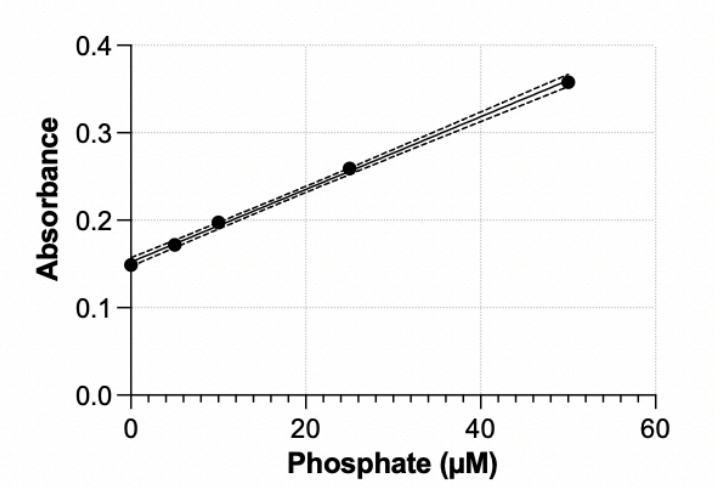

Figure 4.4: Standard curve for phosphate assay. Curve fitted using simple linear regression in GraphPad Prism 9, plotted here with 95% confidence bands. Standards measured in duplicate; points plotted are average values with standard error. In cases where no error bar is shown, this is because the size of the point obscures the error bar. Values for samples presented in **Chapter 4** interpolated from this standard curve.

See Murphy and Riley (1962) for full details of the method for preparation and execution of the P assay. Reagents required were as follows: (i) Ascorbic acid: dissolve 0.88g Ascorbic acid in 50ml MilliQ, (ii) 5N sulfuric acid, (iii) Ammonium molybdate: 2g ammonium molybdate tetrahydrate in 50ml MilliQ, (iv) Potassium antimony tartrate: 0.13715g potassium antimony tartrate in 50ml MilliQ. In a 50ml Falcon tube, 3ml ammonium molybdate tetrahydrate solution, 10ml 5N sulfuric acid, 1ml potassium antimony tartrate solution and 6ml ascorbic acid solution were combined to make a phosphate reagent. Standards for P were made by creating a dilution curve by diluting a working 1000µM NaH_2PO_4 solution with the oxidising reagent. In 1.5ml centrifuge tubes, 800µL sample, standard or blank, was combined with 200µL phosphate reagent. The samples were vortexed well and allowed to react for 30 minutes. In this time, the samples turn an inky blue colour. The phosphate reagent is an acidic molybdate

solution that brings about the formation and reduction of phospho-molybdic acid from the soluble reactive phosphate in solution, resulting in a molybdenum blue colour (Murphy and Riley, 1962). 150µL of each sample was then loaded into a 96-well plate in duplicate and measured on a Tecan SparkControl plate reader at 882nm. The standard curve for this phosphate assay is shown in **Figure 4.4**.

POC:PON (C:N), POC:POP (C:P) and PON:POP (N:P) were tested for significant differences between alkalinity treatments using one-way ANOVA and post-hoc Tukey-Kramer test in GraphPad Prism 9. Before these statistical analyses, data were tested for normality using the Shapiro-Wilks test (Gore et al., 2018; Shafiee et al., 2021). If data did not pass the test for normality using Shapiro-Wilks, the Kruskal-Wallis test for significant difference and Dunn's multiple comparison test were used following best practice guidelines for statistical analysis (Motulsky, GraphPad Statistics Guide).

4.3 Results

There are no particularly strong trends in C:N, C:P or N:P of E*. huxleyi* with increasing Total Alkalinity (TA) in (i) the CO_2-limited system or (ii) the CO_2-replete system (**Figure 4.5**). Some points are significantly different from one another, but no clear patterns, which indicates that the carbonate system is not systematically perturbing the elemental stoichiometry of *E. huxleyi*. The highest TA treatment for *E. huxleyi* in CO_2-limited conditions for Pathway 2 has a statistically significantly higher C:N than the control treatment for the same conditions.

There is a strong trend of lower N:P in the CO_2-replete system for Pathway 1 and Pathway 2 compared to higher N:P in the CO_2-limited system (**Figure 4.5, Panel C**). This is also reflected in **Figure 4.6**, **Panel C**, where the growth rate of the *E. huxleyi* cultures set as the independent variable shows a clear distinction between N:P of CO_2-limited cultures and CO_2-replete cultures. There are no trends with the growth rate for C:N or C:P (**Figure 4.6**, **Panel A & B**).

C. braarudii C:N does not change in CO_2-replete conditions over the TA range tested in either Pathway 1 or Pathway 2 (**Figure 4.7**, **Panel A**). As outlined in **Chapter 3**, the highest growth rate for *C. braarudii* is in the highest TA treatment (TA = 3943 μmol kg^{-1}, see **Table 3.1**), and ROUT analysis (Q = 0.1%) indicates that this highest growth rate point is an outlier in the growth rate dataset. This high growth rate appears to correlate strongly with the highest values for C:P (**Figure 4.8**, **Panel B**) and N:P (**Figure 4.8**, **Panel C**). However, because this is known to be a growth rate outlier, we must discount it from our dataset. Disregarding that one point, *C. braarudii* C:P (**Figure 4.7**, **Panel B**) and N:P (**Figure 4.7**, **Panel C**) therefore do not change increase with increasing TA for Pathway 2, but decrease with increasing TA for Pathway 1. The outlier is very obvious in **Figure 4.8**. There is no apparent correlation between *C. braarudii* growth rate and (i) C:P and (ii) N:P for the cluster of other datapoints (**Figure 4.8**, **Panel B and C**).

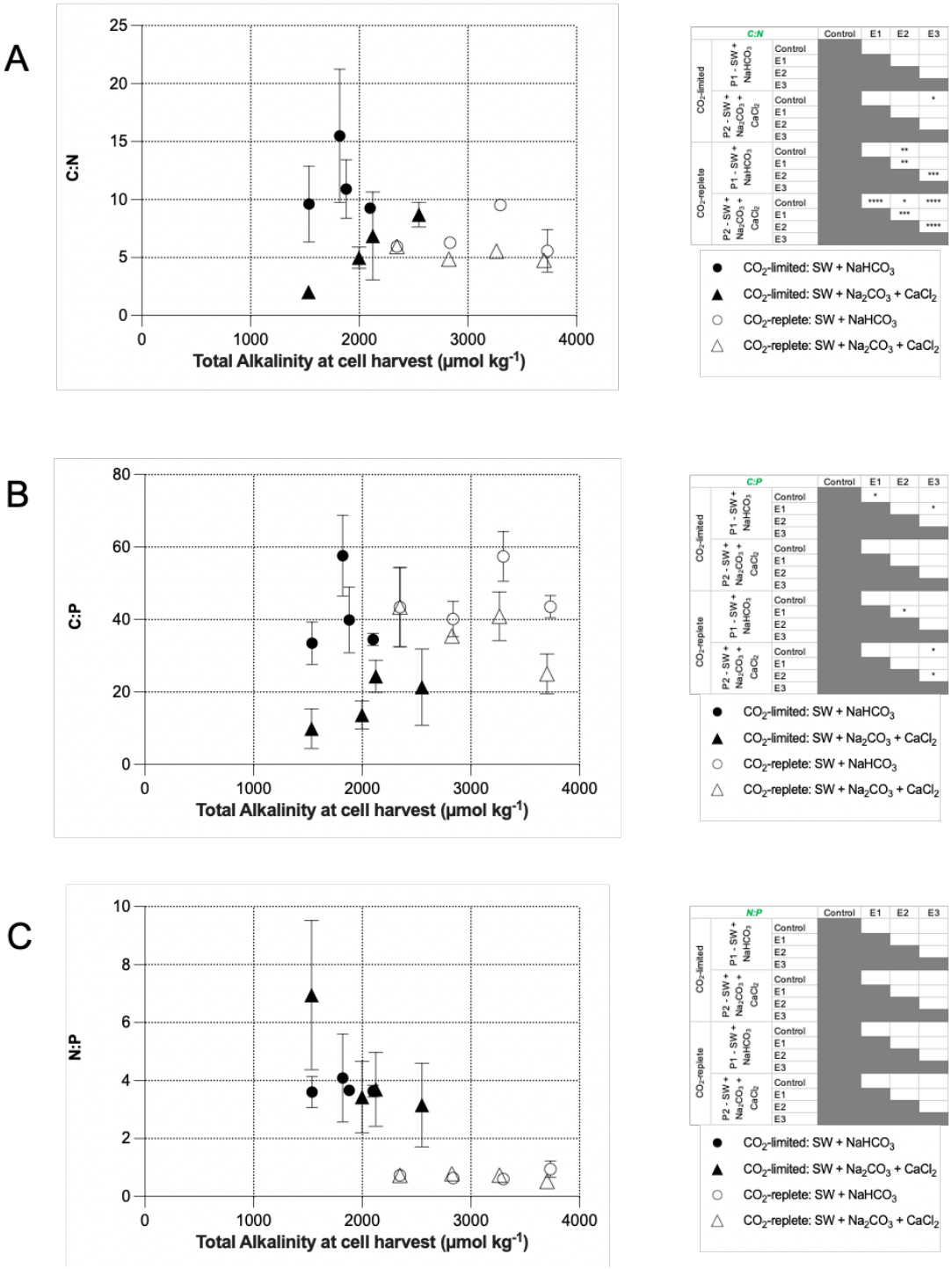

Figure 4.5: Total Alkalinity in culture media at harvest vs. elemental ratios in *E. huxleyi*, with accompanying tables showing statistical significance. Panel (A) shows C:N ratios, panel (B) shows C:P ratios and panel (C) shows N:P ratios. * = P ≤ 0.05, ** = P ≤ 0.01, *** = P ≤ 0.001, **** = P ≤ 0.0001. As outlined in text, Control = Synthetic Ocean Water (SOW), E1 (Control + ~500 µmol kg^{-1}), E2 (Control + ~1000 µmol kg^{-1}), E3 (Control + ~1500 µmol kg^{-1}). Error bars shown are technical replicate values measured on duplicate filters taken from 2L large-volume cultures run alongside biological triplicate cultures, combined with analytical uncertainty (added in quadrature). In cases where no error bar is shown, this is because the size of the symbol obscures the error bar.

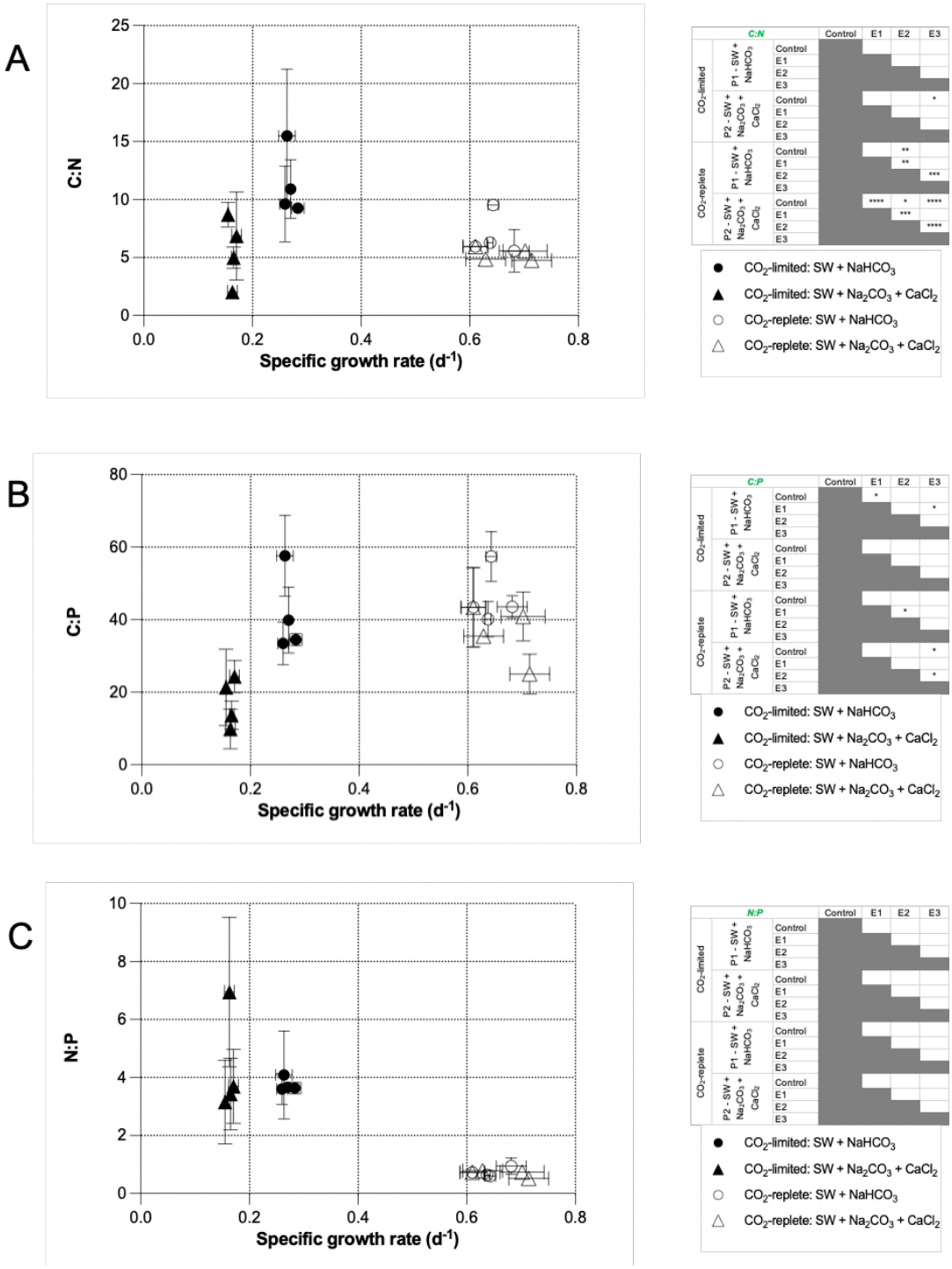

Figure 4.6: Specific growth rate of culture vs. elemental ratios in *E. huxleyi*, with accompanying tables showing statistical significance. Panel (A) shows C:N ratios, panel (B) shows C:P ratios and panel (C) shows N:P ratios. * = P ≤ 0.05, ** = P ≤ 0.01, *** = P ≤ 0.001, **** = P ≤ 0.0001. As outlined in text, Control = Synthetic Ocean Water (SOW), E1 (Control + ~500 µmol kg^{-1}), E2 (Control + ~1000 µmol kg^{-1}), E3 (Control + ~1500 µmol kg^{-1}). Vertical error bars shown are technical replicate values measured on duplicate filters taken from 2L large-volume cultures run alongside biological triplicate cultures, combined with analytical uncertainty (added in quadrature). Horizontal error bars shown are 1 SD of the specific growth rate (see **Chapter 3** for details of specific growth rate measurement and calculation). In cases where no error bar is shown, this is because the size of the symbol obscures the error bar.

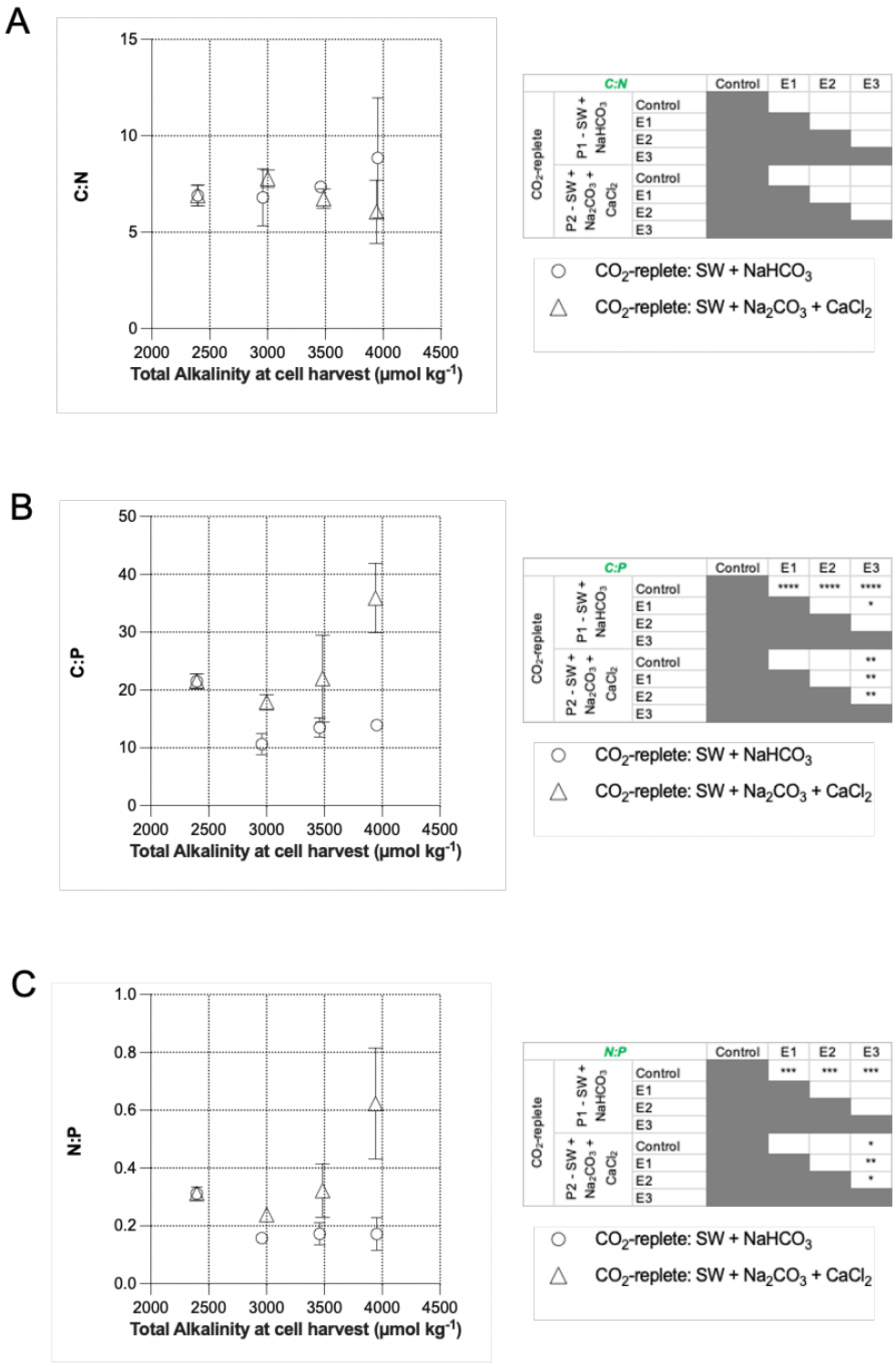

Figure 4.7: Total Alkalinity in culture media at harvest vs. elemental ratios in *C. braarudii*, with accompanying tables showing statistical significance. Panel (A) shows C:N ratios, panel (B) shows C:P ratios and panel (C) shows N:P ratios. * = P ≤ 0.05, ** = P ≤ 0.01, *** = P ≤ 0.001, **** = P ≤ 0.0001. As outlined in text, Control = Synthetic Ocean Water (SOW), E1 (Control + ~500 µmol kg^{-1}), E2 (Control + ~1000 µmol kg^{-1}), E3 (Control + ~1500 µmol kg^{-1}). Error bars shown are technical replicate values measured on duplicate filters taken from 2L large-volume cultures run alongside biological triplicate cultures, combined with analytical uncertainty (added in quadrature). In cases where no error bar is shown, this is because the size of the symbol obscures the error bar.

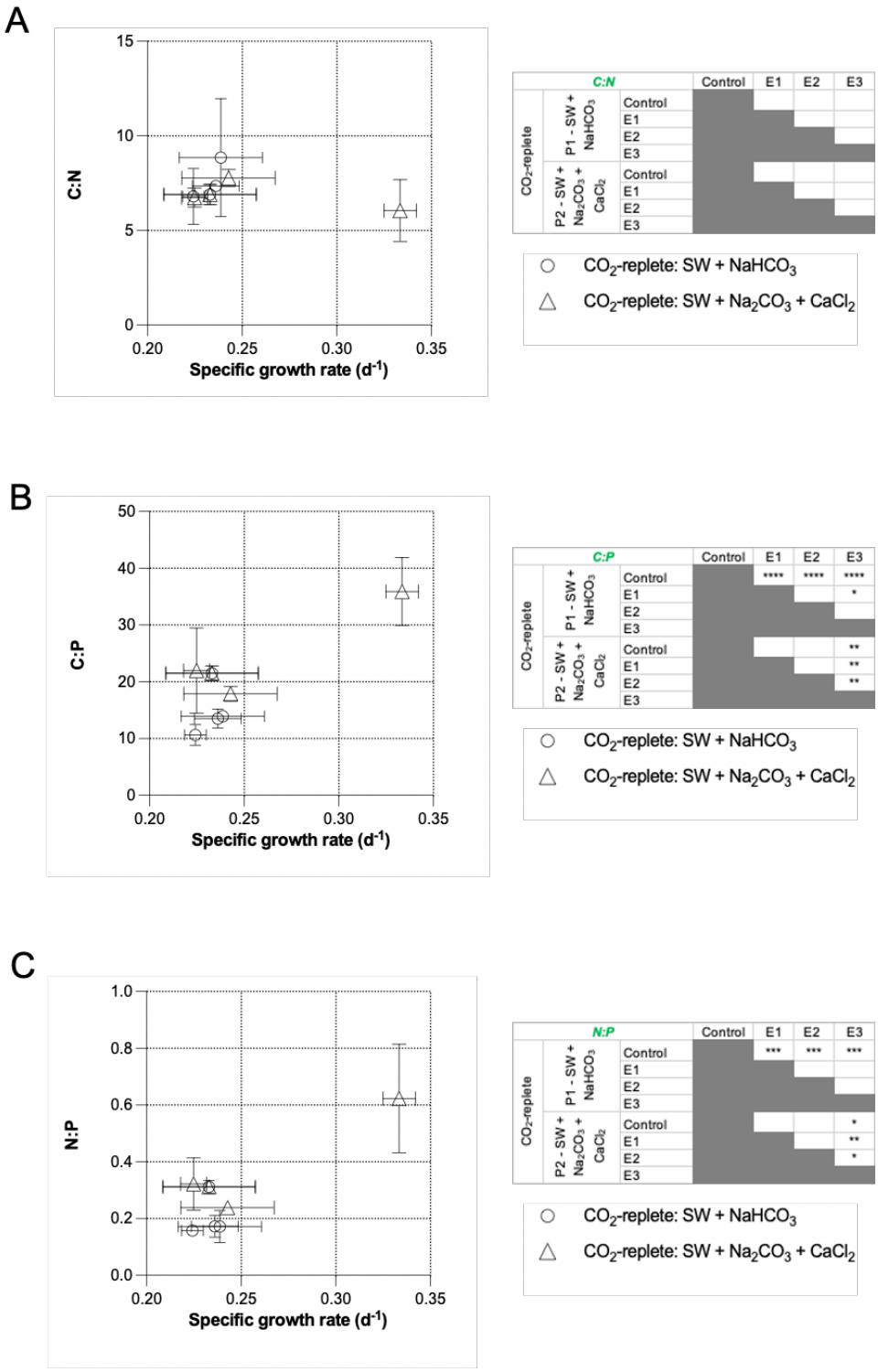

Figure 4.8: Specific growth rate of culture vs elemental ratios in *C. braarudii*, with accompanying tables showing statistical significance. Panel (A) shows C:N ratios, panel (B) shows C:P ratios and panel (C) shows N:P ratios. * = P ≤ 0.05, ** = P ≤ 0.01, *** = P ≤ 0.001, **** = P ≤ 0.0001. As outlined in text, Control = Synthetic Ocean Water (SOW), E1 (Control + ~500 µmol kg^{-1}), E2 (Control + ~1000 µmol kg^{-1}), E3 (Control + ~1500 µmol kg^{-1}). Vertical error bars shown are technical replicate values measured on duplicate filters taken from 2L large-volume cultures run alongside biological triplicate cultures, combined with analytical uncertainty (added in quadrature). Horizontal error bars shown are 1 SD of the specific growth rate (see Chapter 3 for details of specific growth rate measurement and calculation). In cases where no error bar is shown, this is because the size of the symbol obscures the error bar.

4.4 Discussion

4.4.1 Biological mechanisms for shifts in elemental composition

It is clear from the results that growth influences elemental stoichiometry in the experimental manipulations for *E. huxleyi*. Klausmeier et al. (2004) developed a stoichiometrically explicit mathematical model of phytoplankton physiology and resource competition to determine optimal stoichiometry for different physiological and ecological niches. They included a wide variety of phytoplankton taxa in their model: diatoms, cyanobacteria, dinoflagellates, chlorophytes, rhaphydophytes, coccolithophorids (*E. huxleyi*), and pelagophytes. Results from Klausmeier et al. (2004) are used by Arrigo (2005) to outline the concept of the "survivalist" (high N:P, i.e. >30) and "bloomer" (low N:P, i.e. <10) growth strategies for marine plankton. Adherence to one of these growth strategies allows cells to partition elements into the categories of cellular machinery that are helpful to them under nutrient-replete vs nutrient-limited regimes. Proteins and chlorophyll are composed of relatively more N than P (Falkowski, 2000; Geider and Roche, 2002). Proteins and chlorophyll are cellular components that help cells acquire resources and are helpful for cells in nutrient-limited conditions. These allow them to sustain growth when resources are low (Arrigo, 2005). Therefore, a high(er) N:P ratio exhibited by "survivalist" plankton occurs due to a relative partitioning into more PON relative to POP in proteins and chlorophyll. A low(er) N:P ratio exhibited by "bloomer" plankton occurs due to a relative partitioning into more POP relative to PON. More POP is required to support growth machinery such as ribosomal RNA (Arrigo, 2005) in nutrient-replete conditions, as these allow plankton to be adapted for exponential growth.

Arrigo's hypotheses imply a fundamental dependence of elemental stoichiometry on the growth rate of plankton because cellular growth requirements drive relative partitioning between PON and POP. While not with the same elemental ratio, Xie et al. (2021) found evidence that in *E. huxleyi*, growth rate causes changes in cellular partitioning of C and N between macromolecules. We suggest that the shift to higher N:P under CO_2-limitation compared to CO_2-replete conditions in *E. huxleyi,* which we observed in our study, could

therefore be an adaptation to sustain growth when "resources" are low; in this case, the "resource" being [CO_2]. This supports results from Burkhardt et al. (1999), where significant changes in elemental ratios of diatoms and dinoflagellates were observed in CO_2-limited conditions (i.e. [CO_2] < 10 μmol kg^{-1}). We observed high growth rates in **Chapter 3** in the CO_2-replete cultures of *E.* huxleyi, which are driven by the increased supply of HCO_3^- in the OAE treatments, and so these cultures exhibit a shift to lower N:P to sustain their high rates of exponential growth.

The biological mechanisms behind the other changes in elemental stoichiometry we observe in our study are more difficult to identify. The fact that C:P and N:P in *C. braarudii* show an almost identical trend with increasing TA indicates that POP is driving the change in ratio for both those ratios because it is the common factor between them. N:P and C:P of *C. braarudii* decrease with increasing TA for Pathway 1. As outlined, cellular partitioning into relatively more P compared to N (or C, in this case) would suggest that *C. braarudii* growth rate has increased. However, as shown in **Figure 4.8**, there are no trends in C:P or N:P with growth rate, and in **Chapter 3** we did not observe that *C. braarudii* growth rate changed with increasing TA (discounting the outlier). Changing N:P observed in *C. braarudii* does not follow the trends of growth rates presented in **Chapter 3** and is therefore not explained by partitioning into PON and POP to aid growth requirements, unlike for *E. huxleyi*. Although we also observed that *C. braarudii* is not fertilised by extra availability of HCO_3^-, unlike *E. huxleyi*, so perhaps it is not altogether surprising that *C. braarudii* does not exhibit the same growth-rate driven changes in N:P that *E. huxleyi* does.

Changes in marine organic matter C:N and C:P ratios are often dependent on nutrient availability (Weykam et al., 1996; Diehl et al., 2005; Xu et al., 2021; Matsumoto et al., 2020), where a low C:N (C:P) ratio implies high availability of N (P) in the environment, and a high C:N (C:P) ratio indicates low availability of N (P) in the environment. In our study, nitrate and phosphate were spiked into culture media at the same concentration for every TA treatment (see **Methods** in **Chapter 3** for details of culture media preparation). We observed no changes

in C:N for increasing TA for *C. braarudii*, which would fit the availability of N being constant in control and enhanced TA treatments.

However, different C:P and N:P responses for *C. braarudii* C:P were observed in Pathway 1 compared to Pathway 2. There are no differences between Pathway 1 and Pathway 2 culture media conditions other than the addition of Ca (see culture media set up in **Chapter 3**). As shown in **Chapter 3**, added Ca in Pathway 2 does not differently impact growth rates or cellular calcification rates or quota of *C. braarudii* compared to Pathway 1. Therefore it is unlikely that added Ca has a significant impact on C:N or C:P of these species.

To ascertain the biological mechanisms driving the responses of elemental stoichiometry in *C. braarudii* that growth rate drivers in our study cannot explain, it would have been helpful to undertake some proteomics work to ascertain in a more specific way which cellular components are driving changes in elemental stoichiometry, following methods similar to those in Jones et al. (2013), Shire and Kustka (2021) and Shafiee et al., (2021), amongst others. For example, ascertaining which proteins are up-regulated or down-regulated in tandem with the C:P and N:P responses observed would help shed some light on the biological drivers behind these processes.

4.4.2 Implications of changing C:N:P for OAE

As outlined in our **Introduction**, POC formation is thought to be limited by nitrate and phosphate, not DIC. The elemental ratio of C:N indicates whether additional POC formation due to the addition of DIC through OAE may act as a positive feedback on CO_2 drawdown. Our study shows that in higher TA treatments under CO_2-replete conditions, both *E. huxleyi* and *C. braarudii* do not alter their C:N. In CO_2-limited conditions, there is an intimation that *E. huxleyi* may increase its C:N at TA ~4000 µmol kg^{-1} when TA is added as Ca^{2+} (Pathway 2). The same trend is not observed when TA is added as Na^{+} (Pathway 1). As outlined in **Chapter 3**, the experimental manipulations in CO_2-replete conditions are representative of an air-equilibrated OAE scenario, whereas the CO_2-limited conditions are representative of a non-equilibrated OAE scenario (**Figure 3.1**). Therefore, we can conclude that under non-

equilibrated conditions of OAE (analogous to point-source additions of TA to the surface ocean), there is a hint that C:N of coccolithophores increases and would feasibly act as a positive feedback on CO_2 drawdown during OAE. However, during air-equilibrated scenarios of OAE, our study suggests that this is unlikely. The majority of the evidence from our experimental incubations indicates that the C:N of these species of coccolithophores is unlikely to increase and therefore is unlikely to provide a positive feedback on CO_2 drawdown during OAE.

Nevertheless, on a global scale, deep ocean nutrient ratios are controlled by the average C:N:P of the phytoplankton community (Arrigo, 2005). Our study has observed varying changes in C:N, C:P, and N:P in both *E. huxleyi* and *C. braarudii* to OAE treatments. If these changes were scaled up in the real ocean, they would impact nutrient ratios of the deep ocean because coccolithophores contribute up to 10% of global organic carbon fixation (Poulton et al., 2007), which could have knock-on impacts on global biogeochemical cycling. There is also a possibility that increased C:N of phytoplankton could impact the nutritional value for grazers higher up in the marine food web (e.g. bacteria, zooplankton), with further impacts on ecosystem functioning (Riebesell et al., 2007; Sterner and Elser, 2002).

Our study indicates that, to varying degrees, coccolithophores change their cellular partitioning of POC, PON and POP in response to OAE. To constrain the full extent and nature of the impacts of this, further work is needed to quantify *ecosystem* C:N:P response to OAE because coccolithophores are only one group of plankton in a much larger pelagic ecosystem, and as explained in the **Introduction**, contribute to an average C:N:P of phytoplankton organic matter.

This could be ascertained through mesocosm experiments or mesoscale field trials. For example, Bozec et al. (2005) measured the relative changes in elemental ratios of seawater inside the Fe-enrichment patch during a mesoscale iron enrichment experiment (EisenEx) carried out in the Southern Ocean in 2000. The authors then quantified the ratio of biological carbon uptake to Fe added. EisenEx aimed to test the feasibility of another mCDR scheme,

Ocean Iron Fertilization (OIF) (see **Chapter 2** for more details on OIF). This could be repeated but in a mesoscale OAE field trial, coupled with taking samples of plankton within and outside the OAE patch to test shifts in elemental stoichiometry of marine organic matter, using sampling methods similar to those used in OIF plankton experiments (Bakker et al., 2001; Boyd et al., 2007; Boyd et al., 2000; Gall et al., 2001; Assmy et al., 2007; Cavender-Bares, 1999).

4.5 Conclusions

We conclude that N:P of *E. huxleyi* is strongly related to the growth rate. As shown in **Chapter 3**, it is likely that the growth rate of *E. huxleyi* will change as a result of Alkalinity Enhancement, driven by concurrent changes in [CO_2] and [HCO_3^-]. Therefore, we can expect *E. huxleyi* C:N:P to change during OAE. By contrast, *C. braarudii* C:P and N:P do not appear to be linked to growth rate. We have shown that the cellular C:N of the two coccolithophore species, *E. huxleyi* and *C. braarudii* is unlikely to increase in response to the carbonate chemistry conditions resulting from air-equilibrated Ocean Alkalinity Enhancement, and therefore unlikely to provide a positive feedback on atmospheric CO_2 drawdown during this mCDR process. However, there was a hint that under non-equilibrated scenarios of OAE, C:N of *E. huxleyi* may increase. This may warrant further study by conducting whole ecosystem experiments with OAE to examine whether the pelagic ecosystem C:N:P of marine organic matter shifts from the canonical Redfield ratio. If community C:N:P shifts, this could have wide-ranging impacts on biogeochemical cycling and ecosystem structure, that could indirectly affect carbon export.

References

Arrigo, K.R., 2005. Marine microorganisms and global nutrient cycles. Nature 437, 349–355. https://doi.org/10.1038/nature04159

Assmy, P., Henjes, J., Klaas, C., Smetacek, V., 2007. Mechanisms determining species dominance in a phytoplankton bloom induced by the iron fertilization experiment EisenEx in the Southern Ocean. Deep Sea Research Part I: Oceanographic Research Papers 54, 340–362. http://dx.doi.org/10.1016/j.dsr.2006.12.005

Bach, L.T., Gill, S.J., Rickaby, R.E.M., Gore, S., Renforth, P., 2019. CO_2 Removal With Enhanced Weathering and Ocean Alkalinity Enhancement: Potential Risks and Co-benefits for Marine Pelagic Ecosystems. Frontiers in Climate 1. https://doi.org/10.3389/fclim.2019.00007

Bakker, D.C.E., Watson, A.J., Law, C.S., 2001. Southern Ocean iron enrichment promotes inorganic carbon drawdown. Deep Sea Research Part II: Topical Studies in Oceanography, The Southern Ocean Iron Release Experiment (SOIREE) 48, 2483–2507. https://doi.org/10.1016/S0967-0645(01)00005-4

Boyd, P.W., Jickells, T., Law, C.S., Blain, S., Boyle, E.A., Buesseler, K.O., Coale, K.H., Cullen, J.J., Baar, H.J.W. de, Follows, M., Harvey, M., Lancelot, C., Levasseur, M., Owens, N.P.J., Pollard, R., Rivkin, R.B., Sarmiento, J., Schoemann, V., Smetacek, V., Takeda, S., Tsuda, A., Turner, S., Watson, A.J., 2007. Mesoscale Iron Enrichment Experiments 1993-2005: Synthesis and Future Directions. Science 315, 612–617. https://doi.org/10.1126/science.1131669

Boyd, P.W., Watson, A.J., Law, C.S., Abraham, E.R., Trull, T., Murdoch, R., Bakker, D.C.E., Bowie, A.R., Buesseler, K.O., Chang, H., Charette, M., Croot, P., Downing, K., Frew, R., Gall, M., Hadfield, M., Hall, J., Harvey, M., Jameson, G., LaRoche, J., Liddicoat, M., Ling, R., Maldonado, M.T., McKay, R.M., Nodder, S., Pickmere, S., Pridmore, R., Rintoul, S., Safi, K., Sutton, P., Strzepek, R., Tanneberger, K., Turner, S., Waite, A., Zeldis, J., 2000. A mesoscale phytoplankton bloom in the polar Southern Ocean stimulated by iron fertilization. Nature 407, 695–702. https://doi.org/10.1038/35037500

Bozec, Y., Bakker, D.C.E., Hartmann, C., Thomas, H., Bellerby, R.G.J., Nightingale, P.D., Riebesell, U., Watson, A.J., de Baar, H.J.W., 2005. The CO_2 system in a Redfield context during an iron enrichment experiment in the Southern Ocean. Marine Chemistry 95, 89–105. https://doi.org/10.1016/j.marchem.2004.08.004

Broecker, W.S., 1982. Ocean chemistry during glacial time. Geochimica et Cosmochimica Acta 46, 1689–1705. https://doi.org/10.1016/0016-7037(82)90110-7

Cavender-Bares, K.K., 1999. Differential response of equatorial Pacific phytoplankton to iron fertilization. Limnology & Oceanography 44, 237–246.

DeVries, T., Deutsch, C., 2014. Large-scale variations in the stoichiometry of marine organic matter respiration. Nature Geoscience 7, 890–894. https://doi.org/10.1038/ngeo2300

Diehl, S., Berger, S., Wöhrl, R., 2005. Flexible Nutrient Stoichiometry Mediates Environmental Influences on Phytoplankton and Its Resources. Ecology 86, 2931–2945. https://doi.org/10.1890/04-1512

Doane, T.A., Horwáth, W.R., 2003. Spectrophotometric Determination of Nitrate with a Single Reagent. Analytical Letters 36, 2713–2722. https://doi.org/10.1081/AL-120024647

Falkowski, P., Scholes, R.J., Boyle, E., Canadell, J., Canfield, D., Elser, J., Gruber, N., Hibbard, K., Högberg, P., Linder, S., Mackenzie, F.T., Moore III, B., Pedersen, T., Rosenthal, Y., Seitzinger, S., Smetacek, V., Steffen, W., 2000. The Global Carbon Cycle: A Test of Our Knowledge of Earth as a System. Science 290, 291–296. https://doi.org/10.1126/science.290.5490.291

Falkowski, P.G., 2000. Rationalizing elemental ratios in unicellular algae. Journal of Phycology 36, 3–6. https://doi.org/10.1046/j.1529-8817.2000.99161.x

Finkel, Z.V., Beardall, J., Flynn, K.J., Quigg, A., Rees, T.A.V., Raven, J.A., 2010. Phytoplankton in a changing world: cell size and elemental stoichiometry. Journal of Plankton Research 32, 119–137. https://doi.org/10.1093/plankt/fbp098

Galbraith, E.D., Martiny, A.C., 2015. A simple nutrient-dependence mechanism for predicting the stoichiometry of marine ecosystems. PNAS 112, 8199–8204. https://doi.org/10.1073/pnas.1423917112

Gall, M.P., Boyd, P.W., Hall, J., Safi, K.A., Chang, H., 2001. Phytoplankton processes. Part 1: Community structure during the Southern Ocean Iron RElease Experiment (SOIREE). Deep Sea Research Part II: Topical Studies in Oceanography 48, 2551–2570. http://dx.doi.org/10.1016/S0967-0645(01)00008-X

Geider, R., Roche, J.L., 2002. Redfield revisited: variability of C:N:P in marine microalgae and its biochemical basis. European Journal of Phycology 37, 1–17. https://doi.org/10.1017/S0967026201003456

GESAMP, 2019. “High level review of a wide range of proposed marine geoengineering techniques”. (Boyd, P.W. and Vivian, C.M.G., eds.). (IMO/FAO/UNESCO-IOC/UNIDO/WMO/IAEA/UN/UN Environment/ UNDP/ISA Joint Group of Experts on the Scientific Aspects of Marine Environmental Protection). Rep. Stud. GESAMP No. 98, 144 p.

Gore, S., Renforth, P., Perkins, R., 2018. The potential environmental response to increasing ocean alkalinity for negative emissions. Mitigation and Adaptation Strategies for Global Change 24, 1191–1211. https://doi.org/10.1007/s11027-018-9830-z

Henderson, G., Rickaby, R., Bouman, H., 2008. Decreasing Atmosphere CO_2 By Increasing Ocean Alkalinity, The Ocean Dimension: Would The Concept Work And What Would Be The Environmental Consequences?

Hillebrand, H., Steinert, G., Boersma, M., Malzahn, A., Meunier, C.L., Plum, C., Ptacnik, R., 2013. Goldman revisited: Faster-growing phytoplankton has lower N:P and lower stoichiometric flexibility. Limnology and Oceanography 58, 2076–2088. https://doi.org/10.4319/lo.2013.58.6.2076

Irandoust, M., Shariati-Rad, M., Haghighi, M., 2013. Nitrite determination in water samples based on a modified Griess reaction and central composite design. Analytical Methods 5, 5977–5982. https://doi.org/10.1039/C3AY40913A

Jones, B.M., Iglesias-Rodriguez, M.D., Skipp, P.J., Edwards, R.J., Greaves, M.J., Young, J.R., Elderfield, H., O'Connor, C.D., 2013. Responses of the *Emiliania huxleyi* Proteome to Ocean Acidification. PLOS ONE 8, e61868. https://doi.org/10.1371/journal.pone.0061868

Klausmeier, C.A., Litchman, E., Daufresne, T., Levin, S.A., 2008. Phytoplankton stoichiometry. Ecological Research 23, 479–485. https://doi.org/10.1007/s11284-008-0470-8

Klausmeier, C.A., Litchman, E., Daufresne, T., Levin, S.A., 2004. Optimal nitrogen-to-phosphorus stoichiometry of phytoplankton. Nature 429, 171–174. https://doi.org/10.1038/nature02454

Lenton, T.M., Watson, A.J., 2000. Redfield revisited: 1. Regulation of nitrate, phosphate, and oxygen in the ocean. Global Biogeochemical Cycles 14, 225–248. https://doi.org/10.1029/1999GB900065

Matsumoto, K., Tanioka, T., Rickaby, R., 2020. Linkages Between Dynamic Phytoplankton C:N:P and the Ocean Carbon Cycle Under Climate Change. Oceanography 33, 44 - 52. https://doi.org/10.5670/oceanog.2020.203

Motulsky, H.J., GraphPad Statistics Guide. URL http://www.graphpad.com/guides/prism/7/statistics/index.htm (accessed 12.7.21).

Murphy, J., Riley, J.P., 1962. A modified single solution method for the determination of phosphate in natural waters. Analytica Chimica Acta 27, 31–36. https://doi.org/10.1016/S0003-2670(00)88444-5

Oviedo, A.M., Langer, G., Ziveri, P., 2014. Effect of phosphorus limitation on coccolith morphology and element ratios in Mediterranean strains of the coccolithophore *Emiliania huxleyi*. Journal of Experimental Marine Biology and Ecology 459, 105–113. https://doi.org/10.1016/j.jembe.2014.04.021

Poulton, A.J., Adey, T.R., Balch, W.M., Holligan, P.M., 2007. Relating coccolithophore calcification rates to phytoplankton community dynamics: Regional differences and implications for carbon export. Deep-Sea Research Part II: Topical Studies in Oceanography 54, 538–557. https://doi.org/10.1016/j.dsr2.2006.12.003

Ptacnik, R., Andersen, T., Tamminen, T., 2010. Performance of the Redfield Ratio and a Family of Nutrient Limitation Indicators as Thresholds for Phytoplankton N vs. P Limitation. Ecosystems 13, 1201–1214. https://doi.org/10.1007/s10021-010-9380-z

Quigg, A., Al-Ansi, M., Al Din, N.N., Wei, C.-L., Nunnally, C.C., Al-Ansari, I.S., Rowe, G.T., Soliman, Y., Al-Maslamani, I., Mahmoud, I., Youssef, N., Abdel-Moati, M.A., 2013. Phytoplankton along the coastal shelf of an oligotrophic hypersaline environment in a semi-enclosed marginal sea: Qatar (Arabian Gulf). Continental Shelf Research 60, 1–16. https://doi.org/10.1016/j.csr.2013.04.015

Raimbault, P., Diaz, F., Pouvesle, W., Boudjellal, B., 1999. Simultaneous determination of particulate organic carbon, nitrogen and phosphorus collected on filters, using a semi-automatic wet-oxidation method. Marine Ecology Progress Series 180, 289–295. https://doi.org/10.3354/meps180289

Redfield, A.C., 1958. The Biological Control Of Chemical Factors In The Environment. American Scientist 46, 230A–221.

Renforth, P., Henderson, G., 2017. Assessing ocean alkalinity for carbon sequestration. Reviews of Geophysics 55, 636–674. https://doi.org/10.1002/2016RG000533

Riebesell, U., Schulz, K.G., Bellerby, R.G.J., Botros, M., Fritsche, P., Meyerhöfer, M., Neill, C., Nondal, G., Oschlies, A., Wohlers, J., Zöllner, E., 2007. Enhanced biological carbon consumption in a high CO_2 ocean. Nature 450, 06267. https://doi.org/10.1038/nature06267

Schulhof, M.A., Shurin, J.B., Declerck, S.A.J., Van de Waal, D.B., 2019. Phytoplankton growth and stoichiometric responses to warming, nutrient addition and grazing depend on lake productivity and cell size. Global Chang Biology 25, 2751–2762. https://doi.org/10.1111/gcb.14660

Shafiee, R.T., Diver, P.J., Snow, J.T., Zhang, Q., Rickaby, R.E.M., 2021. Marine ammonia-oxidising archaea and bacteria occupy distinct iron and copper niches. ISME Communications. 1, 1–12. https://doi.org/10.1038/s43705-021-00001-7

Shafiee, R.T., Snow, J.T., Hester, S., Zhang, Q., Rickaby, R.E.M., 2021. Proteomic response of the marine ammonia-oxidising archaeon *Nitrosopumilus maritimus* to iron limitation reveals strategies to compensate for nutrient scarcity. Environmental Microbiology 24, 835-849. https://doi.org/10.1111/1462-2920.15491

Shire, D.M., Kustka, A.B., 2021. Proteomic responses of the coccolithophore *Emiliania huxleyi* to zinc limitation and trace metal substitution. Environmental Microbiology 24, 819-834. https://doi.org/10.1111/1462-2920.15644

Sigman, D.M., Boyle, E.A., 2000. Glacial/interglacial variations in atmospheric carbon dioxide. Nature 407, 35038000. https://doi.org/10.1038/35038000

Sterner, R.W., Elser, J.J., 2002. Ecological Stoichiometry: The Biology of Elements From Molecules to the Biosphere. Princeton University Press, Princeton.

Tanioka, T., Matsumoto, K., 2020. A meta-analysis on environmental drivers of marine phytoplankton. Biogeosciences 17, 2939–2954. https://doi.org/10.5194/bg-17-2939-2020

Tanioka, T., Matsumoto, K., 2017. Buffering of Ocean Export Production by Flexible Elemental Stoichiometry of Particulate Organic Matter. Global Biogeochemical Cycles 31, 1528–1541. https://doi.org/10.1002/2017GB005670

They, N.H., Amado, A.M., Cotner, J.B., 2017. Redfield Ratios in Inland Waters: Higher Biological Control of C:N:P Ratios in Tropical Semi-arid High Water Residence Time Lakes. Frontiers in Microbiology 8, 1505. https://doi.org/10.3389/fmicb.2017.01505

Weber, T.S., Deutsch, C., 2010. Ocean nutrient ratios governed by plankton biogeography. Nature 467, 550–554. https://doi.org/10.1038/nature09403

Weykam, G., Gómez, I., Wiencke, C., Iken, K., Klöser, H., 1996. Photosynthetic characteristics and C:N ratios of macroalgae from King George Island (Antarctica). Journal of Experimental Marine Biology and Ecology 204, 1–22. https://doi.org/10.1016/0022-0981(96)02576-2

Xie, E., Xu, K., Li, Z., Li, W., Yi, X., Li, H., Han, Y., Zhang, H., Zhang, Y., 2021. Disentangling the Effects of Ocean Carbonation and Acidification on Elemental Contents and Macromolecules of the Coccolithophore *Emiliania huxleyi*. Frontiers in Microbiology 12, 737454. https://doi.org/10.3389/fmicb.2021.737454

Xu, N., Wang, W., Xu, Y., Ji, D., Chen, C., Xie, C., Xu, K., 2021. Effects of Nutrient Availability on the Release of Dissolved and Particulate Organic Carbon by *Pyropia haitanensis* and Its Implications. Frontiers in Marine Science 8, 856. https://doi.org/10.3389/fmars.2021.696938

Statement of Authorship for joint/multi-authored papers for PGR thesis

To appear at the end of each thesis chapter submitted as an article/paper

The statement shall describe the candidate's and co-authors' independent research contributions in the thesis publications. For each publication there should exist a complete statement that is to be filled out and signed by the candidate and supervisor **(only required where there isn't already a statement of contribution within the paper itself).**

Title of Paper	**Chapter 4:** Changing Redfield ratio of the coccolithophores *Emiliania huxleyi* and *Coccolithus braarudii* in response to Ocean Alkalinity Enhancement: a potential positive feedback for CO_2 drawdown
Publication Status	Unpublished and unsubmitted work written in a manuscript style.
Publication Details	

Student Confirmation

Student Name:	Sophie Gill (SG)		
Contribution to the Paper	SG designed experiments with input from RR and GH. SG conducted all experimental work. SG analysed all data. SG wrote the chapter.		
Signature 		Date	03/01/2022

Supervisor Confirmation

By signing the Statement of Authorship, you are certifying that the candidate made a substantial contribution to the publication, and that the description described above is accurate.

Supervisor name and title: Prof. Rosalind Rickaby		
Supervisor comments: Sophie has clearly stated the authorship above.		
Signature 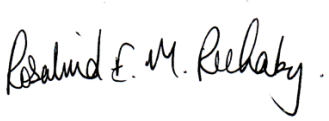	Date	03/01/2022

This completed form should be included in the thesis, at the end of the relevant chapter.

Chapter 5: The response of planktonic foraminifera to enhanced ocean alkalinity - a conceptual study for marine Carbon Dioxide Removal

Sophie J. Gill, Rosalind R. E. M. Rickaby, Jonathan Erez, Gideon M. Henderson, Isabelle Aldridge, Kat Allen, Kate Holland, Oscar Branson, Bärbel Hönisch, Laura Haynes, Steve Eggins

5.1 Introduction

It is now widely recognised that to keep to within 1.5-2 ^{o}C of pre-industrial temperatures, it is not going to be sufficient to reduce our anthropogenic greenhouse gas emissions, and we must actively remove previously emitted carbon dioxide from our atmosphere (Fuss et al., 2014; IPCC, 2018: Summary for Policymakers; Renforth and Henderson, 2017). This is referred to by various terms, such as Carbon Dioxide Removal (CDR), Negative Emissions (NE), and Greenhouse Gas Removal (GGR). Many potential CDR techniques have been proposed to remove historical carbon dioxide from the atmosphere. Many of these are marine-based (marine Carbon Dioxide Removal, mCDR) and focus on careful manipulation of the ocean's carbonate buffer system, such as Enhanced Weathering (EW) or Ocean Alkalinity Enhancement (OAE), which elevate the ocean's natural alkalinity levels to sequester atmospheric CO_2 (Bach et al., 2019; GESAMP, 2019), with an increase in [HCO_3^-] and [CO_3^{2}] and either constant or decreased [CO_2] depending on timescales of air-sea gas exchange between the surface ocean and atmosphere. In addition to alleviating global warming, these schemes also benefit from potentially reversing ocean acidification, which is damaging to calcifying pelagic organisms such as foraminifera. Reduced calcification, increased risk of dissolution and morphological discrepancies have been recorded to occur in response to increased acidification (Lischka et al., 2018; Uthicke et al., 2013; Prazeres et al., 2015). However, calcification produces CO_2 as a by-product, so if the calcification can keep pace with additional alkalinity inputs within the framework of an mCDR scheme, then much of the net sequestration of CO_2 may be undone (Bach et al., 2019; Henderson et al., 2008). In addition,

to remove appreciable amounts of atmospheric CO_2 from the atmosphere, OAE would not just reverse ocean acidification but would bring the ocean to higher alkalinity than its pre-industrial state. Quantifying the potential complications this may cause is a vital step in assessing the viability and safety of OAE for carbon dioxide removal. Therefore, as one of the dominant groups of calcifiers in the pelagic realm, it is crucial to constrain planktonic foraminifera's growth and calcification response to OAE scenarios.

Planktonic foraminifera are calcifying, single-celled amoeboid protists that are ubiquitous throughout the modern surface oceans (Morard et al., 2018). They are heterotrophs that feed in the marine water column by ensnaring passing phytoplankton and zooplankton. They do this using their reticulopodia, calcite spines covered in slightly adhesive extruded cytoplasm, originating from the single-cell amoeba present within the calcite test (Kucera, 2007). It is well-established that many species of planktonic foraminifera also indirectly photosynthesise through the action of associated symbionts. These may be diatoms or dinoflagellates and commonly vary between species and morphotypes of foraminifera (Gastrich, 1987; Erez and Luz, 1983; Henehan et al., 2015; Kucera, 2007; Hemleben et al., 1989).

As such, planktonic foraminifera are vital components of:

(i) the marine food web through both their predation on other plankton and in their role of being grazed by larger filter-feeding planktotrophs (Kucera, 2007),

(ii) the marine organic carbon cycle as hosts of symbiotic algae and associated photosynthetic activity,

(iii) the inorganic marine carbon cycle through their contribution to surface ocean calcification.

It is estimated that foraminiferal calcite provides 25-50% of the annual total pelagic carbonate flux from the surface ocean (Schiebel, 2002; Fox et al., 2020), with 30-80% of that carbonate flux accumulating on the seafloor (Kucera, 2007). The only other plankton group that matches the foraminiferal production of calcite in the pelagic realm is the coccolithophores (Monteiro et al., 2016). Foraminifera calcify by employing a method of fluid-phase seawater endocytosis,

where seawater is drawn directly into the cell via vacuolisation. Ions are supplied directly to the calcification site in the cell from the seawater vacuole (Bentov et al., 2009). As foraminifera calcify, they produce new calcite chambers extracellularly and add a new layer of calcite to previous chambers each time a new chamber is added (de Nooijer et al., 2009).

The influence of altered alkalinity on planktonic foraminifera has been explored before in culturing studies (Bijma et al., 1999; Holland et al., 2020; Russell et al., 2004; Spero et al., 1997). It has been established that shifts in pH and CO_3^{2-} have significant impacts on foraminiferal calcite geochemistry such as the signatures of $\delta^{18}O$ and $\delta^{13}C$ (Bijma et al., 1999; Spero et al., 1997), and U/Ca, Mg/Ca and Sr/Ca (Russell et al., 2004) in symbiotic *Orbulina universa* and non-symbiotic *Globigerina bulloides*. Additionally, the Mg/Ca of foraminiferal calcite in *Orbulina universa* and *Globigerinoides ruber* is sensitive to [Ca] and [DIC] (Holland et al., 2020). These studies have found that calcification in foraminifera does not appear to be impacted by elevated alkalinity; although this could be due to the difficulty of assessing calcification rates (e.g., Holland et al. 2017, Allen et al. 2016).

However, the response of planktonic foraminiferal calcification to the specific chemistries of OAE have never been examined before, and most prior studies, as outlined, have focussed on geochemical measurements of the chemistry of foraminifera tests.

This study quantifies the growth and calcification response of two species of planktonic foraminifera, *Globigerinoides ruber (G. ruber)* and *Globigerinella siphonifera (G. siphonifera)*, to OAE treatments, through a series of live culturing experiments carried out in Eilat, Israel in 2019. We compare these results to prior work on planktonic foraminifera cultures, with the species *Globigerina bulloides* (*G. bulloides*), *Globigerinoides ruber* (*G. ruber*), *Globigerinoides sacculifer* (*G. sacculifer*) and *Orbulina universa* (*O. universa*), to conclude the impact that proposed OAE schemes may have on planktonic foraminifera in our future oceans.

5.2 Methods

5.2.1 Experimental framework

Two different methods in these experiments have been deployed to raise alkalinity either by adding (i) $NaHCO_3$ (Pathway 1) or (ii) Na_2CO_3 and $CaCl_2$ (Pathway 2). These two sets of alkalinity manipulations accurately mimic the chemical conditions which are expected under proposed Ocean Alkalinity Enhancement (OAE) and Enhanced Weathering (EW) schemes (Bach et al., 2019; GESAMP, 2019; Renforth and Henderson, 2017). Pathway 1, using $NaHCO_3$ addition, raises alkalinity and DIC without altering $[Ca^{2+}]$. In Pathway 2, two moles of ALK are added by two conservative Na^+ ions in Na_2CO_3, and 1 mole DIC is added by CO_3^{2-}. $CaCl_2$ does not raise alkalinity because it adds equal amounts of positive and negative conservative charge to the solution from Ca^{2+} and 2 x Cl^-. However, it does raise [Ca] in solution to concentrations relevant for OA . This scheme of experiments allows us to constrain how physiology and calcification respond to these two different modes of alkalinity manipulation. See **Table 5.1** for a summary of the carbonate chemistry conditions of the experiments, including Ca levels.

Our methods result in several other chemical species of the carbonate system co-varying with the alkalinity increases, as illustrated in **Table 5.1**. Co-variance of different species of the carbonate system with enhanced alkalinity is a natural consequence of such manipulations, and it is pertinent to allow this to occur to ensure accurate responses of organisms to OAE and EW schemes. Enhanced alkalinity itself is very unlikely to be a driver for physiological responses. Alkalinity is an analytical concept and hence not “sensed” by organisms. In contrast, concentrations of individual carbon species are directly relevant to organismal physiology and therefore need to be considered as drivers. Foraminifera are physiologically driven by changes in $[CO_3^{2-}]$ (Bijma et al., 1999; Spero et al., 1997; Russell et al., 2004; Lombard et al., 2010; Osborne et al., 2016), and CO_3^{2-} is predicted to rise with increasing TA

in OAE scenarios. Therefore, this is the relevant carbonate system parameter relative to which responses of planktonic foraminifera to OAE scenarios are discussed in this study.

Treatment	Total Alkalinity, TA (μmol kg^{-1})	Dissolved Inorganic Carbon, DIC (μmol kg^{-1})	pH	pCO_2 (μatm)	HCO_3^- (μmol kg^{-1})	CO_3^{2-} (μmol kg^{-1})	CO_2 (μmol kg^{-1})	$\Omega CaCO_3$	Ca concentration (mM L^{-1})
SW (control)	2461	2162	8.072	555	1931	215	15.7	4.9	10.3
SW + $NaHCO_3$	2926	2460	8.237	414	2105	343	11.7	7.9	10.3
	3393	2790	8.320	377	2321	458	10.6	10.5	10.3
SW + Na_2CO_3 + $CaCl_2$	2941	2451	8.263	386	2080	360	10.9	8.2	10.6
	3355	2765	8.312	382	2307	447	10.8	10.2	10.8

Table 5.1: A summary of the experimental alkalinity treatments for this study (after equilibration), measured with an error of TA±2 μmol kg^{-1} on duplicate measurements of the same sample. Seawater is abbreviated to SW. DIC, pCO_2, HCO_3^-, CO_3^{2-}, CO_2 and $\Omega CaCO_3$ were determined from Total Alkalinity and pH measurements using CO2SYS v2.1 (Pierrot et al. 2016), with K1 and K2 constants from Roy, et al. (1993), $KHSO_4$ values from Dickson, pH on the NBS scale and $[B]_T$ value from Lee et al. (2010). Ca levels in solution are calculated using the molar amounts of Ca^{2+} in the volume of $CaCl_2$ added to the enhanced alkalinity treatments.

All seawater (SW) solutions were prepared at the Fredy and Nadine Herrmann Institute of Earth Sciences, Hebrew University of Jerusalem. Control SW from the Gulf of Eilat is collected regularly and stored in jerry cans in the Jerusalem laboratory. The control SW used in this study was ~3 months aged. Enhanced alkalinity solutions were prepared by spiking control SW with calculated amounts of either (i) 0.5M $NaHCO_3$ or (ii) 0.5M Na_2CO_3 + 1M $CaCl_2.2H_2O$ stock solutions. Amounts were calculated for ~500 and ~1000 μmol kg^{-1} increases in alkalinity compared to control alkalinity values (see **Table 5.1**). After the chemistry of these solutions had been adjusted, they were bubbled with ambient water-saturated air overnight to equilibrate with atmospheric CO_2, so these experiments are representative of an air-equilibrated OAE scenario (Bach et al., 2019). The vessels were covered with disposable plastic wrap during bubbling to reduce evaporation, which would have increased the alkalinity. The control SW was not aerated because planktonic foraminifera are incredibly sensitive organisms, so we needed to preserve the exact conditions in the control Gulf of Eilat SW to guarantee that we would get a reliable control response in the experiment. After the enhanced alkalinity solutions had been bubbled, the pH of all solutions (including the control SW) was measured using a Radiometer pH meter. The alkalinity of the solutions was measured by Gran

titration using a Metrohm 716 DMS Titrino (see **Table 5.1**). The titrator is calibrated against NBS buffers daily and a certified seawater reference material (Dickson Batch 155, Scripps Institute of Oceanography). The enhanced alkalinity and control solutions were then 0.45µm filter-sterilised and transferred to 120ml culturing jars and sealed with parafilm and plastic lids to prevent evaporation and CO_2 exchange with the atmosphere before foraminifera culturing. Culturing jars of solutions were packaged and transported to Eilat, ready for culturing foraminifera at the Inter-University Institute of Marine Sciences (IUI).

5.2.2 Culturing

The methods of culturing planktonic foraminifera are well-established, and in-depth procedures are described by various authors (Evans et al., 2018; Kisakürek et al., 2008; Evans et al., 2016b; Lombard et al., 2009; Erez and Luz, 1983). For this specific study, culturing of planktonic foraminifera was completed from 06/11/2019-07/12/2019 at the H. Steinitz Marine Biology Laboratory at the Inter-University Institute of Marine Sciences (IUI), Eilat, Israel. Planktonic foraminifera were collected from the Gulf of Eilat using vertical net tows (100µm mesh size) from 20m to the surface. Nets were towed at water column depths of ~300m, measured by the boat's bathymetry instrument (echosounder), a water depth which was typically encountered ~1km offshore. *Globigerinoides ruber* and *G. siphonifera* were picked and isolated from the plankton tows under a binocular microscope back in the laboratory. Foraminifera were placed in Petri dishes in seawater collected from the same location as the plankton tows and allowed to recover under culturing lights for ~2-3 days. After this recovery period, foraminifera that were healthy and suitable to be placed in experimental conditions were identified by the presence of long calcite spines and a halo of symbionts.

Before being placed in either control or enhanced alkalinity conditions, the diameter of the long axis of each healthy foraminifer was measured using an inverted light microscope. Foraminifera were then placed either individually or in pairs in 120ml glass culture jars. These were sealed with parafilm and a plastic lid to eliminate evaporation (which would increase alkalinity) and minimise CO_2 exchange with the atmosphere. Culture jars were kept at 24 ^{o}C

in temperature-controlled water baths, under a 12h light-dark cycle, with 5 am-5 pm auto-timing in phase with daylight hours in Eilat at this time of year. The irradiance of the culturing lights was approximately equivalent to that at 20m open ocean water depth (~200 µmol photons m^{-2} s^{-1}) (Shaked and Genin, 2006). Each foraminifer was fed daily with a juvenile artemia shrimp using a Pasteur pipette. It was important not to touch the foraminifera directly during feeding as this could have disrupted their growth, so artemia were fired towards the adhesive reticulopodia to simulate how foraminifera would feed in the open ocean water column.

The treatments were staggered in completion because of constraints on how many foraminifera it was possible to pick, isolate, check for recovery and maintain feeding in one working day. Therefore, the early stages of culturing focussed on the control treatments instead of enhanced alkalinity treatments. It is worth noting that there were some difficulties with culturing planktonic foraminifera in the control treatments at the beginning of this experiment due to the prevalence of unicellular ciliates. Consequently, mortality rates (see **Table 5.2**) are slightly higher than would normally be expected because some individuals were overrun by these unicellular ciliates, disrupting the expected growth of the foraminifera. This disproportionately affected *G. siphonifera* compared to *G. ruber* for the control treatments. We surmise that the unicellular ciliates were associated with the foraminifera on their extraction from the water column during plankton tows but were dormant/not visible during an initial inspection under the inverted light microscope. It is unclear whether the unicellular ciliates (i) actively contributed to the death of foraminifera, e.g. by feeding on the foraminifera, or (ii) fed on the foraminifera during and after their death, and were associated with foraminifera which were already unhealthy. At any rate, data for individuals associated with the unicellular ciliate activity are not included in results for gametogenesis rates, lifespan, calcification or morphometrics.

Species	Treatment	#individuals cultured	#individuals died	#individuals gametogenesis	Mortality rate (%)	Gametogenesis rate (%)
G. ruber	2461 µmol kg^{-1} SW (control)	22	11	11	50	50
	2926 µmol kg^{-1} SW + $NaHCO_3$	12	5	7	42	58
	3393 µmol kg^{-1} SW + $NaHCO_3$	14	5	9	36	64
	2941 µmol kg^{-1} SW + Na_2CO_3 + $CaCl_2$	10	1	9	10	90
	3355 µmol kg^{-1} SW + Na_2CO_3 + $CaCl_2$	12	8	4	67	33
G. siphonifera	2461 µmol kg^{-1} SW (control)	22	14	8	64	36
	2926 µmol kg^{-1} SW + $NaHCO_3$	23	3	20	13	87
	2941 µmol kg^{-1} SW + Na_2CO_3 + $CaCl_2$	16	6	10	38	63

Table 5.2: Comparison of how many individuals (i) cultured in enhanced alkalinity treatments compared to control conditions, (ii) died, including deaths attributed to the action of unicellular ciliates, and (iii) underwent gametogenesis. SW = Sea Water. All individual foraminifera that were observed to be healthy and feeding, but that were taken out of culturing jars at the end of the experiment on 07/12/2019 before naturally undergoing gametogenesis, are included in the count of individuals which underwent gametogenesis.

5.2.3 Handling of calcification data

Calcification in this study was estimated using published size-mass relationships after the methods of Kisakürek et al (2011). At the start of culturing, each foraminifer's long axis diameter was measured via inverted light microscopy at the IUI, Eilat. At the end of the experiment, the long axis diameter of each dead or gametogenic foraminifer was measured again. Each foraminifer was then cleaned via three consecutive washes of 18MΩ MilliQ water, labelled, and air-dried on a micro-palaeontological slide. Foraminifera were then transported back to Jerusalem, where the shell mass of individuals with sufficient mass was measured using a Kahn microbalance with a precision of ±0.1µg. Alkalinity drift is negligible from the start to the end of the experiment because calcification of a single or pair of foraminifera in a 120ml culture jar is insufficient to change the Total Alkalinity of the solution (Evans et al., 2016a).

Using the size and mass data for foraminifera from the end of the experiments, it is possible to plot size-mass relationships for both species. **Figure 5.1** compares the size-mass relationships from this experiment with well-constrained size-mass relationships published in Kisakürek et al. (2011). At first glance, data from this experiment seems to fit the published size-mass relationships very well. ROUT statistical analysis quantifies how well the measured data fit the published size-mass relationships. Q (the maximum desired false discovery rate)

was set to 0.1% to identify whether the measured weights were classed as outliers compared to the published data (Motulsky and Brown, 2006). This analysis, the details summarised in **Table 5.3**, returned 0 outliers for either species, which supports using the published size-mass relationships to back-calculate shell initial mass data for the foraminifera in this experiment from the measured long axis diameter data. The relationships from Kisakürek et al. (2011) for *G. ruber* of $m = 0.00008*D^{1.95}$ ($R^2 = 0.89$) and for *G. siphonifera* of $m = 0.93*e^{(0.0055*D)}$ ($R^2 = 0.83$), where m = shell mass and D = shell diameter, are therefore used to calculate mass of foraminifera. The change in shell mass can reliably constrain calcification during the experiment for gametogenic individuals. This is because, after gametogenesis, the foraminifera have no vestige of organic matter remaining attached to their calcite shell due to the expulsion of cellular material and calcite spines during the production of gametes.

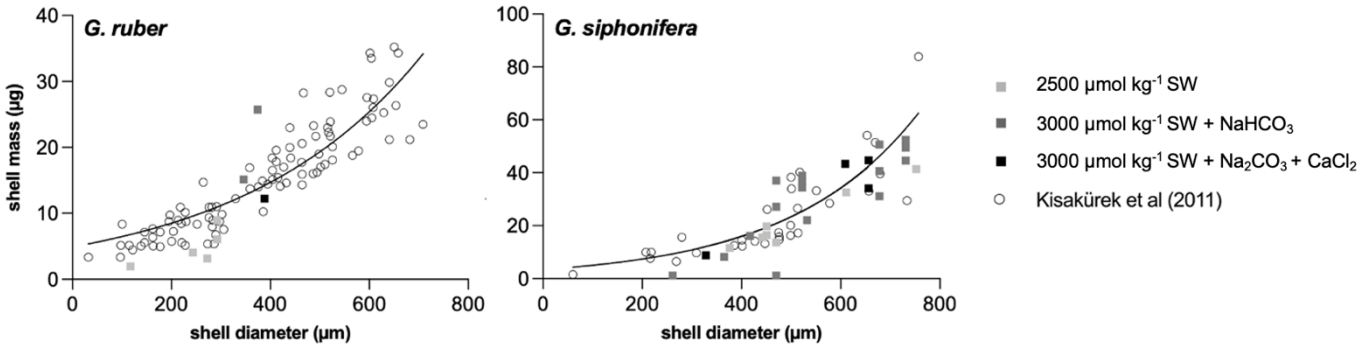

Figure 5.1: Size-mass relationship data for *G. ruber* and *G. siphonifera* from this experiment (solid points) alongside published size-mass relationships from Kisakürek et al (2011). The relationships plotted from Kisakürek et al. (2011) are for *G. ruber* cultured in 2006 and *G. siphonifera* cultured in 2007.

Species	Q (%)	#y values analysed	Outliers identified
G. ruber	0.1	104	0
G. siphonifera	0.1	58	0

Table 5.3: A summary of the ROUT analysis performed in GraphPad Prism 9 of outliers in the size-mass relationship from this experiment compared to published data from Kisakürek et al. (2011).

5.2.4 Compilation of prior data

Due to the presence of unicellular ciliates during culturing, the shell sizes of foraminifera in our OAE treatments were not as large as we had hoped (see **Table 5.4**). It is also difficult to obtain statistically significant relationships from the small number of successful individuals. To

complement our culturing study carried out in Eilat, 2019, we compiled prior data on calcification, lifespan, and where possible, the gametogenic success rate for the species *G. bulloides*, *G. ruber*, *G. sacculifer* and *O. universa*, in carbonate chemistry conditions comparable to the OAE treatments we examined during our Eilat 2019 culturing study.

Species	Treatment	Mortality rate (%)	Gametogenesis rate (%)	#individuals successfully cultured
G. ruber	2461 µmol kg^{-1} SW (control)	31	69	11
	2926 µmol kg^{-1} SW + $NaHCO_3$	13	88	7
	3393 µmol kg^{-1} SW + $NaHCO_3$	31	69	9
	2941 µmol kg^{-1} SW + Na_2CO_3 + $CaCl_2$	10	90	9
	3355 µmol kg^{-1} SW + Na_2CO_3 + $CaCl_2$	50	50	4
G. siphonifera	2461 µmol kg^{-1} SW (control)	47	53	8
	2926 µmol kg^{-1} SW + $NaHCO_3$	5	95	20
	2941 µmol kg^{-1} SW + Na_2CO_3 + $CaCl_2$	17	83	10

Table 5.4: Summary of the mortality and gametogenesis rate of foraminifera for each experimental treatment after exclusion of the unicellular ciliate-attributed deaths from the dataset. SW = Sea Water. As in **Table 5.2**, all individual foraminifera that were observed to be healthy and feeding, but that were taken out of culturing jars at the end of the experiment on 07/12/2019 before naturally undergoing gametogenesis, are included in the count of individuals which underwent gametogenesis. Number of individuals successfully cultured in each OAE treatment is also shown.

Calcification rates for *G. bulloides* (culturing season and location: Santa Catalina Island, California, 2008), *G. ruber* (Catalina 2008), *G. sacculifer* (Puerto Rico 2010) and *O. universa* (Catalina 2008) were previously published by Allen et al. (2016). The total amount of calcite added over the experiment ($\Delta_{shell\ mass}$) was then calculated for each foraminifer using the calcification rate and the corresponding number of days in culture (i.e. lifespan in culture). Lifespan is the same as defined in our Eilat 2019 culturing study (see **Section 5.3.2**).

Lifespan data for *G. bulloides* (Catalina 2008), *G. ruber* (Puerto Rico 2010), *G. sacculifer* (Puerto Rico 2010) and *O. universa* (Catalina 2008) was supplied for this study by K. Allen, who provided unpublished culture log data for the culturing seasons and locations listed. Additional lifespan data for *O. universa* (Catalina 2014) was supplied for this study by K. Holland, who provided unpublished culture log data for that season.

Gametogenic success rate was only calculable for *O. universa* in Catalina, 2014, digitised from culture logs supplied by K. Holland.

Manipulations to change TA/DIC in these prior culturing studies used $NaHCO_3$ (Allen et al., 2016; Holland et al., 2020), representing similar conditions to Pathway 1 in our Eilat 2019 experiments. Only data that exhibited the same trends as in our study, i.e., increasing CO_3^{2-} with increasing TA, were selected for and are presented in this study to ensure that all examined responses are relevant to predicted OAE scenarios. See **Figure 5.2** for the relationship between TA and CO_3^{2-} for all culturing conditions examined in this study.

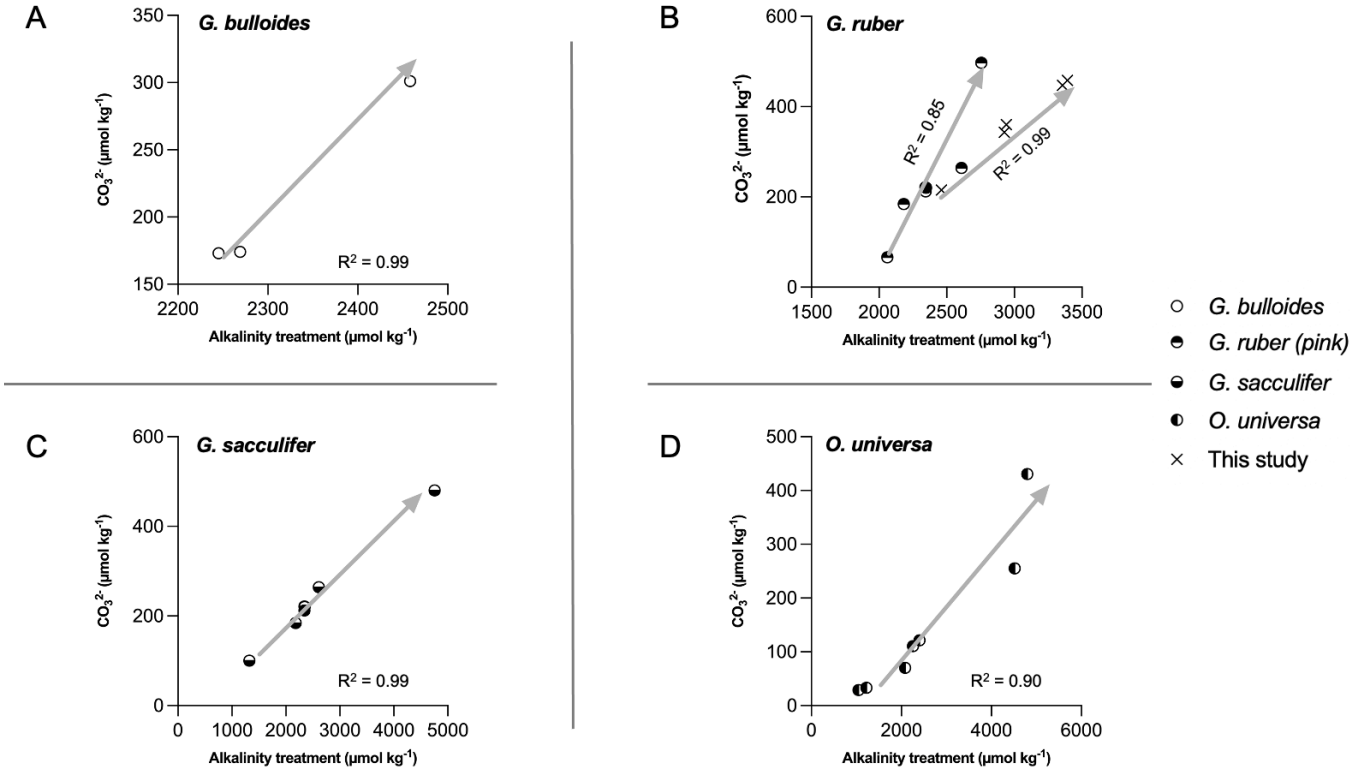

Figure 5.2: Relationship between TA and CO_3^{2-} in all culturing conditions examined from prior work, including "This study" = Eilat 2019. Simple linear regression was performed to illustrate the strength of the co-variance of CO_3^{2-} with TA for these culturing conditions that are relevant to OAE scenarios. Panel (A) shows relationship for *G. bulloides*, panel (B) shows relationship for *G. ruber*, panel (C) shows data for *G. sacculifer* and panel (D) shows data for *O. universa*.

5.3 Results

Here we present results of the cultured planktonic foraminifera to enhanced alkalinity treatments, shown in the context of increasing CO_3^{2-} and pH with increasing Total Alkalinity, as outlined in the Introduction and shown in **Table 5.1**.

5.3.1 Gametogenesis rate

Gametogenesis is the end of an individual foraminifer's life cycle. It is a form of sexual reproduction. During this process, the cytoplasm of a foraminifer divides into thousands of gametes expelled from the calcite test and released into the surrounding seawater column. These then combine to create juvenile foraminifera (Kucera, 2007). There is evidence that this process is synchronised with the lunar cycle (Bijma et al., 1990; Schiebel et al., 1997; Erez et al., 1991). However, planktonic foraminifera have never produced juveniles in culture, despite undergoing gametogenesis, which is observed by cytoplasm expulsion accompanied by the sinking of the calcite test to the bottom of the culturing jar. It is essential to constrain reproductive success. It is a vital aspect of the foraminiferal response to enhanced alkalinity conditions because it will have knock-on effects on the ecology of the surface ocean and the propagation of foraminiferal populations.

As is illustrated in **Table 5.2**, during this experiment, there was an unusual incidence of unicellular ciliates, resulting in elevated mortality rates around twice as high as would usually be expected (Henehan et al., 2013). However, if we exclude individuals associated with unicellular ciliates, we can accurately compare rates of gametogenesis (vs mortality rates) between species and enhanced alkalinity treatments (see **Table 5.4**). For reference, the number of individuals successfully cultured in each OAE treatment is also shown in **Table 5.4**. **Figure 5.3** shows comparisons between the gametogenesis rate (i.e., the percentage of individuals undergoing successful gametogenesis) for different OAE treatments and the two different species cultured in this experiment. Across all panels in **Figure 5.3**, it is clear that both species exhibit higher rates of gametogenic success than in control treatments at [CO_3^{2-}] ~340-360 μmol kg^{-1} in both Pathway 1 and Pathway 2 (TA = ~3000 μmol kg^{-1} in both these

treatments). Rates of gametogenic success for *G. ruber* are 19% higher for Pathway 1 (**Figure 5.3**, **Panel A**) and 21% higher for Pathway 2 (**Figure 5.3**, **Panel B**), relative to the control. For *G. siphonifera*, compared to the control, rates of gametogenesis are 42% and 30% higher for Pathway 1 (**Figure 5.3**, **Panel C**) and Pathway 2 (**Figure 5.3**, **Panel D**), respectively. For *G. siphonifera*, no experiments were run at ~3500 µmol kg^{-1}. However, these experiments were run for *G. ruber*, which, contrasting with the ~3000 µmol kg^{-1} treatments, show either no change or a negative impact on gametogenic success at [CO_3^{2-}] > ~450-460 µmol kg^{-1}. In Pathway 1, there is no impact on gametogenic success, with a 0% change (**Figure 5.3**, **Panel A**). In Pathway 2, there is a 19% reduction in the number of individuals successfully going through gametogenesis (**Figure 5.3**, **Panel B**). This hints at an optimum level of TA increase,

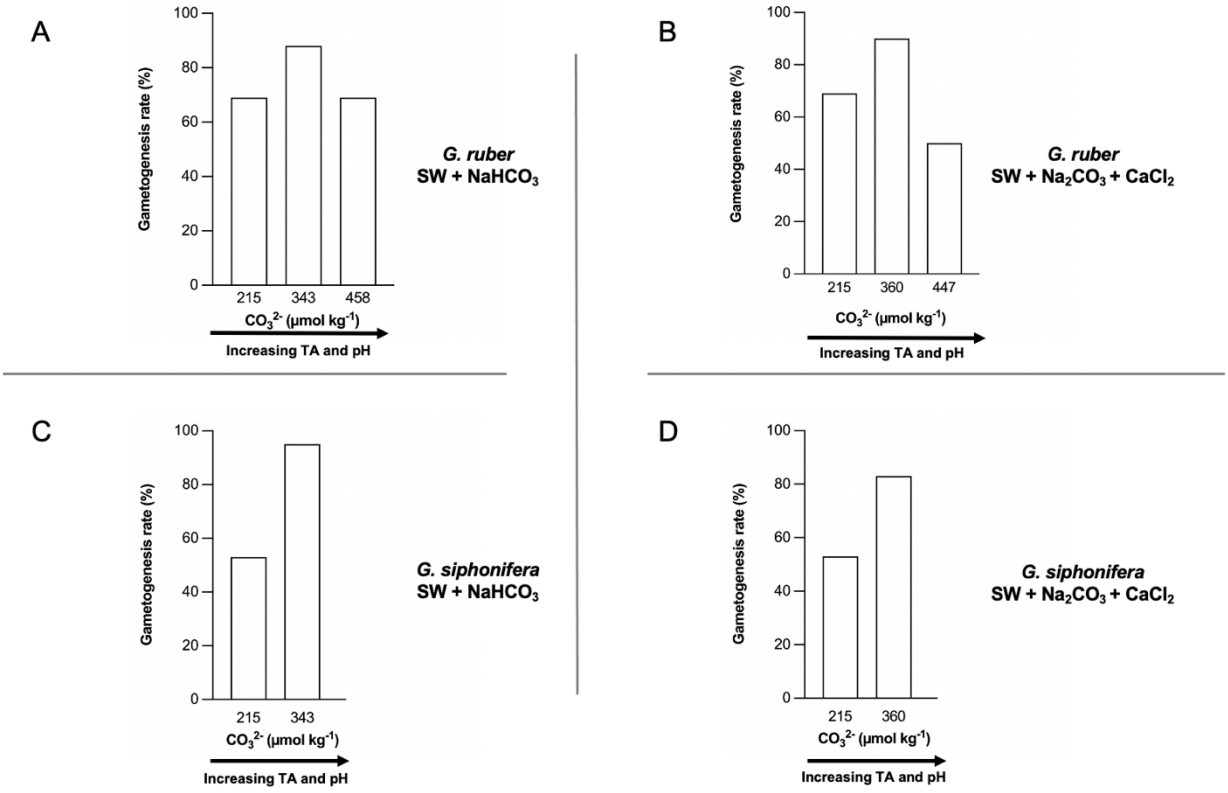

Figure 5.3: Rate of gametogenic success for different alkalinity treatments compared between species, with any deaths attributed to unicellular ciliates excluded from the dataset. Uses data from **Table 5.4**. Panel (A) shows *G. ruber* response to OAE treatments under Pathway 1 (SW + $NaHCO_3$). Panel (B) shows *G. ruber* response to OAE treatments under Pathway 2 (SW + Na_2CO_3 +$CaCl_2$). Panel (C) shows *G. siphonifera* response to OAE treatments under Pathway 1 (SW + $NaHCO_3$). Panel (D) shows *G. siphonifera* response to OAE treatments under Pathway 2 (SW + Na_2CO_3 +$CaCl_2$). Arrow shows direction of Total Alkalinity increase.

and therefore concurrent [CO_3^{2-}] increase, for *G. ruber* in terms of their likely reproductive success in OAE scenarios.

The indication of a possible optimum for TA/ CO_3^{2-} increase is also shown in **Figure 5.4**, which shows the gametogenic success rate for *O. universa* with increasing CO_3^{2-}/increasing TA and pH from compiled literature data (K. Holland, unpub.). Overall, the gametogenesis rates are higher than for our Eilat 2019 study, but this is not surprising. As explained, the incidence of unicellular ciliates has affected the mortality and gametogenesis rates for the Eilat 2019 culturing results. At lower concentrations of CO_3^{2-}, there appears to be a slightly higher chance of a lower gametogenesis rate, although this is not as strong as shown in the Eilat 2019 culturing results (**Figure 5.4**).

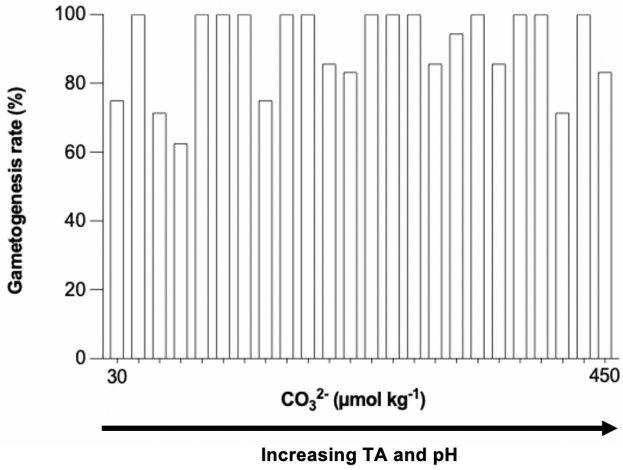

Figure 5.4: Gametogenic success rate of *O. universa* calculated from unpublished data supplied by K. Holland from a culturing season in Catalina, 2014. Arrow shows direction of Total Alkalinity increase.

5.3.2 Lifespan in culture

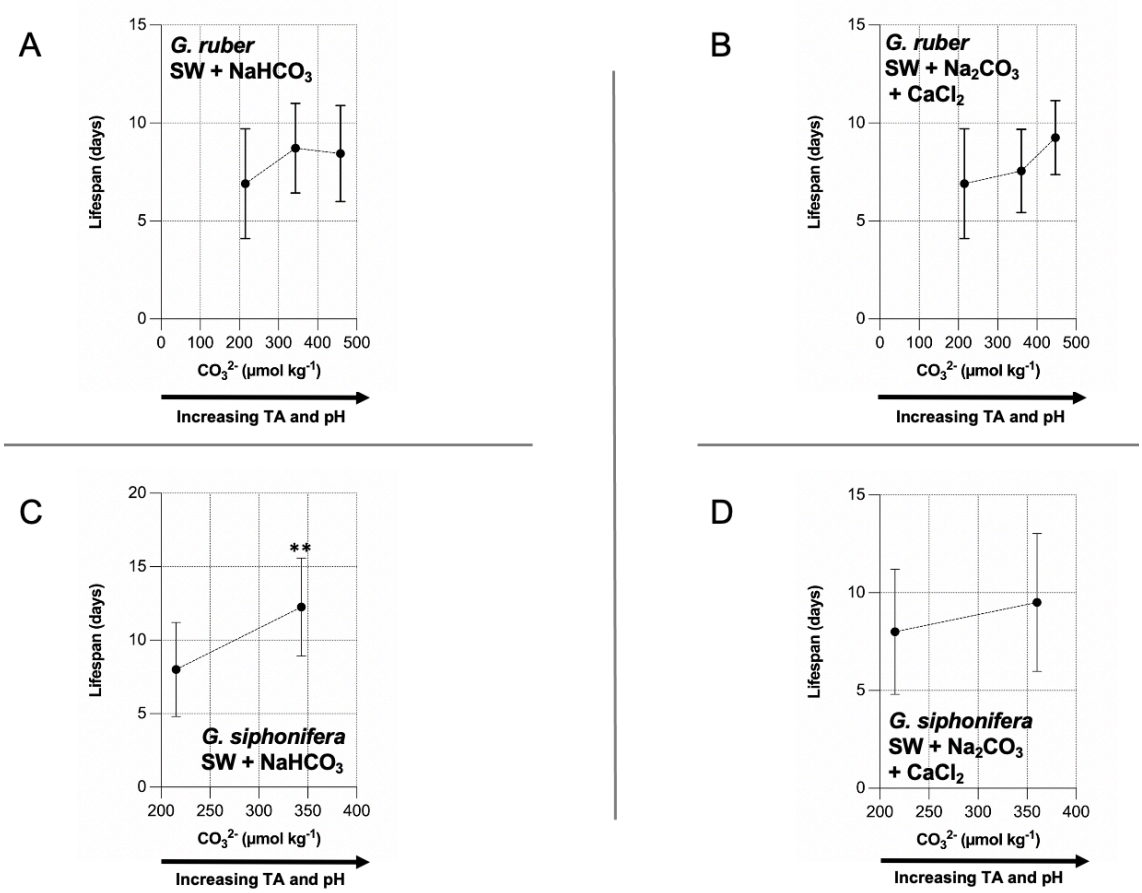

Figure 5.5: Lifespan of foraminifera, i.e., time between collection from the ocean and observation of gametogenesis in the culturing jar. Error is presented as 1 Standard Deviation. Unpaired t-tests with Welch's correction accounting for unequal Standard Deviations were performed on all data. Significant differences are denoted by asterisks above the two datasets in question, where ** $P \leq 0.01$. Graphs created, and statistical analyses performed, in GraphPad Prism 9. Panel (A) shows *G. ruber* response to OAE treatments under Pathway 1 (SW + $NaHCO_3$). Panel (B) shows *G. ruber* response to OAE treatments under Pathway 2 (SW + Na_2CO_3 +$CaCl_2$). Panel (C) shows *G. siphonifera* response to OAE treatments under Pathway 1 (SW + $NaHCO_3$). Panel (D) shows *G. siphonifera* response to OAE treatments under Pathway 2 (SW + Na_2CO_3 +$CaCl_2$). Arrow shows direction of Total Alkalinity increase.

In addition to the gametogenic success rate, we report the average lifespan of the foraminifera in response to enhanced alkalinity treatments (see **Figure 5.5**). The lifespan is measured from the day on which an individual foraminifer was collected from the water column to the day on which that same foraminifer was (i) observed to have undergone gametogenesis, (ii) in the case of healthy individuals still alive at the end of the experiment on 07/12/2019, observed to be long displaying spines and symbionts, indicating that gametogenesis was imminent. It is technically impossible to guarantee that they were all at precisely the same stage of life when

picked for culturing, even when meticulously selecting small, juvenile foraminifera. We present averaged lifespan data for each treatment, so this effect is minimised. We tried to mitigate further the impact of variable age at picking using the fact that foraminifera grow in size as they progress through their life cycle. We considered that a normalisation based on the initial size of individual foraminifera might be appropriate for this lifespan data. However, in **Appendix 3.1**, we present the results of this normalisation and why it is not suitable for this dataset. Therefore, raw averaged lifespan data are presented here.

Across all panels in **Figure 5.5**, we can see that for both OAE treatments raising [CO_3^{2-}] to ~340-360 µmol kg^{-1} in both Pathway 1 and Pathway 2, for both *G. ruber* and *G. siphonifera*, it appears that lifespan is increased compared to control seawater ([CO_3^{2-}] ~215 µmol kg^{-1}). However, only one treatment exhibits a statistically significant difference from the control, which is *G. siphonifera* in Pathway 1, [CO_3^{2-}] ~343 µmol kg^{-1} ($P < 0.01$), where foraminifera live on average four days longer in the enhanced alkalinity treatment relative to the control (**Figure 5.5**, **Panel C**). This difference coincides with the increased likelihood of gametogenic success observed in **Figure 5.3**. *G. ruber* exhibits an increase in lifespan of ~2 days compared to control for Pathway 1 (**Figure 5.5**, **Panel A**) and Pathway 2 (**Figure 5.5**, **Panel B**) at [CO_3^{2-}] ~340-360 µmol kg^{-1}. There is only an increase in lifespan relative to control conditions of ~1.5 days on average for *G. ruber* in Pathway 1 [CO_3^{2-}] = 458 µmol kg^{-1} (TA = 3393 µmol kg^{-1}) (**Figure 5.5**, **Panel A**). This trend is not observed with the corresponding level of OAE Pathway 2 treatment for *G. ruber*, [CO_3^{2-} = 447 µmol kg^{-1}] with a 2.5-day average increase in lifespan compared to the control (**Figure 5.5**, **Panel B**). However, it is important to note that none of the changes other than the one identified in **Figure 5.5** by ** qualify as a significant statistical difference between population groups. Therefore, while there are observable impacts on lifespan in **Figure 5.5**, there is no evidence of a significant effect of the OAE treatments on *G. ruber* lifespan. Testing for statistical significance of the Eilat 2019 culturing data was carried out using unpaired t-tests with Welch's correction accounting for unequal Standard Deviations were performed on these data in GraphPad Prism 9.

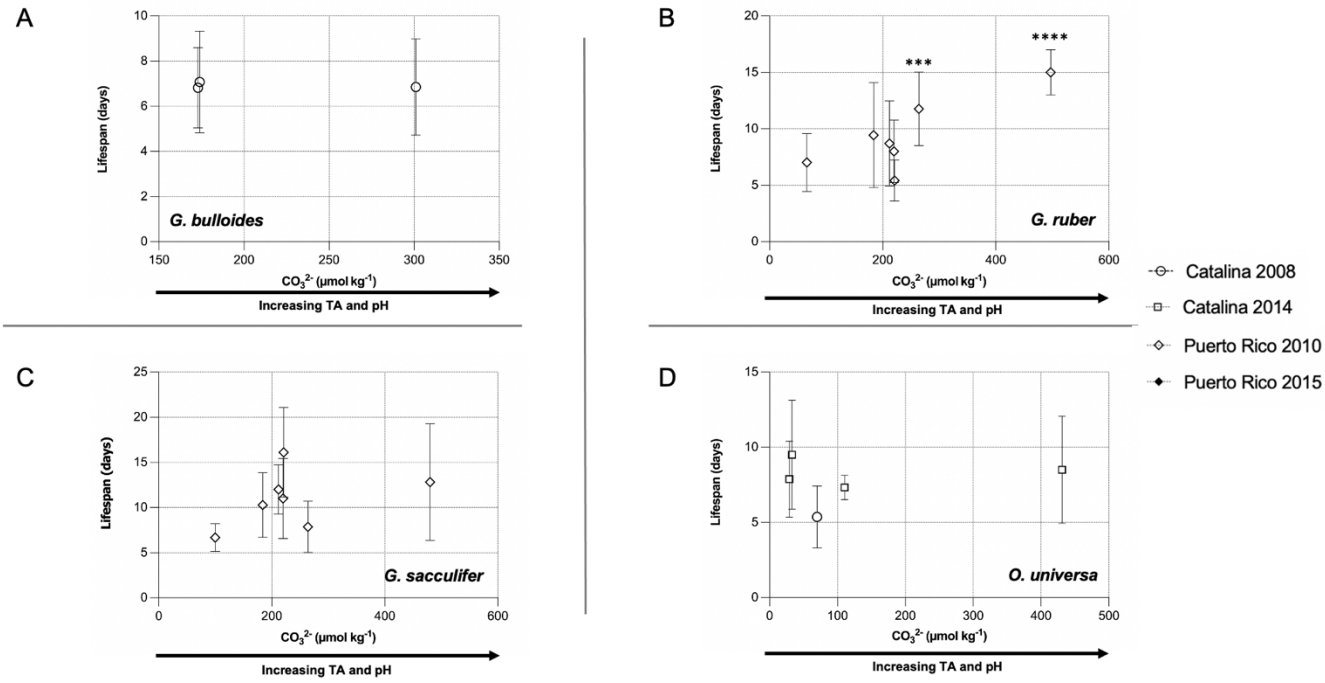

Figure 5.6: Lifespan data from unpublished culture log data compiled for this study from K. Holland and K. Allen. See **5.2 Methods** for full details. Graphs created, and statistical analyses performed, in GraphPad Prism 9. * = P ≤ 0.05, ** = P ≤ 0.01, *** = P ≤ 0.001, **** = P ≤ 0.0001. Panel (A) shows *G. bulloides.* Panel (B) shows *G. ruber*. Panel (C) shows *G. sacculifer.* Panel (D) shows *O. universa*. Arrow shows direction of Total Alkalinity increase.

However, the observation of potential increased lifespan for *G. ruber* with increasing TA/[CO_3^{2-}] in Eilat 2019 is supported by the compiled literature data for *G. ruber* from Puerto Rico 2010 (**Figure 5.6, panel B**; K. Allen, unpub.). There is a statistically significant difference between an average lifespan of ~7 days (+/- 2.6) at [CO_3^{2-}] = 66 µmol kg^{-1} and (i) an average lifespan of ~12 days (+/- 3.2) at [CO_3^{2-}] = 264 µmol kg^{-1} and (ii) an average lifespan of ~15 days (+/- 2.0) at [CO_3^{2-}] = 497 µmol kg^{-1}. For the three other species shown in **Figure 5.6**, *G. bulloides*, *G. sacculifer* and *O. universa*, there are no statistically significant differences in lifespan with changing TA/[CO_3^{2-}]. For full results of statistical testing for compiled literature data, see **Appendix 3**.

5.3.3 Calcification

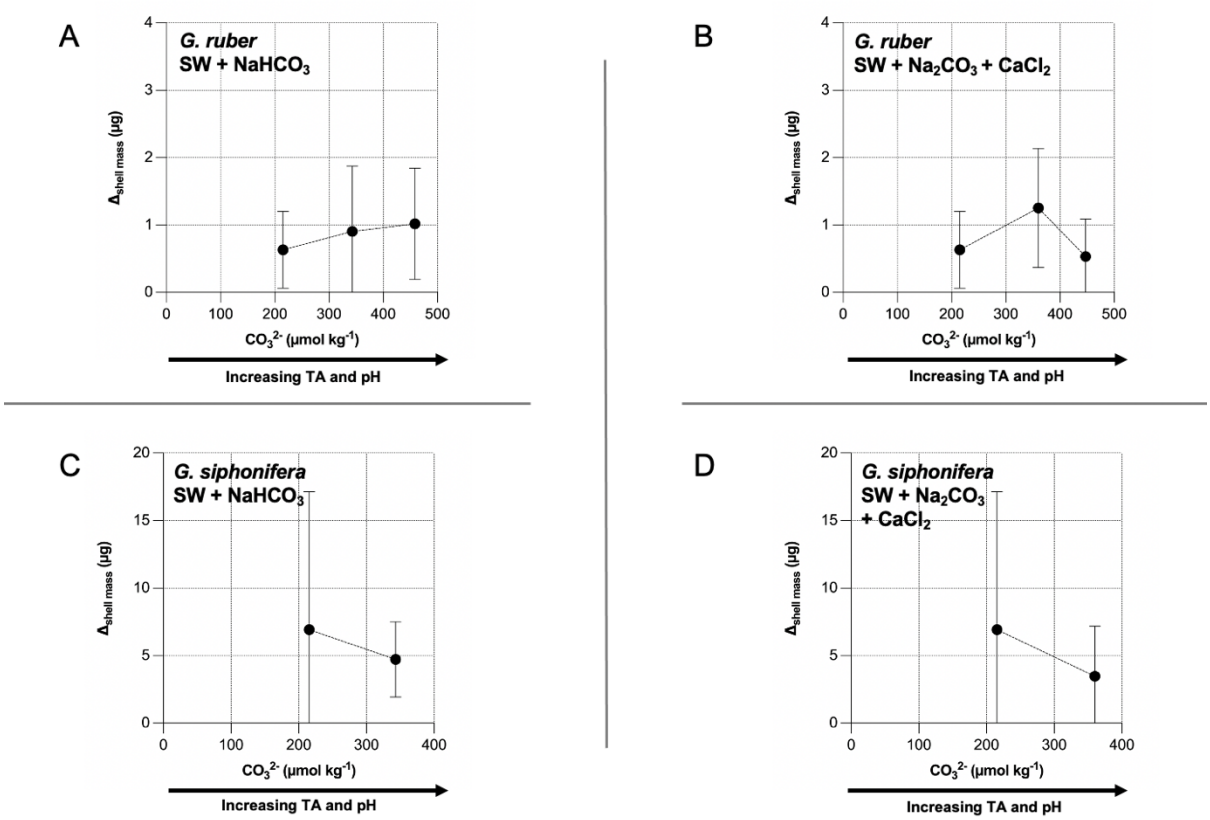

Figure 5.7: Calcification of foraminifera presented as shell mass added over the course of the experiment ($\Delta_{shell\ mass}$). Graphs created, and statistical analysis performed, in GraphPad Prism 9. Panel (A) shows *G. ruber* response to OAE treatments under Pathway 1 (SW + $NaHCO_3$). Panel (B) shows *G. ruber* response to OAE treatments under Pathway 2 (SW + Na_2CO_3 +$CaCl_2$). Panel (C) shows *G. siphonifera* response to OAE treatments under Pathway 1 (SW + $NaHCO_3$). Panel (D) shows *G. siphonifera* response to OAE treatments under Pathway 2 (SW + Na_2CO_3 +$CaCl_2$). Arrow shows direction of Total Alkalinity increase.

To compare calcification response data between *G. ruber* and *G. siphonifera* for different alkalinity treatments, post-experimental long-axis diameter data have been transformed to shell mass data as explained in **Section 5.2.3**. The change in shell mass over the experiment ($\Delta_{shell\ mass}$) is used to provide information on how much each foraminifer has calcified (see **Figure 5.7**).

Unpaired t-tests with Welch's correction accounting for unequal Standard Deviations were performed on these data in GraphPad Prism 9. None of these were deemed significant differences in $\Delta_{shell\ mass}$ between control and enhanced alkalinity treatments due to results

returned by the Welch's t-tests. Therefore, no differences in calcification for either *G. ruber* or *G. siphonifera* with increasing TA/[CO_3^{2-}] were observed for culturing in Eilat, 2019.

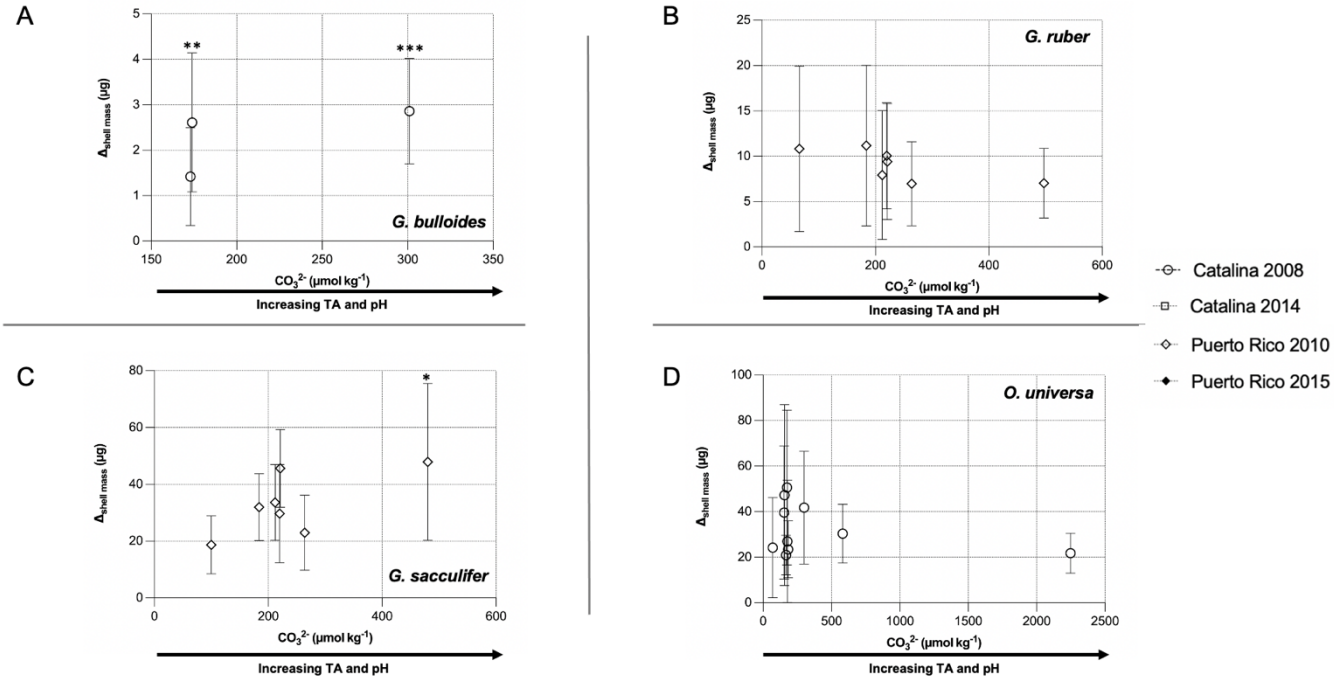

Figure 5.8: Calcification data from Supplementary Material of Allen et al. (2016). See **5.2 Methods** for full details. Graphs created, and statistical analyses performed, in GraphPad Prism 9. * = P ≤ 0.05, ** = P ≤ 0.01, *** = P ≤ 0.001, **** = P ≤ 0.0001. Panel (A) shows *G. bulloides.* Panel (B) shows *G. ruber*. Panel (C) shows *G. sacculifer.* Panel (D) shows *O. universa*. Arrow shows direction of Total Alkalinity increase.

Overall, the same trend of no statistically significant differences with changing TA/[CO_3^{2-}] is observed in compiled calcification data from prior culturing studies (**Figure 5.8**). There is much noise in the data, leading to many overlapping error bars. This is the case for *G. ruber* (**Figure 5.8, Panel B**), *G. sacculifer* (**Figure 5.8, Panel C**), and *O. universa* (**Figure 5.8, Panel D**). There is a statistically significant increase for calcification in *G. bulloides* at [CO_3^{2-}] = 301 µmol kg^{-1} compared to (i) [CO_3^{2-}] = 173 µmol kg^{-1} and (i) [CO_3^{2-}] = 174 µmol kg^{-1} (**Figure 5.8, Panel A**). However, because the error bars overlap so much for [CO_3^{2-}] = 173 µmol kg^{-1} and [CO_3^{2-}] = 174 µmol kg^{-1}, this is likely due to chance. For full results of statistical testing for compiled literature data, see **Appendix 3**.

5.4 Discussion

The differences in *G. ruber* and *G. siphonifera* (Eilat, 2019) response to OAE treatments using Pathway 1 compared to Pathway 2 are negligible. In many cases, the responses to the two pathways are the same at the same level of alkalinity addition. Therefore, our study shows that adding Ca^{2+} compared to Na^{+} as the alkalinity-enhancing material does not significantly affect planktonic foraminifera response to OAE.

This study has examined data trends in lifespan and calcification with increasing TA/[CO_3^{2-}], but these are for minimal observed changes in physiological parameters. It is evident from the vast body of prior work on experiments using filtered seawater only (Bé et al., 1981; Bé et al., 1977; Caron et al., 1982; Caron et al., 1987) that it is normal to see a high level of individual variation in experiments with planktonic foraminifera. It is possible that most of the trends and group differences in our study, particularly for the small-scale culturing completed in Eilat (2019), fall within the range of natural variability seen in past experiments under constant conditions and normal seawater. It is clear from the results that the carbonate system perturbations resulting from the OAE treatments evoke some responses in lifespan and calcification from planktonic foraminifera. However, these are difficult to distinguish above the noise of natural variation in the populations and the sparsity of foraminifera that successfully underwent gametogenesis in the Eilat (2019) study.

Considering the calcification results on their own, there is no significant impact of the OAE treatments on planktonic foraminifera calcification, which has positive ramifications for greenhouse gas removal, i.e., minimal risk of CO_2 production via calcification that would counteract CO_2 drawdown by OAE. Arguably, it could be expected that increased availability of CO_3^{2-} as alkalinity increases would lead to an increase in planktonic foraminifera calcification because of their mode of calcification being highly dependent on the direct supply of ions to the calcification site via seawater vacuolisation (de Nooijer et al., 2009; de Nooijer et al., 2014; Bentov et al., 2009; Kisakürek et al., 2011; Marchitto et al., 2018). However, as explained, even if there were increases in calcification with increasing TA/[CO_3^{2-}], these might

have to be very large to overprint the great natural spread of calcification of individual foraminifera, which causes enough noise to hide responses. We can surmise from our study that lifespan in culture and calcification parameters in planktonic foraminifera are affected by much noise, and therefore do not constitute particularly robust indicators of planktonic foraminifera response to OAE.

By contrast, the gametogenic success rate appears to yield more robust and meaningful results in the context of response to OAE. Unlike calcification or lifespan data, the gametogenic success rate is a discrete, binary indicator (either a foraminifer is successful in gametogenesis, or it is not) of the likely ecological success of planktonic foraminifera to OAE. Therefore, it is not subject to the same risk of "noise" as lifespan or calcification data. The rate of gametogenesis for *G. ruber* (Eilat, 2019) and *O. universa* (Catalina, 2014) appears to indicate an "optimum" for the reproductive success of planktonic foraminifera as TA (and therefore CO_3^{2-}, the physiological driver for foraminifera) is altered. At moderate levels of OAE ([CO_3^{2-}] ~350 µmol kg^{-1}, TA ~3000 µmol kg^{-1}), *G. ruber* (Eilat, 2019), *G. siphonifera* (Eilat, 2019) and *O. universa* (Catalina, 2014) all exhibit an increased likelihood of gametogenic success. At [CO_3^{2-}] above ~350 µmol kg^{-1}, *G. ruber* and *O. universa* show a decreased percentage of individuals undergoing successful gametogenesis. We suggest that perhaps the gametogenesis rate (essentially a measure of reproductive success) may be the most useful metric for assessing the response of planktonic foraminifera to OAE from culture experiments due to (i) its lower susceptibility to noise than other individual physiological parameters and (ii) its ability to highlight population changes in foraminifera that can be used to deduce their response to OAE schemes. For example, if a population of foraminifera exhibit increased likelihood of gametogenic success during OAE at TA ~ 3000 µmol kg^{-1}, as we do in our experiments, this indicates that their population size will gradually increase over time. Projections about calcification could then be made based on population-level statistics rather than individual calcification measurements. If population were to increase, then population levels of calcification could be expected to increase, too. The best way to assess the

population response of planktonic foraminifera to OAE would be using a mesoscale field study of the pelagic ecosystem, where the contribution of planktonic foraminifera to pelagic calcification could be placed into the context of the ecosystem niche within which they reside.

G. ruber and *G. siphonifera* are both globally abundant, tropical-temperate water species, *G. bulloides* is a temperate water species decreasing in abundance towards tropical and equatorial regions, *O. universa* spans a biogeographic range from equatorial to subpolar, and *G. sacculifer* is highly abundant in tropical water masses (Kennett and Srinivasan, 1983; Aze et al., 2011). Therefore, the results of our study are fully applicable to planktonic foraminifera more widely across the globe. However, further work with larger sample sizes of planktonic foraminifera is required to confirm these results and safely and reliably extrapolate planktonic foraminifera responses to OAE chemistries across the entire global ocean. It is also worth noting that the Gulf of Eilat is a higher alkalinity region of the ocean than the average values for the global surface ocean (Lazar et al., 2008). Therefore, repeating our small-scale culturing study in other ocean areas is critical to discover whether similar responses of foraminifera that are adapted to slightly lower alkalinities are recorded.

5.5 Conclusions

This small-scale culturing study (Eilat, 2019) and accompanying data compilation from prior work offers, to our knowledge, the first examination of the response of five species of planktonic foraminifera (*G. ruber*, *G. siphonifera*, *G. bulloides*, *G. sacculifer* and *O. universa*) to the carbonate system conditions specific to OAE and relevant for mCDR. We have shown that adding Ca^{2+} instead of Na^{+} as the alkalinity-enhancing ion does not significantly impact gametogenesis, lifespan or calcification in the planktonic foraminifera *G. ruber* and *G. siphonifera*. This indicates that Ca^{2+} added in the levels expected for OAE will not have significant physiological impacts on planktonic foraminifera. Any responses observed are more likely due to changes in carbonate system parameters, such as CO_3^{2-}, which act as direct physiological drivers. Lifespan and calcification data for all species of planktonic foraminifera, both in our small-scale culturing study of *G. ruber* and *G. siphonifera* (Eilat, 2019) and data

compilation of prior work on *G. bulloides*, *G. ruber*, *G. sacculifer* and *O. universa*, indicate that these parameters are subject to a high degree of individual variation, which makes them challenging to draw meaningful conclusions from. We conclude that the gametogenic success rate may be the most robust and meaningful way to assess the response of planktonic foraminifera to OAE, with a suggestion of increased success at TA ~ 3000 μmol kg^{-1}, and would be best evaluated in mesoscale field experiments that can place the planktonic foraminifera in a whole-ecosystem context.

References

Allen, K.A., Hönisch, B., Eggins, S.M., Haynes, L.L., Rosenthal, Y., Yu, J., 2016. Trace element proxies for surface ocean conditions: A synthesis of culture calibrations with planktic foraminifera. Geochimica et Cosmochimica Acta 193, 197–221. https://doi.org/10.1016/j.gca.2016.08.015

Aze, T., Ezard, T.H.G., Purvis, A., Coxall, H.K., Stewart, D.R.M., Wade, B.S., Pearson, P.N., 2011. A phylogeny of Cenozoic macroperforate planktonic foraminifera from fossil data. Biological Reviews 86, 900–927. https://doi.org/10.1111/j.1469-185X.2011.00178.x

Bach, L.T., Gill, S.J., Rickaby, R.E.M., Gore, S., Renforth, P., 2019. CO_2 Removal With Enhanced Weathering and Ocean Alkalinity Enhancement: Potential Risks and Co-benefits for Marine Pelagic Ecosystems. Frontiers in Climate. 1. https://doi.org/10.3389/fclim.2019.00007

Bé, A.W.H., Caron, D.A., Anderson, O.R., 1981. Effects of feeding frequency on life processes of the planktonic foraminifer *Globigerinoides sacculifer* in laboratory culture. Journal of the Marine Biological Association of the United Kingdom 61, 257–277. https://doi.org/10.1017/S002531540004604X

Bé, A.W.H., Hemleben, C., Anderson, O.R., Spindler, M., Hacunda, J., Tuntivate-Choy, S., 1977. Laboratory and Field Observations of Living Planktonic Foraminifera. Micropaleontology 23, 155–179. https://doi.org/10.2307/1485330

Bentov, S., Brownlee, C., Erez, J., 2009. The role of seawater endocytosis in the biomineralization process in calcareous foraminifera. PNAS 106, 21500–21504. https://doi.org/10.1073/pnas.0906636106

Bijma, J., Faber, W., Hemleben, C., 1990. Temperature and salinity limits for growth and survival of some planktonic foraminifers in laboratory cultures. The Journal of Foraminiferal Research 20, 95–116. https://doi.org/10.2113/gsjfr.20.2.95

Bijma, J., Spero, H.J., Lea, D.W., 1999. Reassessing foraminiferal stable isotope geochemistry: Impact of the oceanic carbonate system (experimental results) In: Fischer, G., Wefer, G. (eds) Use of Proxies in Paleoceanography. Springer, Berlin, Heidelberg. https://doi.org/10.1007/978-3-642-58646-0_20

Caron, D.A., Bé, A.W.H., Anderson, O.R., 1982. Effects of variations in light intensity on life processes of the planktonic foraminifer *Globigerinoides sacculifer* in laboratory culture. Journal of the Marine Biological Association of the United Kingdom 62, 435–451. https://doi.org/10.1017/S0025315400057374

Caron, D.A., Faber, W.W., Bé, A.W.H., 1987. Effects of temperature and salinity on the growth and survival of the planktonic foraminifer *Globigerinoides sacculifer*. Journal of the Marine Biological Association of the United Kingdom 67, 323–341. https://doi.org/10.1017/S0025315400026643

de Nooijer, L.J., Spero, H.J., Erez, J., Bijma, J., Reichart, G.J., 2014. Biomineralization in perforate foraminifera. Earth-Science Reviews 135, 48–58. https://doi.org/10.1016/j.earscirev.2014.03.013

de Nooijer, L.J., Toyofuku, T., Kitazato, H., 2009. Foraminifera promote calcification by elevating their intracellular pH. PNAS 106, 15374–15378. https://doi.org/10.1073/pnas.0904306106

Erez, J., Almogi-Labin, A., Avraham, S., 1991. On the Life History of Planktonic Foraminifera: Lunar Reproduction Cycle in *Globigerinoides Sacculifer (Brady)*. Paleoceanography 6, 295–306. https://doi.org/10.1029/90PA02731

Erez, J., Luz, B., 1983. Experimental paleotemperature equation for planktonic foraminifera. Geochimica et Cosmochimica Acta 47, 1025–1031. https://doi.org/10.1016/0016-7037(83)90232-6

Evans, D., Brierley, C., Raymo, M.E., Erez, J., Müller, W., 2016a. Planktic foraminifera shell chemistry response to seawater chemistry: Pliocene–Pleistocene seawater Mg/Ca, temperature and sea level change. Earth and Planetary Science Letters 438, 139–148. https://doi.org/10.1016/j.epsl.2016.01.013

Evans, D., Müller, W., Erez, J., 2018. Assessing foraminifera biomineralisation models through trace element data of cultures under variable seawater chemistry. Geochimica et Cosmochimica Acta, Chemistry of oceans past and present: A Special Issue in tribute to Harry Elderfield 236, 198–217. https://doi.org/10.1016/j.gca.2018.02.048

Evans, D., Wade, B., Henehan, M., Erez, J., Müller, W., 2016b. Revisiting carbonate chemistry controls on planktic foraminifera Mg/Ca: Implications for sea surface temperature and hydrology shifts over the Paleocene-Eocene Thermal Maximum and Eocene-Oligocene Transition. Climate of the Past 12, 819–835. https://doi.org/10.5194/cp-12-819-2016

Fox, L., Stukins, S., Hill, T., Miller, C.G., 2020. Quantifying the Effect of Anthropogenic Climate Change on Calcifying Plankton. Scientific Reports 10, 1–9. https://doi.org/10.1038/s41598-020-58501-w

Fuss, S., Canadell, J.G., Peters, G.P., Tavoni, M., Andrew, R.M., Ciais, P., Jackson, R.B., Jones, C.D., Kraxner, F., Nakicenovic, N., Quéré, C.L., Raupach, M.R., Sharifi, A., Smith, P., Yamagata, Y., 2014. Betting on negative emissions. Nature Climate Change 4, 850–853. https://doi.org/10.1038/nclimate2392

Gastrich, M.D., 1987. Ultrastructure of a New Intracellular Symbiotic Alga Found Within Planktonic Foraminifera. Journal of Phycology 23, 623–632. https://doi.org/10.1111/j.1529-8817.1987.tb04215.x

GESAMP, 2019. “High level review of a wide range of proposed marine geoengineering techniques”. (Boyd, P.W. and Vivian, C.M.G., eds.). (IMO/FAO/UNESCO-IOC/UNIDO/WMO/IAEA/UN/UN Environment/ UNDP/ISA Joint Group of Experts on the Scientific Aspects of Marine Environmental Protection). Rep. Stud. GESAMP No. 98, 144 p.

Hemleben, C., Spindler, M., Anderson, O.R., 1989. Modern planktonic foraminifera. Springer-Verlag.

Henderson, G., Rickaby, R., Bouman, H., 2008. Decreasing Atmosphere CO_2 By Increasing Ocean Alkalinity, The Ocean Dimension: Would The Concept Work And What Would Be The Environmental Consequences?

Henehan, M.J., Foster, G.L., Rae, J.W.B., Prentice, K.C., Erez, J., Bostock, H.C., Marshall, B.J., Wilson, P.A., 2015. Evaluating the utility of B/Ca ratios in planktic foraminifera as a proxy for the carbonate system: A case study of *Globigerinoides ruber*. Geochemistry, Geophysics, Geosystems 16, 1052–1069. https://doi.org/10.1002/2014GC005514

Henehan, M.J., Rae, J.W.B., Foster, G.L., Erez, J., Prentice, K.C., Kucera, M., Bostock, H.C., Martínez-Botí, M.A., Milton, J.A., Wilson, P.A., Marshall, B.J., Elliott, T., 2013. Calibration of the boron isotope proxy in the planktonic foraminifera *Globigerinoides ruber* for use in palaeo-CO_2 reconstruction. Earth and Planetary Science Letters 364, 111–122. https://doi.org/10.1016/j.epsl.2012.12.029

Holland, K., Branson, O., Haynes, L.L., Hönisch, B., Allen, K.A., Russell, A.D., Fehrenbacher, J.S., Spero, H.J., Eggins, S.M., 2020. Constraining multiple controls on planktic foraminifera Mg/Ca. Geochimica et Cosmochimica Acta 273, 116–136. https://doi.org/10.1016/j.gca.2020.01.015

IPCC, 2018: Summary for Policymakers, In: Global Warming of 1.5°C. An IPCC Special Report on the impacts of global warming of 1.5°C above pre-industrial levels and related global greenhouse gas emission pathways, in the context of strengthening the global response to the threat of climate change, sustainable development, and efforts to eradicate poverty [Masson-Delmotte, V., P. Zhai, H.-O. Pörtner, D. Roberts, J. Skea, P.R. Shukla, A. Pirani, W. Moufouma-Okia, C. Péan, R. Pidcock, S. Connors, J.B.R. Matthews, Y. Chen, X. Zhou, M.I. Gomis, E. Lonnoy, T. Maycock, M. Tignor, and T. Waterfield (eds.)].

Kennett, J.P., Srinivasan, M.S., 1983. Neogene Planktonic Foraminifera: A Phylogenetic Atlas. Hutchinson Ross.

Kısakürek, B., Eisenhauer, A., Böhm, F., Garbe-Schönberg, D., Erez, J., 2008. Controls on shell Mg/Ca and Sr/Ca in cultured planktonic foraminiferan, *Globigerinoides ruber (white)*. Earth and Planetary Science Letters 273, 260–269. https://doi.org/10.1016/j.epsl.2008.06.026

Kısakürek, B., Eisenhauer, A., Böhm, F., Hathorne, E.C., Erez, J., 2011. Controls on calcium isotope fractionation in cultured planktic foraminifera, *Globigerinoides ruber* and *Globigerinella siphonifera*. Geochimica et Cosmochimica Acta 75, 427–443. https://doi.org/10.1016/j.gca.2010.10.015

Kucera, M., 2007. Chapter Six Planktonic Foraminifera as Tracers of Past Oceanic Environments. Developments in Marine Geology Volume 1, 213–262. https://doi.org/10.1016/S1572-5480(07)01011-1

Lazar, B., Erez, J., Silverman, J., T, R., A, R., M, D., Meeder, E., Iluz, D., 2008. Recent environmental changes in the chemical-biological oceanography of the Gulf of Aqaba (Eilat). In: Aqaba-Eilat, the Improbable Gulf - Environment, Biodiversity and Preservation, pp. 49–61.

Lischka, S., Stange, P., Riebesell, U., 2018. Response of Pelagic Calcifiers (Foraminifera, Thecosomata) to Ocean Acidification During Oligotrophic and Simulated Up-Welling Conditions in the Subtropical North Atlantic Off Gran Canaria. Frontiers in Marine Science 5. https://doi.org/10.3389/fmars.2018.00379

Lombard, F., da Rocha, R.E., Bijma, J., Gattuso, J.-P., 2010. Effect of carbonate ion concentration and irradiance on calcification in planktonic foraminifera. Biogeosciences 7, 247–255. https://doi.org/10.5194/bg-7-247-2010

Lombard, F., Erez, J., Michel, E., Labeyrie, L., 2009. Temperature effect on respiration and photosynthesis of the symbiont-bearing planktonic foraminifera *Globigerinoides ruber*, *Orbulina universa*, and *Globigerinella siphonifera*. Limnology and Oceanography 54, 210–218. https://doi.org/10.4319/lo.2009.54.1.0210

Marchitto, T.M., Bryan, S.P., Doss, W., McCulloch, M.T., Montagna, P., 2018. A simple biomineralization model to explain Li, Mg, and Sr incorporation into aragonitic foraminifera and corals. Earth and Planetary Science Letters 481, 20–29. https://doi.org/10.1016/j.epsl.2017.10.022

Monteiro, F.M., Bach, L.T., Brownlee, C., Bown, P., Rickaby, R.E.M., Poulton, A.J., Tyrrell, T., Beaufort, L., Dutkiewicz, S., Gibbs, S., Gutowska, M.A., Lee, R., Riebesell, U., Young, J., Ridgwell, A., 2016. Why marine phytoplankton calcify. Science Advances 2, e1501822. https://doi.org/10.1126/sciadv.1501822

Morard, R., Garet-Delmas, M.-J., Mahé, F., Romac, S., Poulain, J., Kucera, M., de Vargas, C., 2018. Surface ocean metabarcoding confirms limited diversity in planktonic foraminifera but reveals unknown hyper-abundant lineages. Scientific Reports 8, 2539. https://doi.org/10.1038/s41598-018-20833-z

Motulsky, H.J., Brown, R.E., 2006. Detecting outliers when fitting data with nonlinear regression - a new method based on robust nonlinear regression and the false discovery rate. BMC Bioinformatics 7, 123. https://doi.org/10.1186/1471-2105-7-123

Osborne, E.B., Thunell, R.C., Marshall, B.J., Holm, J.A., Tappa, E.J., Benitez-Nelson, C., Cai, W.-J., Chen, B., 2016. Calcification of the planktonic foraminifera *Globigerina bulloides* and carbonate ion concentration: Results from the Santa Barbara Basin. Paleoceanography 31, 1083–1102. https://doi.org/10.1002/2016PA002933

Prazeres, M., Uthicke, S., Pandolfi, J.M., 2015. Ocean acidification induces biochemical and morphological changes in the calcification process of large benthic foraminifera. Proceedings of the Royal Society B: Biological Sciences 282, 20142782. https://doi.org/10.1098/rspb.2014.2782

Renforth, P., Henderson, G., 2017. Assessing ocean alkalinity for carbon sequestration. Reviews of Geophysics 55, 636–674. https://doi.org/10.1002/2016RG000533

Russell, A.D., Hönisch, B., Spero, H.J., Lea, D.W., 2004. Effects of seawater carbonate ion concentration and temperature on shell U, Mg, and Sr in cultured planktonic foraminifera. Geochimica et Cosmochimica Acta 68, 4347–4361. https://doi.org/10.1016/j.gca.2004.03.013

Schiebel, R., 2002. Planktic foraminiferal sedimentation and the marine calcite budget. Global Biogeochemical Cycles 16, 3–1. https://doi.org/10.1029/2001GB001459

Schiebel, R., Bijma, J., Hemleben, C., 1997. Population dynamics of the planktic foraminifer Globigerina bulloides from the eastern North Atlantic. Deep Sea Research Part I: Oceanographic Research Papers 44, 1701–1713. https://doi.org/10.1016/S0967-0637(97)00036-8

Shaked, Y., Genin, A., 2006. The Israel National Monitoring Program in the Northern Gulf of Aqaba, Science report for year 2004 p. 133.

Spero, H.J., Bijma, J., Lea, D.W., Bemis, B.E., 1997. Effect of seawater carbonate concentration on foraminiferal carbon and oxygen isotopes. Nature 390, 497–500. https://doi.org/10.1038/37333

Uthicke, S., Momigliano, P., Fabricius, K.E., 2013. High risk of extinction of benthic foraminifera in this century due to ocean acidification. Scientific Reports 3, 1–5. https://doi.org/10.1038/srep01769

Statement of Authorship for joint/multi-authored papers for PGR thesis

To appear at the end of each thesis chapter submitted as an article/paper

The statement shall describe the candidate's and co-authors' independent research contributions in the thesis publications. For each publication there should exist a complete statement that is to be filled out and signed by the candidate and supervisor **(only required where there isn't already a statement of contribution within the paper itself).**

Title of Paper	**Chapter 5:** The response of planktonic foraminifera to enhanced ocean alkalinity - a conceptual study for marine Carbon Dioxide Removal
Publication Status	Unpublished and unsubmitted work written in a manuscript style.
Publication Details	

Student Confirmation

Student Name:	Sophie Gill (SG)		
Contribution to the Paper	SG designed experiments with input from RR, JE and GH. SG conducted all experimental work in Eilat (2019). SG analysed all data from Eilat (2019) and compiled from literature studies. IA compiled data from literature studies and culture logs provided by KA, KH, OB, LH, and SE. SG wrote the chapter. RR, JE and BH provided comments on the chapter that SG used to redraft before thesis submission.		
Signature 		Date	03/01/2022

Supervisor Confirmation

By signing the Statement of Authorship, you are certifying that the candidate made a substantial contribution to the publication, and that the description described above is accurate.

Supervisor name and title: Prof. Rosalind Rickaby		
Supervisor comments: Sophie has stated the authorship clearly above.		
Signature 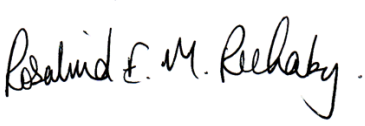	Date	03/01/2022

This completed form should be included in the thesis, at the end of the relevant chapter.

Chapter 6: Discussion and conclusions

6.1 Summary of research chapters

The main findings of this thesis are summarised by research chapter below.

Chapter 2: Meta-analysis of Ocean Carbon Dioxide Removal literature: major focus areas for research identified using elimination criteria

→ Overall, the field of marine Carbon Dioxide Removal (mCDR) research is incredibly nascent in terms of peer-reviewed, published literature.

→ There are six key "elimination" criteria that must be met for any given mCDR approach to be implemented. These can be used to assess the relative advancement of different mCDR approaches.

→ Most mCDR literature focuses on Ocean Iron Fertilisation (OIF). Still, much research into OIF is inconclusive as to whether it could be successfully used at scale as an mCDR technique. We can build on how OIF research has been carried out to drive mCDR research in a timely manner to contribute meaningfully to international climate goals.

→ Alkalinity Enhancement (including Enhanced Weathering (EW), Ocean Alkalinity Enhancement (OAE) and electrochemical approaches) is the most researched mCDR technique, excluding OIF. It has good potential as an mCDR technique due to its co-benefits and relative advancement compared to other mCDR methods.

→ Critical knowledge gaps according to the "elimination" criteria that would significantly advance the mCDR field forward, in particular for Alkalinity Enhancement, include:

1. Completion of field trials, pilot studies and demonstration projects
2. Assessment of governance/finance/social aspects of mCDR
3. Accurate quantification of CO_2 drawdown/CDR potential.

Chapter 3: The growth and calcification response of the coccolithophores *Emiliania huxleyi* and *Coccolithus braarudii* to the Carbon Dioxide Removal technique of Ocean Alkalinity Enhancement

→ The addition of alkalinity using Ca^{2+} compared to Na^{+} does not result in significant differences in coccolithophore growth or calcification response.

→ Cellular calcification rates and quota of *E. huxleyi* (i) do not change in air-equilibrated OAE scenarios and (ii) increase in non-equilibrated OAE scenarios. By contrast, *C. braarudii* calcification rates and quota decrease in air-equilibrated OAE scenarios.

→ The risk of "CO_2 leakage" from coccolithophores re-releasing CO_2 drawn down through OAE is dependent on (i) equilibration conditions and (ii) coccolithophore species.

→ The changes in calcification in these major groups of coccolithophores that we have observed could have major knock-on impacts for global carbon cycling through the role that calcite formation plays in ballasting organic matter to the deep ocean.

→ *E. huxleyi* is fertilised by the increased supply of HCO_3^- during OAE to facilitate growth both in CO_2-replete (air-equilibrated OAE) and CO_2-limited (non-equilibrated OAE) conditions. This was not observed in *C. braarudii*, supporting theories that suggest the coccolithophore genii *Coccolithus and Reticulofenestra* do not have the same cellular carbon utilisation mechanisms, acting in a "static" and an "opportunistic" way respectively.

→ Increased growth of *E. huxleyi* driven by increased HCO_3^- availability resulting from OAE could increase population net calcification, even if cellular calcification is relatively unaffected.

Chapter 4: Changing Redfield ratio of the coccolithophores *Emiliania huxleyi* and *Coccolithus braarudii* in response to Ocean Alkalinity Enhancement: a potential positive feedback for CO_2 drawdown?

→ CO_2-limitation during OAE suppresses *E. huxleyi* growth rate (observed in **Chapter 3**), and this causes *E. huxleyi* to have a higher N:P in CO_2-limited conditions than CO_2-

replete conditions. Redfield ratio (C:N:P) of *E. huxleyi* appears to be primarily driven by changes in growth rate, so as it is likely that growth rate changes as a result of OAE (**Chapter 3**), the C:N:P of *E. huxleyi* will likely shift during OAE.

→ By contrast, growth rate does not appear to drive C:P and N:P partitioning in *C. braarudii*.

→ C:N of *E. huxleyi* and *C. braarudii* in air-equilibrated OAE conditions did not change. This is the key parameter which indicates whether increased POC formation would drive a positive feedback on CO_2 drawdown during OAE, and in air-equilibrated scenarios likely would not operate.

→ However, there is a hint in our data that under non-equilibrated scenarios of OAE, C:N of *E. huxleyi* could increase, implying that additional POC formation may be possible as a positive feedback mechanism on CO_2 drawdown during OAE, which warrants further study.

Chapter 5: The response of planktonic foraminifera to enhanced ocean alkalinity - a conceptual study for marine Carbon Dioxide Removal

→ The addition of alkalinity using Ca^{2+} compared to Na^{+} does not result in significant differences in planktonic foraminifera response to enhanced ocean alkalinity.

→ In our small-scale culturing study in Eilat (2019) and compiled data from unpublished culture logs provided by collaborators, lifespan in culture and calcification data for planktonic foraminifera are subject to a high degree of individual variation, which makes them unsuitable for quantifying response to OAE schemes.

→ The gametogenic success rate may provide a more robust way to assess the response of planktonic foraminifera to OAE schemes, particularly if this were used in mesocosm experiments where a whole-ecosystem approach can be taken.

→ We found that there may be an “optimum” level of alkalinity for gametogenic success at TA ~ 3000 µmol kg^{-1}, observed in *G. siphonifera*, *G. ruber* and *O. universa*, which is likely physiologically driven by [CO_3^{2-}] and/or pH.

6.2 Wider implications of thesis findings

Perhaps the central finding of this thesis is that the possibility of "CO_2 leakage" from CO_2 re-release from calcification as a result of OAE has been assessed for two key "endmember" species of coccolithophore and five key species of planktonic foraminifera and shown to be overall minimal. As found in **Chapter 2**, accurate assessment of CDR potential (including quantification of any CO_2-leakage from calcification responses to CDR) is a critical knowledge gap, which this thesis has addressed.

In Bach et al. (2019), we hypothesised that under air-equilibrated (constant $[CO_2]$/pCO_2) OAE scenarios, pelagic calcification would likely increase because of higher pH and $[HCO_3^-]$. For all species of planktonic foraminifera examined in **Chapter 5**, we found that calcification ($\Delta_{shell\ mass}$) did not significantly change relative to control values. As a caveat, we found that this may be due to difficulties in obtaining good-quality data for change in shell mass for foraminifera. In coccolithophores, the calcification response to air-equilibrated OAE was species-specific. *E. huxleyi* did not significantly change its cellular calcification rate or quota, and *C. braarudii* decreased its cellular calcification rate and quota. We also predicted in Bach et al. (2019) that during non-equilibrated OAE scenarios phytoplankton growth and calcification would likely decrease due to the potential for CO_2-limitation from decreasing $[CO_2]$/pCO_2. In **Chapter 3**, we found that *E. huxleyi* growth did decrease, and cellular calcification rate and quota actually did not decrease relative to CO_2-replete values. Therefore, a wider implication of the outcomes of this thesis is that like many studies of coccolithophore calcification on ocean acidification, responses are likely to be species-specific (Ridgwell et al., 2009). Our data also indicates that a "one-size-fits-all" prediction of calcification responses is not possible.

The observations in **Chapter 3** showing *E. huxleyi* growth responding differently to OAE under CO_2-limited conditions compared to CO_2-replete conditions highlight how remarkably adaptable coccolithophores are. Previous studies have shown that the physiological properties of *E. huxleyi* relate strongly to the carbonate chemistry conditions from which they have been isolated, and therefore adapted to (Rickaby et al., 2016). We have shown that *E.*

huxleyi, unlike *C. braarudii*, is fertilised by an extra supply of HCO_3^- during OAE under CO_2-replete conditions as *E. huxleyi* cells exhibited much-increased growth rates in elevated TA compared to control (**Chapter 3**). *E. huxleyi* also likely used HCO_3^- to sustain growth in CO_2-limited conditions (**Chapter 3**). These observations add to the vast body of knowledge concerning coccolithophore physiology and have implications for understanding the comparative physiology of the *Coccolithus and Reticulofenestra* because these results suggest that *E. huxleyi* and *C. braarudii* do not have the same modes of carbon acquisition. Advancing our understanding of the exact seawater substrate for calcification, and the heterogeneity of the utilisation of carbon for calcification by different species of coccolithophore, will improve our predictive capacity for how coccolithophores will respond to mCDR schemes like OAE.

The observation that *C. braarudii* decreases its cellular calcification rate and quota in response to air-equilibrated OAE could lead to reduced ballasting and decreased organic carbon drawdown. Coccolithophores play a significant role in driving the marine organic carbon pump, ballasting and contributing to marine snow, which removes CO_2 from the atmosphere (Rost and Riebesell, 2004; Honjo et al., 2008). In the modern oceans, the effect of coccolith ballasting on atmospheric CO_2 concentration likely outweighs CO_2 output from calcification (Honjo et al., 2008; Falkowski et al., 2007; De Vargas et al., 2007). If coccolithophore calcification decreases, then less CO_2 will be output from calcification, at the same time as reduced ballasting drawing down less CO_2 from the atmosphere. Therefore, depending on the scale of this ballasting feedback, the net effect may not be significant, or it could fundamentally shift the balance of CO_2 drawdown through ballasting and CO_2 output through calcification.

The finding that coccolithophores change their C:N:P in response to OAE also potentially has wide-ranging impacts. The amount of atmospheric carbon dioxide removal by the oceans is very sensitive to the stoichiometric relationship between phytoplankton and nutrients (Arrigo, 2005). Therefore, evidence of *E. huxleyi* potentially increasing its partitioning of cellular POC relative to PON in response to non-equilibrated OAE may provide a viable pathway for a

positive feedback on CO_2 drawdown during OAE. However, the differences between C:N:P in *E. huxleyi* and *C. braarudii* were somewhat unclear (see **Chapter 4**), so further work to ascertain the elemental stoichiometry of phytoplankton will be required to fully assess the nature and magnitude of the impact of changing C:N:P during OAE on CO_2 drawdown.

Changing C:N:P could also impact the relative success of major phytoplankton functional groups, i.e., calcifiers, silicifiers and nitrogen-fixers. This links into the ideas we presented in Bach et al. (2019), where it was predicted that during EW/OAE scenarios, increased TA and [Ca^{2+}] would benefit calcifiers compared to silicifiers and nitrogen-fixers, meaning their relative abundance would increase (see **Chapter 1** for full details). While the data in this thesis only examines coccolithophores and foraminifera, not all calcifying groups in the pelagic realm, together coccolithophores and foraminifera do comprise the majority of our ocean's calcium carbonate formation (Lebrato et al., 2010; Monteiro et al., 2016; Sarmiento and Gruber, 2006; Tyrrell and Young, 2009; Schiebel, 2002). So, here, the response of calcifiers will be equated to the responses of coccolithophores and foraminifera that have been quantified in this thesis. Some species of planktonic foraminifera increased their reproductive success in response to increased TA, and the coccolithophore *E. huxleyi* increased their growth rate in response to increased TA, whereas the coccolithophore *C. braarudii* did not. Therefore, the hypothesis in Bach et al. (2019) that calcifiers would be favoured by the carbonate chemistry conditions resulting from EW/OAE is true for some calcifiers and not true for others. The laboratory experiments in this thesis do not provide enough data to fully assess whether a shift to a "white(r)" ocean is definitive during EW/OAE – this will have to be evaluated at an ecosystem level during mesocosm and/or mesoscale field trials. However, they suggest that not all calcifiers will respond in the same way to EW/OAE. So even if net community calcification were to stay constant during EW/OAE, the contribution of different calcifying organisms to the calcification budget could shift, which would have fundamental impacts on ecosystems, e.g. change of grazing pressure on coccolithophores.

While this thesis has focused on applying this work to artificial ocean alkalinisation as part of a CDR framework, the research is also applicable to the natural Earth system response to global warming. While most forecasts for future CO_2 uptake by the ocean assume that alkalinity will stay constant over this century (Orr et al., 2005), there may be biological feedbacks that might increase the alkalinity of the surface ocean on human-relevant (and international climate goals-relevant) timescales of this century (Egleston et al., 2010). These could include a reduction in biogenic calcification (observed in coccolithophores in **Chapter 3** of this thesis) or enhanced calcite dissolution in the marine environment. Over geological timescales, increased mineral weathering will occur in response to global warming (Derry, 2009; Berner, 1991; Berner et al., 1983; Walker et al., 1981), and this will increase inputs of alkalinity to the ocean from the terrestrial environment. So the outcomes of this thesis can inform approaches towards artificial alkalinisation as a CDR technique and can be used as a predictor of how biota will respond to conditions that will occur post-ocean acidification as part of the Earth's natural thermostatic processes. Alkalinity enhancement in the geological past may provide a useful analogue for this modern-day situation, in future studies that consider ocean-level processes. The Cretaceous period was characterised by elevated TA, DIC, pH and Ca^{2+}; (Müller, 2019); (Taylor et al., 2017), with HCO_3^- concentrations of between 1.5-2.5mM (Wallmann, 2001), and reasonable upper values for alkalinity in Cretaceous seawater of up to 10mM (Lee and Morse, 2010). These occur in coincidence with a major proliferation of coccolithophores (De Vargas et al., 2007; Stanley et al., 2005; Hönisch et al., 2012), which could plausibly have been driven in part by alkalinity conditions at the time.

6.3 Future work on mCDR and the response of biota

One major limitation of the work in **Chapter 3** is the inadequacy (large error; often ±50-60% of the measured value) of the PIC:POC data collected for *E. huxleyi* and *C. braarudii*. PIC:POC is a key response parameter collected in most major studies of coccolithophore physiology, as a ratio of calcification (PIC) relative to autotrophic productivity (POC) (Findlay et al., 2011; Zondervan et al., 2002; Balch et al., 2018). It directly elucidates the interaction between

organic carbon fixation and inorganic calcium carbonate production (i.e. the carbon export ratio) allowing more nuanced conclusions about the overall carbon drawdown balance between inorganic and organic carbon. It is a shame not to have had access to good quality data for this parameter during this research project. Future studies should prioritise PIC:POC as a key physiological parameter to constrain.

Additionally, it would be interesting to constrain the response of more species and strains of coccolithophore to OAE in laboratory experiments. Do all strains of the same species behave in the same way? From the outcomes of this thesis, it appears that responses to OAE, much like with the vast body of work on biotic responses to ocean acidification (Bach et al., 2011; Riebesell et al., 2007; Riebesell et al., 2000; Iglesias-Rodriguez et al., 2008; Andersson et al., 2008; Beaufort et al., 2011), are species- and taxa-specific. However, does this hold when work on more species has been completed? This thesis examines the response of only one species (*E. huxleyi*) to both CO_2-replete and CO_2-limited conditions in conjunction with OAE treatments. One experiment with *C. braarudii* under CO_2-limited conditions (see **Appendix 4**) was completed to complement the CO_2-replete conditions presented in **Chapter 3**. However, the carbonate chemistry conditions during culturing could not be fully explained and therefore the data could not be interpreted robustly (see **Appendix 4** for full details). As with any hypothesis, a theory can only be fully proven once experiments with multiple species and strains have been completed (Müller, 2019).

Laboratory experiments examining concurrent changes in Mg/Ca ratio and other metals/contaminants (e.g. Fe, Ni – see **Chapter 1**) were beyond the timeframe and scope of this thesis. Depending on the materials and methods proposed for OAE schemes, incorporating these scenario-relevant elements into enhanced TA experiments with calcifiers will be interesting to examine. It would seem prudent for the materials used to enhance alkalinity in laboratory experiments to be decided based on which materials are most likely to be used in real-world scenarios. For example, Gore (2021) examined the response of the

macroalga *Corallina spp.* to olivine, and Guo et al. (2022) examined the response of multiple species of phytoplankton to Ni, a key component of olivine.

The experimental work in this thesis has provided evidence that has implications for large-scale biogeochemical and ecosystem-level research questions. However, to fully quantify answers to these questions, a full biogeochemical and/or ecosystem level has to be taken. For example, our laboratory experiments were conducted under nutrient-replete conditions, and at some point in the natural environment, calcification response to OAE will be limited by lack of available nutrients. Incorporation of the experimental evidence this thesis has collected into biogeochemical/ecosystem/earth system models will be essential to assess:

- Net CO_2 drawdown of OAE. Only computer models of the appropriate complexity (e.g. Earth System Models like UVic, shown in **Figure 6.1** (Kvale et al., 2015) will accurately incorporate the interactions with the atmosphere, ocean circulation and abiotic processes to fully establish the net effect of carbon drawdown through organic and inorganic processes
- How the impact of decreased coccolithophore calcification may impact on ballasting to deeper ocean layers
- Longer timescales of biotic response to OAE
- Relevant regional areas where the efficacy of OAE may be highest depending on local carbonate chemistry conditions
- The broader impact of altered Redfield ratio on biogeochemical cycling.

The experimental work in this thesis does not cover two major critical knowledge gaps identified in **Chapter 2** for mCDR studies. Governance, legal and social implications of OAE were beyond the scope of this thesis. Completing studies with mesocosms and/or field trials was also beyond the timeframe and scope of this thesis – repeating the experiments run in the laboratory in these settings would be another thesis in itself. However, the results of this thesis support the notion that due to the pressing nature of the climate crisis, and as identified

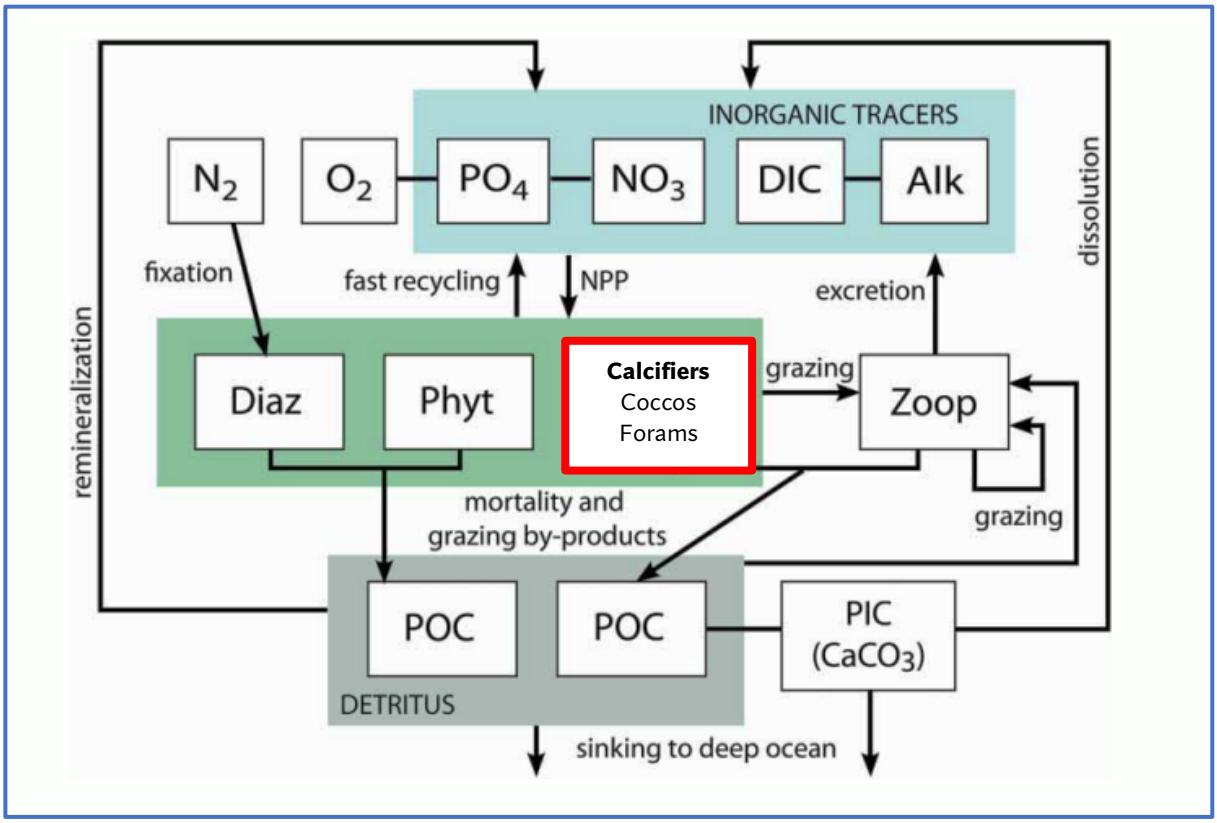

Figure 6.1: UVic ESCM model, original diagram from Kvale et al. (2015). Coccos = coccolithophores, Forams = foraminifera.

in **Chapter 2**, we need to be assessing the feasibility of mCDR studies at a much quicker pace than we currently are. Globally, we are already experiencing some of the predicted extreme impacts of climate change (IPCC, 2019; IPCC AR5, 2014; IPCC et al., 2021; IPCC, 2018: Summary for Policymakers; Kapsenberg and Cyronak, 2019) and there are well-established deadlines of the 2030s (as outlined in the **Introduction**) by which to achieve meaningful climate action within 1.5 °C or 2 °C of warming over pre-industrial temperatures. Due to these time constraints, it would seem that the most efficient way to assess whether proposed mCDR schemes can contribute meaningfully to reducing levels of CO_2 in our atmosphere would be to bypass the time-consuming single-species laboratory experiments completed in this thesis and move straight to the large-scale ecosystem-level assessment of pelagic calcifier growth and calcification response in rigorously assessed and regulated mesocosm and/or mesoscale field trials. These kinds of trials would allow a full evaluation of net community calcification in response to OAE, incorporating all major groups of plankton and corals, if the study site(s)

were carefully chosen. They would also provide the necessary evidence to assess whether a shift to a “white(r)” or a “green(er)” ocean is more likely under OAE scenarios, as they would allow an integrated and interactive assessment of how calcifiers, silicifiers and nitrogen-fixers respond to OAE as they function in an ecosystem, rather than isolated responses observed in laboratory studies. These suggestions are also applicable to all other mCDR approaches which may have impacts on the marine pelagic ecosystem, including and not limited to: OIF, artificial upwelling, artificial downwelling, and macroalgal cultivation.

Above all, future work on mCDR approaches should prioritise a robust scientific assessment of the balance between CDR drawdown and any deleterious ecosystem impacts; in a timely manner so that chances to contribute to climate goals using CDR do not pass us by.

6.4 Conclusions

The research outcomes of this thesis have highlighted the great need for quantitative research into marine Carbon Dioxide Removal (mCDR) techniques that provide tangible measures of CDR potential. The experimental work completed in the field and laboratory has provided the first results quantifying coccolithophore and planktonic foraminifera response to the carbonate chemistries specific to the mCDR approach of Ocean Alkalinity Enhancement (OAE). Together, these two groups contribute an overwhelming majority of the total flux of shallow pelagic calcification and calcite export to the deep ocean. This thesis has shown that the calcification of these two major pelagic calcifiers is unlikely to increase during realistic air-equilibrated OAE scenarios, and even in one species of coccolithophore (*C. braarudii*) may decrease. There is evidence that *E. huxleyi* may increase its calcification in non-equilibrated (CO_2-limited) OAE conditions, but non-equilibrated conditions of OAE are likely to be at point-source additions of alkalinity to the surface ocean and thereby short-lived. Responses to OAE, similar to responses to Ocean Acidification, are likely to be species- and taxa-specific. This thesis has shown that coccolithophores alter their elemental (Redfield) ratios in response to OAE scenarios; there is evidence that *E. huxleyi* may increase its cellular fraction of POC compared to PON. Therefore, increased POC formation providing a positive feedback on CO_2

drawdown is possible. This will require further investigation to ascertain whether average pelagic marine organic matter C:N increases. This thesis has shown that the major bloom-forming coccolithophore *E. huxleyi* may be fertilised by the increased availability of HCO_3^- resulting from OAE in air-equilibrated scenarios. In contrast, the same is not true of *C. braarudii*. This has implications for future work on the physiology of the two major extant lineages of coccolithophore in the modern ocean, *Coccolithus and Reticulofenestra*, and supports prior work from other authors suggesting that *E. huxleyi* may be limited by HCO_3^- in the modern ocean. The work of this thesis highlights the importance of examining biotic responses to OAE in a biogeochemical framework. To build on these findings, future work should focus on (i) whether these results are observed in mesocosm experiments and (ii) quantifying net community calcification during an OAE mesocosm experiment.

References

Andersson, A.J., Mackenzie, F.T., Bates, N.R., 2008. Life on the margin: implications of ocean acidification on Mg-calcite, high latitude and cold-water marine calcifiers. Marine Ecology Progress Series 373, 265–273. https://doi.org/10.3354/meps07639

Arrigo, K.R., 2005. Marine microorganisms and global nutrient cycles. Nature 437, 349–355. https://doi.org/10.1038/nature04159

Bach Lennart Thomas, Riebesell Ulf, Schulz Kai Georg, 2011. Distinguishing between the effects of ocean acidification and ocean carbonation in the coccolithophore *Emiliania huxleyi*. Limnology and Oceanography 56, 2040–2050. https://doi.org/10.4319/lo.2011.56.6.2040

Bach, L.T., Gill, S.J., Rickaby, R.E.M., Gore, S., Renforth, P., 2019. CO_2 Removal With Enhanced Weathering and Ocean Alkalinity Enhancement: Potential Risks and Co-benefits for Marine Pelagic Ecosystems. Frontiers in Climate 1. https://doi.org/10.3389/fclim.2019.00007

Balch, W.M., Bowler, B.C., Drapeau, D.T., Lubelczyk, L.C., Lyczkowski, E., 2018. Vertical Distributions of Coccolithophores, PIC, POC, Biogenic Silica, and Chlorophyll-a Throughout the Global Ocean. Global Biogeochemical Cycles 32, 2–17. https://doi.org/10.1002/2016GB005614

Beaufort, L., Probert, I., de Garidel-Thoron, T., Bendif, E.M., Ruiz-Pino, D., Metzl, N., Goyet, C., Buchet, N., Coupel, P., Grelaud, M., Rost, B., Rickaby, R.E.M., de Vargas, C., 2011. Sensitivity of coccolithophores to carbonate chemistry and ocean acidification. Nature 476, 80–83. https://doi.org/10.1038/nature10295

Berner, R.A., 1991. A model for atmospheric CO_2 over Phanerozoic time. American Journal of Science 291, 339–376. https://doi.org/10.2475/ajs.291.4.339

Berner, R.A., Lasaga, A.C., Garrels, R.M., 1983. The carbonate-silicate geochemical cycle and its effect on atmospheric carbon dioxide over the past 100 million years. American Journal of Science 283, 641–683. https://doi.org/10.2475/ajs.283.7.641

De Vargas, C., Aubry, M.-P., Probert, I., Young, J., 2007. Origin and Evolution of Coccolithophores: From Coastal Hunters to Oceanic Farmers, in: Falkowski, P.G., Knoll, A.H. (Eds.), Evolution of Primary Producers in the Sea. Academic Press, Burlington, pp. 251–285. https://doi.org/10.1016/B978-012370518-1/50013-8

Derry, L.A., 2009. Weathering and Climate, in: Gornitz, V. (Ed.), Encyclopedia of Paleoclimatology and Ancient Environments. Springer Netherlands, Dordrecht, pp. 981–986. https://doi.org/10.1007/978-1-4020-4411-3_228

Egleston, E.S., Sabine, C.L., Morel, F.M.M., 2010. Revelle revisited: Buffer factors that quantify the response of ocean chemistry to changes in DIC and alkalinity. Global Biogeochemical Cycles 24, GB1002. https://doi.org/10.1029/2008GB003407

Falkowski, P.G., Knoll, A.H., ProQuest, 2007. Evolution of primary producers in the sea [electronic resource], Ebook central. Elsevier Academic Press, Amsterdam ; Boston.

Findlay, H.S., Calosi, P., Crawfurd, K., 2011. Determinants of the PIC:POC response in the coccolithophore *Emiliania huxleyi* under future ocean acidification scenarios. Limnology and Oceanography 56, 1168–1178. https://doi.org/10.4319/lo.2011.56.3.1168

Gore, S., 2021. Assessing ocean alkalinity for carbon storage. School of Earth and Environmental Sciences, Cardiff University.

Guo, J.A., Strzepek, R., Willis, A., Ferderer, A., Bach, L.T., 2022. Investigating the effect of nickel concentration on phytoplankton growth to inform the assessment of ocean alkalinity enhancement. Biogeosciences Discussions 1–23. https://doi.org/10.5194/bg-2021-312

Hönisch, B., Ridgwell, A., Schmidt, D.N., Thomas, E., Gibbs, S.J., Sluijs, A., Zeebe, R., Kump, L., Martindale, R.C., Greene, S.E., Kiessling, W., Ries, J., Zachos, J.C., Royer, D.L., Barker, S., Marchitto, T.M., Moyer, R., Pelejero, C., Ziveri, P., Foster, G.L., Williams, B., 2012. The Geological Record of Ocean Acidification. Science 335, 1058–1063. https://doi.org/10.1126/science.1208277

Honjo, S., Manganini, S.J., Krishfield, R.A., Francois, R., 2008. Particulate organic carbon fluxes to the ocean interior and factors controlling the biological pump: A synthesis of global sediment trap programs since 1983. Progress in Oceanography 76, 217–285. https://doi.org/10.1016/j.pocean.2007.11.003

Iglesias-Rodriguez, M.D., Halloran, P.R., Rickaby, R.E.M., Hall, I.R., Colmenero-Hidalgo, E., Gittins, J.R., Green, D.R.H., Tyrrell, T., Gibbs, S.J., Dassow, P. von, Rehm, E., Armbrust, E.V., Boessenkool, K.P., 2008. Phytoplankton Calcification in a High-CO_2 World. Science 320, 336–340. https://doi.org/10.1126/science.1154122

IPCC, 2019. IPCC Special Report on Climate Change, Desertification, Land Degradation, Sustainable Land Management, Food Security, and Greenhouse gas fluxes in Terrestrial Ecosystems.

IPCC, 2018: Summary for Policymakers, In: Global Warming of 1.5°C. An IPCC Special Report on the impacts of global warming of 1.5°C above pre-industrial levels and related global greenhouse gas emission pathways, in the context of strengthening the global response to the threat of climate change, sustainable development, and efforts to eradicate poverty [Masson-Delmotte, V., P. Zhai, H.-O. Pörtner, D. Roberts, J. Skea, P.R. Shukla, A. Pirani, W. Moufouma-Okia, C. Péan, R. Pidcock, S. Connors, J.B.R. Matthews, Y. Chen, X. Zhou, M.I. Gomis, E. Lonnoy, T. Maycock, M. Tignor, and T. Waterfield (eds.)].

IPCC AR5, 2014. Fifth Assessment Report - Mitigation of Climate Change [WWW Document]. URL https://www.ipcc.ch/report/ar5/wg3/mindex.shtml (accessed 10.18.17).

IPCC, Masson-Delmotte, V., Zhai, P., Pirani, A., Connors, S.L., Péan, C., Berger, S., Caud, N., Chen, Y., Goldfarb, L., Gomis, M.I., Huang, M., Leitzell, K., Lonnoy, E., Matthews, J.B.R., Maycock, T.K., Waterfield, T., Yelekçi, O., Yu, R., Zhou, B., 2021. Climate Change 2021: The Physical Science Basis. Contribution of Working Group I to the Sixth Assessment Report of the Intergovernmental Panel on Climate Change. Cambridge University Press.

Kapsenberg, L., Cyronak, T., 2019. Ocean acidification refugia in variable environments. Global Change Biology 25, 3201–3214. https://doi.org/10.1111/gcb.14730

Kvale, K.F., Meissner, K.J., Keller, D.P., Eby, M., Schmittner, A., 2015. Explicit Planktic Calcifiers in the University of Victoria Earth System Climate Model, Version 2.9. Atmosphere-Ocean 53, 332–350. https://doi.org/10.1080/07055900.2015.1049112

Lebrato, M., Iglesias-Rodríguez, D., Feely, R.A., Greeley, D., Jones, D.O.B., Suarez-Bosche, N., Lampitt, R.S., Cartes, J.E., Green, D.R.H., Alker, B., 2010. Global contribution of echinoderms to the marine carbon cycle: $CaCO_3$ budget and benthic compartments. Ecological Monographs 80, 441–467. https://doi.org/10.1890/09-0553.1

Lee, J., Morse, J.W., 2010. Influences of alkalinity and pCO_2 on $CaCO_3$ nucleation from estimated Cretaceous composition seawater representative of “calcite seas.” Geology 38, 115–118. https://doi.org/10.1130/G30537.1

Monteiro, F.M., Bach, L.T., Brownlee, C., Bown, P., Rickaby, R.E.M., Poulton, A.J., Tyrrell, T., Beaufort, L., Dutkiewicz, S., Gibbs, S., Gutowska, M.A., Lee, R., Riebesell, U., Young, J., Ridgwell, A., 2016. Why marine phytoplankton calcify. Science Advances 2, e1501822. https://doi.org/10.1126/sciadv.1501822

Müller, M.N., 2019. On the genesis and function of coccolithophore calcification. Frontiers in Marine Science 6. https://doi.org/10.3389/fmars.2019.00049

Orr, J.C., Fabry, V.J., Aumont, O., Bopp, L., Doney, S.C., Feely, R.A., Gnanadesikan, A., Gruber, N., Ishida, A., Joos, F., Key, R.M., Lindsay, K., Maier-Reimer, E., Matear, R., Monfray, P., Mouchet, A., Najjar, R.G., Plattner, G.-K., Rodgers, K.B., Sabine, C.L., Sarmiento, J.L., Schlitzer, R., Slater, R.D., Totterdell, I.J., Weirig, M.-F., Yamanaka, Y., Yool, A., 2005. Anthropogenic ocean acidification over the twenty-first century and its impact on calcifying organisms. Nature 437, 681–686. https://doi.org/10.1038/nature04095

Rickaby, R.E.M., Hermoso, M., Lee, R.B.Y., Rae, B.D., Heureux, A.M.C., Balestreri, C., Chakravarti, L., Schroeder, D.C., Brownlee, C., 2016. Environmental carbonate chemistry selects for phenotype of recently isolated strains of *Emiliania huxleyi*. Deep Sea Research Part II: Topical Studies in Oceanography, Impacts of surface ocean acidification in polar seas and globally: a field-based approach 127, 28–40. https://doi.org/10.1016/j.dsr2.2016.02.010

Ridgwell, A., Schmidt, D.N., Turley, C., Brownlee, C., Maldonado, M.T., Tortell, P., Young, J.R., 2009. From laboratory manipulations to Earth system models: scaling calcification impacts of ocean acidification. Biogeosciences 6, 2611–2623. https://doi.org/10.5194/bg-6-2611-2009

Riebesell, U., Schulz, K.G., Bellerby, R.G.J., Botros, M., Fritsche, P., Meyerhöfer, M., Neill, C., Nondal, G., Oschlies, A., Wohlers, J., Zöllner, E., 2007. Enhanced biological carbon consumption in a high CO_2 ocean. Nature 450, 545–548. https://doi.org/10.1038/nature06267

Riebesell, U., Zondervan, I., Rost, B., Tortell, P.D., Zeebe, R.E., Morel, F.M.M., 2000. Reduced calcification of marine plankton in response to increased atmospheric CO_2. Nature 407, 364–367. https://doi.org/10.1038/35030078

Rost, B., Riebesell, U., 2004. Coccolithophores and the biological pump: responses to environmental changes, in: Thierstein, H.R., Young, J.R. (Eds.), Coccolithophores: From Molecular Processes to Global Impact. Springer, Berlin, Heidelberg, pp. 99–125. https://doi.org/10.1007/978-3-662-06278-4_5

Sarmiento, J.L., Gruber, N., 2006. Ocean biogeochemical dynamics. Princeton University Press, Princeton, N.J. ; Woodstock.

Schiebel, R., 2002. Planktic foraminiferal sedimentation and the marine calcite budget. Global Biogeochemical Cycles 16, 3–1. https://doi.org/10.1029/2001GB001459

Stanley, S.M., Ries, J.B., Hardie, L.A., 2005. Seawater chemistry, coccolithophore population growth, and the origin of Cretaceous chalk. Geology 33, 593–596. https://doi.org/10.1130/G21405.1

Taylor, A.R., Brownlee, C., Wheeler, G., 2017. Coccolithophore Cell Biology: Chalking Up Progress. Ann Rev Mar Sci 9, 283–310. https://doi.org/10.1146/annurev-marine-122414-034032

Tyrrell, T., Young, J.R., 2009. Coccolithophores, in: Encyclopedia of Ocean Sciences.

Walker, J.C.G., Hays, P.B., Kasting, J.F., 1981. A negative feedback mechanism for the long-term stabilization of Earth's surface temperature. Journal of Geophysical Research: Oceans 86, 9776–9782. https://doi.org/10.1029/JC086iC10p09776

Wallmann, K., 2001. Controls on the cretaceous and cenozoic evolution of seawater composition, atmospheric CO_2 and climate. Geochimica et Cosmochimica Acta 65, 3005–3025. https://doi.org/10.1016/S0016-7037(01)00638-X

Zondervan, I., Rost, B., Riebesell, U., 2002. Effect of CO_2 concentration on the PIC/POC ratio in the coccolithophore *Emiliania huxleyi* grown under light-limiting conditions and different daylengths. Journal of Experimental Marine Biology and Ecology 272, 55–70. https://doi.org/10.1016/S0022-0981(02)00037-0

Appendix 1: Supplementary Material for Chapter 2, Zotero searches, ground-truthing, and reviewing of publications

The Zotero database was searched for studies on Ocean Iron Fertilization (OIF), Macronutrient (N and P) fertilization, Alkalinity Enhancement, Deep Storage, Artificial Upwelling, Artificial Downwelling, and Macroalgal cultivation. Following is a breakdown of the search terms used to capture publications on each mCDR approach. Zotero searches used were a combination of (i) the advanced search function, and (ii) the compound Boolean search function, run through the title, abstract and publication name of each item in Zotero. For reference, % captures all suffixes after the % sign in Zotero e.g. for fert%, fertilization, fertilizing, fertilised, fertilisation etc.

Ocean Iron Fertilization (OIF) and ***Macronutrient (N and P) fertilization:*** marine, ocean, sea%, fert%, iron%enrich%, ocean nourishment

In the manuscript, we have separated out Ocean Iron Fertilization (OIF) and Macronutrient (N and P) fertilization, but when Zotero searches were carried out, the searches were carried out to include all ocean fertilization.

Alkalinity Enhancement: marine, ocean, sea%, alk%, enhanc%weather%, weather% olivine, accelerat% dissol%, lime%, liming

In the manuscript, the majority of the time we have amalgamated all approaches to alkalinity generation under Alkalinity Enhancement. When Zotero searches were carried out, we were categorising electrochemical removal of CO2 as distinct from alkalinity generation via direct addition of alkaline materials to seawater or enhanced weathering.

Electrochemical removal: marine, ocean, sea%, strip%, reverse osmosis, electrodialysis, electro% split%, electrolysis, scrub%, CO2 mitigation, indirect ocean capture

Deep Storage: marine, ocean, sea%, stor% geol%, deep storage, injection, CCS, crop residue%, crop% residue, stor% sediment%

Artificial Upwelling: artificial upwelling, geoengineer% upwelling, controlled upwelling, deep water upwelling, enhanc% ocean upwelling, ocean pip%, nutrient translocation

Artificial Downwelling: artificial downwelling, ocean pipes, enhanc% downwelling, geoengineer% downwelling

Macroalgal cultivation: seaweed, macroalga%, ocean afforestation, CO2 capture alga%, marine macrophytes

The searches were conducted initially in September 2020. Ground-truthing was carried out after Tawfik et al. (2019), where authors SG and JG separately picked key papers to check that the searches were capturing. The database was updated with new papers in July 2021, and searches were then conducted for a second time on only the new papers, to add to the final list of publications from which to collect meta-data as outlined in the manuscript.

Following filtration by keywords in Zotero, references were manually reviewed by reading the abstract and/or full paper. At this stage, references were further checked for relevance to our analyses according to the following selection criteria:

1. References must be peer-reviewed publications. The following forms of reference were therefore omitted from the final analysis: news articles (any form of print or online press coverage), blog posts, books or book chapters, theses (Bachelors, Masters or PhD), conference proceedings, introductory papers to a particular volume/special proceedings edition to a journal, working [group] papers, white papers, podcasts, policy documents e.g. IPCC reports, technical reports e.g. documents produced by private or public consultants, and lectures.
2. References must include a significant ocean component to be included. Specifically relating to enhanced weathering publications, if the publication only cursorily mentions a benefit to ocean acidification mitigation of alkalinity enhancement from land-based enhanced weathering, but there is no original data presented relating to oceans, we do not count it. Therefore, publications included in our final analysis may have a blended terrestrial and ocean focus.
3. References were only classified in a particular mCDR category if they (i) actively contribute to advancing the field of knowledge in intentional mCDR, or (ii) cover natural mCDR studied with the explicit stated aim of application to future intentional mCDR e.g. studies of the Kerguelen Plateau in ocean iron fertilization studies. In the case of the “Macroalgal cultivation” category, references were only included when the focus was mCDR. For example, marine macroalgal cultivation to increase C storage in kelp forests counts as mCDR, but macroalgal cultivation for biofuels does not count as mCDR.

Appendix 2: Supplementary Material for Chapter 3, The growth and calcification response of the coccolithophores *Emiliania huxleyi* and *Coccolithus braarudii* to the Carbon Dioxide Removal technique of Ocean Alkalinity Enhancement

A2.1 Calculation for CO_2 drawdown per unit addition of Total Alkalinity to the surface ocean

From Renforth and Henderson (2017): 1.4-1.7 moles CO_2 uptake from atmosphere into surface ocean per mole of added divalent cation (e.g. Ca^{2+})

Bach et al. (2019): Predict surface ocean Total Alkalinity (TA) raised 100-2000 µmol kg^{-1}

So if TA is raised by 100-2000 µmol kg^{-1} by 2100, how much CO_2 uptake is that equivalent to?

70-1700 µmol CO_2 per kg SW that has had TA raised – equivalent to 3-74 mg CO_2 per kg SW

Assume that the epipelagic zone = upper 200m of ocean

Volume of epipelagic zone = 7.5 x 10^{16} m^3 → 7.5 x 10^{19} kg accounting for density of SW (1.03 g cm^{-3}).

So for 3-74 mg CO_2 per kg SW, over the entire epipelagic zone, that is equivalent to between 22.5 x 10^{19} mg CO_2 – 555 x 10^{19} mg CO_2

= ~225-5550 Gt CO_2 drawdown through Alkalinity Enhancement if surface ocean TA were raised between 100-2000 µmol kg^{-1}.

NOTE: this is based on molar equivalents for divalent cations - uptake for monovalent cation (e.g. Na^+) would be ~half that if the same amount of Na^+ was added to the surface ocean as Ca^{2+} = 0.7-0.85 moles of CO_2 uptake per kg SW. To achieve the same amount of CO_2 drawdown over the same volume of epipelagic zone, it would require double the amount of Na^+ as Ca^{2+} to account for the charge difference.

A2.2 Malformation statistics

	Not malformed	Mildly malformed	Severely malformed
C. braarudii RCC1198			
E. huxleyi RCC911			
E. huxleyi SO 14-2			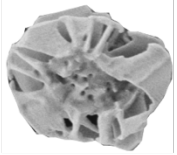

Table A2.1: SEM images showing representative liths for each species and strain in each category used to assign malformation information. For details and explanation see **Chapter 3**. Not to scale.

C. braarudii										
Pathway	**CO_2 condition**	**Strain**	**TA (µmol kg^{-1})**	**Liths (total)**		**Liths (mildly malformed)**		**Liths (severely malformed)**		**Liths (total malformed)**	
				N	%	N	%	N	%	N	%
P1 - SOW + $NaHCO_3$	CO_2-replete	RCC1198	2398	38	100.00	4	10.52	4	10.52	8	21.05
			2959	56	100.00	12	21.43	10	17.86	22	39.29
			3459	38	100.00	8	21.05	16	42.11	24	63.16
			3953	68	100.00	12	17.65	28	41.18	40	58.82
P2 - SOW + Na_2CO_3 + $CaCl_2$			2398	38	100.00	4	10.52	4	10.52	8	21.05
			3000	36	100.00	8	22.22	16	44.44	24	66.66
			3484	46	100.00	6	13.04	18	39.13	24	52.17
			3943	84	100.00	14	16.67	40	47.62	54	64.29

Table A2.2: Number and percentage of *C. braarudii* liths for each enhanced alkalinity treatment exhibiting mild and severe malformation, including total malformation and total counts for liths analysed using methods outlined in **Chapter 3.**

E. huxleyi											
Pathway	**CO_2 condition**	**Strain**	**TA (µmol kg^{-1})**	**Liths (total)**		**Liths (mildly malformed)**		**Liths (severely malformed)**		**Liths (total malformed)**	
				N	**%**	**N**	**%**	**N**	**%**	**N**	**%**
P1 - SOW + $NaHCO_3$	CO_2-limited	SO 14-2	1537	53	100.00	2	3.77	0	0.00	2	3.77
			1819	47	100.00	1	2.13	1	2.13	2	4.26
			1881	107	100.00	14	13.08	3	2.80	17	15.89
			2100	46	100.00	6	13.04	0	0.00	6	13.04
	CO_2-replete	RCC911	2346	129	100.00	25	19.38	3	2.33	28	21.71
			2835	156	100.00	50	32.05	6	3.85	56	35.90
			3299	98	100.00	27	27.55	7	7.14	34	34.69
			3732	68	100.00	18	26.47	11	16.18	29	42.65
P2 - SOW + Na_2CO_3 + $CaCl_2$	CO_2-limited	SO 14-2	1534	185	100.00	4	2.16	2	1.08	6	3.24
			1997	187	100.00	8	4.28	3	1.60	11	5.88
			2125	119	100.00	8	6.72	3	2.52	11	9.24
			2550	118	100.00	8	6.78	2	1.69	10	8.47
	CO_2-replete	RCC911	2346	129	100.00	25	19.38	3	2.33	28	21.71
			2825	64	100.00	23	35.94	2	3.13	25	39.06
			3263	70	100.00	18	25.71	18	25.71	36	51.43
			3701	91	100.00	20	21.98	30	32.97	50	54.95

Table A2.3: Number and percentage of *E. huxleyi* liths for each enhanced alkalinity treatment exhibiting mild and severe malformation, including total malformation and total counts for liths analysed using methods outlined in **Chapter 3.**

Appendix 3: Supplementary Material for Chapter 5, The response of planktonic foraminifera to enhanced ocean alkalinity for Carbon Dioxide Removal

A3.1 Normalisation of time to gametogenesis using individual foraminifera growth rates

When foraminifera are picked from the water column, the age of each foraminifer is unknown (i.e. how far through their life cycle they are). However, it is well-established that foraminifera grow in size as they progress through their life cycle by adding additional chambers to their calcite test and successive layers of calcite to their existing chambers (Hemleben et al., 1989; Nooijer et al., 2009). During the experiment in this study, "time to gametogenesis" is recorded as the number of days between the time when an individual was collected from the water column and when that individual underwent gametogenesis in its culturing jar. Technically, to properly compare time to gametogenesis between species, and indeed in between individuals, it would be helpful to normalise this "time to gametogenesis", for each foraminifer, by the stage of their life cycle they were at when they were extracted from the water column. To do this, we have performed a robust species-specific normalisation. Here, we set out the methods of this normalisation.

Firstly, we considered normalising based on the assumption that all foraminifera of the same species grow at the same rate. However, once we had calculated growth rate [change in long-axis diameter over the course of the experiment (μm)/time between picking and gametogenesis (hours)] for each foraminifer, the results showed more than an order of magnitude variation between individuals within species. In **Figure A3.1**, this can be observed, where the growth rate is plotted against raw time to gametogenesis for each species (shown by the blue crosses labelled "Raw Time"). Therefore, we opted for a normalisation using each foraminifer's growth rate. This relies on two key assumptions, according to published literature concerning the physiology and lifespan of planktonic foraminifera: (i) each foraminifer was, at some point previously in their cycle, once the size of the smallest foraminifer of that species picked from the water column, (ii) the length of time since the foraminifer was that smallest recorded size can be back-calculated from its growth rate.

To normalise the size of the smallest foraminifer in each species dataset, the size of the smallest foraminifer in the dataset was subtracted from each foraminifer's initial size. This "difference in size" was then divided by each foraminifer's growth rate. This provides an estimate of the "additional time" each foraminifer must have been alive compared to the

smallest size in the dataset when they were picked from the water column. This "additional time" is then added onto the raw "time to gametogenesis" to provide an estimate of the "normalised time", shown by the orange crosses in **Figure A3.1**.

Figure A3.1 shows that small growth rates are greatly affected by the normalisation for each dataset, whereas fast growth rates are minimally affected. This suggests that the assumptions of all foraminifera adhering to the same linear growth rates and progression of size in their cycle might not be valid, certainly for this dataset. Therefore, we do not normalise our data for "time to gametogenesis" and present the raw data for each species in **Chapter 5.**

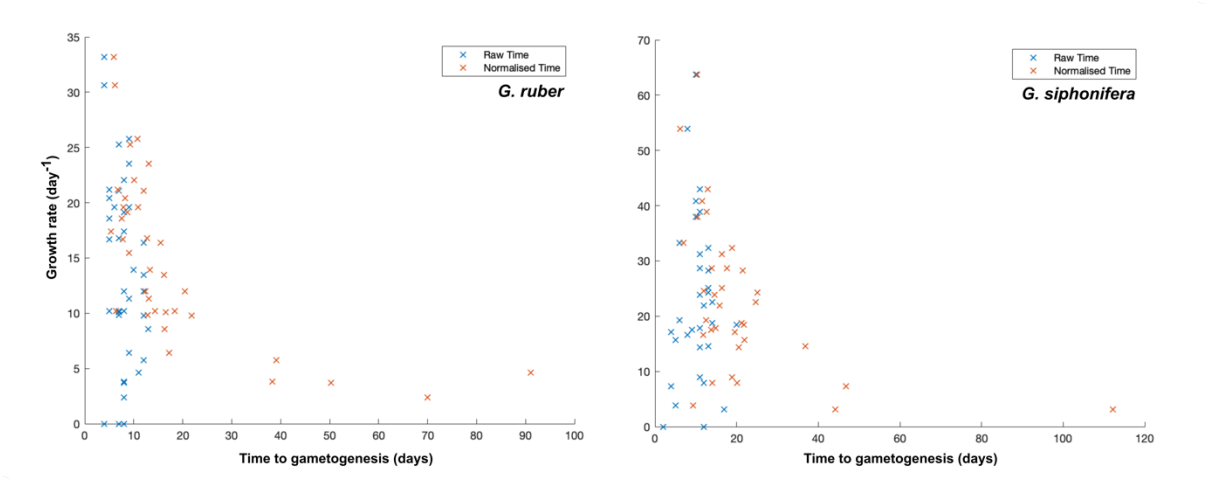

Fig. A3.1: Normalisation of time to gametogenesis compared to the raw data for each species (species labelled on the graphs). The growth rate is provided in units of μm day^{-1}. Time to gametogenesis is in units of days. Graphs were created, and normalisations were performed in MATLAB_R2019a.

A3.2 Morphometric analyses of planktonic foraminifera

A3.2.1 Methods

After culturing was completed and foraminifera were washed, dried and weighed as explained in **Chapter 5** (**Section 5.2.3**), the foraminifera were shipped back to the UK. Breakages of some foraminifera were inevitable during their transport due to the nature of the shipping process. As many foraminifera as possible have been imaged through SEM analysis; however, some breakages of foraminifera meant that not all foraminifera cultured could be imaged because they were too delicate/fractured to mount on an SEM stub. This means sample sizes of SEM images are not as high as would be ideally required to make inferences about morphological differences between alkalinity treatments, especially for morphometric analyses. Percentages for how many individuals have been imaged are recorded in **Table A3.1**. These percentages provide context for the significance of the inferences drawn from morphometric analyses performed on the images regarding the proportion of each population imaged. Light microscope images were taken via inverted light microscopy of foraminifera at the end of the experiment in culture at the Biogeochemistry laboratory at the Inter-University Institute of Marine Sciences, Eilat, Israel. SEM images were taken with a Zeiss Sigma 300 Field Emission Gun Scanning Electron Microscope (FEG-SEM) after mounting individual foraminifera onto SEM stubs and gold-coating in a vacuum evaporation system at the William-Dunn School of Pathology at the University of Oxford, UK. See Figures **A3.2a-e** for a selection of SEM and Light Microscope images exhibiting interesting aspects of foraminifera morphology pertinent to the discussion in this appendix.

species	treatment	%SEM	%LM	%SEM + LM
G. ruber	2461 µmol kg^{-1} SW (control)	9	9	0
	2926 µmol kg^{-1} SW + $NaHCO_3$	43	71	29
	3393 µmol kg^{-1} SW + $NaHCO_3$	33	44	33
	2941 µmol kg^{-1} SW + Na_2CO_3 + $CaCl_2$	44	78	33
	3355 µmol kg^{-1} SW + Na_2CO_3 + $CaCl_2$	50	25	25
G. siphonifera	2461 µmol kg^{-1} SW (control)	50	25	13
	3393 µmol kg^{-1} SW + $NaHCO_3$	25	10	0
	3355 µmol kg^{-1} SW + Na_2CO_3 + $CaCl_2$	20	50	0

Table A3.1: Summary table to show what proportion of individuals have been imaged by SEM, Light Microscope (LM), and SEM and LM in each treatment and for each species.

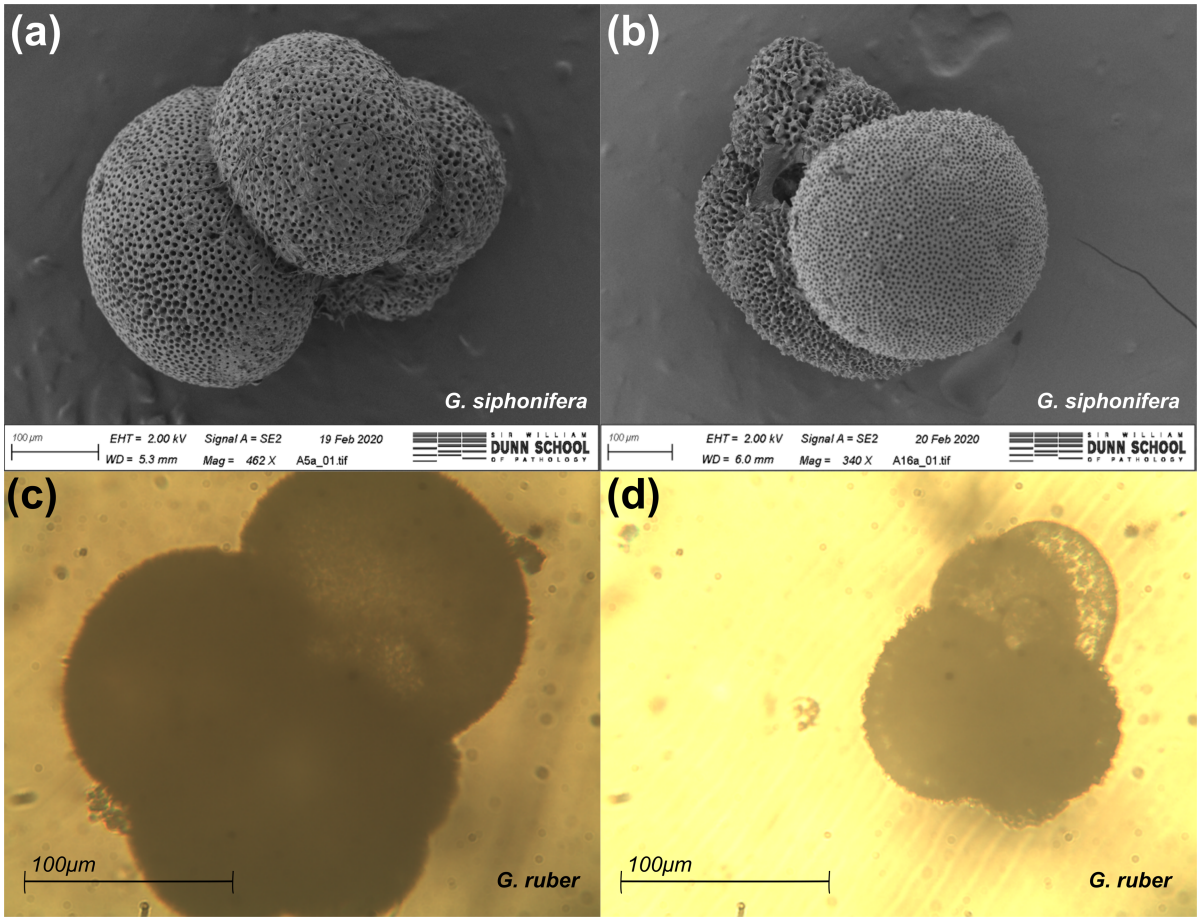

Figure A3.2a: SEM and LM images of foraminifera in control SW (TA = 2461 µmol kg^{-1}).

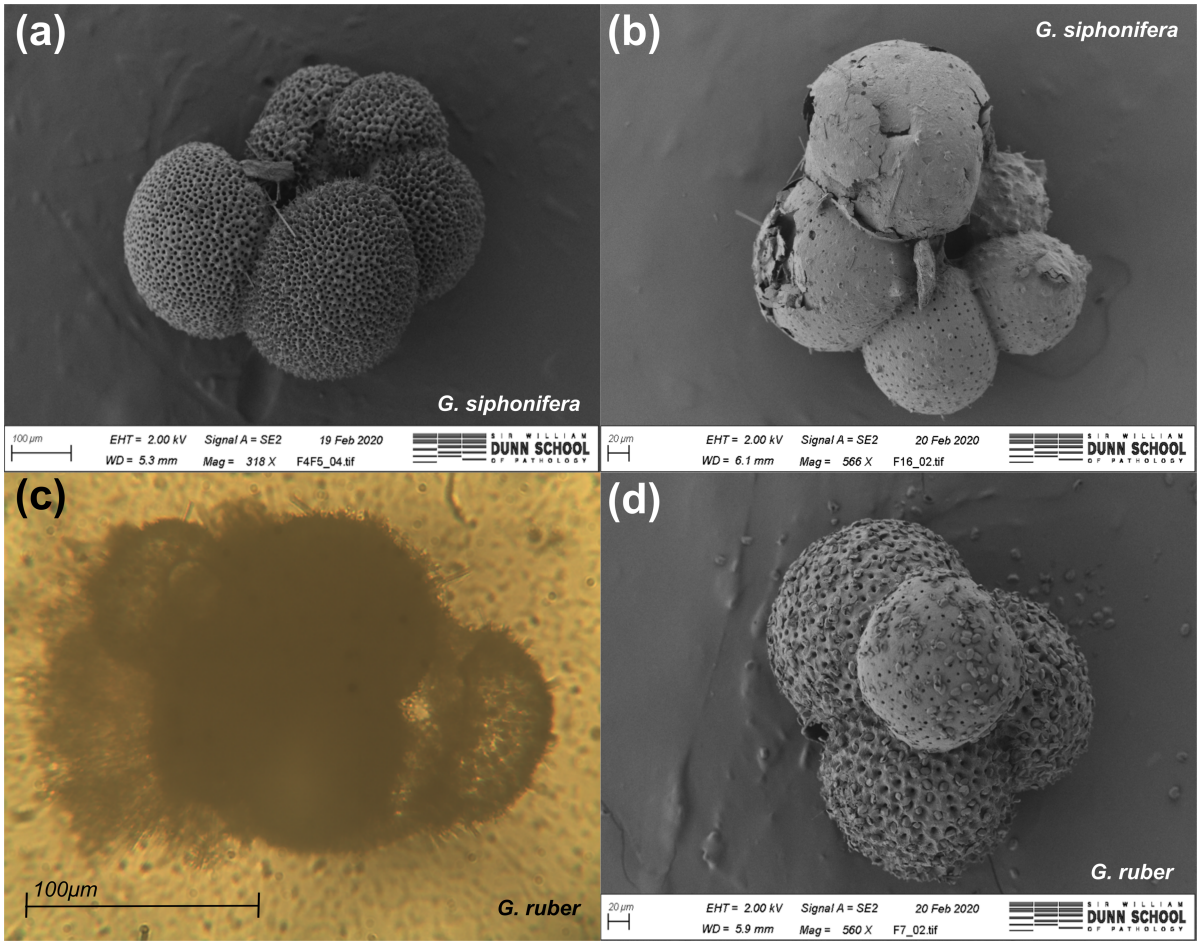

Figure A3.2b: SEM and LM images of foraminifera in SW + $NaHCO_3$ (TA = 2926 µmol kg^{-1}).

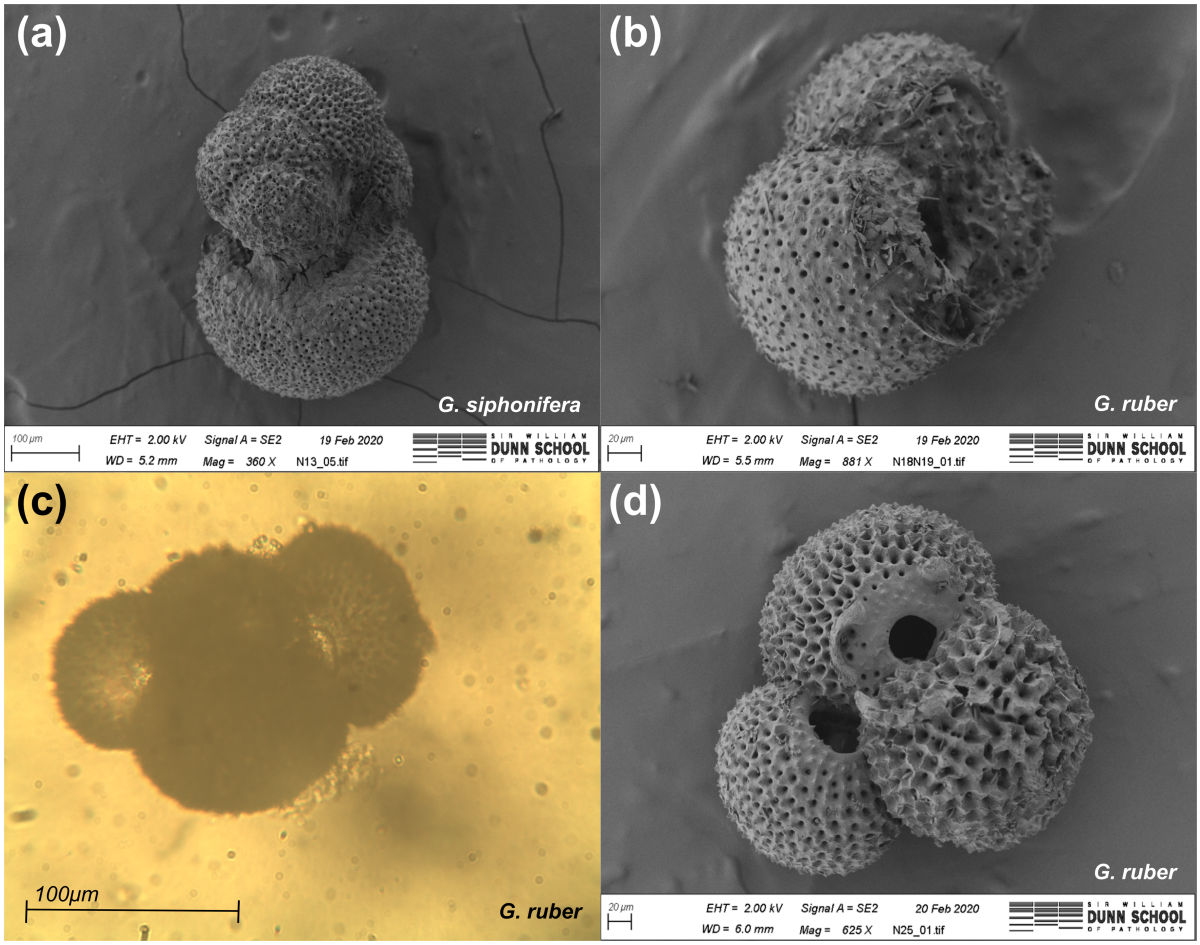

Figure A3.2c: SEM and LM images of foraminifera in SW+Na_2CO_3+$CaCl_2$ (TA = 2941 µmol kg^{-1}).

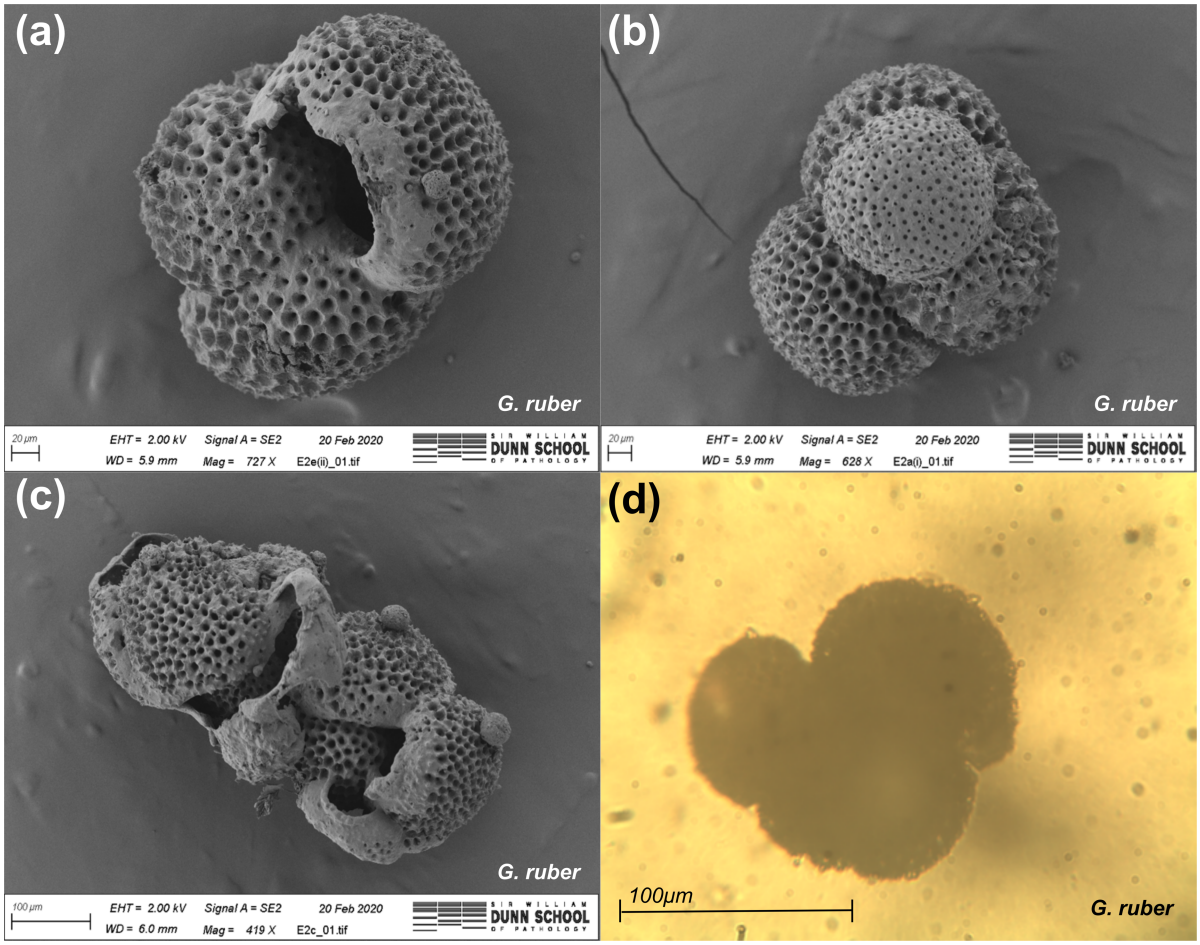

Figure A3.2d: SEM and LM images of foraminifera in SW + $NaHCO_3$ (TA = 3393 µmol kg^{-1}).

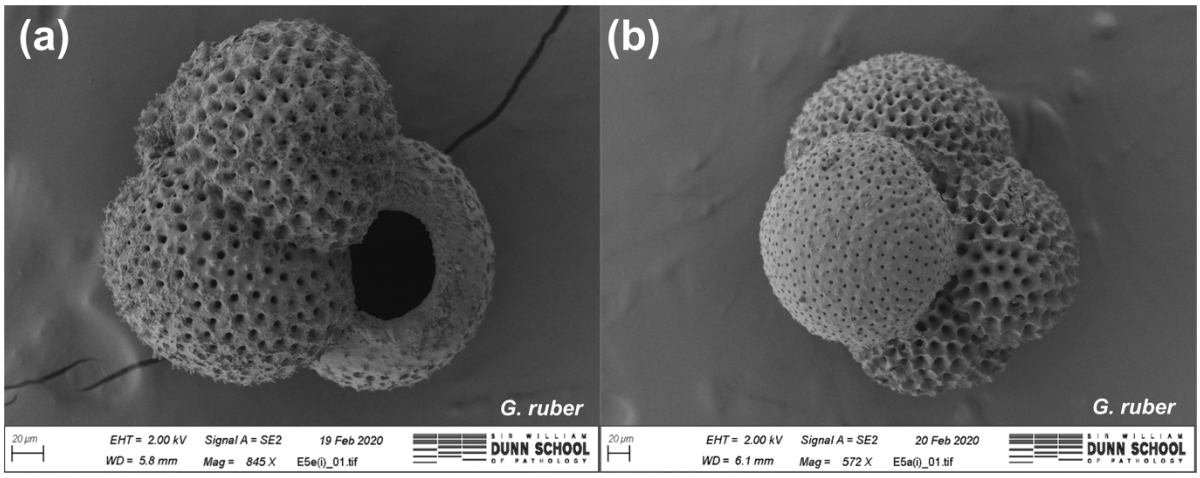

Figure A3.2e: SEM and LM images of foraminifera in SW+Na_2CO_3+$CaCl_2$ (TA = 3355 µmol kg^{-1}).

It is usual for planktonic foraminifera to exhibit a range of morphological plasticity (Kucera, 2007), and the morphology of an individual foraminifer's calcite test may change substantially during growth (Caromel et al., 2016; Hemleben et al., 1989). It is essential to distinguish between abnormal morphological deviations of *G. ruber* and *G. siphonifera* that result from being placed in enhanced alkalinity treatments and "normal" ranges of morphological plasticity for the species. "endlessforams.org" (Hsiang et al., 2019) has provided an invaluable encyclopaedic reference collection of images of *G. ruber* and *G. siphonifera* to establish what we can define as the "normal" range of morphological plasticity for these species in control SW.

We can also define what is "normal" for the populations of foraminifera from the Gulf of Eilat based on the images from **Figure A3.2a**, which are for foraminifera in control SW. Generally, for *G. ruber*, we observe trochospiral, subspherical chambers with a primary aperture symmetrically placed above a suture (Aze et al., 2011; Kennett and Srinivasan, 1983). For *G. siphonifera*, we observe planispiral subspherical chambers arranged around a central wide-rimmed aperture (Aze et al., 2011; Kennett and Srinivasan, 1983). **Figure A3.2b** shows images of *G. ruber* and *G. siphonifera* in Pathway 1, TA = 2926 µmol kg^{-1}. In *G. siphonifera,* we can see a potential decrease in the perforation level. In *G. ruber,* we can see the addition of a kummerform chamber atop the primary aperture in one specimen, which adheres to the normal morphology expected for this species. However, an individual of G. ruber also adds two kummerform chambers, one on either side of the test, which does not adhere to the trochospiral blueprint usually followed by this species. Figure **A3.2c** shows images of *G. ruber* and *G. siphonifera* in Pathway 2, TA = 2941 µmol kg^{-1}. In *G. siphonifera,* we see a potential reduction in perforation compared to control SW, but otherwise no change to morphology. In *G. ruber*, by contrast, we see most individuals following the normal morphology observed in panel (b) and a repeat of the two abnormal kummerform chamber arrangements from **Figure A3.2b** in panel (c). We can also clearly see one individual with a double aperture, rather than one primary aperture, in panel (d). **Figure A3.2d** shows images of *G. ruber* in Pathway 1, TA = 3393 µmol kg^{-1}. We can observe two individuals, in panel (a) and (b), which adhere to the trochospiral arrangement of chambers expected for *G. ruber*, where panel (d) is the same individual as in (b), just shown from a different orientation and via light microscopy. However, panel (c) shows two individuals exhibiting deformities of chamber morphology, despite adhering to the characteristic *G. ruber* trochospiral shape. **Figure A3.2e** shows images of *G. ruber* in Pathway 2, TA = 3355 µmol kg^{-1}. There were no morphological deformities or abnormalities noted in *G. ruber* in this treatment. In summary, there is a hint that some individuals of *G. siphonifera* have decreased perforation in enhanced alkalinity treatments

compared to control SW. Some individuals of *G. ruber* exhibit deviations from typical morphologies in enhanced alkalinity treatments.

From observation of these SEM and Light Microscope images, it is clear that some morphological deviation from the norm was observed in some individuals exposed to the enhanced alkalinity treatments. To place some quantifiable constraints on these observations, we have performed two kinds of morphometric analysis in ImagePro® v10: (i) quantification of the aspect ratio of foraminifera in SEM and light microscope images, and (ii) quantification of the perforation in foraminifera in SEM images (it is not possible to do perforation analysis on light microscope images).

Morphometric analysis for these two parameters was performed in ImagePro® v10 as follows. Each image of a single foraminifer was loaded into ImagePro® v10. Aspect ratio is the ratio between the major axis and minor axis of the ellipse equivalent to the perimeter of the individual foraminifer being analysed. This analysis is relatively straightforward and involves the software recognising the outline of the foraminifer relative to the background and then returning the measurement for aspect ratio. For aspect ratio analyses, only those foraminifera imaged in SEM and/or Light Microscopy with the long axis visible were measured. For %perforation analyses, all images from SEM and Light Microscopy were used, even those not imaged along the long axis, because %perforation analysis does not depend on a reliable image of the long axis. To quantify %perforation, the area of the foraminifera, defined by its outline only, was measured. ImagePro® v10 can distinguish the colour difference between perforations and the calcite of the foraminifer. Because of this, it is possible to delineate the perforations and then set ImagePro® v10 to calculate the total area of the perforations. This can then be subtracted from the total area, and a %perforation calculated for each foraminifer.

Data from these morphometric analyses are presented in **Figure A3.3** and **A3.4**. There appears to be no observable difference between treatments here, though this may simply be a result of the sparse nature of the datasets. Significant differences between *G. ruber* aspect ratio datasets (shown in **Figure A3.3**) were tested for using the t-test, with Welch's correction for unequal Standard Deviations. It was not possible to perform this statistical test with other datasets due to the sparsity of the data points. There is no significant difference between any of the treatments apart from between ~3000 and ~3500 µmol kg^{-1} SW + Na_2CO_3 + $CaCl_2$ for *G. ruber*. Considering that there are only two data points for ~3500 µmol kg^{-1} SW + Na_2CO_3 + $CaCl_2$, we are unsure of the reliability of this statistical test.

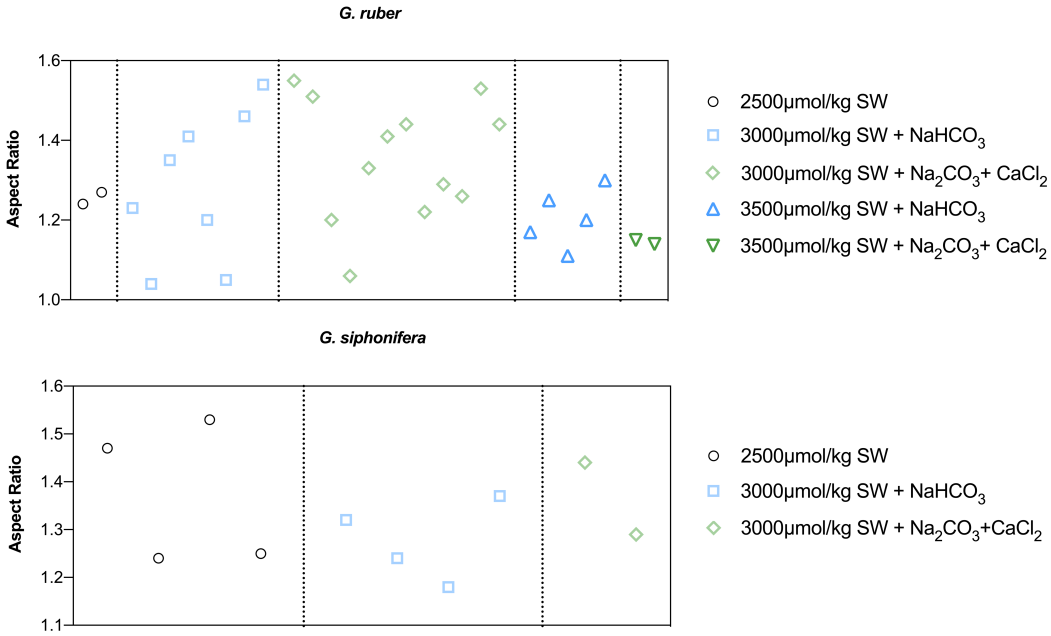

Figure A3.3: Morphometric analysis of foraminifera aspect ratio. Graphs created in GraphPad Prism 9. Each data point represents one single foraminifer.

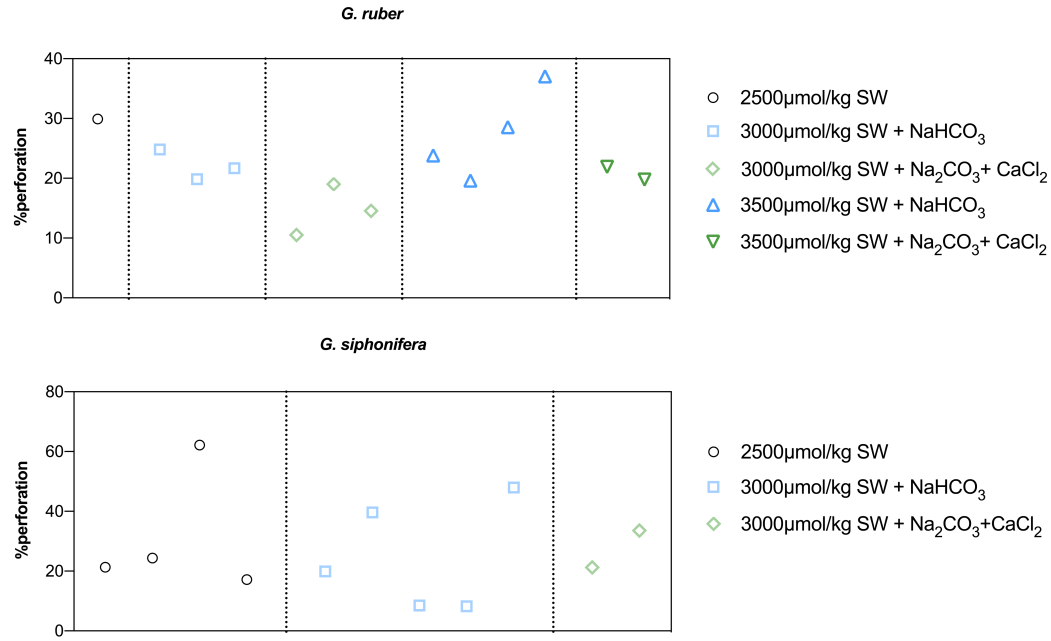

Figure A3.4: Morphometric analysis of foraminifera %perforation. Graphs created in GraphPad Prism 9. Each data point represents one single foraminifer.

A3.2.2 Discussion

Morphometric analysis (Aspect Ratio and %perforation) of both species of foraminifera did not return any significant difference between alkalinity treatments and control seawater. However, the fact remains that some individuals of *G. siphonifera* and *G. ruber* in enhanced alkalinity treatments exhibit morphological abnormalities. In control conditions, there was not a single individual of *G. siphonifera* or *G. ruber* which exhibited deviation from normal morphologies of their respective species. Therefore, we suggest that the probability of abnormal growth/malformation is higher in enhanced alkalinity treatments compared to the control.

The reason for this might lie in how planktonic foraminifera respond to external chemical perturbations. For example, the supplementary apertures which we observe in *G. ruber* at ~3000µmol kg^{-1} SW + Na_2CO_3 + $CaCl_2$ are not unusual amongst this species, however they tend to only be observed in individuals under notable environmental stress (Arenillas et al., 2018; Hsiang et al., 2019). Arenillas et al. (2018) report a wide range of extreme planktonic foraminifera morphologies across the K/Pg boundary in the Western Tethys, which was a time of extreme environmental stress. They observe abnormal chambers, double or twinned ultimate chambers, distortion in test coiling, amongst other “general monstrosities”. The tendency for foraminifera to change their morphologies under environmental stress might be related to the idea of “bet-hedging”, discussed in Weinkauf et al. (2014). The central tenet of this argument lies in the idea that the higher the range of morphologies exhibited by a species of foraminifera during times of environmental stress, the more likely that species is to survive the environmental stress. However, it is also postulated that under stress, the ability of foraminifera to constrain shape of shells is limited (Caron et al., 1987). A suggestion arising from our study is that this could be due to a diversion of focus from morphological control towards more “core” functions, for example maintaining normal calcification function. This is supported by our results showing that calcification is not significantly perturbed by the enhanced alkalinity treatments for either *G. ruber* or *G. siphonifera*. Geometry of foraminifera shells is controlled by cytoskeleton assembly during the calcification process (Bé, 1980). There is clearly some debate here as to whether abnormal morphologies under environmental stress are driven by an external evolutionary pressure to survive, or an internal physiological constraint on cytoskeleton assembly. At any rate, both of these explanations would suggest that the deviations from normal foraminiferal shell morphology which we observe in this study are a stress response to the associated changes in the carbonate system which accompany raised alkalinity.

A3.3 Statistical testing of compiled literature and culture logs

Data were tested for significant difference using one-way ANOVA and post-hoc Tukey-Kramer test in GraphPad Prism 9. Before these statistical analyses, data were tested for normality using the Shapiro-Wilks test (Gore et al., 2018) (Shafiee et al., 2021). If data did not pass the test for normality using Shapiro-Wilks, the Kruskal-Wallis test for significant difference and Dunn's multiple comparison test were used following best practice guidelines for statistical analysis (Motulsky, GraphPad Statistics Guide).

Full results of statistical testing are included below for each species, where * = P ≤ 0.05, ** = P ≤ 0.01, *** = P ≤ 0.001, **** = P ≤ 0.0001, and ns = not significant.

G. bulloides - Change in shell mass	
CO_3^{2-} comparison (µmol kg^{-1})	Summary of statistical significance
173 vs. 174	**
173 vs. 301	***
174 vs. 301	ns

G. bulloides - Lifespan	
CO_3^{2-} comparison (µmol kg^{-1})	Summary of statistical significance
173 vs. 174	ns
173 vs. 301	ns
174 vs. 301	ns

G. ruber - Change in shell mass	
CO_3^{2-} comparison (µmol kg^{-1})	Summary of statistical significance
66 vs. 184	ns
66 vs. 221	ns
66 vs. 212	ns
66 vs. 220	ns
66 vs. 264	ns
66 vs. 497	ns
184 vs. 221	ns
184 vs. 212	ns
184 vs. 220	ns
184 vs. 264	ns
184 vs. 497	ns
221 vs. 212	ns
221 vs. 220	ns
221 vs. 264	ns
221 vs. 497	ns
212 vs. 220	ns
212 vs. 264	ns
212 vs. 497	ns
220 vs. 264	ns
220 vs. 497	ns
264 vs. 497	ns

G. ruber - Lifespan	
CO_3^{2-} comparison (µmol kg^{-1})	Summary of statistical significance
66 vs. 184	ns
66 vs. 221	ns
66 vs. 212	ns
66 vs. 220	ns
66 vs. 264	***
66 vs. 497	****
184 vs. 221	*
184 vs. 212	ns
184 vs. 220	ns
184 vs. 264	ns
184 vs. 497	*
221 vs. 212	ns
221 vs. 220	ns
221 vs. 264	****
221 vs. 497	****
212 vs. 220	ns
212 vs. 264	ns
212 vs. 497	*
220 vs. 264	ns
220 vs. 497	**
264 vs. 497	ns

G. sacculifer - Change in shell mass	
CO_3^{2-} comparison (µmol kg^{-1})	Summary of statistical significance
100 vs. 184	ns
100 vs. 221	ns
100 vs. 212	ns
100 vs. 220	ns
100 vs. 264	ns
100 vs. 480	ns
184 vs. 221	ns
184 vs. 212	ns
184 vs. 220	ns
184 vs. 264	ns
184 vs. 480	ns
221 vs. 212	ns
221 vs. 220	ns
221 vs. 264	***
221 vs. 480	ns
212 vs. 220	ns
212 vs. 264	ns
212 vs. 480	ns
220 vs. 264	ns
220 vs. 480	ns
264 vs. 480	*

G. sacculifer - Lifespan	
CO_3^{2-} comparison (µmol kg^{-1})	Summary of statistical significance
100 vs. 184	ns
100 vs. 221	*
100 vs. 212	ns
100 vs. 220	ns
100 vs. 264	ns
100 vs. 480	ns
184 vs. 221	ns
184 vs. 212	ns
184 vs. 220	ns
184 vs. 264	ns
184 vs. 480	ns
221 vs. 212	ns
221 vs. 220	ns
221 vs. 264	****
221 vs. 480	ns
212 vs. 220	ns
212 vs. 264	ns
212 vs. 480	ns
220 vs. 264	ns
220 vs. 480	ns
264 vs. 480	ns

O. universa - Change in shell mass	
CO_3^{2-} comparison (µmol kg^{-1})	Summary of statistical significance
154 vs. 70	ns
154 vs. 157	ns
154 vs. 2248	ns
154 vs. 174	ns
154 vs. 168	ns
154 vs. 177	ns
154 vs. 183	ns
154 vs. 299	ns
154 vs. 581	ns
70 vs. 157	ns
70 vs. 2248	ns
70 vs. 174	ns
70 vs. 168	ns
70 vs. 177	ns
70 vs. 183	ns
70 vs. 299	ns
70 vs. 581	ns
157 vs. 2248	ns
157 vs. 174	ns
157 vs. 168	ns
157 vs. 177	ns
157 vs. 183	ns
157 vs. 299	ns
157 vs. 581	ns
2248 vs. 174	ns
2248 vs. 168	ns
2248 vs. 177	ns
2248 vs. 183	ns
2248 vs. 299	ns
2248 vs. 581	ns
174 vs. 168	ns
174 vs. 177	ns
174 vs. 183	ns
174 vs. 299	ns
174 vs. 581	ns
168 vs. 177	ns
168 vs. 183	ns
168 vs. 299	ns
168 vs. 581	ns
177 vs. 183	ns
177 vs. 299	ns
177 vs. 581	ns
183 vs. 299	ns
183 vs. 581	ns
299 vs. 581	ns

O. universa - Lifespan	
CO_3^{2-} comparison (µmol kg^{-1})	Summary of statistical significance
29.1348523 vs. 32.9401790	ns
29.1348523 vs. 70.0000000	ns
29.1348523 vs. 110.5831280	ns
29.1348523 vs. 430.8303640	ns
32.9401790 vs. 70.0000000	*
32.9401790 vs. 110.5831280	ns
32.9401790 vs. 430.8303640	ns
70.0000000 vs. 110.5831280	ns
70.0000000 vs. 430.8303640	ns
110.5831280 vs. 430.8303640	ns

Table A3.2: Statistical testing of compiled literature and culture logs.

References

Arenillas, I., Arz, J., Gilabert, V., 2018. Blooms of aberrant planktic foraminifera across the K/Pg boundary in the Western Tethys: Causes and evolutionary implications. Paleobiology 44, 1–30. https://doi.org/10.1017/pab.2018.16

Aze, T., Ezard, T.H.G., Purvis, A., Coxall, H.K., Stewart, D.R.M., Wade, B.S., Pearson, P.N., 2011. A phylogeny of Cenozoic macroperforate planktonic foraminifera from fossil data. Biological Reviews 86, 900–927. https://doi.org/10.1111/j.1469-185X.2011.00178.x

Bé, A.W.H., 1980. Gametogenic calcification in a spinose planktonic foraminifer, *Globigerinoides sacculifer (Brady)*. Marine Micropaleontology 5, 283–310. https://doi.org/10.1016/0377-8398(80)90014-6

Caromel, A.G.M., Schmidt, D.N., Fletcher, I., Rayfield, E.J., 2016. Morphological Change During The Ontogeny Of The Planktic Foraminifera. Journal of Micropalaeontology 35, 2–19. https://doi.org/10.1144/jmpaleo2014-017

Caron, D.A., Faber, W.W., Bé, A.W.H., 1987. Effects of temperature and salinity on the growth and survival of the planktonic foraminifer *Globigerinoides sacculifer*. Journal of the Marine Biological Association of the United Kingdom 67, 323–341. https://doi.org/10.1017/S0025315400026643

Hemleben, C., Spindler, M., Anderson, O.R., 1989. Modern planktonic foraminifera. Springer-Verlag.

Hsiang, A.Y., Brombacher, A., Rillo, M.C., Mleneck-Vautravers, M.J., Conn, S., Lordsmith, S., Jentzen, A., Henehan, M.J., Metcalfe, B., Fenton, I.S., Wade, B.S., Fox, L., Meilland, J., Davis, C.V., Baranowski, U., Groeneveld, J., Edgar, K.M., Movellan, A., Aze, T., Dowsett, H.J., Miller, C.G., Rios, N., Hull, P.M., 2019. Endless Forams: >34,000 Modern Planktonic Foraminiferal Images for Taxonomic Training and Automated Species Recognition Using Convolutional Neural Networks. Paleoceanography and Paleoclimatology 34, 1157–1177. https://doi.org/10.1029/2019PA003612

Kennett, J.P., Srinivasan, M.S., 1983. Neogene Planktonic Foraminifera: A Phylogenetic Atlas. Hutchinson Ross.

Kucera, M., 2007. Chapter Six Planktonic Foraminifera as Tracers of Past Oceanic Environments. Developments in Marine Geology Volume 1, 213–262. https://doi.org/10.1016/S1572-5480(07)01011-1

Nooijer, L.J. de, Toyofuku, T., Kitazato, H., 2009. Foraminifera promote calcification by elevating their intracellular pH. PNAS 106, 15374–15378. https://doi.org/10.1073/pnas.0904306106

Weinkauf, M.F.G., Moller, T., Koch, M.C., Kučera, M., 2014. Disruptive selection and bet-hedging in planktonic Foraminifera: shell morphology as predictor of extinctions. Frontiers in Ecology and Evoution, 2. https://doi.org/10.3389/fevo.2014.00064

Appendix 4: The response of *Coccolithus braarudii* strain RCC1198 to OAE using $NaHCO_3$ under CO_2-limited conditions

The set-up of the following CO_2-limited experiment is identical to the coccolithophore cultures described in **Chapter 3** for CO2-limited cultures, including aspects of sample analyses for the Redfield ratio outlined in **Chapter 4**. Statistical analyses were all carried out following methods outlined in **Chapter 3**.

In addition to examining the response of *C. braarudii* strain RCC1198 to OAE under CO_2-replete conditions, presented in **Chapter 3**, I also examined the response of *C. braarudii* RCC1198 to OAE CO_2-limited conditions for Pathway 1 (SOW + $NaHCO_3$). However, the experiment had some problems, which meant I could not include it in the final dataset presented in **Chapter 3**.

Typically, over the course of a culture, it is expected that [CO_2] will decrease in solution because the cells are respiring and taking resources out of the culture media to fuel their growth. However, in my experiment using concentrated cultures of *C. braarudii* strain RCC1198 (~5000 cells ml^{-1} inoculated, ~200,000 cells ml^{-1} at harvest), CO_2 in solution rose from inoculation to the time of harvest (see **Table A4.1**). This was despite no increase in calcification (see **Figure A4.1(b)**). One explanation could be that another organism (such as a contaminating bacteria) was respiring in solution. If this were the case, then the culture was not monospecific or axenic, which would render the culturing study null. No bacteria were imaged during SEMs (see **Figure A4.2**). However, the pore size of the polycarbonate filters used to collect SEM samples was 0.6µm, so bacteria may have been smaller than this and then passed through the filter.

Because it has been impossible to conclude what happened to this culture, I have chosen to exclude it from the final dataset because the data cannot be considered watertight. However, I include it in this Appendix in case it is useful and for completeness.

C. braarudii (RCC1198) – CO_2-limited conditions before inoculation										
	Initial alkalinity treatment	Total alkalinity ($\mu molkg^{-1}$)	DIC ($\mu molkg^{-1}$)	pH (NBS scale)	pCO_2 (μatm)	$[CO_2]$ ($\mu molkg^{-1}$)	HCO_3^- ($\mu molkg^{-1}$)	CO_3^{2-} ($\mu molkg^{-1}$)	$\Omega CaCO_3$	Ca (mM)
Pathway 1 – SOW + $NaHCO_3$	Control (SOW)	2651	2379	7.983	786	22.3	2175	182	4.4	10.5
	E1 (Control + ~500 $\mu molkg^{-1}$)	3238	2875	8.061	785	22.2	2594	259	6.2	10.5
	E2 (Control + ~1000 $\mu molkg^{-1}$)	3677	3231	8.122	758	21.4	2879	331	8.0	10.5
	E3 (Control + ~1500 $\mu molkg^{-1}$)	4191	3549	8.268	578	16.4	3042	490	11.8	10.5
C. braarudii (RCC1198) – CO_2-limited conditions at harvest										
	Initial alkalinity treatment	Total alkalinity ($\mu molkg^{-1}$)	DIC ($\mu molkg^{-1}$)	pH (NBS scale)	pCO_2 (μatm)	$[CO_2]$ ($\mu molkg^{-1}$)	HCO_3^- ($\mu molkg^{-1}$)	CO_3^{2-} ($\mu molkg^{-1}$)	$\Omega CaCO_3$	Ca (mM)
Pathway 1 – SOW + $NaHCO_3$	Control (SOW)	934	894	7.385	1209	34.2	842	18	0.4	10.5
	E1 (Control + ~500 $\mu molkg^{-1}$)	1076	1030	7.429	1261	35.7	972	23	0.5	10.5
	E2 (Control + ~1000 $\mu molkg^{-1}$)	1050	995	7.492	1085	30.7	936	26	0.6	10.5
	E3 (Control + ~1500 $\mu molkg^{-1}$)	4190	3678	8.143	799	23.1	3262	393	9.5	10.5

Table A4.1: Carbonate chemistry for culture media conditions before inoculation and at harvest. Total Alkalinity and pH were measured via Gran titration and pH probe respectively (as outlined in **Chapter 3**), and then used as inputs for calculation of the rest of the carbonate system in CO2SYS v2.1 (Pierrot et al. 2016), with K1 and K2 constants from Roy, et al. (1993), $KHSO_4$ values from Dickson, pH on the NBS scale and $[B]_T$ value from Lee et al. (2010). Ca levels in solution are calculated using the molar amounts of Ca^{2+} in the volume of $CaCl_2$ added to the enhanced alkalinity treatments.

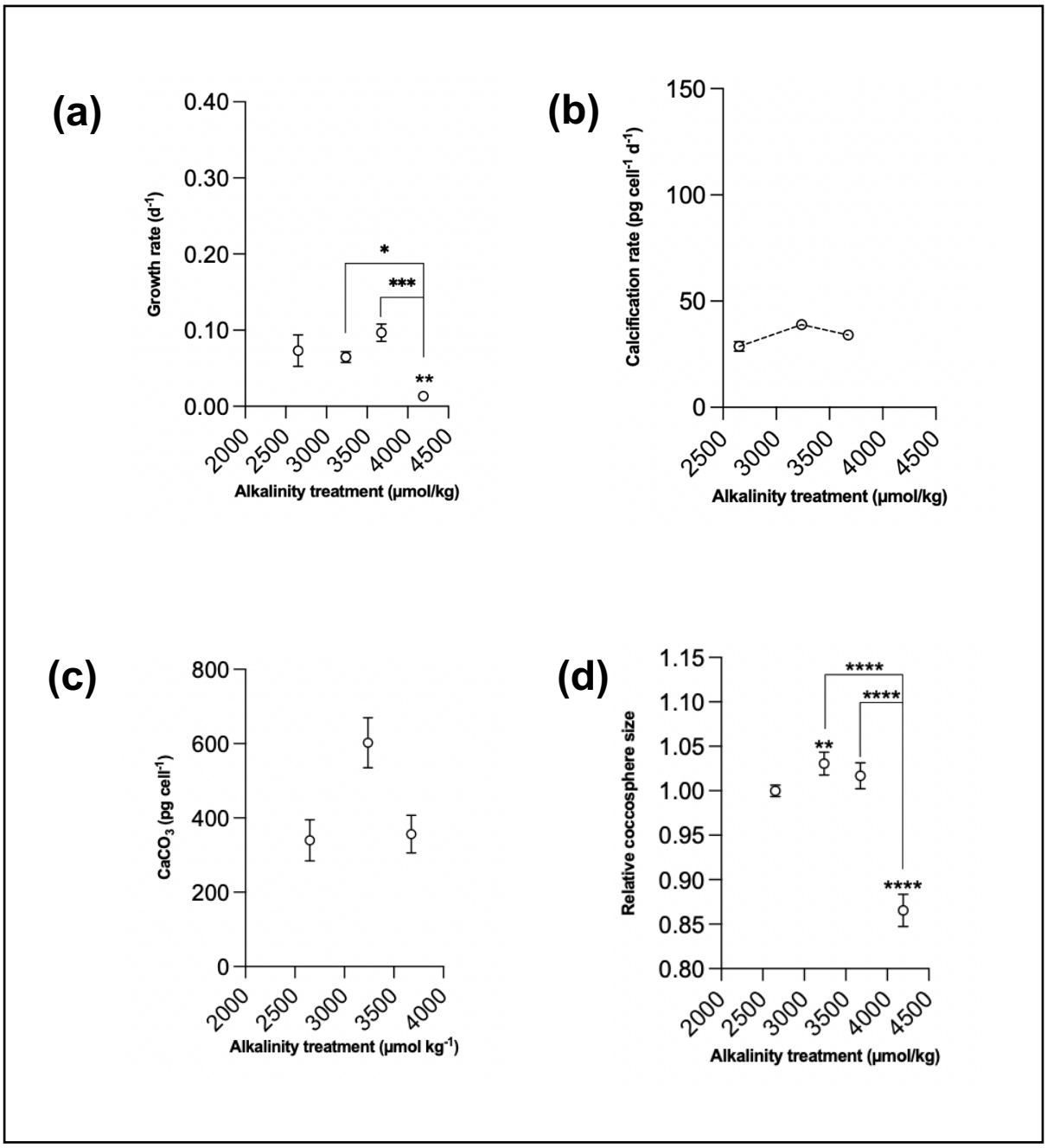

Figure A4.1: Initial alkalinity treatment (i.e. alkalinity before inoculation) vs (a) growth rate, (b) calcification rate, (c) calcite quota per cell, and (d) relative coccosphere size. Statistical significance: * = P ≤ 0.05, ** = P ≤ 0.01, *** = P ≤ 0.001, **** = P ≤ 0.0001. Error bars shown are triplicate values from biological triplicate cultures. In cases where no error bar is shown, this is because the size of the symbol obscures the error bar.

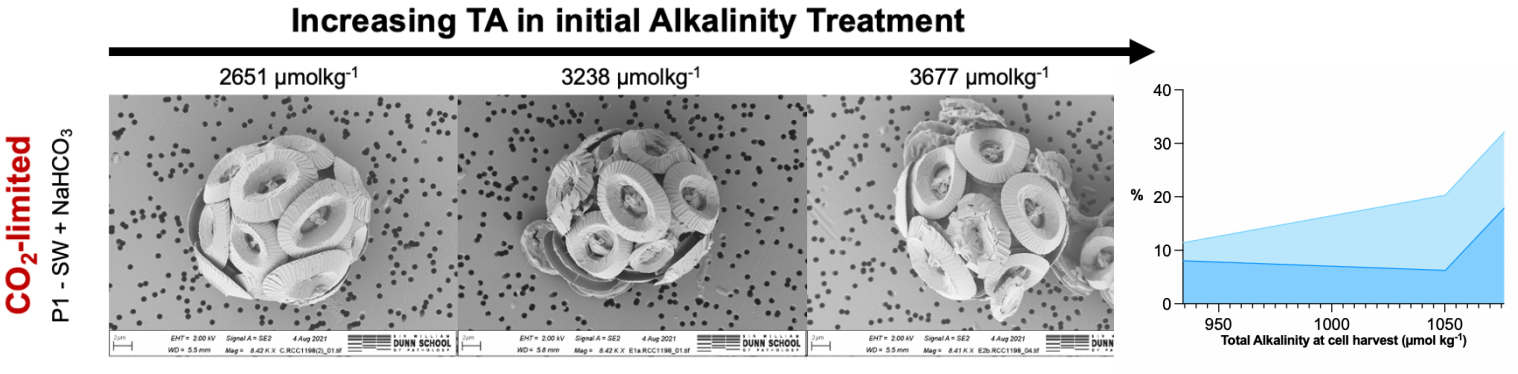

Figure A4.2: SEM images of *C. braarudii* in CO_2-limited OAE Pathway 1, alongside graph showing % malformation of liths in culture. Unfortunately, the highest TA treatment (TA = 4191) SEM samples had not captured any cells, so no SEM images were procured for this alkalinity treatment. Malformation (%) graph follows the framework set out in **Chapter 3**. The upper line on each chart = total % of lith malformation observed. Lighter blue area = % of liths exhibiting severe malformation. Darker blue area = % of liths showing mild malformation. For full details of these categorisations, please see **Chapter 3**.

	Initial alkalinity treatment	Total alkalinity ($\mu molkg^{-1}$)	Average POC (pg $cell^{-1}$)	SD	Average PON (pg $cell^{-1}$)	SD	Average POP (pg $cell^{-1}$)	SD
Pathway 1 – SOW + $NaHCO_3$	Control (SOW)	2651	53.2	20.26	2.4	0.08	1.9	0.27
	E1 (Control + ~500 $\mu molkg^{-1}$)	3238	-	-	3.5	0.04	1.6	0.27
	E2 (Control + ~1000 $\mu molkg^{-1}$)	3677	186.6	-	6.0	1.32	1.6	0.19
	E3 (Control + ~1500 $\mu molkg^{-1}$)	4191	25.7	7.18	-	-	1.5	0.06

Table A4.2: POC, PON, POP values for each initial alkalinity treatment. SD = Standard Deviation. Missing POC, PON and POP values are due to technical failures in mass spectrometer runs or spectrophotometric assays. Missing SD values are due to a lack of values to calculate SD, i.e. n < 1. POC values are from measurements on a SERCON 20/22 Isotope ratio mass spectrometer (IRMS) coupled to a SERCON GSL elemental analyser in the School of Archaeology, the University of Oxford – see **Chapter 3** for complete details. PON and POP values are from N and P assays run on a Tecan SparkControl plate reader – see **Chapter 4** for full details.